Universidade Federal de Minas Gerais
Instituto de Ciências Biológicas
Programa de Pós-Graduação em Genética

Thaís Cristina Vilela Rodrigues

**COMPREHENSIVE CHARACTERIZATION OF THE PROTEIN MICROBIAL
ANTI-INFLAMMATORY MOLECULE (MAM) FROM THE GENUS**
***Faecalibacterium*: structural, diversity, and anti-inflammatory implications**

Belo Horizonte
2025

Thaís Vilela Rodrigues

COMPREHENSIVE CHARACTERIZATION OF THE PROTEIN MICROBIAL ANTI-INFLAMMATORY MOLECULE (MAM) FROM THE GENUS *Faecalibacterium*: structural, diversity, and anti-inflammatory implications

Tese apresentada ao Programa de Pós-Graduação em Genética da Universidade Federal de Minas Gerais como requisito parcial para obtenção do grau de Doutor(a) em Genética, área de concentração: Genética Molecular e de Microrganismos.

Orientadores: Dr. Jean-Marc Chatel e Dr. Vasco Azevedo

Coorientador: Siomar de Castro Soares

Belo Horizonte
2025

ATA DE DEFESA DE DISSERTAÇÃO/TESE

ATA DA DEFESA DE TESE	197/2025
Thaís Cristina Vilela Rodrigues	entrada 1º/2021 CPF: 126.791.666-47

Às nove horas do dia **29 de abril de 2025**, reuniu-se, no Instituto de Ciências Biológicas da UFMG, a Comissão Examinadora de Tese, indicada pelo Colegiado do Programa, para julgar, em exame final, o trabalho intitulado: **"Comprehensive Characterization Of The Protein Microbial Anti-inflammatory Molecule (mam) From The Genus Faecalibacterium Structural, Diversity, And Anti-inflammatory Implications"**, requisito para obtenção do grau de Doutora em **Genética.** Abrindo a sessão, o Presidente da Comissão, **Dr. Vasco Ariston de Carvalho Azevedo**, após dar a conhecer aos presentes o teor das Normas Regulamentares do Trabalho Final, passou a palavra à candidata, para apresentação de seu trabalho. Seguiu-se a arguição pelos Examinadores, com a respectiva defesa da candidata. Logo após, a Comissão se reuniu, sem a presença da candidata e do público, para julgamento e expedição de resultado final. Foram atribuídas as seguintes indicações:

Prof./Pesq.	Instituição	Indicação
Dr. Vasco Ariston de Carvalho Azevedo	Universidade Federal de Minas Gerais	APROVADA
Dr. Jean-Marc (Orientador)	Institut national de la recherche agronomique - Micalis	APROVADA
Dr. Siomar Soares (Co-orientador)	Universidade Federal do Triângulo Mineiro	APROVADA
Dr. Anderson Miyoshi	Universidade Federal de Minas Gerais	APROVADA
Dr. Frederico Gueiros Filho	Universidade de São Paulo	APROVADA
Dra. Stéphanie BURY-MONÉ	Professeure Université Paris-Saclay	APROVADA

Pelas indicações, a candidata foi considerada: **APROVADA**

O resultado final foi comunicado publicamente à candidata pelo Presidente da Comissão. Nada mais havendo a tratar, o Presidente encerrou a reunião e lavrou a presente ATA, que será assinada por todos os membros participantes da Comissão Examinadora.

Belo Horizonte, 29 de abril de 2025.

Dr. Vasco Ariston de Carvalho Azevedo - Orientador

Dr. Jean-Marc -Orientador

Dr. Siomar Soares - Co-orientador

Dr. Anderson Miyoshi

Dr. Frederico Gueiros Filho

Dra. Stéphanie BURY-MONÉ

Assinatura dos membros da banca examinadora:

Documento assinado eletronicamente por **Siomar de Castro Soares**, **Usuário Externo**, em 29/04/2025, às 16:38, conforme horário oficial de Brasília, com fundamento no art. 5º do Decreto nº 10.543, de 13 de novembro de 2020.

Documento assinado eletronicamente por **Bury-Moné Stephanie Germaine Marie-Madelaine**, **Usuária Externa**, em 30/04/2025, às 02:52, conforme horário oficial de Brasília, com fundamento no art. 5º do Decreto nº 10.543, de 13 de novembro de 2020.

Documento assinado eletronicamente por **Anderson Miyoshi**, **Membro**, em 30/04/2025, às 08:44, conforme horário oficial de Brasília, com fundamento no art. 5º do Decreto nº 10.543, de 13 de novembro de 2020.

Documento assinado eletronicamente por **Jean-Marc Bernard Chatel**, **Usuário Externo**, em 30/04/2025, às 12:14, conforme horário oficial de Brasília, com fundamento no art. 5º do Decreto nº 10.543, de 13 de novembro de 2020.

Documento assinado eletronicamente por **Vasco Ariston de Carvalho Azevedo**, **Professor do Magistério Superior**, em 30/04/2025, às 14:16, conforme horário oficial de Brasília, com fundamento no art. 5º do Decreto nº 10.543, de 13 de novembro de 2020.

Documento assinado eletronicamente por **Frederico José Gueiros Filho**, **Usuário Externo**, em 05/05/2025, às 11:00, conforme horário oficial de Brasília, com fundamento no art. 5º do Decreto nº 10.543, de 13 de novembro de 2020.

A autenticidade deste documento pode ser conferida no site https://sei.ufmg.br/sei/controlador_externo.php?acao=documento_conferir&id_orgao_acesso_externo=0, informando o código verificador **4163159** e o código CRC **F42C3571**.

UNIVERSIDADE FEDERAL DE MINAS GERAIS

"Comprehensive Characterization Of The Protein Microbial Anti-inflammatory Molecule (mam) From The Genus Faecalibacterium Structural, Diversity, And Anti-inflammatory Implications"

Thaís Cristina Vilela Rodrigues

Tese aprovada pela banca examinadora constituída pelos Professores:

Prof. Vasco Ariston de Carvalho Azevedo - Orientador

Universidade Federal de Minas Gerais

Jean-Marc (Orientador)

Institut national de la recherche agronomique - Micalis

Siomar Soares (Co-orientador)

Universidade Federal do Triângulo Mineiro

Anderson Miyoshi

Universidade Federal de Minas Gerais

Frederico Gueiros Filho

Universidade de São Paulo

Stéphanie BURY-MONÉ

Professeure Université Paris-Saclay

Belo Horizonte, 29 de abril de 2025

Aos meus pais Fábio Rodrigues Flora e Maria Marta Vilela Rodrigues, e ao meu irmão Lucas, por serem a base.

ACKNOWLEDGMENTS

"By the means of Telescopes, there is nothing so far distant but may be represented to our view; and by the help of Microscopes, there is nothing so small as to escape our inquiry; hence there is a new visible World discovered to the understanding. By this means the Heavens are open'd and a vast number of new Stars and new Motions, and new Productions appear in them, to which all the ancient Astronomers were utterly strangers. By this the Earth it self, which lyes so neer to us, under our feet, shews quite a new thing to us, and in every little particle of its matter, we now behold almost as great a variety of Creatures, as we were able before to reckon up in the whole Universe itself."

Robert Hooke, 1665
(in the Preface of Micrographia)

RESUMO

A Microbial Anti-inflammatory Molecule (MAM) é uma proteína única produzida pelo gênero *Faecalibacterium*, um grupo essencial de bactérias comensais do intestino humano. Entre essas, *Faecalibacterium duncaniae* (anteriormente *F. prausnitzii*) é altamente abundante e está intimamente associada à homeostase intestinal e à saúde geral. MAM demonstrou propriedades anti-inflamatórias significativas; no entanto, suas características moleculares e funcionais, bem como seus mecanismos de ação, permanecem pouco compreendidos. Este trabalho tem como objetivo investigar o papel fisiológico da MAM em *Faecalibacterium* e sua interação com o hospedeiro. Utilizando proteômica, bioinformática estrutural e técnicas de microscopia, caracterizamos as propriedades moleculares da MAM e sua diversidade dentro do gênero. Além disso, avaliamos a atividade imunomoduladora da MAM por meio de ensaios *in vitro* e *in vivo*. Nossos achados revelam que a MAM é processada e transportada via o transportador ABC PCAT para o envelope celular de *F. duncaniae*, onde forma uma rede supramolecular hexamérica, contribuindo provavelmente para a organização do envelope celular. Essa estrutura hexamérica é conservada em múltiplas espécies de *Faecalibacterium*, conforme demonstrado por análises *in silico*. Embora a exata localização dessa rede no envelope celular ainda não esteja determinada, *F. duncaniae* exibe uma arquitetura de envelope distintiva, caracterizada por uma camada fina de peptidoglicano e uma camada externa que diverge das bactérias monodérmicas/didérmicas clássicas. Ensaios funcionais revelaram que a MAM recombinante purificada foi capaz de melhorar significativamente os sinais macroscópicos em um modelo murino de inflamação intestinal, além de promover respostas anti-inflamatórias *in vitro*. Este trabalho representa a primeira caracterização detalhada da MAM, elucidando suas propriedades moleculares e implicações funcionais para a organização do envelope celular de *F. duncaniae*. Além disso, contribui para a compreensão do papel do *Faecalibacterium* na promoção da saúde intestinal e seu potencial bioterapêutico. Esses achados também enriquecem discussões mais amplas sobre a organização única do envelope celular do gênero e a base molecular das interações hospedeiro-bactéria.

Palavras-chave: microbiota intestinal; envelope celular; doença inflamatória intestinal; probiótico de próxima geração; moléculas efetoras.

ABSTRACT

The Microbial Anti-inflammatory Molecule (MAM) is a unique protein produced by the genus *Faecalibacterium*, a key group of commensal bacteria in the human gut. Among these, *Faecalibacterium duncaniae* (formerly *F. prausnitzii*) is highly abundant and closely associated with gut homeostasis and overall health. MAM has demonstrated significant anti-inflammatory properties; however, its molecular and functional characteristics, as well as its mechanisms of action, remain poorly understood. This work aims to investigate the physiological role of MAM in *Faecalibacterium* and its interaction with the host. Using proteomics, structural bioinformatics, and microscopy techniques, we characterized MAM's molecular properties and its diversity within the genus. Additionally, we evaluated MAM's immunomodulatory activity through *in vitro* and *in vivo* assays. Our findings reveal that MAM is processed and transported via the PCAT ABC transporter to the cell envelope of *F. duncaniae*, where it forms a supramolecular hexameric lattice, likely contributing to cell envelope organization. This hexameric structure was conserved across multiple *Faecalibacterium* species, as demonstrated by *in silico* analyses. Although the exact positioning of the lattice within the cell envelope remains undetermined, *F. duncaniae* exhibits a distinctive envelope architecture with a thin peptidoglycan layer and an outer layer that diverges from classical monoderm/diderm bacteria. Functional assays revealed that purified recombinant MAM effectively improved macroscopic signs in a murine model of intestinal inflammation, alongside promoting anti-inflammatory responses *in vitro*. This work provides a pioneering characterization of MAM, elucidating its molecular attributes and functional implications for the cell envelope organization of *F. duncaniae*. Additionally, it advances the understanding of *Faecalibacterium*'s role in promoting gut health and its biotherapeutic potential. These findings also contribute to broader discussions on the unique envelope organization of the genus and the molecular basis of host-microbe interactions.

Keywords: gut microbiota; cell envelope; inflammatory bowel disease; next-generation probiotic; effector molecules.

LIST OF FIGURES

LIST OF ABBREVIATIONS

(5-ASA)	5-Aminosalicylic Acid
Å	Angstroms
ABC	Atp-Binding Cassette
ABIES	Agriculture, Alimentation, Biologie, Environnement, Santé
AFM	Atomic Force Microscopy
AMP	Antimicrobial Peptides
ANI	Average Nucleotide Identity
Bam	B-Barrel Assembly Machinery
Ca	Calcium
CD	Crohn's Disease
cDNA	Complementary DNA
CFU	Colonies Forming Units
CNS	Central Nervous System
COPD	Chronic Obstructive Pulmonary Disease
CRC	Colorectal Cancer
Cryo-EM	Cryo-Electron Microscopy
CTL	Cytotoxic T Lymphocytes
DC	Dendritic Cell
DNA	Deoxyribonucleic Acid
DNBS	Dinitrobenzene Sulfate
DSS	Dextran Sodium Sulfate
ECM	Extracellular Matrix
EDTA	Ethylenediaminetetraacetic Acid (Ácido Etilenodiamino Tetra-Acético)
EFSA	European Food Safety Authority
EM	Electron Microscopy
emPAI	Exponentially Modified Protein Abundance Index.
ENS	Enteric Nervous System
EOS	Extremely Oxygen-Sensitive
ES	Early Stationary Phase
EV	Extracellular Vesicles
EX	Exponential Phase
FDA	United States Food And Drug Administration
FMT	Fecal Microbiota Transplantation
FOS	Fructooligosaccharides
GABA	Gamma-Aminobutyric Acid
GAPDH	Glyceraldehyde-3-Phosphate Dehydrogenase
GIT	Gastrointestinal Tract
Glu	Glutamate
GPR43	G-Protein-Coupled Receptor 43
GRAS	Generally Regarded As Safe
GuHCL	Guanidine Hydrochloride

HDAC	Histone Deacetylases
HEK	Human Embryonic Kidney
HO-1	Heme Oxygenase-1
HPA	Hypothalamic-Pituitary-Adrenal
HT29	Human Colorectal Adenocarcinoma Cell Line-29
IBD	Inflammatory Bowel Diseases
IBS	Irritable Bowel Syndrome
IFN-γ	Interferon Gama
IL	Interleukyne
IM	Inner Membrane
INRAE	Institut National De La Recherche Agronomique
ISAPP	International Scientific Association For Probiotics And Prebiotics
JAK-STAT	Janus Kinase/Signal Transducers And Activators Of Transcription
LAB	Lactic Acid Bacteria
LamB	Lambda Phage Receptor
LBP	Live Biotherapeutic Products
LC-MS/MS	Liquid Chromatography-Tandem Mass Spectrometry
LiCl	Lithium Chloride
LP	Leader Peptide
LPS	Lipopolysaccharides
LptA	Lipopolysaccharide Transport Protein A
LS	Late Stationary Phase
MAM	Microbial Anti-Inflammatory Molecule
MD2	Myeloid Differentiation Factor 2
MDCF	Microbiota-Directed Complementary Food
Mg	Magnesium
MlaF	Maintenance Of Lipid Asymmetry Protein F
MlaFEDB	Maintenance Of Lipid Asymmetry Complex (F, E, D, B Components
MLN	Mesenteric Lymph Nodes
MRI	Magnetic Resonance Imaging
MscL	Mechanosensitive Ion Channel
MW	Molecular Weight
NaCl	Sodium Chloride (Cloreto De Sódio)
NF-kb	Nuclear Factor-Kappa B
NGP	Next Generation Probiotics
NOD	Nucleotide Oligomerization Domain
NP-40	Nonidet P-40
Nrf2	Nuclear Factor Erythroid 2-Related Factor
NSAF	Normalized Spectral Abundance Factor
NSAID	Non-Steroidal Anti-Inflammatory Drug
OD	Optical Density
OM	Outer Membrane
OMP	Outer Membrane Protein
PBMC	Peripheral Blood Mononuclear Cells

PCAT	Peptidase-Containing ABC Transporter
PCR	Polymerase Chain Reaction
PFP	Pore-Forming Proteins
PG	Peptidoglycan
PLDDT	Predicted Local Distance Difference Test
PSA	Capsular Polysaccharide A
RNA	Ribonucleic Acid
RNS	Reactive Nitrogen Species
ROS	Reactive Oxygen Species
SAXS	X-Ray Scattering Nanometer Scale
SCFA	Short-Chain Fatty Acid
SDS-PAGE	Sodium Dodecyl Sulfate - Polyacrylamide Gel Electrophoresis.
SHM	Sequence Homology Modeling
SLH	S-Layer Homology
SLP	S-Layer Proteins
SMFS	Single-Molecular Force Spectroscopy
SN	Supernatant
T2D	Type 2 Diabetes
Th1	T Helper Cell Type 1
TLR	Toll-Like Receptors
TMD	Transmembrane Domains
TNBS	Trinitrobenzene Sulfonic Acid
TNF	Tumor Necrosis Fator
Treg	T Regulatory Cells
Tris–HCl	Tris(Hydroxymethyl)Aminomethane Hydrochloride
Trp	Tryptophan
UC	Ulcerative Colitis
UFMG	Universidade Federal De Minas Gerais
USA	United States Of America
ZO-1	Zona Occludens

THESIS CONTENT AND STRUCTURE

1. INTRODUCTION

Provides the theme introduction, research problem, questions, and objectives of the study (Figure 1).

2. OBJECTIVES

This thesis aims to characterize MAM's molecular attributes to elucidate its functions in relation to the cell biology of *Faecalibacterium* in addition to its effects and mechanisms of action towards the host.

3. LITERATURE REVIEW

This includes background related to the gut microbiota, Intestinal Bowel Disease (IBD) *Faecalibacterium*. It includes a submitted review paper about bacterial cell envelope components, particularly those of gut commensals, and their roles in host-microbe interactions.

4. CHAPTER I: MAM IS A KEY PROTEIN PROCESSED AND EXPORTED TO THE *Faecalibacterium duncaniae* ENVELOPE, WHICH IS ITS MAIN PROTEIN TO ORGANIZE ITS UNIQUE STRUCTURE

The chapter demonstrates that MAM is a key protein processed and exported to the *F. duncaniae* envelope, where it serves as a main structural component organizing the unique cell envelope architecture. It includes a submitted research paper regarding MAM characterization.

5. CHAPTER II: IMMUNOMODULATORY CHARACTERIZATION OF MAM FROM *F. duncaniae*

It focuses on the immunomodulatory characterization of MAM in *F. duncaniae*, including a paper with both *in vitro* and *in vivo* studies with unfolded recombined MAM.

6. CHAPTER III: MOLECULAR DIVERSITY OF MAM WITHIN THE GENUS *Faecalibacterium*

Explores the molecular diversity of MAM across the *Faecalibacterium* genus, highlighting conserved and variable features among different species.

7. GENERAL DISCUSSION

This section synthesizes findings from all chapters to propose new perspectives on the role of MAM in *Faecalibacterium* biology and its implications for gut health

8. CONCLUSION

THESIS GRAPHICAL ABSTRACT

Figure 1. Thesis graphical abstract: The figure indicates the organization of the thesis in the literature review and the three chapters, with the scientific production for each section. Source: Author's elaboration
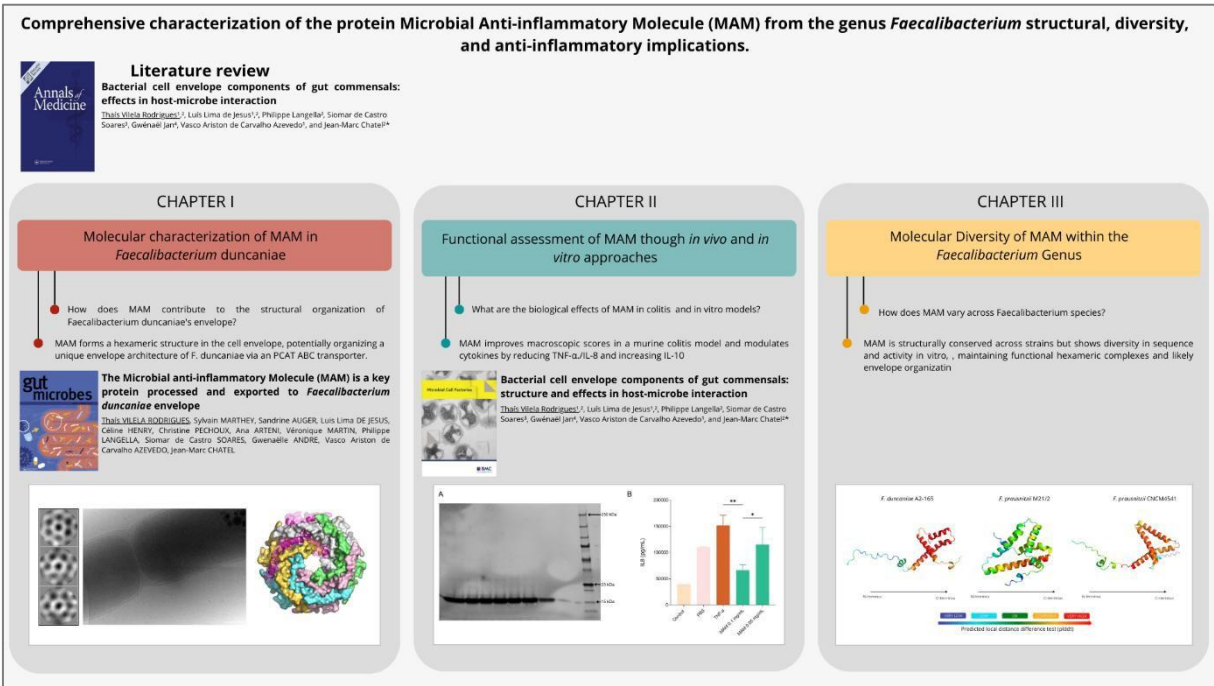
1. INTRODUCTION

The human gut microbiota is a complex and dynamic ecosystem essential for maintaining health and homeostasis. Within this environment, the genus *Faecalibacterium* represents one of the most abundant and studied groups due to its health-promoting properties, which include its ability to produce butyrate and other bioactive molecules. Among its molecular effectors, the Microbial Anti-inflammatory Molecule (MAM) is known for its anti-inflammatory properties and protective properties observed in inflammatory bowel diseases (IBD) mice model. However, despite its recognized significance, the molecular characteristics and functional roles of MAM remain poorly understood, as do the mechanisms underlying its interactions with the host. Moreover, the diversity of MAM across species within the *Faecalibacterium* genus has not yet been fully explored.

The lack of comprehensive information about MAM hinders our understanding of its physiological role within *Faecalibacterium* and its contribution to host-microbe interactions. Addressing these knowledge gaps is crucial for elucidating the biological functions of MAM and its potential as a biotherapeutic target. Thus, this thesis aims to investigate the structural, functional, and molecular diversity of MAM, with a particular focus on its physiological role in the most studied species, *F. duncaniae*, and its implications for intestinal health.

2. OBJECTIVES

This thesis aims to characterize MAM's molecular attributes to elucidate its functions in relation to the cell biology of *Faecalibacterium* in addition to its effects towards the host.

2.1 Specific objectives

- **Characterize the molecular aspects of MAM in the cellular organization and biology of *Faecalibacterium duncaniae***

  1. Investigate the localization, structural features, and protein interactions.
  2. Assess its potential biological functions, including its contribution to cellular organization and structural integrity.

- **Evaluate the properties of MAM on host physiology and immune responses**

  1. Purify recombinant MAM and assess its effects in a DiNitroBenzene Sulfate (DNBS)-induced colitis murine model.
  2. Perform *in vitro* assays using HT29 cells and PBMCs to investigate its anti-inflammatory potential.
  3. Perform *in vivo* assays to assess MAM's properties in intestinal inflammatory the mice model.

- **Explore the molecular diversity of MAM within the *Faecalibacterium* genus:**

  1. Investigate the structure, localization, and interactions of MAM across three different *Faecalibacterium* species.
  2. Highlight interspecies variations and their possible implications for host-microbe interactions.

3. LITERATURE REVIEW

3.1. The microbiota and the genus *Faecalibacterium*

The discovery of microorganisms in the 1600s by Robert Hooke and Antoni van Leeuwenhock revolutionized our understanding of biology[1], leading to advancements such as vaccines and antibiotics that have drastically improved human health. Over time, it became evident that most microorganisms engage in mutualistic relationships with their hosts, playing essential roles in maintaining health and homeostasis[2,3]. From these early discoveries, microbiological research has evolved significantly, leading to an advanced understanding of microbial ecosystems, such as the microbiota, and their intricate interactions with human hosts.

The microbiome refers to the community of microorganisms inhabiting a specific environment with distinct physio-chemical properties. The microbiota represents the set of microorganisms, Prokaryotes (Bacteria, Archaea), Eukaryotes (e.g., Protozoa, Fungi, and Algae), and viruses, as well as their cellular components, their metabolites, genetic elements, and DNA. Harboring genetic material around 150 times the abundance of the human genome (Figure 2), the microbiota is present in the respiratory tract, the oral cavity, the skin, the vagina, and the gut[4,5]. Each of those complex ecosystems has its own dynamic and interactions between its components and towards the host, having key roles in biological processes and health[6]. The understanding of microbiota highlights the significance of studying specific microbial communities, and their profound impact on host health, including the changes associated with various disorders.
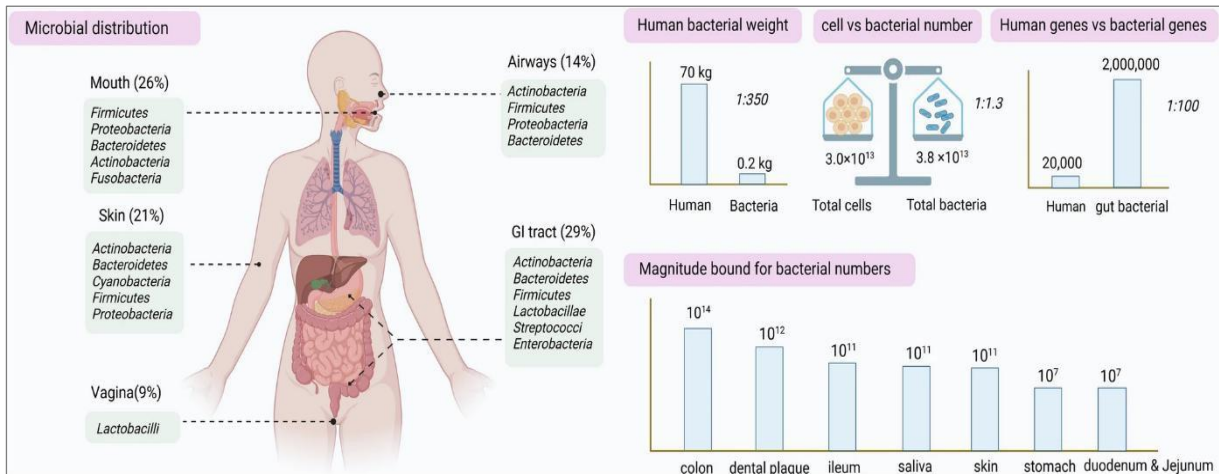
Figure 2. Characteristics of the human microbiome: The figure illustrates the distribution and characteristics of the human microbiome across different body sites, including the mouth, airways, skin, gastrointestinal tract, and vagina. The microbial composition in each niche is represented by dominant phyla and genera. The figure highlights the weight of the human microbiome, the bacterial-to-human cell ratio, and the extensive genetic contribution of the microbiota. Additionally, the magnitude of bacterial numbers is shown across various locations. Source: Adapted from Ziqi Ma et al, 2024.

3.2.   The human gut microbiota

The gut microbiota is the most enriched microbial ecosystem in the human body, hosting trillions of microbe cells, of which 90% are bacterial cells[7]. Through millions of years of co-evolution, gut commensals, and the hosts have developed mutually beneficial relationships. These interactions have shaped adaptive strategies that optimize nutrient exchange and environmental stability, promoting the growth and maintenance of microbial communities precisely suited to the host's gastrointestinal environment[8–10].

The gastrointestinal tract has the most significant surface area of the human body, allowing cross-talk between microorganisms and the host, having broad impacts on local and systemic homeostasis[11,12]. The physiological role of the gut microbiota includes nutrient absorption, pathogen protection, digestion of dietary fibers, intestinal barrier maintenance, and immunomodulation. Among the various mechanisms through which gut commensals promote host health, effector molecules involve a diverse set of peptides, proteins, and metabolites that have been associated with positive effects on the host[13]. Moreover, the gut microbiota plays a role in brain health through the gut-brain axis, influencing behavior, mood, and neurological conditions[14]. Nevertheless, the microbiota community is a dynamic system that can be altered by different factors, which can lead to positive, neutral, or negative effects on the host[4,6,15].

The isolation and cultivation of gut microbiota-associated organisms are challenging, especially as many of them are obligate anaerobes[16]. Thus, advances in metagenomics have profoundly enhanced our understanding of the gut microbiota's community profile and its

dynamic nature and capacity for regeneration after disturbances[17]. The ability of the gut ecosystem to return to a balanced baseline state, known as resilience, plays a crucial role in maintaining gut homeostasis and overall health. Although the precise composition of a healthy gut microbiota remains under debate, it is well established that microbial communities can lead to several health conditions, including IBD, colorectal cancer, type 2 diabetes, and other systemic disorders[18]. A resilient microbiota is, therefore, essential for preventing or mitigating the impact of these imbalances, emphasizing the need for strategies that promote microbial recovery and stability[5,19].

Understanding the components of this complex microbial community under normal conditions, as well as the consequences of its imbalance, is essential for developing innovative therapeutic strategies and determining the mechanisms for promoting gut homeostasis. Modulating the gut microbiota has become a focal point in developing therapeutic strategies to restore microbial balance and enhance host health.

3.3.   Composition of human gut microbiota

The composition of microorganisms inhabiting the human gut varies across gastrointestinal regions, in addition to individual host differences[20]. Overall, abundance and diversity increase from the proximal intestine towards the distal intestine due to variable conditions. For example, oxygen gradients decrease towards the caudal intestine area, pH shifts are higher on the gut extremities, and mucus thickness also varies between anatomic regions. The higher abundance diversity is observed in the ascending colon, with about 10^{10}-10^{12} CFU/ml (Colonies Forming Units per milliliter). In the duodenum, abundance rates range from 10^1 to 10^3 CFU/ml, in the jejunum from 10^4 to 10^7 CFU/ml, and in the ileum from 10^3 to 10^8 CFU/ml[21].

The composition of the gut microbiota varies significantly among individuals, even within the same population, with some exhibiting a dominance of specific phyla such as Bacteroidota or Fusobacteria, while others display a more balanced distribution of Bacillota and Bacteroidota[12,22,23]. Whole-metagenome studies involving large cohorts reveal that the microbial composition similarity between two individuals is approximately 45%. Although these individuals share fewer microbial species, they exhibit a greater overlap in metabolic pathways. This overlap is more closely linked to systemic and fecal metabolites than to species composition alone. These are indications of redundant mechanisms to guarantee functional and metabolic processes even with variable microbiota composition[24–26].

Despite the diversity between individuals, metaproteomic studies have identified a "core" microbiota, which is broadly identified in the overall population. The microbiota core is primarily composed of Bacillota (Firmicutes), which represent about 60% of the bacterial community, and Bacteroidota (Bacteroidetes), comprising approximately 35%. Other phyla, such as Actinomycetota (Actinobacteria) and Pseudomonadota (Proteobacteria), account for smaller proportions, with Fusobacteria and Verrucomicrobia also present in healthy microbiota (Figure 3)[27–29]. In a global analysis of healthy microbiota, 20 bacterial genera were consistently identified as part of the universal core. Among these, *Faecalibacterium* was identified as one of the most abundant genera, with the lowest coefficient of variation, indicating its strong consistency across populations. Indeed, studies indicate the genus *Faecalibacterium* varies in a range from 5-15% of the complete bacterial gut composition, representing a massive colonization dominance[30–32]. In contrast, *Prevotella*, despite its high relative abundance, exhibited significant variability between individuals[27,33].
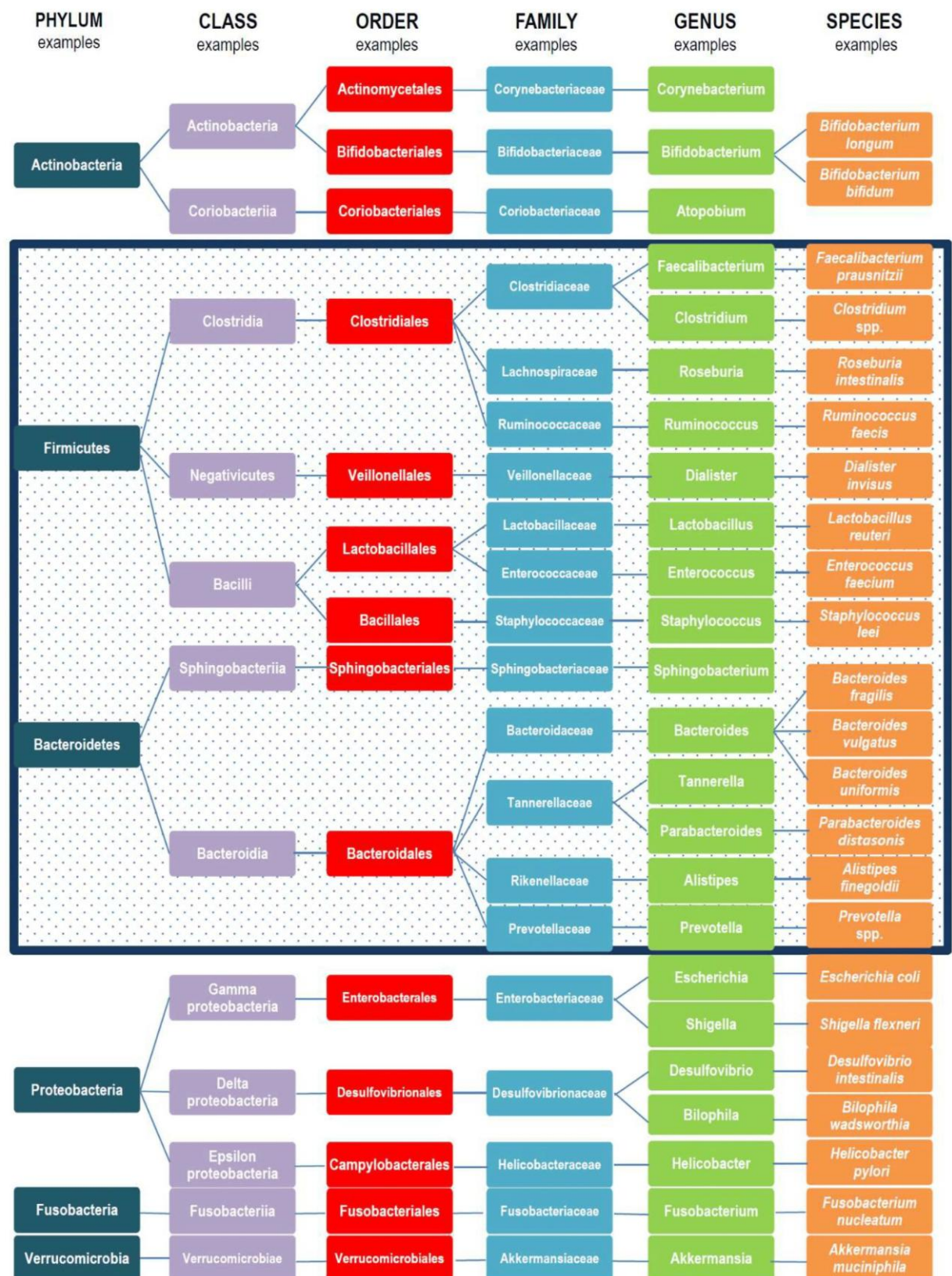
Figure 3. Examples of the taxonomic composition of the core gut microbiota: The figure indicates the taxonomic diversity of the gut microbiota. The box highlights bacterial species from the phyla Firmicutes and Bacteroidetes, which together account for approximately 90% of the gut microbial community. Source: Rinninella et al, 2019.

The colonization of the gastrointestinal (GI) tract, particularly during the early stages of life, remains a topic of debate[34]. Nevertheless, factors such as the modern diet during gestation, antibiotic use, and delivery mode are among the most critical determinants impacting the transmission and colonization of the infant microbiome[35].

At birth, *Bifidobacterium* spp. are considered pioneer species in gut colonization. Over the first year of life, *Clostridium* and *Bacteroides* spp. gradually join the microbial community, shaping its development. Post-birth, factors such as diet, geography, and lifestyle play a significant role in influencing the initial colonization. Generally, this period sees an increase in the abundance and diversity of *Bacteroides* spp. and Bacillota, including *Faecalibacterium*. By the ages of 3–6 years, the gut microbiota reaches its peak diversity and density, with *Firmicutes* and *Bacteroidetes* emerging as the dominant phyla. During adulthood, the microbiota stabilizes into a relatively resilient community characterized by functional and compositional balance. However, this stability remains susceptible to external influences such as diet, medication, and environmental changes. Aging introduces notable shifts in the gut microbiota, with a broad reduction in diversity and abundance, particularly of *Bifidobacterium*, *Bacteroides*, and *Lactobacillus*. Concurrently, members of the Enterobacteriaceae family have an increased susceptibility to colonization, which can potentially compromise gut health[19,35].

The gut microbiota is a dynamic and complex ecosystem that, despite its resilience, is constantly influenced by genetic and environmental conditions. Understanding its composition at different stages of life and under varying circumstances is essential for uncovering the mechanisms that maintain balance and homeostasis.

3.4.   Role of microbiota in health and disease

The concept of healthy gut microbiota remains highly debated due to individual variability, environmental influences, and the dynamic nature of health. Rather than a single ideal microbiome, research suggests multiple configurations can support host homeostasis[36].

Being crucial for the host's health, the gut microbiota processes complex carbohydrates, synthetizes vitamins, and controls the immunologic responses. Also, gut microbiota members compete with pathogens for nutrients and maintenance, hampering the colonization by harmful species[26]. The gut microbiota resides on the whole intestinal surface, representing an enormous interface for constant connection with the host. It interacts dynamically with the host's immune, endocrine, and nervous systems, indicating its role as a central regulator of local and systemic homeostasis[5].

3.4.1. Metabolites production

One key role of the gut microbiota is the production of metabolites, which are essential for maintaining homeostasis. Short-chain fatty acids (SCFAs), including butyrate, propionate, and acetate, are key metabolites produced through microbial fermentation. These compounds are crucial for health, influencing immune responses, lipid metabolism, and glucose regulation. Butyrate, particularly, acts as an energy source for colonocytes and suppresses pro-inflammatory signaling pathways like NF-Kb[37–39]. In addition to SCFAs, other microbiota-derived metabolites, such as tryptophan (Trp) and bile acids (BA), play critical roles in immunological pathways. BA metabolites influence immune responses via T-cell regulation, while Trp derivatives promote macrophage differentiation and further suppress NF-κB signaling, contributing to immune homeostasis[37]. These metabolites also support the intestinal barrier, which acts as a physical and immunological interface between the gut lumen and the host[5,40].

Another marker of a healthy gut microbiota is the production of gases such as hydrogen, methane, and carbon dioxide. Derived from the fermentation of carbohydrates and amino acid metabolization, an imbalance in the production of those gases indicates gut microbiota alterations, which are associated with irritable bowel syndrome (IBS)[41,42]. Moreover, vitamins, such as vitamin K and B-complex components, are also produced by the microbiota, enhancing protein digestion through bacterial enzymes and supporting nutrient absorption and metabolic balance[43,44].

3.4.2. Gut barrier and immune system

The gut barrier is a structure composed of the luminal mucus layer, the epithelial layer, and the mucosal internal immune layer. The selective permeability of this barrier is crucial for enabling the absorption of essential dietary nutrients, electrolytes, amino acids, SCFA, sugars, water, and specific microbial metabolites from the intestinal lumen into the bloodstream. The gut barrier is also a physical limit that defends against the passage of bacteria, toxins, and pathogens from the lumen[26].

At the epithelial surface, goblet cells and Paneth cells are responsible for mucosal protection and lubrification through mucin secretion and antimicrobial peptides (AMPs) production, respectively, serving as the initial line of defense against microbial invasion. The mucus layer is constituted with a protective gel-like structure that acts as a primary defense mechanism against bacterial colonization, thereby preventing microbial adherence and

subsequent penetration of the epithelium. The composition and characteristics of this mucus layer vary depending on the specific region of the gastrointestinal tract[45].

The epithelial layer consists mainly of enterocytes, Paneth cells, and goblet cells. They are arranged in a monolayer that separates the lumen from the lamina propria[46]. Enterocytes are the major cell type in the epithelium and are important for the uptake of diverse compounds. Paneth cells, present especially in the small intestine, secrete host defense mediators to protect against pathogens[47,48]. The intestinal barrier is supported by multiple components that enhance its structural integrity (Figure 4). The core structural elements of tight junctions (TJs) include claudins, a class of integral membrane proteins that interact with the actin cytoskeleton through scaffold proteins of the zonula occludens (ZO) family, specifically ZO-1 and ZO-2. These junctions restrict molecules' uncontrolled translocation from the cell surface to the underlying membrane, being fundamental in regulating paracellular permeability[48,49]. Moreover, a healthy gut microbiota supports the development of goblet cells and the formation of the mucus barrier, consequently supporting homeostasis[50].
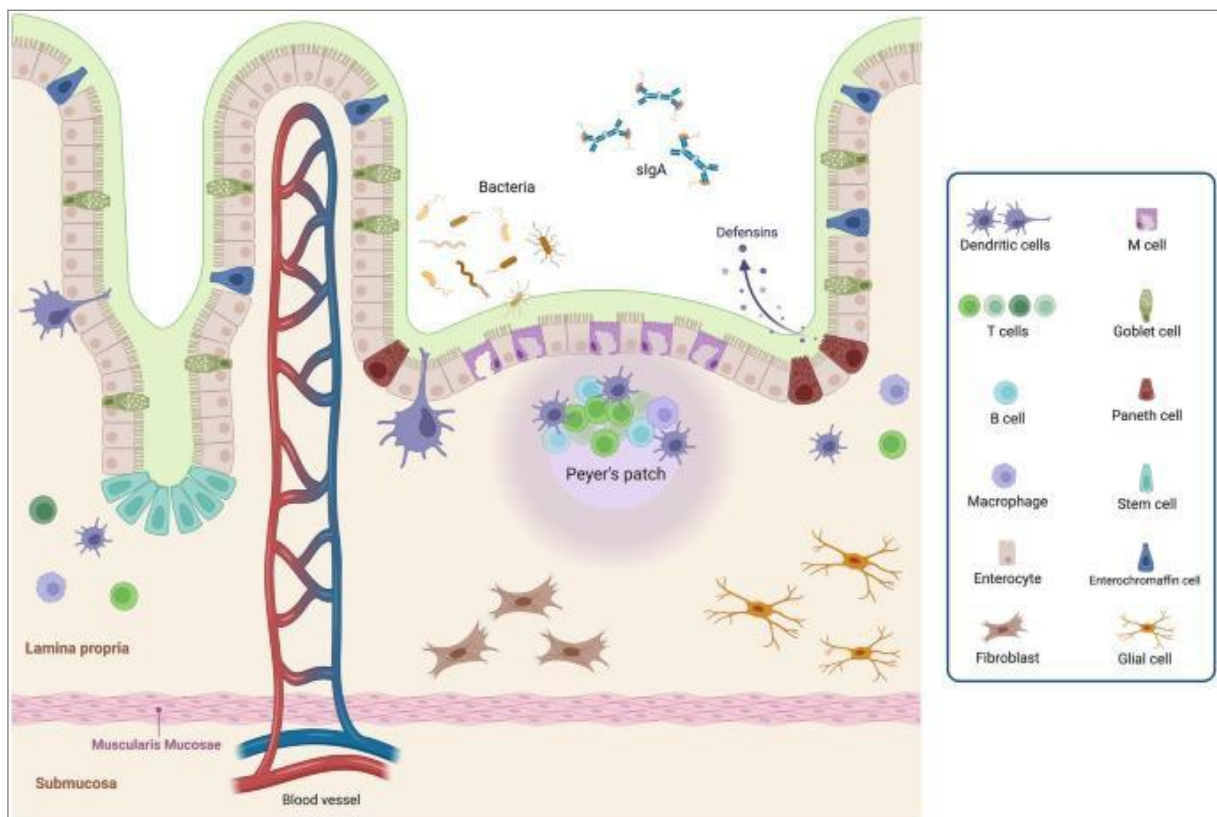
Figure 4. Key components of the intestinal barrier. The figure shows the epithelial layer components: enterocytes, goblet cells, Paneth cells, enterochromaffin cells (neuroendocrine function), intestinal stem cells (crypt regeneration), dendritic cells, and M cells (antigen presentation in Peyer's patches). The mucus barrier is highlighted in green is rich in mucins, secretory IgA, and defensins. Beneath the epithelium, the lamina propria contains immune cells, fibroblasts, glial cells, blood vessels, Peyer's patches, elements of the enteric nervous system, and connective tissue. Source: Sabatino et al, 2023.

Beneath the epithelial lining, the lamina propria constitutes a sub-epithelial region rich in immune cells, enteric nervous system (ENS) components, and connective tissue. This compartment harbors key immune effectors, including intraepithelial CD8+ lymphocytes, lamina propria lymphocytes (both B and T cells), eosinophils, dendritic cells (DCs), mast cells, and macrophages. These immune cells collectively contribute to intestinal immune surveillance and homeostasis. Furthermore, the gut-associated lymphoid tissue (GALT) is a specialized structure within the lamina propria that organizes immune responses. It comprises lymphoid follicles, Peyer's patches (aggregations of lymphoid follicles), and mesenteric lymph nodes, serving as essential hubs for antigen presentation and immune activation[51,52].

The intricate interaction between the immune system and the gut microbiota is a complex system in which the microbiota supports the development and regulation of both innate and adaptive immune systems. The gut microbiota supports the maturation of the immune system during early life[53]. On the other hand, the immune system helps sustain and shape the growth of microbial communities. Although the exact mechanisms of these interconnections are not fully elucidated, it highlights an essential capacity of the host to direct resistance or susceptibility to pathogens and establish immune tolerance to commensal bacteria[54,55].

3.4.3. Gut-brain axis

The microbiota-gut-brain axis describes the bidirectional communication between the GI tract (GIT) and the brain[14,56]. It involves the immune, enteric nervous, circulatory, and endocrine systems, as well as the vagus nerve[50]. Alterations in gut microbiota have been associated with neurodegenerative conditions[57–59], altered social behavior as autism[57–59], anxiety and depression[60–62], and physical performance and motivation[63,64]. This indicates the important functional roles that the gut microbiota play in modulating central nervous system activity, neuroimmune interactions, and overall behavioral outcomes.

The gut-brain interaction occurs through multiple pathways: the immune pathway (involving cytokines and SCFAs); the neuroactive pathway (with neurotransmitters such as γ-aminobutyric acid [GABA]); the neural pathway (via the enteric nervous system and vagus nerve); and the endocrine pathway (mediated by the hypothalamic-pituitary-adrenal [HPA] axis)[65]. The HPA axis, for instance, triggers cortisol production, thereby regulating neuroimmune signaling and stress responses. Metabolic compounds, such as bile acids, SCFAs, glutamate (Glu), GABA, dopamine, norepinephrine, serotonin, and histamine, produced by the

gut microbiota, have a role in mediating communication with the nervous system[66,67]. The brain responds with signals to the gut barrier mucosa, including enterochromaffin and enteroendocrine cells, thus regulating inflammatory immune responses and barrier integrity[68,69]. Moreover, the connections of microbiota with the enteric nervous system regulate intestinal motility and secretion, as well as signal the development of epithelial cells, including goblet and Paneth cells[54,70].

3.5. Dysbiosis and Inflammatory Bowel Disease (IBD)

3.5.1. Dysbiosis

A loss of homeostatic equilibrium in the resident microbial community is characteristic of dysbiosis. Fecal microbiota analysis of patients with cardiovascular conditions[71], diabetes[72], colorectal cancer (CRC)[73,74], chronic kidney disease[75,76], and IBD supports the profiling of dysbiotic environments, which is crucial to determining key players in gut microbiota health and disease[77,78].

Dysbiosis is generally categorized into three types: (1) a loss of beneficial bacteria, such as *Akkermansia muciniphila*, *Ruminococcus bromii*, *Roseburia*, and *F. duncaniae*; (2) an overgrowth of pathobionts, particularly members of the Enterobacteriaceae family, and the phylum Proteobacteria; and (3) a reduction in microbial diversity, notably affecting the two major phyla, Bacillota and Bacteroidota[79–81].

Dysbiosis can originate from various factors that disrupt the balance of the gut microbiota[82]. Enteric infections, such as those caused by *Citrobacter rodentium* or *Salmonella enterica*, trigger inflammation that compromises the microbiota's ability to provide colonization resistance, enabling the overgrowth of pathogenic bacteria[83]. Diet is another significant factor, with low-fiber or high-fat diets reducing microbial diversity over time, while dietary xenobiotics, such as antibiotics and emulsifiers, further alter microbial colonization. Host genetics also influence dysbiosis, as specific genetic loci, such as those encoding the vitamin D receptor or lactase, have been linked to shifts in microbial taxa[84–86]. The familial and environmental transmission also acts in shaping individual microbiomes, with maternal microbiota, delivery mode, and shared household environments contributing to microbiota composition. Additional factors, such as circadian disruptions, and physical injury, also contribute to dysbiosis, reflecting its multifaceted origins and the complex interplay between environmental and genetic influences[87].

Dysbiosis impacts both the intestinal barrier and the systemic immune system (Figure 5). Pathobiont-derived signals can alter immune responses, epigenetic patterns, and gene

expression, thereby promoting chronic inflammation[53,87]. For instance, a reduced microbiota population capable of production of SCFA and tryptophan derivatives can impair regulatory T-cell (Treg) function and compromise epithelial barrier integrity[88,89]. As the intestinal barrier becomes disrupted, increased permeability allows microbial components such as LPS to enter the bloodstream, triggering systemic inflammation[90]. Moreover, these metabolites and microbial components activate Toll-like receptors (TLRs) and Nod-like receptors (NLRs), driving the overproduction of pro-inflammatory cytokines, including IL6, TNF-α, and IL1-β[91]. This chronic inflammatory state skews the Th17/Treg balance and disrupts the gut-associated lymphoid tissue, thereby inciting a self-perpetuating cycle of inflammation[92].
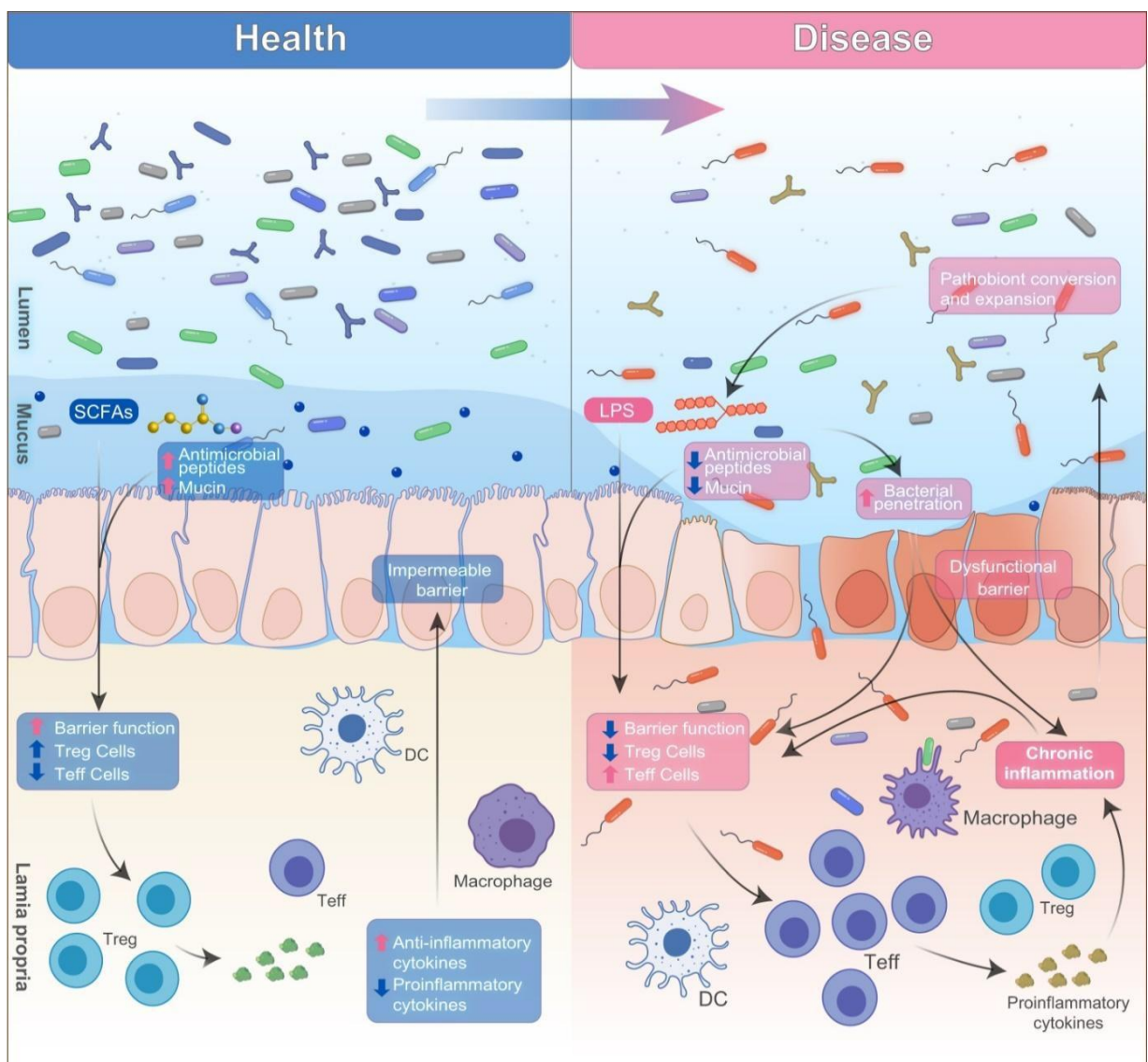
Figure 5. Determinants of microbiota-induced chronic inflammation in health and disease: The figure illustrates the contrasting states of the intestinal barrier in health and disease. On the left, in health, the microbiota is characterized by the presence of beneficial metabolites like SCFAs, AMPs, and mucin, with the presence of immune cells. On the right, in disease, dysbiosis leads to reduced antimicrobial peptides, mucin degradation, bacterial penetration, and pathobiont expansion. Increased pro-inflammatory cytokines, and Teff (effector T cell) activation, macrophage recruitment, and chronic inflammation is also indicated. Source: Kaijian Hou et al, 2022.

3.5.2. Inflammatory Bowel Disease (IBD)

IBD is a significant global health burden, with prevalence and incidence exhibiting considerable variation across different regions and demographic groups. IBD is traditionally considered a problem prevalent in industrial-urbanized societies due to its strong association with Westernized lifestyles. However, its incidence and prevalence in developing countries are steadily rising, attributed to these populations' rapid modernization[93].

As reported in 2019, approximately 4.9 million individuals worldwide were living with IBD, with China and the USA having the highest number of cases, 911,405 and 762,890, respectively (Figure 6). Moreover, from 1990 to 2021, the incidence rates increased from 4.22 per 100000 to 4.45 per 10000, with mortality rates in 2021 reaching the highest yet reported, with 12,791 fatalities in Western Europe[94]. Demographically, IBD affects both males and females, with a slightly higher prevalence observed in females. The disease also commonly manifests between the ages of 15 and 30, with a secondary peak occurring in individuals over 60 years old[95–97].
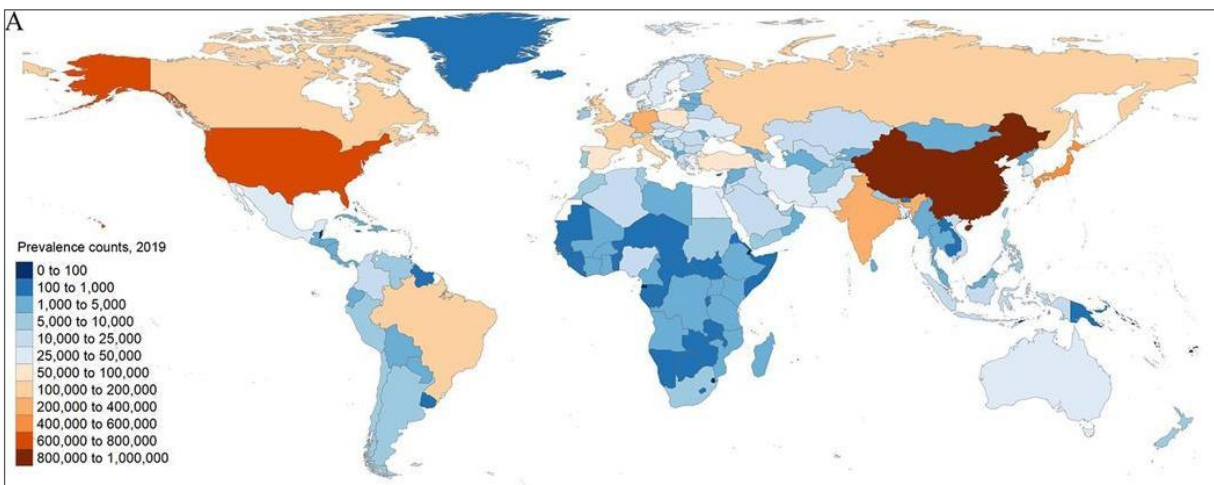
Figure 6. Global, burden of inflammatory bowel disease in 204 countries and territories from 1990 to 2019. The figure represents a world map in which countries are color-coded to indicate IBD prevalence counts, ranging from low prevalence (light blue) to high prevalence (dark red). Source: Wang R et al, 2019.

IBD is a multifactorial disorder that arises in genetically predisposed individuals when exposed to environmental risk factors, leading to disruptions in intestinal homeostasis[98]. IBD encompasses two primary conditions: Crohn's disease (CD) and ulcerative colitis (UC), which differ in their pathological features and distribution. The CD is characterized by transmural inflammation, most frequently affecting the terminal ileum and colon, though it can involve any part of the gastrointestinal tract. In contrast, UC is limited to the colonic mucosa and submucosa, progressing proximally from the rectum in a continuous pattern[99,100].

3.5.3. Pathophysiology of IBD

Damage to the mucosal epithelial barrier and the subsequent development of inflammation are central to IBD pathophysiology[101]. Injuries caused by infectious agents, chemical irritants, or metabolic-derived ulcerations can lead to unresolved inflammation[102]. Increased permeability of the compromised epithelium disrupts the secretion of AMPs and mucus, exposing the host to luminal microbiota and facilitating the translocation of microbial antigens into the bloodstream. This further activates the immune system and damages the organization of tight junction proteins, perpetuating mucosal inflammation[103].

Macrophages and dendritic cells are central to intestinal homeostasis, clearing debris and regulating epithelial re-establishment via anti-inflammatory cytokines. In IBD, however, there is a marked shift: the recruitment of specific monocytes generates pro-inflammatory macrophages that secrete TNF-α, and IL6, driving tissue injury and fibrosis through excessive deposition of extracellular matrix (ECM) components like collagen[104]. At the same time, tolerogenic dendritic cell subsets, such as CD103$^+$ cDC2, are reduced, impairing immune tolerance and antigen presentation. Instead, DCs adopt a pro-inflammatory phenotype with enhanced TLR expression. These shifts impair antigen presentation and reinforce chronic inflammation. These shifts impair immune tolerance, disrupt antigen presentation, and contribute to tissue remodeling, strictures, and complications in disease management[103].

Central inflammatory pathways, including NF-κB and JAK-STAT, further sustain inflammation. NF-κB activation leads to the production of pro-inflammatory cytokines, while dysregulated JAK-STAT signaling amplifies immune cell activation and cytokine responses[73]. Accumulation of inflammatory T-cells in the intestinal barrier together with the release of pro-inflammatory cytokines are crucial in the progression of IBD[105]. Moreover, excessive activation of neutrophils and macrophages results in overproduction of matrix metalloproteinases, neutrophil elastase, and reactive oxygen species (ROS), which exacerbate epithelial damage by inducing lipid peroxidation, DNA damage, protein oxidation, and mitochondrial disruption. Weakened antioxidant defenses amplify oxidative stress, creating a vicious cycle that drives disease progression[106–108].

Additionally, the activity of the enteric nervous system (ENS) in mucosal immunity is implicated in IBD evolution. Chronic pain and visceral hypersensitivity reflect the altered bidirectional communication between the intestinal mucosa, the ENS, and the central nervous system (CNS), leading to disrupted gut motility[109,110].

Together, these interconnected mechanisms reveal the complexity of IBD pathophysiology and challenges in identifying trigger factors and unraveling the multifaceted disease mechanisms.

3.5.4. Risk factors of IBD

IBD pathogenesis involves three main factors: genetics, the internal environment, including the immune system and the gut microbiota, and external environmental triggers (Figure 7)[5].

Genetic background is associated with the pathogenesis of both CD and UC. Genome-wide association studies have identified several gene loci linked to IBD, many being shared between CD and UC[111,112]. In this context, mutations in the NOD2 gene have been broadly studied in the pathogenesis of CD[113]. NOD2 encodes a receptor that recognizes bacterial cell wall components and triggers autophagy in intestinal epithelial cells and monocytes, having its genetic variants commonly associated with IBD. Other specific loci, including FOXO3, IGFBP1, and XACT, are also associated with CF and may even serve as predictive markers for the condition[114]. Moreover, alterations in other autophagy-related genes, such as ATG16L1, LRRK2, and IRGM, as well as mutations in the IL10 receptor genes, have also been implicated in IBD pathogenesis[115,116]. Several of these genetic variations have been reported to impact immune system function, intestinal barrier integrity, oxidative stress response, microbial defense, and antimicrobial activity. Interestingly, recent studies have highlighted that genetic predisposition is mainly linked to CD development in young adulthood, although environmental risks still modulate its effects[117,118].

IBD patients have a decrease in gut microbiota diversity in general. Dysbiosis in IBD is marked by lower levels of bacteria from the phylum Firmicutes (especially *Faecalibacterium*), Bacteroidetes, and Verrucomicrobia. At the same time, there is an increase in Proteobacteria, Actinobacteria, and Fusobacteria[119,120]. This imbalance is associated with immune dysfunction, leading to local and systemic inflammation.[121]

Environmental factors such as lifestyle, smoking, diet, exposure to toxins and pollutants, and the use of medicaments are essential players in IBD[122,123]. One of the strongest associations with IBDs is a low intake of fruits and vegetables. The fiber from those aliments is metabolized by the microbiota components, producing SCFA, which has strong anti-inflammatory properties[124,125]. Contrastingly, high-fat diets rich in refined sugars and animal fats, in addition to the intake of processed meals rich in additives, disrupt microbiota, damage the intestinal barrier, and promote pro-inflammatory immune responses[126,127]. The use of medicaments such

as NSAIDs (Non-steroidal anti-inflammatory drugs), aspirin, oral contraceptives, and postmenopausal therapy has also been linked to IBD development.[128] Moreover, the increasing exposition to microplastic, endocrine-disruption-related toxins, herbicides, heavy metals, and persistent pollutants is related to an increase in intestinal inflammation followed by gut barrier damage and increased permeability, contributing to IBD development[129].

Stress, sleep quality, and physical activity are also significant lifestyle factors related to IBD. Stress can broadly induce inflammation through the connections between the hypothalamus–pituitary–adrenal (HPA) axis and the autonomic nervous system, producing proinflammatory cytokines, activating macrophages, and leading to alterations in intestinal permeability and gut microbiota composition[130]. In addition, major life stressors, anxiety, and depression are deeply associated with an increased risk of IBD. In patients with established disease, these factors are linked to higher relapse rates, hospitalizations, surgeries, and reduced treatment responsiveness[131]. Moreover, physical activity shows protective effects, with studies indicating up to a 44% reduction in CD risk among active individuals. Even without a complete understanding of how these protective effects unfold, it's evident that more sedentary behavior is associated with a higher risk of developing CD[132].
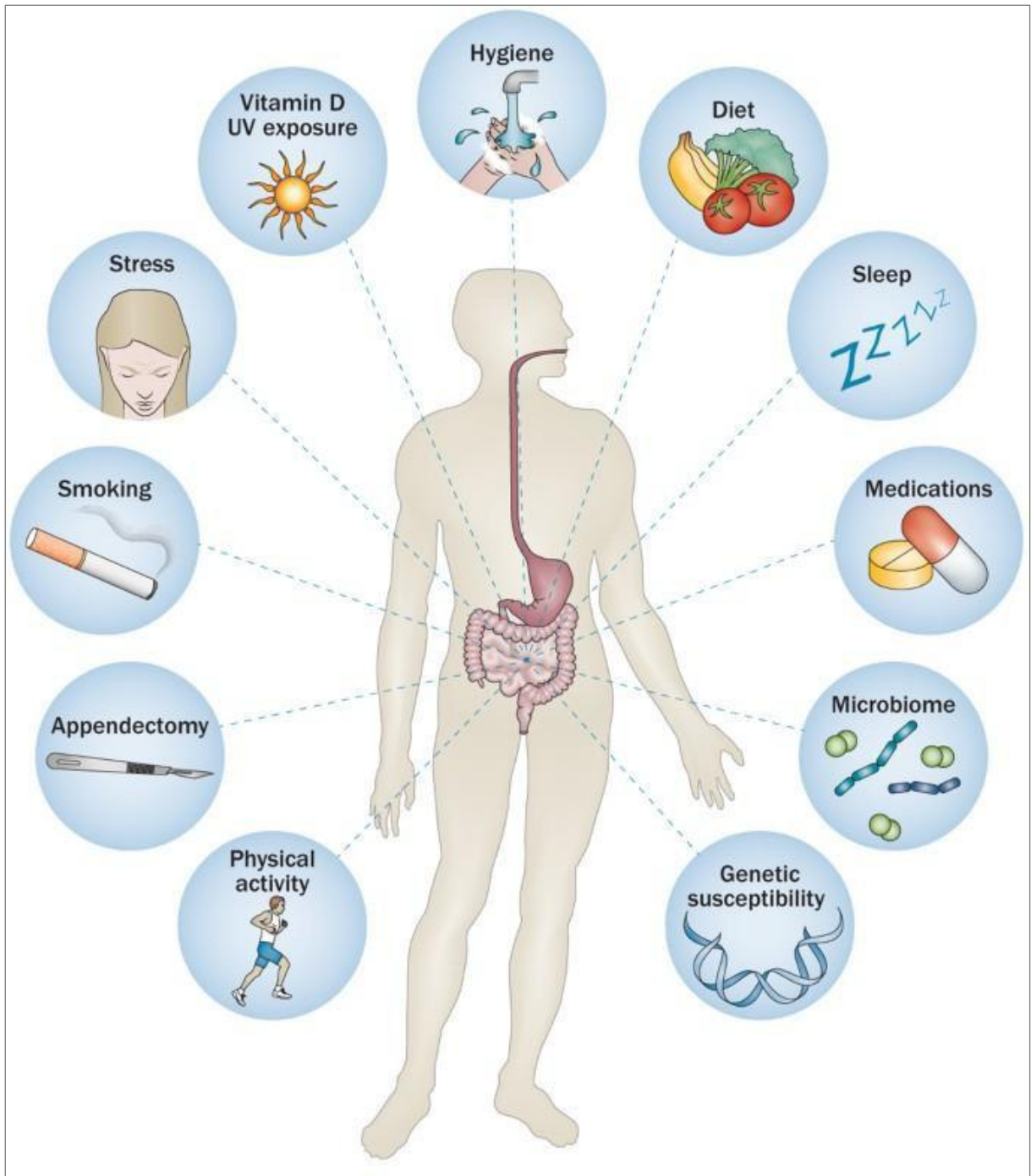
Figure 7. The influences related to dysbiosis and IBD development. The figure demonstrates several factors influencing gut health. Source: Adapted from Ashwin N. Ananthakrishnan, 2015.

3.5.5. Symptoms and diagnosis

The general clinical symptoms of IBD include abdominal pain, bloody diarrhea, and vomiting, with notable differences between UC and CD. UC is often characterized by the presence of blood and mucus in stool, lower abdominal cramping, and rectal bleeding. In contrast, CD symptoms vary based on the location and extent of the disease but may include postprandial abdominal pain, weight loss, and diarrhea, which may or may not be bloody. CD

patients may also present with bowel wall thickening, swelling, and complications such as fistulae or strictures, which are less common in UC[133]. In addition, extraintestinal manifestations are also observed in IBD, resulting in a decrease in life quality that might need additional treatment. Affecting both UC and CD patients, these symptoms are axial and peripheral arthritis, skin lesions, rashes or ulcers, liver and bile duct disorders, and conjunctivitis[134].

Microscopically, UC is characterized by disruptions in mucosal architecture, including crypt atrophy, branching, and irregularities in the villous mucosal surface. Inflammatory infiltrates, primarily composed of lymphocytes and plasma cells, are confined to the mucosa and superficial submucosa. Neutrophilic infiltration often leads to cryptitis and the formation of crypt abscesses. In contrast, CD exhibits discontinuous chronic inflammation, with inflammatory infiltrates in the lamina propria that extend beyond the superficial mucosa to deeper layers of the intestinal wall. Crypt abnormalities, such as distortion and irregular branching, are present. Another feature of CD is the presence of non-caveating granulomas, which are aggregates of macrophages and can aid in distinguishing CD from UC[135,136].

Diagnosing IBD involves a combination of clinical evaluation, endoscopic procedures, imaging studies, laboratory tests, and histopathological analysis to ensure accurate differentiation between CD and UC. Endoscopy remains a key strategy for identifying characteristic lesions, such as ulcerations, inflammation, and mucosal damage. These procedures also allow for tissue biopsies, essential for confirming the diagnosis by revealing microscopic features like crypt abnormalities, granulomas, and inflammatory infiltrates[137–139].

Laboratory tests further support the diagnostic process. Blood tests measure markers of inflammation such as C-reactive protein (CRP) and erythrocyte sedimentation rate (ESR), autoimmune responses, hemolysis, and vitamin deficiencies[140]. Stool analysis, including fecal calprotectin and lactoferrin, provides non-invasive markers of intestinal inflammation, helping to differentiate IBD from non-inflammatory conditions like irritable bowel syndrome (IBS)[141].

In addition to standard methods, advanced techniques like capsule endoscopy allow visualization of the small intestine in cases where traditional endoscopy cannot reach, which is particularly useful for detecting subtle CD lesions[142].

3.5.6. IBD treatments

IBD is a treatable condition but currently has no cure. Additionally, the deteriorating quality of life and increased susceptibility to colorectal cancer highlight the importance of developing effective and ongoing therapies[143,144].

Several treatments are available for IBD, especially with the aim of reducing inflammation and maintaining remission. Nevertheless, despite the development of new treatment options, about 50% of the patients do not achieve remission after 1 year of treatment. Due to the complexity of the inflammatory pathways involved in IBD, as well as the variable clinical manifestations, the combination of several therapeutical agents is required[145].

Standard therapies for IBD include anti-inflammatory drugs like aminosalicylates, such as 5-aminosalicylic acid (5-ASA), acting in important inflammatory segments such as the prostaglandin and reactive oxygen species[146]. Glucocorticoids also bring an important option in the control of inflammation, although infections and dependence can be associated with side effects[147,148]. Anti-TNF and immunomodulators are also among the conventional therapies for IBD[149].

In respect to immunomodulators, thiopurines, methotrexate, calcineurin inhibitors, and Janus Kinase (JAK) inhibitors can suppress pro-inflammatory responses, inhibiting T lymphocyte proliferation and downregulating several pro-inflammatory cytokines[150]. Monoclonal antibodies targeting cytokines are also a relevant option for IBD treatment, especially in cases where patients do not respond to immunomodulators or cannot use steroids. In this case, anti-TNF and anti-IL12/23 antibodies are capable of targeting pro-inflammatory precursors inhibiting the development of immune responses[150].

IBD patients can have long-term disease and clinical remission after immunomodulators and other cited therapies; however, around 47% of patients with CD and 16% of UC need surgical treatment[151]. Total proctocolectomy with ileal pouch-anal anastomosis (IPAA) can be curative for UC patients as it eliminates the disease from the colon and rectum[152]. On the other hand, CD patients might undergo surgical procedures during their lifetime to address complications such as strictures, fistulas, or abscesses; however, surgery is not curative for CD, as the disease can recur in other parts of the gastrointestinal tract[153,154]. Advancements in minimally invasive techniques, including laparoscopic and robotic-assisted surgeries, have improved patient outcomes by reducing complications and postoperative pain, shortening hospital stays, and facilitating quicker returns to daily activities[155].

Fecal microbiota transplantation (FMT) is an emerging therapeutic approach in the treatment of IBD, aimed at restoring the gut microbiota by transferring fecal matter from a healthy donor to the patient[156]. FMT has shown promising results, particularly in UC, with studies reporting improvements in microbiota diversity, clinical symptoms, and mucosal restoration[157]. Some patients have achieved long-term clinical remission, as demonstrated in case studies and trials[158]. Although the efficacy of FMT in CD remains less consistent, studies

reported significant improvements in clinical symptoms such as abdominal pain, diarrhea, hematochezia, and fever. Despite long-term remission being less frequent, nearly half of patients achieve clinical response after one or multiple courses of FMT, with sustained benefits linked to microbiota diversity restoration.[159] Although there are challenges regarding sample/donor diversity, microbial taxonomy, and interactions with the receptor environment, FMT holds significant potential for IBD therapy and other conditions in which microbiota restoration can lead to beneficial impact[160].

In addition to pharmacological, FMT, and surgical interventions, therapies targeting the gut microbiota, such as probiotics, prebiotics, postbiotics, and probiotics, are promising strategies to restore microbial composition in IBD.

3.6. Microbiota-Based Therapies: Probiotics, Prebiotics, Postbiotics, Parabiotics and Symbiotics

Probiotics, prebiotics, postbiotics, parabiotics and symbiotics have been associated as promising alternative options for IBD therapy (Figure 8)[161]. With the current challenges of the traditional treatments primarily focusing on suppressing the immune response and managing inflammation, microbiota-based therapies offer a novel approach by directly targeting and modulating the intestinal ecosystem. Those treatments aim to restore microbial balance which promotes favorable impacts such as enhancing intestinal barrier function and modulating immune responses, thereby addressing several ramifications in which dysbiosis conducts IBD[162]. In this context, the concept of next-generation probiotics (NGPs), which will be discussed in detail later, further expands the therapeutic potential of microbiota modulation.

3.6.1. Probiotics

Probiotics are described as 'Live microorganisms which, when administered in adequate amounts, confer a health benefit on the host[163].' Differing from gut commensals, to be classified as probiotics, the strains need to be isolated, characterized, and correlated with host beneficial effects[164]. Moreover, probiotic bacteria have a long tradition of usage besides being certificated by safety organizations as the United States Food and Drug Administration (FDA) having the GRAS status (Generally Regarded as Safe) (https://www.fda.gov/animal-veterinary/animal-food-feeds/generally-recognized-safe-gras-notification-program) or by the European Food Safety Authority (EFSA)[165].

Common sources of probiotics include fermented foods such as yogurt, kefir, sauerkraut, kimchi, and miso[166,167]. The beneficial bacteria associated with probiotic effects are

especially Lactic acid bacteria (LAB) such as *Lactobacilli* and *Bifidobacteria*[168]. Additionally, *Bacillus*, *Escherichia*, and *Propionibacterium* genera, as well as the yeast *Saccharomyces*, have strains considered probiotics[169,170].

Probiotics contribute to maintaining human health by enhancing the population of healthy gut microbiota, supporting diversity, and competing against pathogenic bacteria. They have immunomodulatory activity, which is essential for reducing inflammatory responses while promoting anti-inflammatory mediators. Additionally, probiotics are associated with the integrity of the intestinal barrier by reducing permeability and producing beneficial compounds such as SCFAs[171].

In the context of IBD, various native commensal probiotics and genetically modified probiotics have been explored as potential treatment options[172]. *Bifidobacterium breve* has been studied for its role in modulating gut inflammation and barrier integrity by modulating tight junctions, supporting the maintenance of remission in IBD patients[173,174]. *L. rhamnosus* GG is another example that has shown efficacy in remission induction in UC patients[175]. Beyond utilizing naturally occurring strains, advancements in genetic engineering have enabled the development of modified probiotics capable of delivering therapeutic agents directly to inflamed intestinal tissues. For example, engineered *L. lactis* has been designed to secrete anti-inflammatory cytokines, offering targeted treatment options for IBD[176]. These innovations represent a significant improvement in exploiting the gut microbiome for therapeutic purposes.

3.6.2. Prebiotics

Prebiotics are described as "a substrate that is selectively utilized by host microorganisms conferring a health benefit" by the International Scientific Association for Probiotics and Prebiotics (ISAPP)[177]. Common dietary sources of prebiotics include whole grains, oats, bananas, onions, garlic, soybeans, artichokes, and many others[178]. To be classified as a prebiotic, the ingredient must resist gastric pH and GIT enzymes and needs to be fermented by the intestinal microbiota components, selectively inducing the growth of beneficial intestinal bacteria[178]. The product of the fermentation of prebiotics is principally SCFA as propionate, butyrate, and lactic acid, which has several essential properties for intestinal and systemic homeostasis[179].

Non-digestible fibers, such as inulin, oligofructose, and fructooligosaccharides (FOS), are examples of prebiotics that serve as nourishment for beneficial gut bacteria, particularly *Bifidobacteria* and *Lactobacilli*, promoting their growth and activity[180]. Prebiotics also

influence the gut microbiota composition, contributing to digestion, nutrient absorption, and immune functions[181].

The competitive dynamics among gut microbes for prebiotic substrates present a significant challenge when evaluating the efficacy of these compounds in selectively targeting beneficial species[182]. Nevertheless, experimental studies in patients with inflammatory conditions have revealed positive outcomes. For instance, supplementation with oligosaccharides and inulin has been shown to reduce fecal calprotectin levels and alleviate symptoms in patients with UC[183]. Inulin has also been associated with an increase in beneficial gut bacteria, particularly *Bifidobacterium*, *Lactobacillus*, and *F. prausnitzii*, which in turn enhances colonic production of short-chain fatty acids. Germinated barley food (GBF), which is rich in dietary fiber and glutamine, has demonstrated efficacy in reducing clinical activity and maintaining remission in patients with mild-to-moderate UC[184]. Moreover, a range of health benefits has been observed, including improved intestinal barrier integrity, better bowel regularity, increased insulin sensitivity, and reduced triglyceride levels[185].
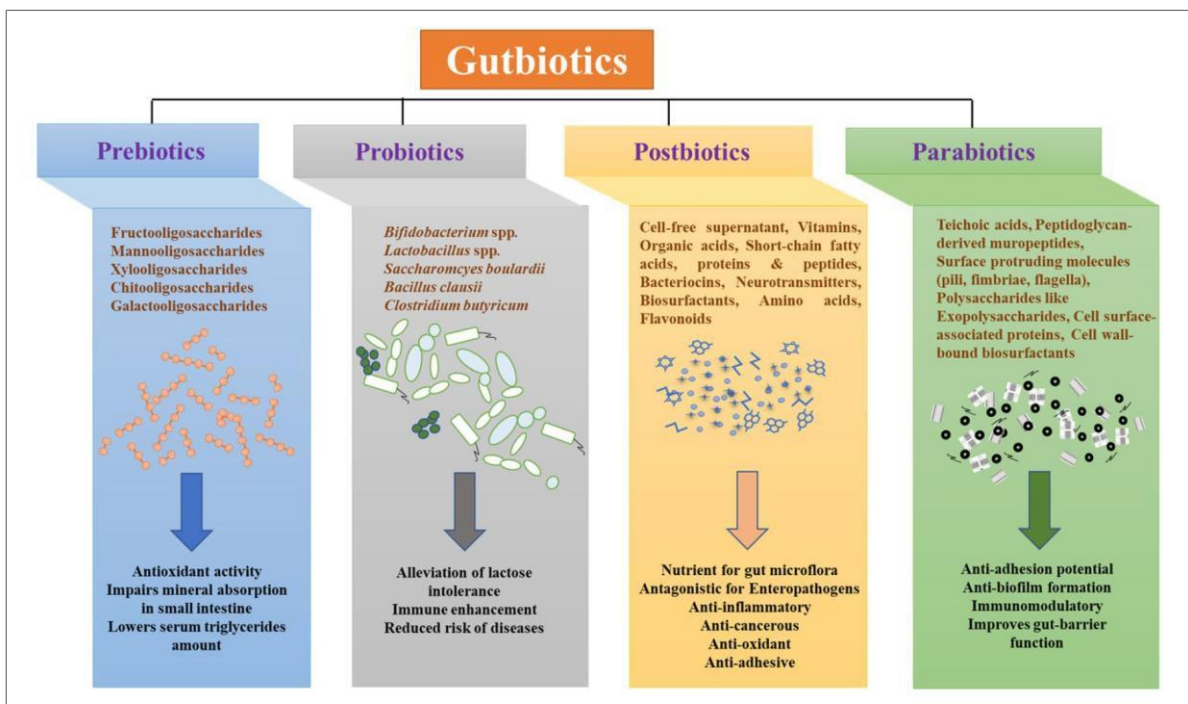
Figure 8. Health-promoting effects of gutbiotics. Source: Kango and Nath, 2024.

3.6.3. Postbiotics and Parabiotics

Postbiotics and parabiotics emerge as promising alternatives to conventional probiotics in microbiota-based therapies. Postbiotics refer to the bioactive compounds produced or released during the metabolic activities of probiotics, which confer health benefits to the host

without involving live microorganisms, thereby minimizing potential risks associated with microbial viability[186,187]. Examples of postbiotics include vitamins, amino acids, peptides, organic acids, SCFA, bacterial supernatants, enzymes, etc[188,189].

In contrast, parabiotics encompass the inactivated or dead probiotic cells along with their cellular residues. These inactivated forms can be generated through methods such as heat treatment, chemical agents (e.g., formalin), irradiation, or sonication, with heat treatment being the most commonly employed approach[189]. These components include teichoic acids, peptidoglycan-derived muropeptides, and surface structures like pili, fimbriae, and flagella, along with polysaccharides (for example, exopolysaccharides), cell surface-associated proteins, and cell wall-bound biosurfactants[189].

Both postbiotics and parabiotics have been shown to interact with immune cell populations and exert antimicrobial effects against enteropathogens, contributing to the maintenance of intestinal barrier function and overall gut homeostasis[190,191].

Postibiotics, as the fermentation products of *L. paracasei* CBA L74, demonstrated anti-inflammatory properties *in vitro* and *ex-vivo* assays, further enhancing responsivity against pathogenic bacteria *Salmonella typhimurium*. Furthermore, such products showed protective effects against colitis *in vivo*.[192] Several other studies have evaluated microbiota-derived peptidoglycan-driven beneficial properties, especially in immunomodulation[193–195].

Among the parabiotics, pasteurized *A. muciniphila* demonstrated beneficial properties in lipid metabolism in minimizing cardiovascular disease risk[196]. In a clinical trial involving non-viable *L. reuteri* DSM17648 cells, the formulation decreased *Helicobacter pylori* loads in addition to ameliorating gastrointestinal symptoms[197]. Moreover, studies with other *Lactobacillus* and *Bifidobacterium* strains have been performed to evaluate the applicability in the production of parabiotics[198].

3.6.4. Synbiotics

Synbiotics are combinations of probiotics (live microorganisms) and prebiotics (substrates) that synergistically confer health benefits to the host[199]. This approach aims to enhance the survival and activity of beneficial microorganisms in the gastrointestinal tract by providing both live beneficial bacteria and the substrates that promote their growth. There are two types of synbiotics: complementary, in which probiotic and prebiotic have independent roles, and synergistic, in which the prebiotic is targeted to select the probiotic[200]. The synergistic action of synbiotics supports gut health by enhancing the colonization and activity of beneficial bacteria, improving the balance of the intestinal microbiota, and inhibiting the growth of

pathogenic organisms[201]. This dual approach also enhances the production of beneficial metabolites, such as SCFAs, promoting immunological balance and intestinal health maintenance[182,202].

Examples of complementary synbiotics are formulations with *Lactiplantibacillus plantarum* and fructooligosaccharides (FOS) tested in clinical trials and having important achievements in sepsis and mortality[203]. *B. breve* combined with FOS also demonstrated the capacity to increase abundance in the organism and increase lactate and acetate production[204]. Among the synergistic probiotics, *L. rhamnosus* GG cultivated with arginine amino acid demonstrated improvement of the growth rate of the bacteria, thus supporting the inhibition of pathogenic *Streptococus mutans*[205].

In the context of IBD, synbiotics have been investigated for their potential therapeutic effects. Studies have indicated that synbiotic supplementation can reduce inflammation and improve macroscopic and microscopic disease indicators in patients with ulcerative colitis[206]. For instance, a combination of *B. longum* and prebiotic inulin demonstrated that it can increase beneficial bacteria, reduce pro-inflammatory cytokines like TNF-α, and alleviate symptoms like abdominal pain and diarrhea in a clinical study[207].

In summary, dysbiosis plays a pivotal role in the progression of IBD, disrupting the complex balance of the gut microbiota and triggering immune dysfunction, intestinal inflammation, and compromised barrier integrity. This points to the crucial role of targeted therapies in restoring microbial balance and managing IBD symptoms. While traditional therapies have focused on managing inflammation, the emergence of microbiota-based therapies offers a promising alternative to directly address dysbiosis. In the following sections, we will explore a new classification of beneficial bacteria, the NGPs exploring their potential therapy options for IBD and other conditions.

3.7. Next Generation Probiotics

3.7.1. Definition and Criteria

Historically, probiotics were originally isolated from fermented dairy products and fecal samples. However, most gut microorganisms have long remained uncharacterized due to their anaerobic nature and cultivation challenges. With the development of techniques, particularly 16S rRNA gene PCR (polymerase chain reaction), next-generation sequencing, and bioinformatic tolls, the precise identification of numerous previously undetected bacterial strains has been achieved[167]. Since then, advances in whole-genome sequencing and innovative

culture methods have further enabled the isolation and detailed characterization of novel microbes with promising health benefits[16,208].

Those advancements enabled the identification of organisms from the gut that confer targeted therapeutical benefits toward the host's needs. Consequently, the terms: "Next Generation Probiotics" (NGP) and "Live Biotherapeutic Products" (LBPs) were adopted[209]. NGP is defined as "live microorganisms identified on the basis of comparative microbiota analyses that, when administered in adequate amounts, confer a health benefit on the host"[167]. These newly identified strains, termed NGP, extend beyond traditional LAB and bifidobacteria to include a broader array of species that show potential in managing inflammatory diseases, cancer, and metabolic disorders[167].

Contrasting with classical probiotics, NGP doesn't have a long history of use; they were identified principally due to metagenomics, usually comparing the microbiota of healthy and non-healthy organisms[210]. Moreover, the safety regulations of NGP differ from the classical probiotics due to the recent categorizations and can include genetically modified organisms [211]. On the other hand, the definition of LBP is more restrictive: "a biological product that contains live organisms; is applicable to the prevention, treatment or cure of a disease or condition of human beings; and is not a vaccine[210]".

3.7.2. Examples and activity

The main known potential NGP are *Roseburia intestinalis*, *Eubacterium* spp., A. *muciniphila*, *Christensenella minuta*, *F. prausnitzii*, *Parabacteroides goldsteinii,* and *Bacteroides fragilis*[167]. Such organisms have been associated with favorable properties towards the host, for example, in the regulation of intestinal immunity, preserving gut barrier, and production of peptides and metabolites (Figure 9)[212].

A. muciniphila is a member of the Verrucomicrobiota phylum, capable of degrading mucin, and is responsible for up to 5% of the gut microbiota composition[213]. The species has garnered attention after it was identified in reduced abundance in diabetic and obese patients, as well as patients with metabolic disorders, hypertension, and bowel conditions[214]. *A. muciniphila* has thus been characterized as NGP due to its activity regarding metabolic activity involved with gut barrier function and immunomodulation[167,215–217].
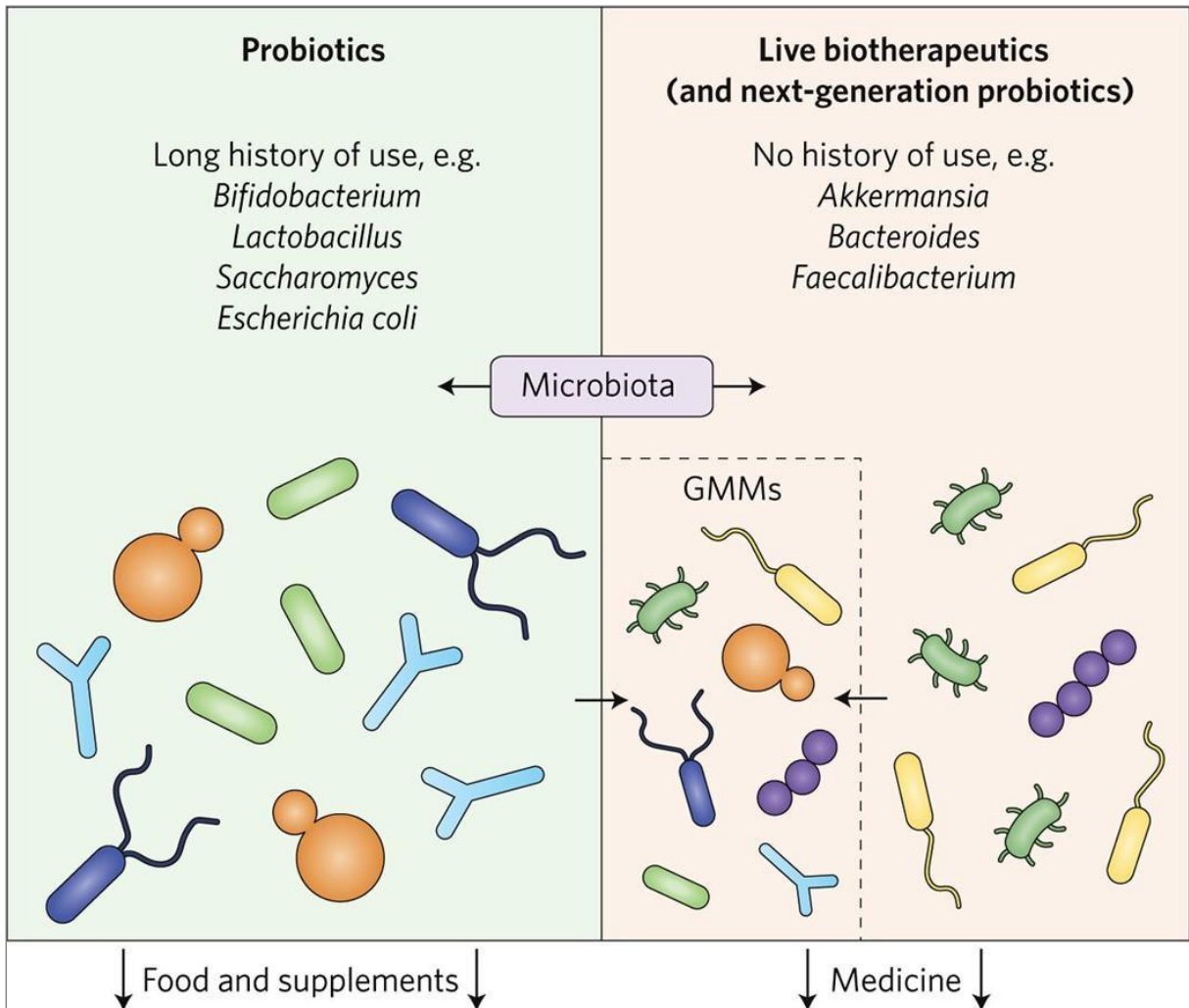
Figure 9. Probiotics and Next-generation probiotics. The figure contrasts traditional probiotics, left panel, with live biotherapeutics/next-generation probiotics, right panel. Source: Paul W. O'Toole et al, 2017.

However, studies in murine models of colorectal cancer have produced contradictory results. While some investigations report a protective effect of *A. muciniphila*, others indicate that its administration may exacerbate tumor development[218,219]. This complex interplay highlights the need for further research to delineate the precise conditions under which *A. muciniphila* confers health benefits versus pathogenic effects.

Belonging to Firmicutes phylum, *R. intestinalis* is a butyric acid producer bacteria considered as potential NGP due to its beneficial effects in disturbs as IBD, atherosclerosis, and colorectal cancer[220,221]. *R. intestinalis* can metabolize several prebiotics and act in immunomodulation contributing to intestinal integrity by enhancing the expression of tight junctions[222].

Also, from the Firmicutes phylum, it is a butyrate and propionate-producer. *Anaerobutyricum hallii* (formerly *Eubacterium hallii*) is a bacterium that constitutes around 3%

of the gut microbiota population. As a metabolically versatile bacterium, *E. hallii* has the capacity to metabolize glucose and intermediate fermentation products such as acetate and lactate for butyrate production[223]. Moreover, it converts glycerol to 3-hydroxypropionaldehyde (3-HPA, reuterin), a compound with antimicrobial activity[224].

C. minuta is a gram-negative bacteria belonging to the Firmicutes phylum in the Clostridiales order[225], that, although strictly anaerobic, can tolerate oxygen[226]. Being able to metabolize several monosaccharides, *C. minuta* produces SCFA as acetic and butyric acid. The species represents 0,2% – 2% of the colonic bacterial population of healthy adults, and its depletion was correlated with IBD patients[227].

Prevotella copri belongs to the Bacteroidetes phylum[228], and conflicting associations have hampered its classification as NGP. *P. copri* have been associated with both beneficial and harmful effects on host health. Such contrasting correlations were observed in patients with neurological conditions, diarrhea, metabolic conditions[229–231], and rheumatoid arthritis (RA), in which enriched gut microbial composition with *P. copri* was observed[232,233]. The duality of associated involvement of *P. copri* in the insulin metabolism has also been observed, as in type 2 diabetes patients had increased abundance of the species[234], while in other studies, the species were linked with the regulation of glucose in the blood[235].

With around 30 species, the order Bacteroidales is present in the human gut in high amounts, ranging from 10^9 - 10^{11} CFU per gram of feces[236]. *B. fragilis* is the group's best-known potential NGP. Capsular polysaccharide A (PSA) from *B. fragilis* NCTC9343 plays a crucial role in its probiotic effect by modulating the immune system, reducing brainstem inflammation during viral infections, and promoting the production of regulatory T cells that secrete IL10, helping to control inflammatory responses.[237] In both *in vitro* and *in vivo* studies, *B. fragilis* attenuated inflammation, improved cell viability, and protected against Dextran Sodium Sulfate (DSS)-induced colitis, highlighting its potential as a probiotic for managing inflammatory conditions such as colitis[238].

3.7.3. Challenges and future directions in NGP

The rise of NGP represents a crucial shift in microbiome-based therapies, offering targeted solutions for various health conditions through their microbiota-modulating effects. Unlike traditional probiotics, NGPs such as *A. muciniphila, B. fragilis, E. hallii, and Roseburia* spp. are not limited by a historical reliance on safe usage but are instead identified through advanced metagenomics and bioinformatics tools. These microorganisms hold immense promise for addressing gastrointestinal, metabolic, and immune disorders through their unique

mechanisms, including immunomodulation and the production of bioactive metabolites. In spite of that, divergent beneficial/harmful activity has also been observed in some NGP, evincing the complexity of properly describing those species.

Significant challenges remain in translating NGPs from laboratory research to clinical practice. These include understanding their complex metabolic activities, ensuring their ecological stability within the gut microbiota, and evaluating potential risks related to immune stimulation, adverse gastrointestinal effects, or the presence of antibiotic-resistant genes. Rigorous safety assessments and deeper insights into their mechanisms of action are essential to unravel their full therapeutic potential. Nevertheless, advancements in microbiome research and biotechnological innovations provide strong efficacy examples for therapies that need further evaluation[217].

In addition to these emerging NGPs, species from the genus *Faecalibacterium* are among the most abundant and critical members of the gut microbiota. Recognized as gut health biomarkers, their depletion has been linked to conditions beyond intestinal inflammation, such as metabolic and neurological disorders. These findings strengthen the relevance of *Faecalibacterium* in NGP research, indicating its potential therapeutic applications[239]. The next sections will further describe the genus *Faecalibacterium*, with a particular focus on *F. duncaniae* (formerly *F. prausniztii*).

3.8. The genus *Faecalibacterium*

Among the diversity of its gut microbiota ecosystem, the genus *Faecalibacterium* stands as a ubiquitous commensal organism, being one of the most abundant in the human colon. It contributes to gut homeostasis by producing short-chain fatty acids, particularly butyrate, and bioactive peptides, such as those derived from the protein MAM[239]. The importance of the *Faecalibacterium* as an NGP was initially highlighted by its protective effects against inflammatory intestinal diseases[240]. With advances in the meta-omics and genome sequencing technologies field, its role has also been associated with neurological and systemic conditions, including obesity and diabetes[241–244].

Although *Faecalibacterium* is widely recognized for its abundance and functional significance in the gut, the specific mechanisms and molecular effectors responsible for its benefits remain poorly understood. Furthermore, a diverse range of effects is observed among this genus representatives. New species have been recently identified, indicating that substantial variability and their specific outcomes in relation to the host remain largely unexplored[239].

Addressing these topics presents substantial biotechnological opportunities for developing innovative therapeutics and a more profound understanding of host-microbiota interactions.

Faecalibacterium species have been identified in other mammals, avian species, and occasionally in cattle milk[245]. They are characterized by small rod-shaped non-motile cells. Although *Faecalibacterium* was described as Gram-negative bacteria[246], phylogenetic analyses using cell envelope markers indicate that it is more closely related to Gram-positive, specific members of the clostridial cluster IV and *Bacillus subtilis* than to classical Gram-negative organisms like *E. coli*. Moreover, *Faecalibacterium* lacks characteristic outer membrane proteins and shows no evidence of LPS, indicating its possible non-classical gram-staining architecture[247]. Although sporulation-related genes have been identified in *Faecalibacterium* species, they are considered non-spore-forming. Genomic studies reveal a G+C content ranging from 45% to 57%[246]. *Faecalibacterium* is also extremely oxygen-sensitive (EOS), with most strains resisting oxygen exposure for only about two minutes, though this varies by species and strain[248]. This strict anaerobic nature plays a critical role in its oxidative stress responses and is essential for maintaining gut anaerobiosis. Such characteristics are important regarding the oxidative stress responses as they impact gut anaerobiosis, which is, therefore, related to the colonization capacity of the species and intestinal inflammation[248].

Although lacking information regarding how gut colonization by *Faecalibacterium* occurs, evidence demonstrates that the species is barely detected at early stages of life but increases significantly from late infancy to toddlerhood (8-19 months old), reaching similar levels with adults between 2-5 years old. The highest levels of *Faecalibacterium* are observed in adult populations, gradually declining as individuals age[249–251].

3.8.1. Taxonomy and diversity

Faecalibacterium prausnitzii was first isolated in 1992 by J. Prausnitz[252]. It was originally named *Bacteroides prausnitzii* in 1937 due to its rod-shaped morphology and anaerobic characteristics[253]. In 1974, due to its great butyrate production, it was reclassified as *Bacteroides prausnitzii*[254]. In 2002, phylogenetic analysis revealed that the species had a lower identity with Fusobacterium species, while a closer relationship was observed with members from the *Clostridium* cluster IV (*Clostridium leptum* group). Moreover, contrasting oxygen resistance levels and metabolic capacities were observed between the species. Thus, the new classification has determined the new genus, *Faecalibacterium*. At first, the genus was composed of the type strain *F. prausnitzii* ATCC 27768 and the strains ATCC 27766, A2-165, and L2-6 (Figure 10)[246].
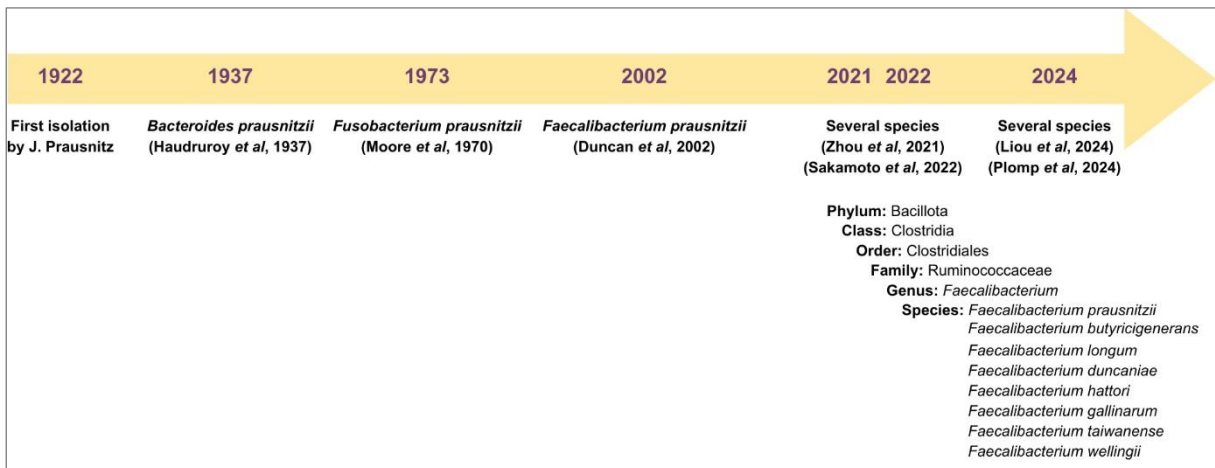
Figure 10. Timeline of *Faecalibacterium* taxonomy. Source: Adapted from Martín et al, 2023.

F. prausnitzii has long been considered the sole species within the genus *Faecalibacterium*. Phylogenetic analysis of 16S rRNA sequencing has primarily identified two phylogroups within *Faecalibacterium* species. The phylogroups show minimal differences in pH tolerance, bile resistance, or substrate metabolism, but their distinct prevalence in health and disease indicates their potential clinical relevance.[255] Phylogroup I shows reduced abundance in conditions such as CD, UC, and CRC, while Phylogroup II appears predominantly affected in CD[74].

Later analyses employing advanced genomic techniques, including whole genome sequencing, phylogenomics, and Average Nucleotide Identity (ANI), revealed a more complex picture of *Faecalibacterium* diversity. Instead of two phylogroups, the genus was found to comprise at least three distinct clusters—A, B, and C—derived from a common recent ancestor. Each cluster represents a genospecies with distinct genetic and functional profiles. In addition, the pangenome of *Faecalibacterium* demonstrated high fragmentation, whereas the pangenomes of the individual clusters were highly homogeneous[256].

With the advancement of metagenomic studies, approximately 3,000 *Faecalibacterium* genomes have been obtained from humans and non-human primates, revealing the existence of around 200 species-level genome bins (SGBs) across 21 clades. These comprehensive analyses indicate that *Faecalibacterium* diversity and abundance are influenced by factors such as age, geographic origin, and lifestyle (Figure 11). For example, higher abundance levels of *F. prausnitzii* were correlated with non-Western populations and non-industrialized countries. In addition, significant functional diversity is also observed, such as in carbohydrate metabolism capacities and protein degradation, suggesting adaptations to different conditions[251].
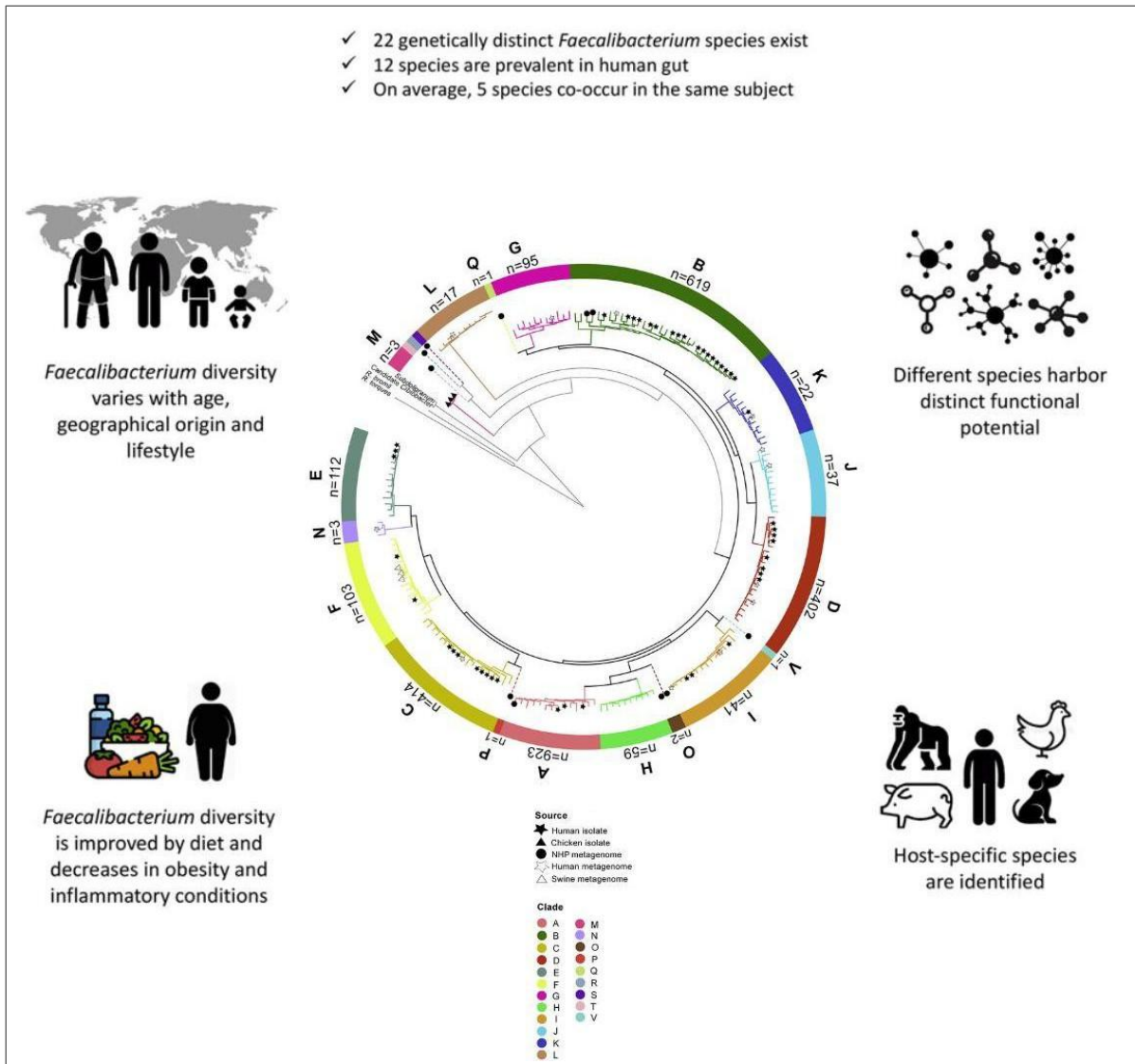
Figure 11. *Faecalibacterium* diversity is observed in different hosts, species activity, age and diet. Source: Filippis, Pasolli and Ecorlini, 2020.

A recent analysis of 136 *Faecalibacterium* genomes identified 11 clusters, five of which have been formally named *Oscillospiraceae* of the Bacillota genus, which harbors extremely oxygen-sensitive (EOS) bacteria. There are seven validated species: *F. prausnitzii*, *F. longum*, *F. butyricigenerans*[257], *F. duncaniae (*previously *F. prausnitzii* strain A2-165*), F. gallinarum, F. hattorii*[258]*, F. taiwanense*[259] and *F. wellingii*[260].

Thus, these studies highlight the complexity of the genus *Faecalibacterium* within the human gut, demonstrating a remarkable species diversity and prevalence that may correlate with intestinal and systemic disorders. The next section will explore the metabolites produced by *Faecalibacterium* and their oxygen sensitivity, which are critical to understanding their impact on gut health.

3.8.2. Metabolism

The genus *Faecalibacterium* is recognized for its ability to produce significant quantities of SCFAs, particularly butyrate, one of the most abundant gut metabolites, being central to gut homeostasis. Butyrate is synthesized via the butyryl-CoA: acetate CoA- transferase pathway, in which acetate serves as a substrate, another highly abundant SCFA[261,262]. This acetate cross-feeding mechanism highlights the metabolic interdependence within gut microbial communities, as *Faecalibacterium* utilizes acetate produced by other microorganisms from the *Bifidobacterium* genus. Such behavior is highlighted by co-culture experiments using *B. adolescentis*, in which the cross-feeding enhanced butyrate production by *F. duncaniae*[263].

In a mice model assay, metabolomic analysis of the colon of animals co-colonized with *E. coli* and *F. duncaniae* revealed a distinct enrichment of metabolites attributable to *F. duncaniae*, including butyrate, shikimic acid, indole-3-lactate, and, in the ileum, raffinose[262].

Faecalibacterium exhibits a notable ability to metabolize simpler substrates such as dietary fiber and inulin-type fructans through specific enzymatic pathways[239]. The fructose phosphotransferase system (PTS) is central to this process, which facilitates the uptake and metabolism of fructose derived from inulin degradation[264]. Intracellular metabolomic studies have revealed that *F. duncaniae* utilizes fructose as an energy source to support inulin metabolism, enhancing its growth and metabolic activity[265]. Research in gnotobiotic rodent models and human dietary interventions further demonstrated the importance of inulin in promoting *Faecalibacterium* populations and increasing butyrate production[239].

Beyond SCFAs, *Faecalibacterium* species can utilize metabolites derived from host intake and microbial activities, including N-acetylglucosamine, d-glucosamine, and d-glucuronic acid. Furthermore, *Faecalibacterium* can metabolize avenanthramides, phenolic compounds from oats, into dihydro-avenanthramides, which exhibit anti-inflammatory and antioxidant properties. These metabolic capacities reflect the genus's adaptability and pivotal role in sustaining a functional and symbiotic gut microbiota[266,267].

3.8.3. Oxygen resistance

Members of the genus *Faecalibacterium* are obligate anaerobes that are highly sensitive to oxygen. This vulnerability is exacerbated during gut inflammation when reactive oxygen species (ROS) and elevated oxygen levels are observed. Despite this sensitivity, certain strains, such as *F. duncaniae* A2-165, demonstrate enhanced oxidative stress tolerance by employing an extracellular electron shuttle system that uses flavins and thiols to transfer electrons to oxygen, thereby reducing it to hydrogen peroxide (H_2O_2)[239]. Overall, all strains are highly

sensitive to oxygen but with varying degrees of tolerance. *F. prausnitzii* CNCM4543 was observed to be the most vulnerable, with complete mortality shortly after exposure. *F. duncaniae* strains and *F. prausnitzii* L2-6 exhibited intermediate sensitivity, showing brief survival before rapidly declining. In contrast, *F. prausnitzii* M21/2 demonstrated the highest resistance, with a small fraction of cells persisting even after prolonged exposure. This increased tolerance is correlated with a greater number of genes encoding O_2- and ROS-detoxifying enzymes, whereas strains with fewer of these enzymes, like CNCM4543, showed extreme susceptibility[239,248].

Together, These findings provide molecular insights into the metabolic adaptations of *Faecalibacterium* and the mediators that enable it to thrive in inulin-rich environments, and to grow under low-oxygen, reinforcing its role in gut homeostasis and cross-feeding within the microbiota.

3.9. *F. duncaniae* and gut homeostasis

Analysis with 7,907 human gut metagenomes demonstrated that *Faecalibacterium* species are widely distributed and highly abundant throughout diverse populations globally, reaching 85% detection in all samples[251]. The depletion of *Faecalibacterium* representatives in the gut has been associated with several gut and systemic disorders, which indicates its important contribution to maintaining host homeostasis. Anti-inflammatory activity, microbiota modulation, and gut barrier maintenance are the best-known mechanisms by which *Faecalibacterium* species promote health. Despite the significance of these studies, it is important to note that most have relied on *in vitro* and in animal models, highlighting the need for future research, specially to elucidate the underlying mechanisms and the role of host factors in these interactions.

3.9.1. *F. duncaniae* and IBD

F. duncaniae was associated with inflammatory bowel diseases in a study by Sokol et al. 2008, which demonstrated a reduction in the abundance and diversity of the Bacillota phylum, particularly *F. duncaniae*, in patients with Crohn's disease[240]. In addition, reductions in the richness of two mucosa-associated *Faecalibacterium* phylotypes have been observed in cases of IBD, indicating specific impacts on its subpopulations and diversity[268]. This reduction was correlated with an increased risk of postoperative ileal surgery recurrence and endoscopic recurrence six months later. Since then, several studies with different cohorts have reinforced such correlations in both CD and UC[268–274]. For instance, a meta-analysis study revealed that,

the reduction of *F. duncaniae* levels is consistently observed in both remission and active disease stages of CD and UC patients, with the most significant reduction seen during active disease[275].

The supernatant (SN) of *F. duncaniae* was also observed to exhibit stronger anti-inflammatory effects than the bacterium itself. In a TNBS-induced colitis model, *F. duncaniae* SN significantly increased TGFβ1 and IL10 levels while triggering only mild production of the pro-inflammatory cytokine IL12p70 or reducing levels of IL17 and IL12[240,276]. Similarly, another study reported that both *F. duncaniae* and its SN alleviated colitis severity in murine models of severe and moderate chronic colitis. This effect was associated with reduced intestinal permeability, lower colonic cytokine levels (IL6, IFN-γ, IL4, and IL22), and decreased serotonin concentrations, further supporting its anti-inflammatory role[277].

Such evidences were reinforced by other studies with *in vivo* models of chronic low-grade inflammation, in which F. duncaniae's SN demonstrated beneficial effects on colonic permeability. These effects are mediated, at least in part, by the restoration of claudin-4 levels and the regulation of tight junctions and junctional adhesion molecules, which are critical for maintaining intestinal barrier integrity[278,279].

Beyond cytokine modulation, *Faecalibacterium* has been identified as a key inducer of regulatory Tregs, particularly CCR6+CSCR6+DP8α Treg leukocytes, which are crucial for microbiota-host cross-talk during IBD. Notably, patients with active IBD exhibit impaired responsiveness of these leukocytes to *Faecalibacterium*, whereas those in remission or healthy individuals maintain this response, suggesting a potential link between disease state and immune modulation[280,281].

3.9.2. *F. duncaniae* and other associated disorders

The association of decreased *F. duncaniae* in the gut microbiota extends beyond intestinal diseases. In a study involving 65 chronic kidney disease patients, a significant depletion of *F. duncaniae* was observed in their feces compared to healthy controls. The reduction in butyrate production, attributed to the loss of this species, has been identified as a contributing factor[282].

Obesity, a multifactorial condition characterized by decreased microbial diversity, is also associated with reduced levels of *Faecalibacterium*. One critical outcome for obese patients is the development of type 2 diabetes (T2D) and insulin resistance. A metagenomic study linked *F. duncaniae* depletion to T2D, suggesting that the absence of this species disrupts

the homeostatic functions of the gut microbiome, leading to chronic inflammation and metabolic imbalance[72].

Negative correlations between *Faecalibacterium* abundance and neurological conditions have also been reported, though many studies remain preliminary. *Faecalibacterium* have been positively associated with clinical depression[283], bipolar disorder[284,285], anxiety[286], schizophrenia[287], and Alzheimer's disease[288].

Other diseases, such as Dermatitis and infectious diseases like COVID-19, are also correlated with decreased *Faecalibacterium* abundance[249,289]. In both conditions, the disbalance in immunological responses is suggested as a key mediator of pathogenicity.

Taken together, these findings highlight the critical role of *Faecalibacterium* in a wide range of health conditions. Despite further research being needed to clarify the mechanisms underlying these associations, the evidence strongly positions *Faecalibacterium* as a pivotal health biomarker with therapeutic potential across diverse physiological and pathological axes.

3.10. Mechanisms of action of *F. duncaniae* for gut homeostasis: effector molecules

Despite *F. duncaniae* having demonstrated those beneficial properties in several *in vivo* and *in vitro* models, in addition to the positive correlation with several intestinal and systemic conditions, the effector molecules and the mechanisms behind those properties are poorly described. The best-known promoters of such properties are the protein MAM, extracellular vesicles, metabolites such as butyrate, and the extracellular polymeric matrix present in some species (Figure 12)[261,290–292].
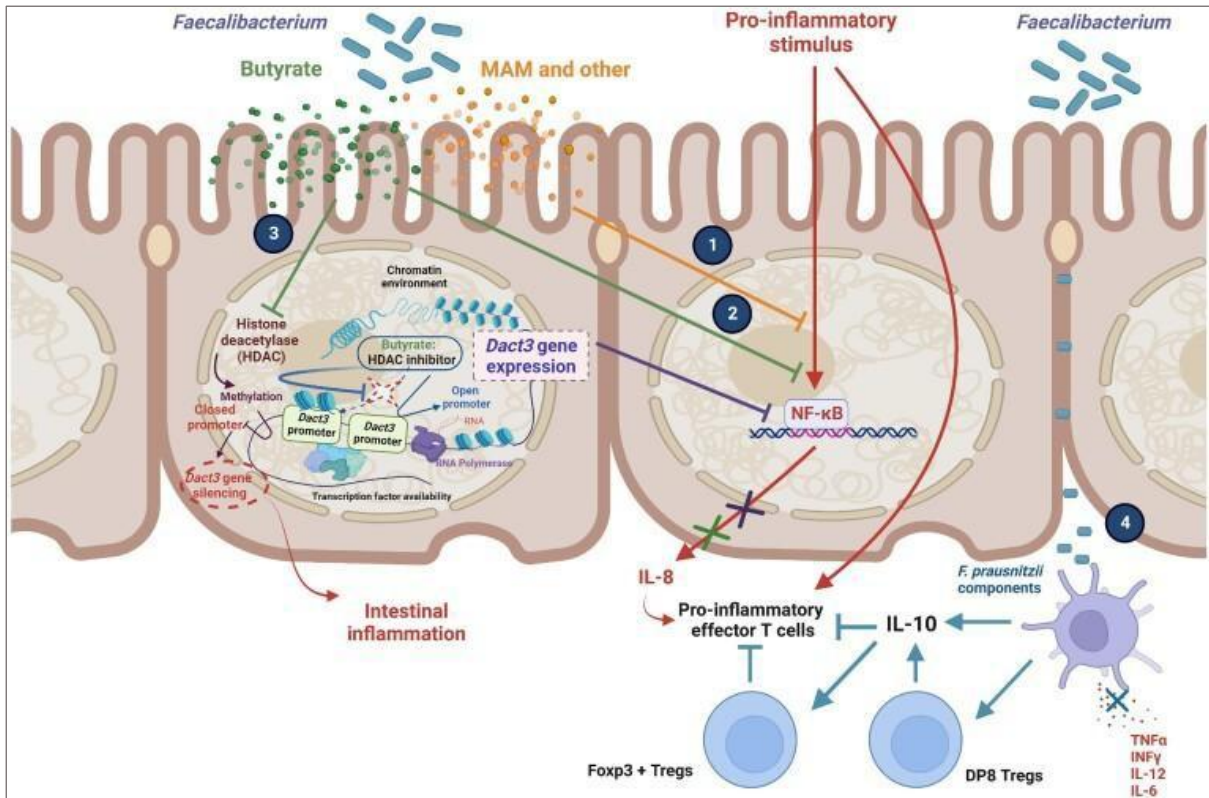
Figure 12. Associated mechanisms of action of *Faecalibacterium*. (1) *Faecalibacterium*-derived components as MAM and butyrate inhibit NF-κB activation triggered by proinflammatory stimuli. (2) Butyrate blocks NF-κB activation and reduces IL8 production in TNF-α-stimulated intestinal epithelial cells. (3) By inhibiting HDAC (Histone deacetylases), butyrate promotes Dact3 expression, a negative regulator of the inflammatory Wnt/JNK pathway, further suppressing IL8 production. (4) Source: Martin et al, 2023.

3.10.1. Metabolites production

Faecalibacterium is a key acetate consumer; the genus is capable of processing various carbohydrates and is among the main butyrate producers in the gut[261]. Butyrate serves as an essential energy source for colonocytes and exhibits potent anti-inflammatory effects by enhancing mucosal immunity and maintaining barrier integrity[293,294]. It regulates tight junction expression and modulates mucus production, besides its anti-inflammatory response mediation (Figure 12)[295].

The immunomodulatory properties of *Faecalibacterium*-derived metabolites were evaluated *in vitro* with HT-29 cells. Notably, butyrate and salicylic acid (a derivative of shikimic acid) significantly reduced IL8 production while inhibiting NF-κB signaling, whereas shikimic acid and raffinose did not exhibit such anti-inflammatory effects. Such findings indicate partially the mechanism of action of *Faecalibacterium*[242,262].

3.10.2. Extracellular vesicles

Extracellular Vesicles (EVs) are structures delimited by a membrane characterized by exosomes or microvesicles. Their cargo is very heterogeneous, and they act by delivering bioactive molecules to other cells[296].

EVs from *Faecalibacterium duncaniae* A2-165 have been observed to modulate serotonin levels in *in vitro* assays[297]. Intestinal motility is a fundamental physiological process that becomes dysregulated in gut disorders, with serotonin playing a central role in modulating peristalsis, secretion, and neural signaling[298,299]. In this context, altered serotonin levels are associated with motility and sensitivity dysfunctions in IBD patients[300]. Notably, both the supernatant and cellular components of *Faecalibacterium prausnitzii* have been shown to restore serotonin concentrations to normal levels, highlighting the potential of these bacteria in maintaining gut function and mitigating dysmotility-related disorders[279].

In a colitis mouse model, purified *F. duncaniae* EVs demonstrated significant ameliorative effects on DSS-induced colitis by reducing both macroscopic and microscopic disease scores. These included reductions in weight loss, disease activity index (DAI) scores, histological damage, and immune cell infiltration. The immunomodulatory properties of the EVs were linked to an anti-inflammatory cytokine profile characterized by increased levels of IL4, IL10, and TGF-β and decreased levels of IL1β, IL6, IL17a, and TNF-α[290]. The study also assessed barrier function, reporting upregulation of tight junction proteins, including zona occludens-1 (ZO-1) and occludin, which contribute to improved gut barrier integrity. Furthermore, the EVs enhanced antioxidant defense mechanisms by increasing the expression of nuclear factor erythroid 2-related factor (Nrf2) and heme oxygenase-1 (HO-1), which help mitigate oxidative stress and ROS damage[290].

In another prospection, EVs from *F. duncaniae* were demonstrated to have properties against fibrosis, a recurrent symptom of CD, which is characterized by the accumulation of collagen in the extracellular matrix, besides increasing mesenchymal cells. EV treatment markedly improved survival rates in DSS-induced colitis and alleviated intestinal inflammation and fibrosis. Additionally, EVs induce macrophage polarization towards the M2b phenotype, which plays a crucial anti-fibrotic and immunomodulatory role, further enhancing their capacity to modulate immune responses and support intestinal healing[301].

3.11. Microbial anti-inflammatory Molecule - MAM

3.11.1. Identification and physicochemical properties

The growing recognition of *F. duncaniae* as a key player in intestinal homeostasis has driven investigations into the molecular mediators underlying its beneficial effects. Given the challenges associated with cultivating *F. duncaniae* for potential biotherapeutic applications, identifying specific proteins or molecules responsible for its therapeutic properties represents a crucial step in advancing IBD treatment. Notably, research has demonstrated that beyond the bacterium itself, the SN of *F. duncaniae* exhibits significant anti-inflammatory activity, further supporting its potential as a next-generation probiotic[278,302].

To further elucidate the molecular components present in the SN responsible for these effects, a peptidomic analysis of *F. duncaniae* supernatant was conducted using MALDI-TOF MS to characterize its peptide composition. *De novo* sequencing of the detected ions identified seven peptides, all corresponding to the MAM (protein accession number ZP 05614546.1). MAM is a 15kDa protein that has been identified only in the genus *Faecalibacterium* so far[303]. Structural *in silico* predictions suggest that MAM adopts a globular conformation featuring a five-stranded β-sheet core surrounded by five α-helices. This protein lacks regions of low complexity or intrinsic disorder, and despite its significant hydrophobicity, no transmembrane domains or other functional motifs were detected[304].

3.11.2. MAM diversity

Overall, genomic analyses of *Faecalibacterium* strains have consistently identified at least one MAM gene in the sequenced genomes studied. To date, only one strain, *F. prausnitzii* L2/6, had two distinct MAM gene copies identified[303]. The genomic region encoding MAM frequently includes a peptidase-containing ABC transporter (PCAT) gene alongside open reading frames (ORFs) for hypothetical proteins, Ig domain-containing proteins, HlyD family efflux transporter periplasmic adaptor subunits, and genes associated with sporulation processes. RNAseq analyses of MAM promoter regions have revealed significant organizational variability in the upstream nucleotide sequences across different species and strains, suggesting diverse regulatory mechanisms for MAM expression (Figure 13)[303].
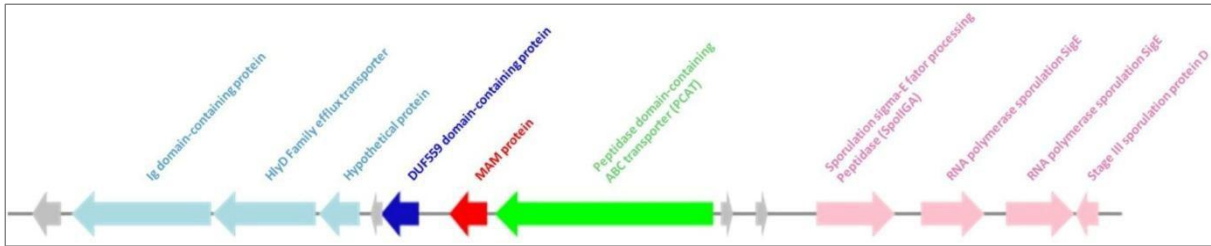
Figure 13. MAM's genetic environment in *F. duncaniae* A2-165. The MAM protein gene is highlighted in red, flanked by genes associated with different functions. Upstream, there are genes encoding an Ig domain-containing protein, an HlyD family efflux transporter, a hypothetical protein, and a DUF559 domain-containing protein (in blue). Downstream, genes encoding a peptidase domain-containing ABC transporter (PCAT, in green) are present, followed by genes linked to sporulation processes, including RNA polymerase sigma factors and sporulation proteins (in pink). Source: Adapted from Auger et al, 2021.

Phylogenetic analysis of MAM sequences from 108 genomes identified at least 10 distinct clades, revealing the protein's remarkable diversity. This genetic variation may influence MAM's structure and its anti-inflammatory potential, highlighting the need for further studies to elucidate functional differences across clades (Figure 14)[303].
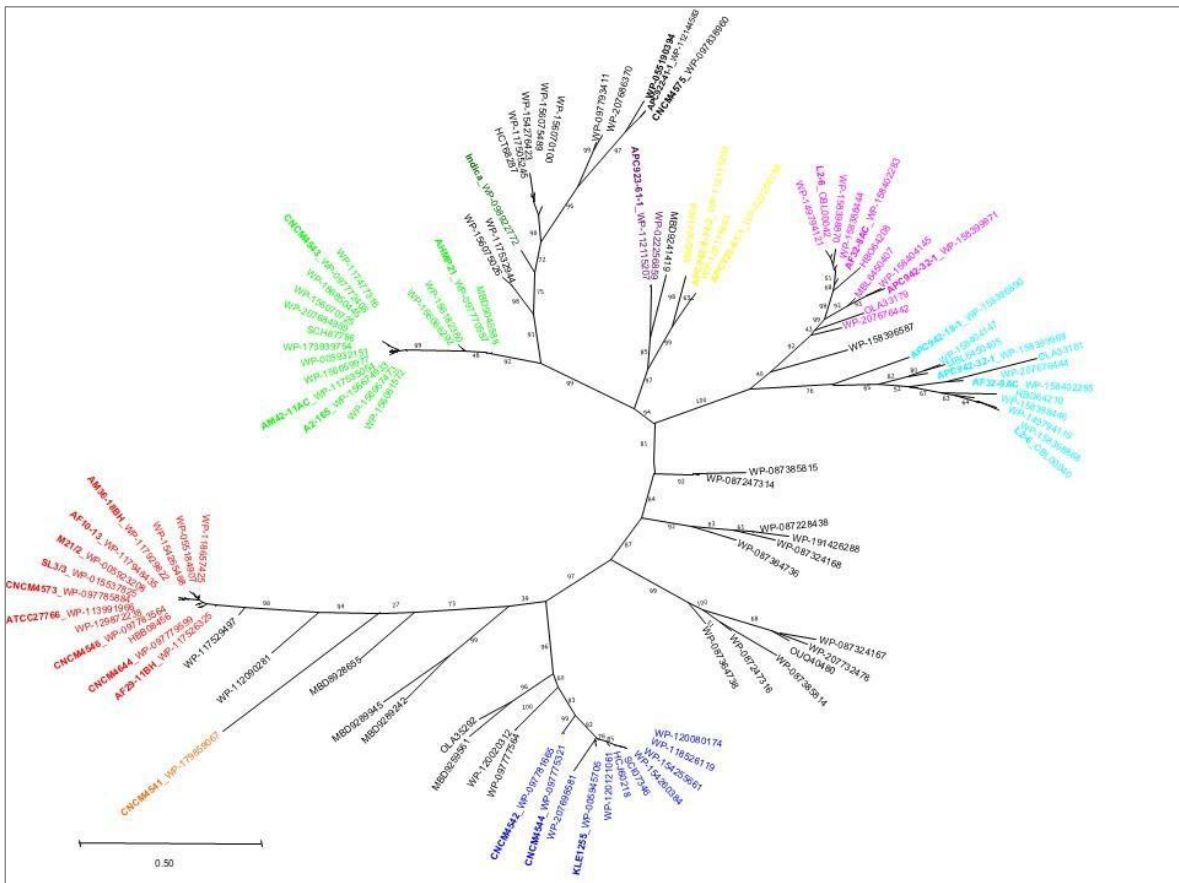
Figure 14. Phylogenetic tree of MAM proteins across 10 distinct clans. Each branch represents a unique evolutionary lineage, with clusters grouped by color to signify their respective family affiliations. Branch lengths reflect evolutionary distances, and bootstrap values (on nodes) indicate the confidence of branch placements. Source: Auger et al, 2021.

3.11.3. Anti-inflammatory potential

After the identification of MAM peptides in the supernatant, the effects of MAM were evaluated *in vitro* by transfecting epithelial cell lines, including HEK293T, MD2-TLR4-CD14 HEK293T, and intestinal HT29 cells. It was revealed that MAM influences the NF-κB signaling cascade, inhibiting this pro-inflammatory pathway. Additionally, in a mouse model of DNBS-induced colitis, the bacterium *L. lactis* was engineered to deliver MAM cDNA directly to the intestinal mucosa, facilitating localized MAM expression. This approach significantly alleviated disease symptoms, as evidenced by reduced weight loss, lower disease activity scores, and decreased secretion of pro-inflammatory cytokines IL17A and IFN-γ[304].

Later, the immunomodulatory effects of MAM were investigated *in vivo* by transfecting its cDNA, driven by a eukaryotic promoter, into transgenic mice engineered to express luciferase under the control of the NF-κB promoter. These mice were subjected to chemically induced colitis using either DSS or DNBS. In the DNBS-induced colitis model, MAM effectively inhibited NF-κB activation, as evidenced by a reduction in luminescence. Additionally, MAM suppressed the production of pro-inflammatory cytokines in mesenteric lymph nodes (MLN) and colon tissue, including IL17, IFNγ, and IL5. Notably, in colon tissue, significant decreases in IL17 and IL5 were detected. In the DSS-induced colitis model, MAM further demonstrated anti-inflammatory effects by reducing the levels of IL17 and IFNγ in MLN and IL6 in colonic tissue, reinforcing its role in mitigating inflammation *in vivo*[305].

Another study aimed to evaluate the anti-inflammatory properties diversity of MAM from several strains. HEK 293 cells were engineered to express luciferase under the NF-κB promoter, activated by Carma 1 cDNA, and co-transformed with MAM cDNA in the eukaryotic expression to evaluate the anti-inflammatory properties of different MAM variants. A broad range of anti-inflammatory activity was observed among the species/strains evaluated. For example, MAM from *F. prausnitzii* CNCM4541 did not inhibit NF-κB responses, while *F. prausnitzii* M21/2 showed the highest inhibition level. *F. duncaniae* A2-165 had an average inhibition capacity of about 40% (Figure 15). In the same study, *L. lactis* was used to deliver a eukaryotic expression plasmid containing MAM from both A2-165 and M21/2 in models of acute and chronic DNBS-induced colitis. In the acute colitis model, MAM from M21/2 significantly reduced macroscopic damage scores, whereas MAM from A2-165 showed no notable effect. In the chronic colitis model, both MAM variants improved macroscopic scores; however, MAM from M21/2 was more effective in preventing weight loss. Such results were crucial to highlight the variable anti-inflammatory properties of MAM from different

strains/species, highlighting the complexity of mechanisms related to the *Faecalibacterium* towards the host[303].
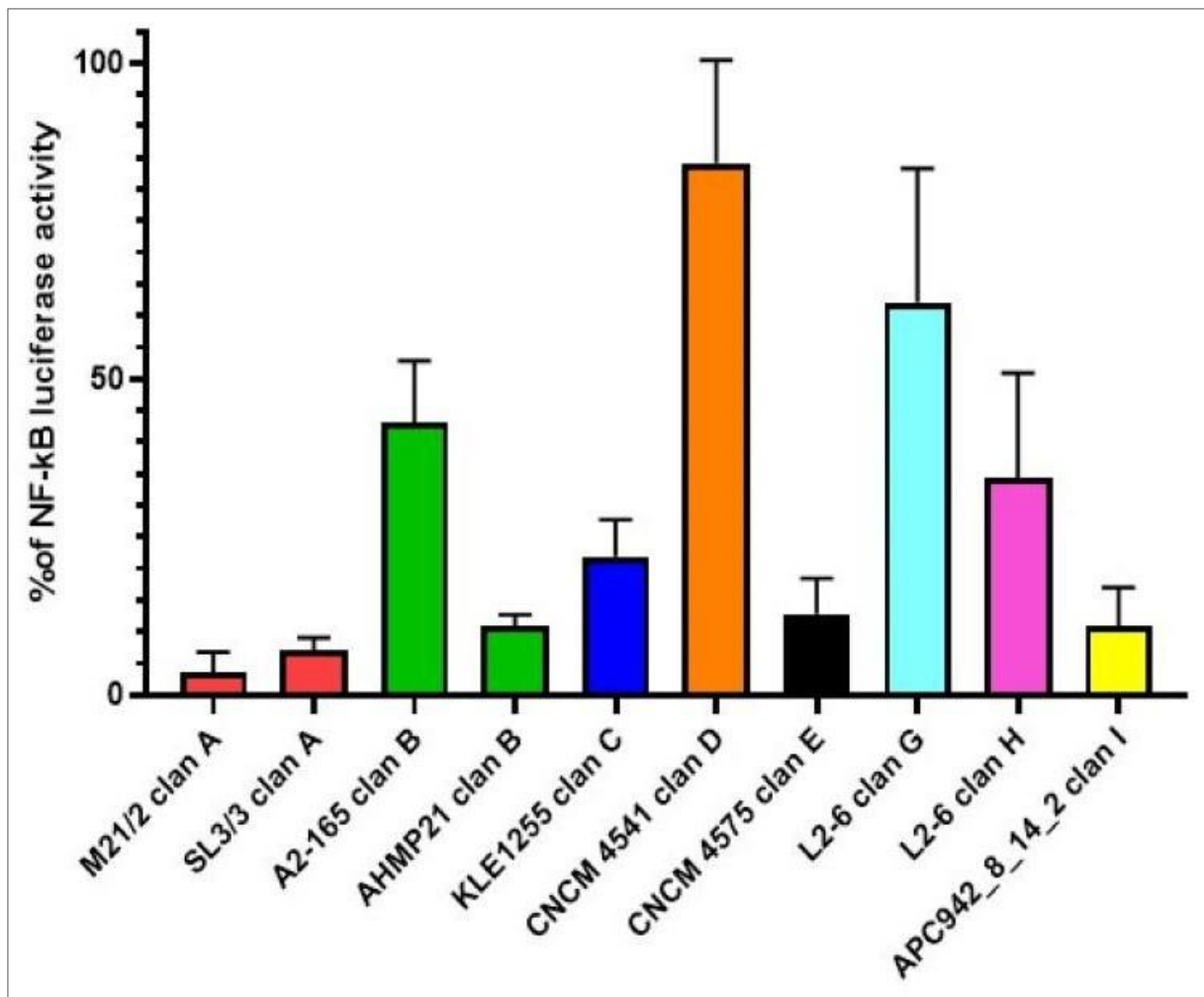
Figure 15. MAM variable activity between variants**.** The bar graph represents the percentage of NF-κB luciferase activity inhibition by MAM proteins derived from different *Faecalibacterium* variants (clans A to I). Each bar corresponds to a specific MAM variant and colors refer from the clans in the phylogenetic tree. Source: Auger et al, 2021.

This section highlights the significant anti-inflammatory and protective effects of F. duncaniae, particularly regarding MAM, in gut inflammatory conditions. However, these findings have been derived primarily from indirect assays due to the challenges associated with obtaining purified MAM. Moreover, this section evidences the limited understanding of MAM's physiological characteristics and its role within the *Faecalibacterium* genus, describing essential gaps regarding the properties and activity of this protein.

3.12. Bacterial cell envelope components of gut commensals: effects in host-microbe interaction

The current pivotal role of effector molecules, such as butyrate, EVs, and MAM, in mediating the health-promoting effects of *F. duncaniae* is evident. However, these molecules' precise mechanisms and structural features remain poorly characterized. These findings highlight the necessity of a deeper exploration into the identification of molecular and structural aspects of *F. duncaniae*'s effector molecules, including MAM. This leads to the next section, which examines bacterial cell envelope components, a central yet underexplored player in shaping host-microbe interactions. This investigation is particularly important among gut commensals, as they represents a promising candidate for and potential therapeutic targets in the context of intestinal inflammation.

Review

Bacterial cell envelope components of gut commensals: effects in host-microbe interaction

Thaís Vilela Rodrigues[1,2], Luís Lima de Jesus[1,2], Philippe Langella[2], Siomar de Castro Soares[3], Gwénaël Jan[4], Vasco Ariston de Carvalho Azevedo[1], and Jean-Marc Chatel[2]*

[1] Federal University of Minas Gerais, Institute of Biological Sciences, Belo Horizonte, Minas Gerais, Brazil.

[2] Université Paris-Saclay, INRAE (National Institute for Agriculture, Food, and Environment), AgroParisTech, MICALIS, Jouy-en-Josas, France.

[3] Federal University of Triângulo Mineiro, Institute of Biological and Natural Sciences, Uberaba, Minas Gerais, Brazil.

[4] INRAE, STLO, Institut Agro, Rennes, France.*****

Corresponding author: jean-marc.chatel@inrae

Abstract: The bacterial cell envelope is a complex structure composed of proteins, lipids, and other molecules that form the physical boundary between bacteria and the environment. In the gut microbiome, commensal bacteria play a fundamental role in maintaining intestinal homeostasis and modulating host physiology. Due to their strategic location, bacterial cell envelope components interact directly with the host immune system, intestinal cells, mucus, and other gut structures, leading to diverse biological effects. Even though beneficial bacteriaproduce effector molecules, the functional diversity of these molecules, especially among gut bacteria, remains largely unknown. This review compiles current knowledge on the structure and function of bacterial cell envelope components, with a specific focus on gut microbiome commensals and their role in host interactions. It highlights key molecules and mechanisms involved in these interactions and emphasizes the need for further research. Understanding these molecular interactions is crucial for identifying novel biotherapeutic targets, particularly in the context of inflammatory bowel diseases and other gut-related disorders. By addressing existing knowledge gaps, this review contributes to a deeper understanding of how bacterial cell envelope components shape host-microbe interactions.

Keywords: Bacterial Cell envelope, surface bacterial components, gut microbiota, host interaction, commensal

1. Introduction

The human gastrointestinal tract harbors a vast microbial community known as the gut microbiome, which includes bacteria, archaea, viruses, and fungi that coexist symbiotically and play a crucial role in host homeostasis and metabolism[1]. Among these microorganisms, commensal bacteria are the most abundant group and establish mutualistic relationships that benefit the host without causing harm, contributing to intestinal homeostasis and overall health [2]. These commensal bacteria are essential for key physiological processes, including nutrient metabolism, immune modulation, and protection against pathogens[3].

The colon, in particular, harbors the highest density of bacteria in the human body, accounting for approximately 70% of the body's total microbiota. The predominant bacterial phyla include Firmicutes and Bacteroidetes, followed by Actinobacteria, Proteobacteria, Fusobacteria, and Verrucomicrobia[4] Key genera, such as *Akkermansia*, *Faecalibacterium*, *Bifidobacterium*, *Bacteroides* and *Roseburia,* show potential as next-generation probiotics (NGP) due to their critical roles in health and disease prevention[5]. Dysbiosis, or microbial imbalance, is a condition in which a disrupted gut microbiota leads to abnormal host-microbiome interactions, compromising the mucosal barrier, enabling systemic microbial dissemination, and heightening susceptibility to infections and immune dysregulation. These disruptions are linked to diseases such as inflammatory bowel disease (IBD), diabetes, and cancer[1,6].

Host-microbiome communication involves various microbial molecules, including metabolites like short-chain fatty acids, secreted proteins, peptides, and bacterial cell envelope components[7,8]. Large-scale studies, including the Human Microbiome Project (HMP) and enterotype studies[9–11], have significantly advanced our understanding of microbial diversity.[12] In spite of successful efforts to characterize microbiota composition, it remains imperative to identify the key molecules influencing host-microbiota interactions, as well as their immunogenic and beneficial properties. The mechanisms of effector molecules mediating host interactions are relatively well-characterized in model organisms such as *Lactobacillus spp.* and *Bifidobacterium spp.*[13–15]. However, considering the broad diversity of gut microbiota species much less is known about other gut commensals' molecular components and their interchange pathways with the host[16–18].

Bacterial cell envelope components are strategically positioned at the interface between bacteria and the host. These molecules serve as the first point of contact, playing fundamental roles in resilience and growth, immune recognition, adhesion, colonization of the intestinal mucosa, and cellular signaling[7,19]. These molecules act as crucial mediators of localized host- microbiome recognition and immune modulation by interacting with pattern recognition receptors (PRRs) on epithelial and immune cells[20].

2. The bacterial cell envelope

The bacterial cell envelope is a complex, multi-layered structure that provides protection, regulates nutrient diffusion, and mediates bacterial interactions with the environment. Traditionally, bacteria are classified as Gram-positive or Gram-negative based on their envelope characteristics: Gram-positive bacteria have a thick peptidoglycan layer. In contrast, Gram-negative bacteria possess both a thin peptidoglycan layer and an outer membrane (OM) (Figure 1)[21]. Despite the widespread use of this dichotomy, recent studies have revealed diverse cell envelope organizations that deviate from these categories, including additional layers such as intra-cytoplasmic membranes and S-layers, composed of proteins, lipids, and other components yet to be further explored[22].

The structural diversity of bacterial cell envelopes reflects their adaptability to different ecological niches and environmental pressures, including fluctuations in temperature, osmolarity, and biochemical conditions[23]. Beyond these structural functions, the cell envelope, being the primary interface for bacterial interactions with the host and other microbes, plays a central role in adhesion, immune recognition, and colonization[7,24]. This section provides an

overview of the key components and organization of the cell envelope, focusing on features relevant to host-commensal interactions.

2.1. Cell envelope organization and components

The bacterial cell envelope consists of multiple layers, including the inner membrane (IM), peptidoglycan (PG) layer, and, in Gram-negative bacteria, the OM. Each of these components has unique structural and functional roles that contribute to bacterial survival and host interactions.

Inner Membrane

The inner membrane, also known as the cytoplasmic membrane, is a phospholipid bilayer embedded with transmembrane proteins and lipoproteins. It facilitates envelope biogenesis, metabolism, protein secretion, and nutrient transport, serving as the foundation for cell envelope assembly[22,25].

Outer Membrane

Exclusive to Gram-negative bacteria, the OM is an asymmetric lipid bilayer with lipopolysaccharides (LPS) in its outer leaflet and phospholipids in the inner leaflet. This structure forms a robust permeability barrier, incorporating LPS, lipoproteins, and porins to regulate nutrient diffusion and environmental sensing[25].

Peptidoglycan

The peptidoglycan layer is a mesh-like structure composed of glycan chains cross-linked by peptides, providing shape and rigidity to the bacterial cell. In Gram-negative bacteria, it is thin and located within the periplasmic space, while in Gram-positive bacteria, it is much thicker (10–30 times thicker) and cross-linked to provide additional stability. This layer is critical for bacterial growth, septation, and survival under environmental stress[23,26].

Teichoic Acids (TAs)

Teichoic acids are anionic polymers unique to Gram-positive bacteria, where they are either covalently attached to the peptidoglycan (wall teichoic acids, WTAs) or anchored to the membrane (lipoteichoic acids, LTAs). These molecules contribute to structural integrity, ion transport, and interactions with host tissues, making them key components in adhesion and immune modulation[27].

Surface Polysaccharides (PSA)

Polysaccharide layers, including capsular polysaccharides (CPS) and exopolysaccharides (EPS), form the outermost interface of bacterial cells. These carbohydrate structures are critical for adhesion, biofilm formation, and immune evasion. Their structural diversity allows bacteria to adapt to varying environments and mediate host interactions.[27]

Pili and Fimbriae

Pili and fimbriae are proteinaceous appendages that facilitate bacterial adhesion to host cells and mediate aggregation with other bacteria. These structures contribute to bacterial

colonization and biofilm formation, playing a crucial role in the persistence and resilience of commensal bacteria within host-associated environments[28].

S-Layers

S-layers are proteinaceous two-dimensional arrays that coat the cell surface in some Gram-positive and Gram-negative bacteria. These layers provide structural support, mediate adhesion, and protect against environmental stress. While not present in all bacteria, S-layers are significant in certain commensal species, where they facilitate host colonization and immune interactions[29,30].
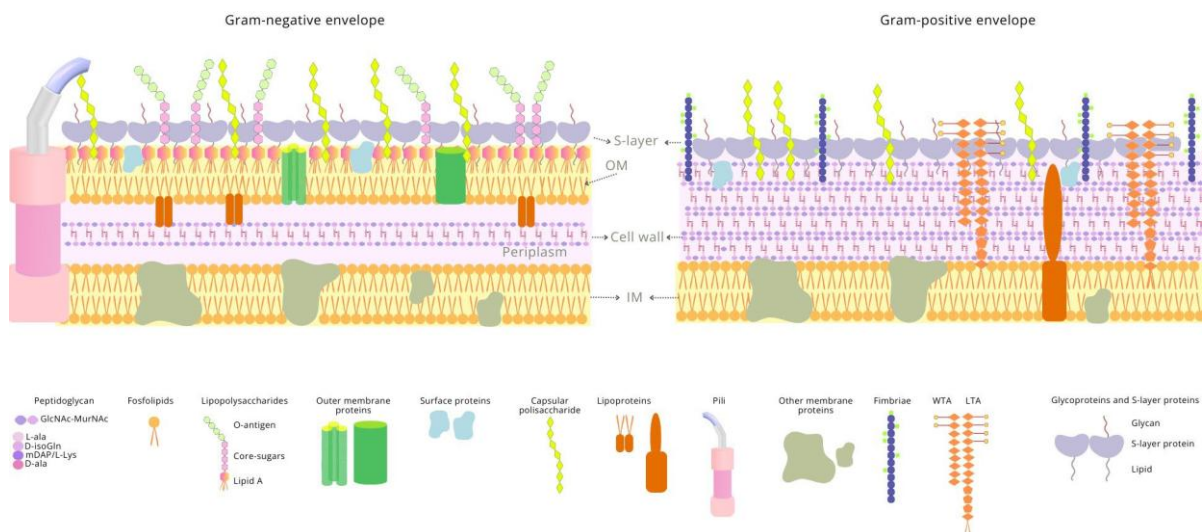
Figure 1. Structural components of Gram-positive and Gram-negative bacterial cell envelopes.

The figure illustrates on the left, the Gram-negative envelope having exclusive components such as the OM with associated LPS, the periplasm, and a thin PG layer. On the right, the envelope of Gram-positive bacteria evidences its thicker PG cell wall and other components, such as TA, fimbriae, and CPS. Below the cell envelope representations, a copy of each one of the elements and their respective names is shown. Created using Canva (www.canva.com)

3. host receptors for envelope molecule identification

The intestinal lumen harbors trillions of bacterial cells that are in constant interaction with intestinal epithelial cells (IECs) and immune cells, triggering innate and adaptive immune responses. These responses vary based on the microbiota community and can range from pro-inflammatory to anti-inflammatory outcomes.[31]

To maintain immune balance, the host must accurately detect and respond to microbial signals. This is achieved through PRRS, which serves as a key immune sensor by recognizing bacterial cell envelope components. The recognition of these microbial components is mediated by PRRs such as Toll-like receptors (TLRs), NOD-like receptors (NLRs), and C-type lectin receptors (CLRs)[32]. These receptors detect conserved microbial molecular patterns, known as microbe-associated molecular patterns (MAMPs), including PG, proteins, LTA, and LPS.

The activation of PRRs triggers intracellular signaling pathways that regulate both host immunity and intestinal barrier integrity, ensuring a balanced immune response and microbial homeostasis[33,34]. While MAMPs are structurally conserved across pathogens and commensals, PRRs rely on additional factors, such as molecular modifications and host-derived signals, to distinguish between harmful and beneficial microbes. Even subtle structural variations in microbial components can shape immune activation pathways, influencing the downstream immunological response[7].

PRRs thus function cooperatively to detect commensal-associated molecules, promoting tolerogenic immune responses that reinforce gut barrier function, modulate immune activity, and prevent excessive inflammation. However, disruptions in PRR signaling can shift this balance, leading to uncontrolled immune activation. Dysregulated PRR activity, often influenced by gut microbiota alterations, has been implicated in chronic inflammatory conditions such as IBD[32,35].

Below, we provide an overview of the primary receptors involved in the bacteria-host interactions.

3.1. Toll-like receptors (TLRs)

TLRs are critical immune sensors that detect molecular patterns associated with microorganisms. They play a fundamental role in distinguishing between commensal and pathogenic bacteria in the intestine by recognizing specific bacterial cell envelope components and modulating the host immune response[36].

TLRs are among the most well-characterized classes of PRRs. These receptors comprise transmembrane proteins with an extracellular leucine-rich repeat (LRR) domain responsible for ligand binding and an intracellular Toll/interleukin-1 receptor (TIR) domain, which mediates downstream signaling[37]. These receptors are localized on the cell surface or within intracellular compartments, within IECs, and innate immune cells. TLR may recognize various MAMPs, including lipoproteins, peptidoglycan, LTA, or glycoproteins. Upon activation, TLRs relay signals to the cell's interior via various adaptor molecules, including Myeloid differentiation primary-response protein 88 (MyD88). This activation of downstream intracellular signaling pathways triggers immune responses, producing inflammatory markers such as cytokines, anti-microbial peptides (AMPs), and tight junction proteins[38].

TLRs play a critical role in combating pathogenic infections and maintaining a balanced interaction between the host and its commensal microbiota. Despite continuous exposure to TLR ligands in the gut lumen, IECs express low baseline levels of TLRs. This controlled expression helps maintain tolerance to commensal bacteria and prevents unnecessary inflammation. However, TLR expressions are upregulated during pathogenic infections, with TLR2, TLR4, TLR5, and TLR9 being particularly responsive[39]. Therefore, TLR signaling must be carefully regulated in the gut epithelium. In response to TLR activation, proteins such as Toll-interacting protein (Tollip), A20, and SIGIRR (Single immunoglobulin interleukin-1 receptor-related molecule are upregulated and act as negative regulators, preventing prolonged or excessive TLR activation and mitigating the risk of inflammation in response to commensal bacteria[40–42].

Disruption of the equilibrium between TLR signaling and gut microbiota can lead to immune dysregulation and the development of various diseases. For example, the expression of TLR4 and TLR2 is demonstrated to be increased in the intestinal mucosa of patients with ulcerative colitis (UC), which leads to the activation of the TLR/Nuclear factor kappa B (NF-κB) signaling pathway and to the subsequent release of pro-inflammatory cytokines. This increased activation is also associated with changes in the gut microbiota, including an overrepresentation of pathogenic bacteria such as *Enterobacteriaceae* and *Streptococcus*, as well as alterations in beneficial species like *Faecalibacterium*[43,44]. Although the correlation between TLR activation and IBD is well established, the precise molecular mechanisms through which specific bacterial components trigger TLR-mediated inflammation remain to be fully elucidated[45].

3.2. NOD-like receptors (NLRs)

NODs constitute another key family within the PPRs. NLRs are located in the cytoplasm of various cell types, including IEC and immune cells such as macrophages, lymphocytes, and dendritic cells[46]. NLRs possess an N-terminal interaction domain, which may be a CARD (Caspase Recruitment Domain) or PYRIN domain. This N-terminal interaction domain is followed by a central NOD domain and a C-terminal LRR domain[47].

NODs are critical receptors of the components of the intestinal innate immune system, contributing to the activation of key immune pathways, such as NF-κB and MAPK (Mitogen-Activated Protein Kinase). These receptors cooperate with TLR signaling to promote the production of cytokines in response to bacterial infections but are also essential for regulating tolerance to commensal bacteria. In this context, NOD1 signaling in dendritic cells promotes their maturation into a tolerogenic state that produces cytokines such as interleukin-10 (IL10). IL10 facilitates the differentiation of regulatory T cells (Tregs), which are crucial for preventing excessive immune reactions against commensals[48,49].

NLRs maintain intestinal barrier integrity and modulate interactions in the interface host-microbiota through signaling pathways involving caspase-1, RIPK2 (Receptor-interacting protein kinase 2), and NF-κB signaling[50]. Specific NLRs have distinct roles in maintaining gut homeostasis. For instance, NLRP6 promotes *Akkermansia muciniphila* colonization and protects against colitis by enhancing IL18 expression, which is essential for epithelial repair and mucosal integrity[51]. Similarly, NLRP3 regulates IL1β and IL18 production to facilitate epithelial proliferation and immune modulation[50,52].

NLRs play another important role in gut homeostasis by detecting bacterial membrane vesicles (BMVs) produced by commensal and probiotic bacteria. Through the activation of NOD1 and NOD2 receptors, these vesicles modulate immune responses by inducing cytokine production, including anti-inflammatory IL10, contributing to maintaining a balanced immune environment in the gut[53].

Dysregulation of NLRs, such as NOD2 and NLRP3, has been closely linked to intestinal inflammation and IBD, interfering in microbiota composition and epithelial barrier function[54]. NOD2 deficiency was associated with impaired Paneth cell bactericidal activity and increased intestinal inflammation, driven by reduced antimicrobial peptide production and dysregulated commensal bacteria[55]. Additionally, NLRP12 supports gut homeostasis by suppressing

excessive inflammatory cytokines, including IL6 and IL1β, and maintaining protective commensal strains[56].

Nevertheless, excessive or impaired NRLs activity may lead to inflammation and tissue damage. Despite advancements in understanding NLRs in IBD, their precise roles remain controversial, and further research is needed to clarify the biochemical mechanisms underlying their activation[50].

3.3. C-type lectin receptors (CLRs)

CLRs form a diverse superfamily of transmembrane or soluble PRRs primarily expressed by myeloid cells, such as dendritic cells and macrophages[57]. This family includes receptors like DC-SIGN (dendritic cell-specific ICAM-3-grabbing non-integrin), Dectin-1, Dectin-2, Dectin-3, and macrophage-inducible C-type lectin (Mincle). CLRs contain one or more C-type lectin-like domains (CTLDs) that recognize carbohydrate structures, including β-glucans, mannose-rich glycans, and fucose, which are found on the surface of pathogens, as well as damage-associated molecular patterns (DAMPs) from self-antigens[58,59].

CLRs are well known for their role in recognizing PAMPs, but their interactions with commensal bacteria are still limited[18,60]. Among their properties, the antifungal activity is mediated by Dectin-1, which recognizes β-glucans in *Candida albicans*, while Dectin-2 detects fungal α-mannans. These protective interactions are particularly important during dysbiosis, helping to prevent the overgrowth of harmful species and maintain immune homeostasis[61].

Mincle and Dectin-3 are involved in responses to both bacterial and fungal ligands. For example, Mincle recognizes bacterial glycolipids from *Listeria monocytogenes* and *Escherichia coli*, both associated with inflammatory diseases such as Crohn's disease[62]. Similarly, Dectin-3 plays a role in antifungal immunity and colitis protection, highlighting its potential contribution to gut immune regulation[62].

The recognition of microbial molecules by host receptors such as CLRs, TLRs, and NLRs demonstrated the complexity of host-microbe interactions in the gut. Despite the progress made in the relations of those key recognition molecules towards gut commensals, there is still a long way to go to determine what the molecules involved in this recognition are, especially when they share similarities with pathogens. In the next section, we delve into the specific components of the bacterial cell envelope, exploring their structural roles and the mechanisms by which they influence host physiology and immunity.

4. Bacterial cell envelope molecules and host effects

Bacterial surface molecules are key to this host-microbe communication, as they constitute the first point of contact with the host. In this context, unlike pathogens[63] and well-characterized probiotic species,[8,64,65] the functional properties of the cell envelope structures of commensal bacteria remain relatively underexplored in the scientific literature[19,66,67].

In this section, we focus exclusively on specific cell envelope molecules that play a defined role in host-commensal interactions. By narrowing our scope to molecules with a known mechanism of action in host modulation, we aim to highlight their effects on immunity, gut barrier integrity, and homeostasis. This approach does not aim to discuss all bacteria with

probiotic or commensal properties exhaustively but rather to provide a molecular perspective on the mediators involved in these interactions and their specific contributions to the host.
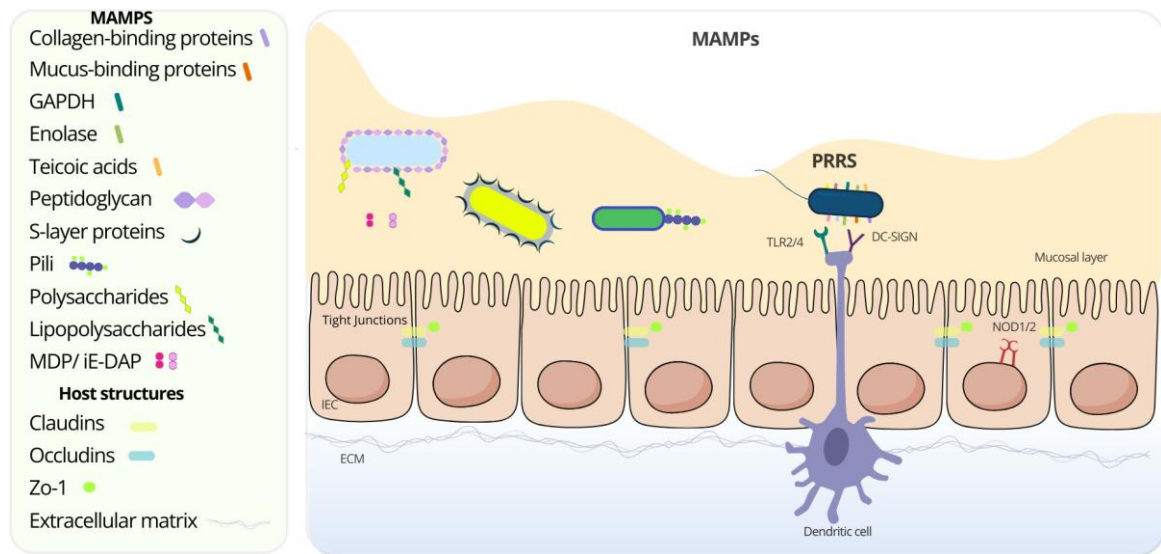
Figure 2. MAMPs from gut microbiota in association with the host intestinal mucosa receptors.

This figure depicts the interaction of bacterial MAMPs with the intestinal mucosa. It illustrates various bacterial surface molecules, including collagen-binding proteins, mucus-binding proteins, GAPDH, enolase, teichoic acids, peptidoglycan, S-layer proteins, pili, polysaccharides, lipopolysaccharides, and MDP/iE-DAP. The intestinal epithelial layer consists of IECs, and tight junctions, which include Claudins, Occludins, and Zo-1. A dendritic cell extends projections below the epithelium. The ECM is shown beneath the epithelium, and the mucosal layer is represented at the apical side of the epithelial barrier in yellow. Host PRRs, including Toll-like receptors (TLR2/4), DC-SIGN, and NOD1/2, are displayed. Created using Canva (www.canva.com)

4.1. Peptidoglycan in host interaction

PG is one of the most abundant components in the bacterial cell wall. It contributes to gut homeostasis and immune processes, including gut-brain axis signaling and stress responses[68]. Microbiota-derived PG was found to be systemically correlated with innate immune response regulation. PG, as well as its constitutive small molecules: Myramyl dipeptide (MDP), N-Acetylglucosamine (NAG), and γ-D-glutamyl-meso-Diaminopimelic acid (iE-DAP), induce signals via several innate immune receptors[69]. PG can be recognized on the bacterial surface, or its fragmented molecules can disseminate through the host intestinal barrier, leading to a variable range of responses through its recognition, from physiologic to pathogenicity effects[70].

The role of TLR2 in recognizing PG remains a topic of debate. While some studies suggest that PG is a ligand for TLR2, others argue that lipoproteins or LTA, which co-purify with PG, are the actual TLR2 ligands[71]. Supporting this, further purification of PG has been shown to diminish TLR2 activation, indicating that PG alone may not be sufficient to trigger TLR2 signaling[72]. However, soluble PG from penicillin-treated bacteria has been reported to activate TLR2 and induce TNF production in macrophages[73,74]. Additionally, muramyl tripeptides and muramyl tetrapeptides have been found to bind TLR2 *in vitro*, and highly purified PG from various Gram-positive and Gram-negative bacteria can activate human monocyte MonoMac6 cells[74].

Adding complexity, a study on *Bacillus anthracis* demonstrated that PG-induced pro-inflammatory cytokine production required its internalization and degradation, suggesting an additional regulatory mechanism[69]. These conflicting findings likely stem from variations in PG structure across bacterial species and differences in purification methods. Given that TLR2 plays a key role in recognizing commensals and promoting immune tolerance, it is possible that structural variations in PG influence how commensals modulate host immunity[70,75]. Unlike pathogenic PG, which may trigger inflammatory responses, PG from commensals could contribute to gut homeostasis by fine-tuning TLR2 activation. Further studies are needed to explore whether distinct PG modifications in commensal bacteria influence TLR2 signaling and support immune balance[69,76].

Contrastingly with TLR2, the role of NOD1 and NOD2 in sensing PG is well established. These cytoplasmic receptors recognize specific PG fragments to trigger immune responses[69]. MDP has been well-documented as a minimal immunogenic component of PG. The NOD2 ligand is MDP, covalently bound to L-alanyl-L-glutamate, the first two residues of the PG peptide crosslinker[77]. Interestingly, phosphorylation of muramyl peptides by N-acetylglucosamine kinase (NAGK) at the hydroxyl group of its C6 position, yielding 6-O-phospho-MDP, is required for NOD2 activation[78]. This NOD2 ligand is present in PG from both Gram-negative and Gram-positive bacteria. By contrast, the ligand of NOD1, iE-DAP, is found exclusively in Gram-negative bacteria[79]. The binding of the corresponding ligand to the LRR domain leads to self-oligomerization and recruits serine/threonine protein kinase 2 (RIPK2). This interaction activates two distinct signaling cascades: one leading to NF-κB activation via phosphorylation of its inhibitor, IκBα, mediated by inhibitory kappa B kinase (IKK), and another activating mitogen-activated protein kinase 7 (MAP3K7, formerly TAK1). Both pathways result in the production of inflammatory cytokines and chemokines, amplifying the immune response[80].

In the context on gut microbiota interactions, PG recognition by PRRs like NOD1 demonstrated enhanced neutrophil activity to defend against pathogens, while healthy microbiota depletion showed increased susceptibility[81]. This activation also leads to macrophage activation and the maturation of dendritic cells to drive antigen-specific adaptive immune response[47]. In addition, PG fragments from *A. muciniphila* were found to activate both NOD1 and NOD2, despite structural modifications like NAG and N-acetylmuramic acid (MurNAc). This indicates that *A. muciniphila* PG effectively triggers innate immune responses through these receptors, indicating an effect of those molecules in host interactions[82].

As an alternative, PG fragments may be targeted to NOD receptors via different transporter-independent mechanisms. Indeed, NOD ligands may be delivered into the cell via bacterial secretion systems, pore-forming toxins, or extracellular vesicles (EVs)[83]. EVs are described as molecular cargos and may contain envelope constituents, including PG. Hence, PG from non-invasive commensal bacteria may be delivered to cytosolic NODS through EVs internalized via endocytosis[84].

Thus, those studies indicate PG as a key and ample component of host-microbe interactions. Still, much remains unknown about how the host recognizes and interprets its structural variations to drive either pro- or anti-inflammatory responses.

4.2. Surface polysaccharides (PSA) in host interaction

4.2.1. EPS and CPS

Commensal gut bacteria, including *Lactobacilli*[85] and *Bifidobacterium* strains,[86] as well as in species such as *Ruminococcus gnavus*[87]*,* and *F. prausnitzii* strain HTF-F,[88] are notable producers of PSA, especially EPS. These biopolymers play critical roles in bacterial colonization, gut health, immune modulation, and interactions with host cells, having great importance in probiosis[89–92].

Among these*, Bacteroides fragilis* produces the zwitterionic polysaccharide (ZPS) known for its immunomodulatory properties[93]. ZPS carry both positive and negative charges, allowing them to interact uniquely with the host immune system, promoting immunological balance and reducing inflammation[94]. In an *in vivo* study, dendritic cells (DCs) presented surface polysaccharides to CD4+ T cells, leading to Foxp3+ Treg activation, IL10 secretion, and CD39 expression while suppressing pro-inflammatory Th17 and Th2 responses and inducing TH1 cytokines like IFN-γ (Interferon gamma)[95–97]. Similarly, ZPS TP2 from *B. fragilis* strain ZY-312 showed protective effects in a DNBS-induced colitis model and supported the colonization of beneficial gut commensals, including *Faecalibacterium*, and *Ruminococcaceae*[96,98].

In an IBD model, *B. fragilis* PSA demonstrated a protective effect, requiring IL10-producing CD4+ T cells to suppress pro-inflammatory IL17 and TNF production in intestinal immune cells, thereby preventing leukocyte infiltration in colonic tissues[99]. Studies further show that PSA induces cytokine production via TLR2-dependent mechanisms[100,101], emphasizing the essential role of PSA-producing commensal bacteria in immune regulation.

Beyond *Bacteroides*, Bifidobacterium-derived EPS has also shown significant immunomodulatory effects. The EPS from *B. longum* BCRC 14634 enhanced macrophage proliferation and IL10 secretion while counteracting LPS-induced TNF-α production and growth inhibition of macrophages. This EPS also demonstrated antimicrobial activity against infectious bacteria. These findings suggest that EPS may function as a mild immune modulator, supporting both immune regulation and antimicrobial defense[102]. In contrast, a mutant for CPS/EPS gene cluster in *B. longum* strain 150-A was efficiently able to bind human intestinal cells. At the same time, the wild-type could not attach to those cells and resisted macrophage internalization, indicating that EPS plays a key role in bacterial attachment and colonization in the gut[103].

The importance of EPS in immune modulation was further demonstrated in studies with *B. breve* UCC2003. Animals treated with EPS-positive strains did not induce an accumulation of pro-inflammatory immune cells such as natural killer (NK) cells or neutrophils, in contrast to EPS-deficient strains, which triggered a stronger immune response. Additionally, mice treated with EPS-deficient *B. breve* exhibited higher levels of IL12, IFN-γ, and TNF-α-positive T cells, suggesting that EPS may help *B. breve* evade excessive host immune activation, while its absence provokes a heightened adaptive immune response[104,105]. Regarding other species, the EPS of *B. longum* 35624 was associated with the prevention of exacerbated immune responses triggered by Th17 cells, and the EPS from *B. bifidum* induces the generation of T-reg cells[106].

The gut commensal *Ruminococcus gnavus* also produces different EPS depending on the strain. These molecules can induce different quantities and types of pro- and anti-inflammatory

cytokines, including IL6 and IL10, and modulate the NF-κB pathway observed in monocytes. This process was demonstrated to involve signaling via immune receptors such as TLR4[87].

Regarding *Lactobacilli,* their EPS constitutes a key molecule in the formation of biofilm and cross-talk with the host, although duality between pro and anti-inflammatory activity is observed. Different strains of *Lactobacillus* produce EPSs with varying capacities to stimulate pro-inflammatory cytokines such as TNF-α, IL6, and IL12, as well as the anti-inflammatory cytokine IL10[107]. As an example, the EPS116 from *L. plantarum* NCU116 was associated with improvements in intestinal barrier function by enhancing the expression of Occludin and Zonula Occludens (ZO-1) through the regulation of the STAT3 pathway in both *in vitro* and *in vivo* models, ultimately protecting mice from colitis[108].

Together, these findings highlight the diverse immunomodulatory roles of EPS from different gut commensals, reinforcing their potential to maintain gut homeostasis, modulate host immunity, and even offer therapeutic benefits against inflammatory diseases.

4.2.2. LPS

Although LPS is widely studied for its pro-inflammatory properties, it is also involved in antagonistic interactions within the gut microbiota, influencing immune modulation. Commensal bacteria, particularly species from the Bacteroidetes phylum, contribute to nearly 80% of LPS identified in healthy adults[109,110]. This suggests that a delicate balance exists between LPS and mucosal immune mechanisms under normal conditions, allowing tolerance to LPS-containing commensals without excessive inflammation[111].

A key factor in commensal LPS immunomodulation is lipid A modification. Bacteroides species, unlike enterobacterial LPS producers, exhibit hypoacylation and hypophosphorylation of the diglucosamine core, reducing TLR4 activation and LPS toxicity[112]. This structural adaptation, driven by the enzyme LpxF, removes a phosphate group from lipid A, decreasing negative surface charge, which limits AMP binding and dampens immune stimulation[113].

This distinct lipid A modification has been described across several Bacteroides species, influencing their interaction with the immune system. For instance, *B. fragilis* LPS signals through a CD14/MD2-dependent TLR4 pathway but does not activate TLR2, contrary to previous claims. Instead, this structural divergence balances immune responses, promoting gut homeostasis rather than excessive inflammation[114].Similarly, *Bacteroides vulgatus* mpk LPS has been shown to function as a weak agonist of the MD-2/TLR4 receptor complex, mitigating intestinal inflammation in colitis models. Unlike highly immunostimulatory LPS from proteobacteria, BVMPK induces semi-mature CD11c+ cells in the lamina propria, modulating inflammatory responses without triggering excessive immune activation[115].

Another example is *Bacteroides dorei* LPS, which exhibits significantly reduced TLR4-mediated immune activation compared to *E. coli* LPS. Studies show that *B. dorei* LPS fails to stimulate NF-κB-dependent cytokines (IL10, TNF-α, IL1β, and IL6) in immune cells, whereas *E. coli* LPS induces a strong pro-inflammatory response[116]. These findings reinforce that Bacteroides-derived LPS plays a regulatory role in gut immunity rather than acting as a classical endotoxin[117]. In another study, the immunomodulatory effects of Bacteroides LPS are further demonstrated by *B. fragilis* HCK-B3 and *Bacteroides ovatus* ELH-B2, which counteract LPS-

induced inflammation by reducing TNF-α and increasing IL10 production. Together, such studies demonstrate how *Bacteroides* strains contribute to gut homeostasis by preserving intestinal barrier integrity and restoring the Treg/Th-17 balance, thereby preventing excessive immune activation[118].

More broadly, gut commensal LPS contributes to immune crosstalk, regulating host responses. Hennezel et al. demonstrated that LPS from gut-resident microbes antagonizes the TLR4-NF-κB pathway, effectively inhibiting inflammatory cytokine production[119]. In contrast, LPS from pathogenic *E. coli* is highly immunostimulatory, inducing TNF, IL1β, and IL6 via TLR4-NF-κB activation[120]. These findings highlight that microbiome-derived LPS can facilitate host tolerance to gut microbes, preventing excessive immune activation[121].

LPS is a key modulator of gut immune balance, but its effects vary widely depending on its structural composition. These findings reinforce the functional divergence of LPS among gut commensals, where modifications in lipid A structure influence bacterial persistence, host-microbe interactions, and intestinal homeostasis. Notably, elevated LPS levels in the blood of IBD patients have been observed, but whether this is due to gut barrier dysfunction or other processes remains unclear[122,123]. Understanding these diverse LPS functions is essential for unraveling how gut microbiota shape immune homeostasis and inflammation regulation.

4.2.3. Lipoteichoic acids (LTA) in host interaction

Among the earliest studied MAMP involved in host-microbe crosstalk is LTA, a major structural component of the Gram-positive bacterial cell wall. Known for its role in inducing inflammatory responses, LTA binds to TLR2 and forms a heterodimer with TLR6, CD14, and CD36 (also referred to as GP4), which function as co-receptors[124].

Despite its immunostimulatory nature, LTA from commensal bacteria plays an important role in immune tolerance. TLR2 activation by commensal LTA induces antimicrobial activity in skin mast cells, promoting host defense mechanisms at epithelial barriers[125]. Considering the elevated population of Gram-positive bacteria harboring LTA in the intestinal content, human IECs have adapted as LTA-unresponsive cells, which allows tolerance towards these MAMP, thus avoiding excessive inflammatory response[126]. This tolerance mechanism includes the downregulation of TLR2 co-receptors and the upregulation of Tollip, which inhibits TLR2 signaling. However, macrophages remain highly responsive to LTA, where TLR2 activation plays a key role in immune regulation[127].

The effects of LTA on inflammation vary among commensal species, with different Lactobacillus strains showing contrasting immunomodulatory properties. In a colitis model, *L. rhamnosus* GG worsened dextran sulfate sodium (DSS)-induced colitis in mice. At the same time, its *dltD* mutant disrupted D-alanylation of LTA, hampering LTA biosynthesis, reduced disease severity, and downregulated TLR2 expression and inflammatory cytokines[128]. Furthermore, LTA from *L. rhamnosus* has been shown to induce both pro- and anti-inflammatory cytokines in DCs and T cells, demonstrating a complex role in immune modulation[129].

Contrastingly, LTA from *L. plantarum* has been shown to suppress excessive pro-inflammatory cytokine production, which is in line with the demonstrated ability of an *L. plantarum* lysate to

reduce the severity of DSS-induced colitis in rats[130]. Additionally, a mutant of *L. plantarum* with reduced D-alanine incorporation in TA induced higher IL10 production in peripheral blood mononuclear cells (PBMCs), resulting in greater protection against TNBS (2,4,6-trinitrobenzene sulfonic acid)-induced colitis compared to its wild-type (WT) counterpart[131]. Similarly, LTA from *L. paracasei* was found to ameliorate age-related intestinal permeability ("leaky gut") and inflammation in mice[132].

These findings highlight that TA and LTA structure and function vary widely among commensal and probiotic bacteria, influencing their immune-modulatory roles. While some LTA molecules drive inflammation, others support immune regulation and gut homeostasis, emphasizing bacterial surface components' complex and strain-specific effects in host interactions.
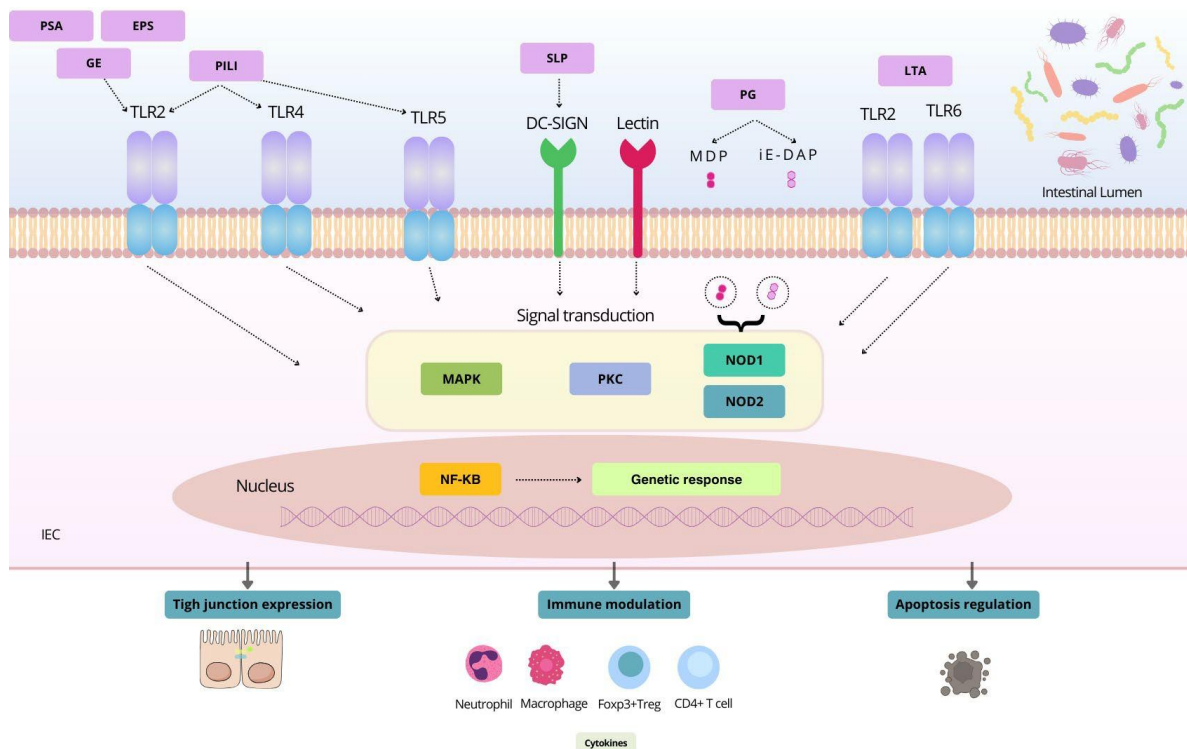
Figure 3. Immunological signaling pathways activated by MAMPs in the intestinal mucosa

This image illustrates an IEC highlighting the main immunological pathways activated by bacterial MAMPs. Various bacterial components, including PSA, EPS, glycolytic enzymes, pili, PG, S-layer protein (SLPs), and LTA, interact with key PRRs such as TLR2, TLR4, TLR5, TLR6, as well as lectins and DC-SIGN. Upon recognition, these receptors initiate signal transduction pathways like MAPK, PKC, and NOD1/2, which activate transcription factors such as NF-κB. This leads to genetic responses influencing tight junction expression, immune modulation (impacting neutrophils, macrophages, Foxp3+ Tregs, and CD4+ T cells), cytokine production, and apoptosis regulation. Created using Canva (www.canva.com)

4.3. Surface proteins in host interaction

4.3.1. Glycolytic enzymes and moonlighting proteins

Glycolytic enzymes, central to energy metabolism, catalyze the conversion of glucose to pyruvate, generating ATP (Adenosine triphosphate), a fundamental process in living organisms[133,134]. Beyond their well-known metabolic role, these enzymes have been found to perform diverse functions, including transcriptional regulation, apoptosis control, and cell mobility. In gut commensal bacteria, they are also involved in adhesion to host tissues, revealing an intriguing aspect of their multifunctionality[135].

Glycolytic enzymes in gut commensals, particularly enolase (ENO) and Glycoceraldehyde 3-phosphate dehydrogenase (GAPDH), engage in non-metabolic processes like adhesion and interaction with the host. These "moonlighting" proteins- initially known for their intracellular functions, have been identified on the cell surface of various gut-associated bacteria, drive metabolic processes, and facilitate the colonization of the gut mucosa, a critical factor in host-microbe interactions[136–138]. In addition to glycolytic enzymes, other moonlighting proteins, such as elongation factors (EF-Tu and EF-G), hydrolases, chaperones, synthetases, and mutases, have been associated with host-microbe interactions[139].

In *Bifidobacterium* species (*B. lactis*, *B. bifidum*, and *B. longum),* ENO functions as a surface receptor for human plasminogen, suggesting a role in host interaction. Other proteins, such as Bile salt hydrolase and Dna K, respectively, glutamine synthetase and phosphoglycerate mutase, were also linked to plasminogen binding in the genus[140]. Similarly, the alpha-enolase of *L. plantarum* LM3 has been shown to bind type I collagen[141]. Moreover, GAPDH adhesive activity was observed in *L. plantarum* LA 318, binding human colonic mucin, potentially hampering pathogens' attachment in the gut through a competitive behavior[142].

Other Lactobacillus species have been found to express moonlighting proteins that contribute to adhesion and gut homeostasis. In *L. johnsonii* MG, GAPDH has been demonstrated to specifically bind to junctional adhesion molecule-2 (JAM-2) in Caco-2 cells, where it restores damaged tight junctions[143]. Additionally, in *L. johnsonii* NCC533, elongation factor EF-Tu was identified on the bacterial surface, where it binds to intestinal epithelial cells and mucins, functioning as an adhesin-like factor[144]. Another study with the same strain identified heat shock protein GroEL as a surface-associated protein capable of binding to mucins and epithelial cells while also stimulating IL8 production via a CD14-mediated mechanism, suggesting a role in gut homeostasis[145].

Beyond their adhesive properties, those moonlighting proteins in gut commensals, such as *Lactobacillus*, have also been linked to immunomodulatory activities, though further studies are needed to clarify their precise mechanisms[146].

These multifunctional roles of moonlighting proteins in gut microbiota-host interactions, particularly in adhesion to the intestinal mucosa, facilitate bacterial colonization and contribute to gut homeostasis. Given that some moonlighting proteins are shared between commensals and pathogens, understanding their binding mechanisms may provide insights into microbiota stability and competitive exclusion. Nevertheless, the processes by which these proteins are secreted and anchored to the bacterial surface remain to be determined.

4.3.2. Pili

Proteinaceous appendages on the bacterial cell surface, including flagella, fimbriae, and pili, are widespread in bacterial communities[19]. Pili are key molecules involved in host-microbiota communication because of their adhesive and immunomodulatory properties. They interacts with macrophages, being recognized by TLR2 receptors also regulating pro- and anti-inflammatory cytokine production. Among them, Type IV pili (T4P) plays a significant role[147].Genomic analyses of gut microbiota species have revealed that approximately 30–45% of tested bacterial species harbor the necessary genes for Type IV pili (T4P) production[19].

In human intestinal cell assays, the presence of pili promoted bacterial attachment and was associated with reduced IL8 mRNA expression, indicating an indirect anti-inflammatory effect[148,149.] In the commensal *L. rhamnosus* GG (LGG), pili facilitate attachment to intestinal cells and interactions with the mucus layer. Notably, strains lacking the SpaCBA pili system genetic region show reduced adhesive capacities[150].

Moreover, post-translational modifications of pili in Gram-positive bacteria, particularly glycosylation, are commonly mediated by sortases. In *L. rhamnosus* GG (LGG), glycan modifications in SpaCBA pili have been shown to interact with the DC-SIGN lectin on human dendritic cells. These glycan-associated MAMPs trigger distinct signaling pathways, where mannose residues activate TLRs and promote pro-inflammatory cytokine production, whereas fucose induces IL10 responses while inhibiting IL6 and IL12 secretion[147].

Another study with human fetal ileal organ culture and IECs, demonstrated that the SpaC of *L. rhamnosus* (ATCC 53013) modulates host immune responses by reducing TLR4 expression and downregulating IL1β-induced IL6 secretion, contributing to anti-inflammatory effects in IECs[151].

In Bifidobacterium species, pili have been identified as critical for gut colonization and host interaction. In *B. breve* UCC2003, the *tad* locus (Type IVb tight adherence pili) is conserved across strains and is essential for murine gut colonization[152]. Additionally, TadE, a structural component of Tad pili, was found to induce intestinal epithelial cell proliferation, and although the underlying mechanisms remain unclear, evidence suggests that TLR receptors may be involved in this process[153].

Similarly, in *B. bifidum* PRL2010, pili play an essential role in bacterium-host interactions. Using *L. lactis* as an expression system, pil3PRL2010 pili showed significant adhesion to Caco-2 cells, while pil2PRL2010 did not, demonstrating species- and substrate-specific adhesion properties. Bifidobacterium pili also bind to ECM proteins, such as fibronectin, plasminogen, and laminin, with their immunomodulatory effects varying by species. In *B. bifidum* PRL2010, pili induced TNF-α production while reducing IL10, indicating a role in immune modulation[154].

Pili-like structures in *A. muciniphila* have been also identified, encoded by the surface-exposed Amuc_1100 protein, which induces TLR2 signaling and cytokine production (IL6, IL8, and IL10) in PBMCs, suggesting an immune-regulatory function.[155] Since *A. muciniphila* recognizes N-acetyllactosamine for O-glycan attachment, further research is needed to determine whether pili contribute to this adhesion mechanism.[156]

Another example of bacterial appendages is the F1C fimbriae from *E. coli* Nissle 1917, which is a key factor in the adhesiveness to abiotic or biotic environments. This property is crucial in

biofilm formation and commensal colonization[157]. The recognition of those molecules by the host cell is mediated by receptors such as TLR4, responding to fimbriae from both commensal and pathogenic bacteria. In *E. coli*, fimbriae can engage distinct co-receptors and adaptor proteins within lipid rafts, triggering signaling pathways that influence bacterial clearance. In commensals, these interactions often promote beneficial colonization, strengthening the gut barrier and modulating immune responses[158].

4.3.3. Collagen-binding proteins (CBP) and S-layer proteins

The stable attachment of bacteria to host tissues is a critical step for gut colonization and immune modulation. Gut commensal bacteria use surface proteins like CBPs and SLPs as adhesive mediators, which play essential roles in their interaction with the host's intestinal epithelium[159]. The ECM, rich in components such as collagen, laminin, fibronectin, and mucin, provides surfaces for bacterial adhesion. Collagen, particularly type V, is abundant in the intestinal mucosa and facilitates bacterial adherence[160]. CBPs mediate direct interactions with ECM components and, together with SLPs, they have a dual purpose: they favor adhesion to the host's tissues and protect against pathogens, thus contributing to the maintenance of gut homeostasis[159,161].

Many *Lactobacillus* isolates demonstrate collagen-binding capabilities through various adhesin proteins, including CBP, which has been linked to colonization processes that reduce pathogen attachment[159]. For instance, *L. reuteri* expresses the mucus adhesion-promoting protein (MapA), which binds to mucus, collagen type I, and Caco-2 cells[162]. Similarly, CBPs derived from *L. plantarum* Lp91 have shown strong adhesive capacity and the ability to inhibit *E. coli* O157 attachment to human type I collagen *in vitro*[159].

SLPs play pivotal roles in protecting the intestinal barrier, inhibiting pathogen colonization, and interacting with host cells. A well-characterized example is *L. acidophilus*, which possesses a complex S-layer composed of major SLPs (SlpA, SlpB, and SlpX). SlpA (S-layer protein A) functions as a commensal ligand that binds to DC-SIGN receptors, promoting a Th2 immune response[163]. *L. acidophilus*, or its purified SlpA, has been shown to protect mice from inflammation and dysbiosis in a murine colitis model. This effect is mediated by the recognition of the SLPa by a C-lectin receptor called SIGNR3 (specific intracellular adhesion molecule-3 grabbing non-integrin homolog-related 3)[164]. *L. acidophilus* NCFM's SLP has been also shown to reduce the production of IL-1β, TNF-α, and reactive oxygen species in LPS-stimulated macrophages by inhibiting the MAPK and NF-κB signaling pathways[165]. In another study, the SLP isolated from *L. acidophilus* CICC 6074 activates pro-inflammatory pathways such as MAPK and NF-κB. However, PKC inhibition was also observed, suggesting that this effect can be modulated and reveal a potential duality in its immune function.[166] The S-layer from *L. brevis* was described to recognize the receptor CLR mincle. The interaction triggers signaling cascades that induce both pro- and anti-inflammatory cytokine responses, particularly IL10[167]

Beyond immune modulation, SLPs contribute to the maintenance of gut barrier integrity. For instance, *L. acidophilus* NCFM's SLP has been associated with maintaining gut barrier integrity in a TNF-α-induced inflammatory model using Caco-2 cells. Notably, these protective effects were absent in SIGNR3-deficient mice[165]. Moreover, it enhanced the expression of tight junction proteins ZO-1 and Occludin in Caco-2 cells subjected to TNF-α-induced inflammation,

leading to reduced NF-κB pathway activation, decreased IL8 production, and prevented apoptosis[168]. S-layer beneficial properties have been also observed in *L. plantarum.* SLPs enhanced tight junctions, reduced permeability, and increased transepithelial resistance (TEER) in response to enteropathogenic *E. coli*[169]. In *Bifidobacterium*, two surface proteins from *B. adolescentis* BB-119, with molecular masses of 36 kDa and 52 kDa, bind to type V collagen via galactose chains, facilitating bacterial adhesion through lectin-like activity[170]. The protective effects of *L. acidophilus* SLPs have also been demonstrated against pathogens such as *Salmonella typhimurium.* In Caco-2 cells, SLP were associated with blocking signaling pathways like ERK1/2, JNK, and p38, thus reducing IL8 secretion and preserving gut barrier integrity.[171]

Other gut microbiota members also utilize SLPs for pathogens protection. *Propionibacterium freudenreichii*, a gut microbiota member commonly found in breast-fed infants, has been linked to protection against necrotizing enterocolitis[172]. These properties were indicated to tightly rely on surface-extractable proteins,[173] including SLPs and other factors such as InlA and LspA[65]. SlpB and SlpE from *P. freudenreichii* were shown to play a key role in the induction of IL10 in PBMCs[174]. Additionally, *P. freudenreichii* has been shown to inhibit LPS-induced IL8 expression in HT-29 enterocytes, whereas its ΔslpB mutant lacks this ability, highlighting the role of SlpB in mitigating intestinal inflammation and damage in murine models of mucositis[175].

Taken together, collagen-binding proteins and SLP serve as critical mediators of host-microbe interactions, playing essential roles in bacterial adhesion, immune modulation, and gut barrier integrity.

4.3.4. Mucus-binding proteins

The intestinal mucosal layer is a protective matrix coating epithelial cells, protecting against pathogens while supporting gut commensals adhering and thriving within the microbiota. Bacterial adherence to mucus involves nonspecific interactions and mucus-binding proteins (MUBs) on the bacterial surface[176]. Though not fully understood, these proteins binding mucosal carbohydrates represent a key mechanism for bacterial adherence[177].

In several *Lactobacillus* species, MUBs facilitate attachment to the mucosal matrix[178]. The MUB protein from *L. acidophilus* NCFM attaches to intestinal cells and mucin[179]. In the commensal *L. reuteri*, mucus adhesins, including MUB and CmbA, exert immunomodulatory effects on human monocyte-derived dendritic cells, hence modulating the production of anti- and pro-inflammatory cytokines IL10, TNF-α, IL1ß, IL6, and IL12. Purified *L. reuteri* MUB binds to CLRs, inducing Th1-polarized immune responses associated with increased IFN-γ production[180,181].

In the context of mucus-binding proteins, studies on *B. bifidum* ATCC 15696 have highlighted the role of the extracellular sialidase SiaBb2 in enhancing mucosal adhesion. This enzyme facilitates the utilization of human milk oligosaccharides and mucin-derived carbohydrates, promoting bacterial adhesion to both human epithelial cells and mucosal surfaces, thereby reinforcing host-microbe interactions[15]. Several *B. bifidum* strains demonstrated the capacity to produce a surface enzyme called transaldolase (Tal). The protein demonstrated autoaggregative properties with a binding capacity to mucin, suggesting participation in gut colonization[182].

Moreover, several mucus-binding proteins that are also moonlighting proteins were identified in EVs derived from *B. longum* NCC2705. The proteins were phosphoketolase, GroEL, EF-Tu, phosphoglycerate kinase, Tal, and heat shock protein 20 (Hsp20)

Finally, regarding the NGP *A. muciniphila*, proteins involved in binding O-glycans on mucins were identified. Throughout the activity of neuraminidases, those glycans are exposed to the attachment to mucin-binding proteins, an essential mechanism for bacterial colonization[183].

5. Concluding remarks

This review has explored the structural and functional diversity of bacterial cell envelope components, emphasizing their pivotal roles as mediators in host-microbiota interactions. These molecules form the primary interface between commensal bacteria and the host, influencing adhesion, immune modulation, and gut homeostasis. Their ability to interact with intestinal epithelial cells, immune receptors, and the mucus layer is evidence of their importance in shaping host physiology.

Despite significant advances in microbiota research, our understanding of the molecular mechanisms and specific effector molecules driving host-microbe communication remains limited, particularly for the lesser-studied commensals. Especially regarding the emerging NGP, characterized molecular effectors derived from those gut bacteria can confer targeted health benefits with critical biotherapeutic applications. Moreover, a deeper understanding of these molecular effectors is crucial for elucidating fundamental host-microbe interactions. Structural and comparative analyses, including advanced techniques such as cryo-electron microscopy, molecular docking simulations, and targeted mutagenesis, can provide insights into ligand-receptor interactions. Synthetic biology and molecular engineering approaches also offer promising avenues to enhance bacterial surface component knowledge, enabling the rational design of probiotics with optimized immunomodulatory properties.

Furthermore, culture-independent techniques, such as metagenomics, transcriptomics, and proteomics, continue to reveal new bacterial effectors and their functional roles. Integrating these approaches with *in vivo* and *in vitro* models will be fundamental across molecular characterization and clinical applications.

With a focus on these bacterial effectors, this review reinforces the importance of future efforts in the characterization of those molecules, especially among less-studied commensals and the emerging NGP. Understanding the molecular signatures of commensal-host interactions will provide essential advances for innovative therapeutic strategies targeting inflammatory diseases, metabolic disorders, and gut health restoration. Those future investigations will support the expansion of the therapeutic potential of commensal bacteria, transforming our ability to modulate the gut microbiota for precision medicine applications.

Interest statement

All authors declare no competing financial or non-financial interests.

Acknowledgments

References

1.   Hou, K. *et al.* Microbiota in health and diseases. *Signal Transduction and Targeted Therapy 2022 7:1* **7**, 1–28 (2022).

2.   Haque, S. Z. & Haque, M. The ecological community of commensal, symbiotic, and pathogenic gastrointestinal microorganisms – an appraisal. *Clin Exp Gastroenterol* **10**, 91 (2017).

3.   Kern, L., Abdeen, S. K., Kolodziejczyk, A. A. & Elinav, E. Commensal inter-bacterial interactions shaping the microbiota. *Curr Opin Microbiol* **63**, 158–171 (2021).

4.   Rinninella, E. *et al.* What is the Healthy Gut Microbiota Composition? A Changing Ecosystem across Age, Environment, Diet, and Diseases. *Microorganisms* **7**, 14 (2019).

5.   O'Toole, P. W., Marchesi, J. R. & Hill, C. Next-generation probiotics: the spectrum from probiotics to live biotherapeutics. *Nature Microbiology 2017 2:5* **2**, 1–6 (2017).

6.   Shan, Y., Lee, M. & Chang, E. B. The Gut Microbiome and Inflammatory Bowel Diseases. *Annu Rev Med* **73**, 455 (2022).

7.   Lebeer, S., Vanderleyden, J. & De Keersmaecker, S. C. J. Host interactions of probiotic bacterial surface molecules: comparison with commensals and pathogens. *Nat Rev Microbiol* **8**, 171–184 (2010).

8.   Sengupta, R. *et al.* The Role of Cell Surface Architecture of Lactobacilli in Host-Microbe Interactions in the Gastrointestinal Tract. *Mediators Inflamm* **2013**, 237921 (2013).

9.   Arumugam, M. *et al.* Enterotypes of the human gut microbiome. *Nature* **473**, 174–180 (2011).

10.   Huttenhower, C. *et al.* Structure, function and diversity of the healthy human microbiome. *Nature* **486**, 207–214 (2012).

11.   Proctor, L. M. *et al.* The Integrative Human Microbiome Project. *Nature 2019 569:7758* **569**, 641–648 (2019).

12.   Rajilić-Stojanović, M. & de Vos, W. M. The first 1000 cultured species of the human gastrointestinal microbiota. *FEMS Microbiol Rev* **38**, 996–1047 (2014).

13.   Muscariello, L., De Siena, B. & Marasco, R. Lactobacillus Cell Surface Proteins Involved in Interaction with Mucus and Extracellular Matrix Components. *Curr Microbiol* **77**, 3831–3841 (2020).

14.   Salazar, N., Gueimonde, M., de los Reyes-Gavilán, C. G. & Ruas-Madiedo, P. Exopolysaccharides Produced by Lactic Acid Bacteria and Bifidobacteria as Fermentable Substrates by the Intestinal Microbiota. *Crit Rev Food Sci Nutr* **56**, 1440–1453 (2016).

15.   Gavzy, S. J. *et al.* Bifidobacterium mechanisms of immune modulation and tolerance. *Gut Microbes* **15**, (2023).

16. Zheng, D., Liwinski, T. & Elinav, E. Interaction between microbiota and immunity in health and disease. *Cell Research 2020 30:6* **30**, 492–506 (2020).

17. Cohen, L. J. *et al.* Functional metagenomic discovery of bacterial effectors in the human microbiome and isolation of commendamide, a GPCR G2A/132 agonist. *Proc Natl Acad Sci U S A* **112**, E4825–E4834 (2015).

18. Tytgat, H. L. P. & de Vos, W. M. Sugar Coating the Envelope: Glycoconjugates for Microbe–Host Crosstalk. *Trends Microbiol* **24**, 853–861 (2016).

19. Ligthart, K., Belzer, C., de Vos, W. M. & Tytgat, H. L. P. Bridging Bacteria and the Gut: Functional Aspects of Type IV Pili. *Trends Microbiol* **28**, 340–348 (2020).

20. van Hensbergen, V. P. & Hu, X. Pattern recognition receptors and the innate immune network. *Molecular Medical Microbiology, Third Edition* 407–441 (2024) doi:10.1016/B978-0-12-818619-0.00131-3.

21. Viljoen, A., Foster, S. J., Fantner, G. E., Hobbs, J. K. & Dufrêne, Y. F. Scratching the surface: bacterial cell envelopes at the nanoscale. *mBio* **11**, (2020).

22. Beaud Benyahia, B., Taib, N., Beloin, C. & Gribaldo, S. Terrabacteria: redefining bacterial envelope diversity, biogenesis and evolution. *Nat Rev Microbiol* **23**, (2025).

23. Silhavy, T. J., Kahne, D. & Walker, S. The Bacterial Cell Envelope. *Cold Spring Harb Perspect Biol* **2**, (2010).

24. Caselli, M. *et al.* Structural Bacterial Molecules as Potential Candidates for an Evolution of the Classical Concept of Probiotics. *Advances in Nutrition* **2**, 372–376 (2011).

25. Lithgow, T., Stubenrauch, C. J. & Stumpf, M. P. H. Surveying membrane landscapes: a new look at the bacterial cell surface. *Nature Reviews Microbiology 2023 21:8* **21**, 502–518 (2023).

26. Sibinelli-Sousa, S., Hespanhol, J. T. & Bayer-Santos, E. Targeting the achilles' heel of bacteria: Different mechanisms to break down the peptidoglycan cell wall during bacterial warfare. *J Bacteriol* **203**, 478–498 (2021).

27. Limoli, D. H., Jones, C. J. & Wozniak, D. J. Bacterial Extracellular Polysaccharides in Biofilm Formation and Function. *Microbiol Spectr* **3**, 10.1128/microbiolspec.MB-0011–2014 (2015).

28. Jin, X. & Marshall, J. S. Mechanics of biofilms formed of bacteria with fimbriae appendages. *PLoS One* **15**, e0243280 (2020).

29. Royer, A. L. M. *et al.* Clostridioides difficile S-Layer Protein A (SlpA) Serves as a General Phage Receptor. *Microbiol Spectr* **11**, (2023).

30. Alp, D., Kuleaşan, H. & Korkut Altıntaş, A. The importance of the S-layer on the adhesion and aggregation ability of Lactic acid bacteria. *Mol Biol Rep* **47**, 3449–3457 (2020).

31. Takiishi, T., Fenero, C. I. M. & Câmara, N. O. S. Intestinal barrier and gut microbiota: Shaping our immune responses throughout life. *Tissue Barriers* **5**, (2017).

32. Li, D. & Wu, M. Pattern recognition receptors in health and diseases. *Signal Transduction and Targeted Therapy 2021 6:1* **6**, 1–24 (2021).

33. Burgueño, J. F. & Abreu, M. T. Epithelial Toll-like receptors and their role in gut homeostasis and disease. *Nature Reviews Gastroenterology & Hepatology 2020 17:5* **17**, 263–278 (2020).

34. Jiao, Y., Wu, L., Huntington, N. D. & Zhang, X. Crosstalk Between Gut Microbiota and Innate Immunity and Its Implication in Autoimmune Diseases. *Front Immunol* **11**, (2020).

35. Abraham, C., Abreu, M. T. & Turner, J. R. Pattern Recognition Receptor Signaling and Cytokine Networks in Microbial Defenses and Regulation of Intestinal Barriers: Implications for Inflammatory Bowel Disease. *Gastroenterology* **162**, 1602-1616.e6 (2022).

36. Le Noci, V. *et al.* Toll Like Receptors as Sensors of the Tumor Microbial Dysbiosis: Implications in Cancer Progression. *Front Cell Dev Biol* **9**, 732192 (2021).

37. Sameer, A. S. & Nissar, S. Toll-Like Receptors (TLRs): Structure, Functions, Signaling, and Role of Their Polymorphisms in Colorectal Cancer Susceptibility. *Biomed Res Int* **2021**, (2021).

38. Akira, S. & Takeda, K. Toll-like receptor signalling. *Nature Reviews Immunology 2004 4:7* **4**, 499–511 (2004).

39. Keogh, C. E., Rude, K. M. & Gareau, M. G. Role of pattern recognition receptors and the microbiota in neurological disorders. *Journal of Physiology* **599**, 1379–1389 (2021).

40. Kubinak, J. L. & Round, J. L. Toll-Like Receptors Promote Mutually Beneficial Commensal-Host Interactions. *PLoS Pathog* **8**, e1002785 (2012).

41. Oshima, N. *et al.* A20 is an early responding negative regulator of Toll-like receptor 5 signalling in intestinal epithelial cells during inflammation. *Clin Exp Immunol* **159**, 185–198 (2010).

42. Kowalski, E. J. A. & Li, L. Toll-Interacting Protein in Resolving and Non-Resolving Inflammation. *Front Immunol* **8**, 511 (2017).

43. Xu, N. *et al.* Changes in intestinal microbiota and correlation with TLRs in ulcerative colitis in the coastal area of northern China. *Microb Pathog* **150**, 104707 (2021).

44. Machiels, K. *et al.* A decrease of the butyrate-producing species Roseburia hominis and Faecalibacterium prausnitzii defines dysbiosis in patients with ulcerative colitis. *Gut* **63**, 1275–1283 (2014).

45. Lee, M. & Chang, E. B. Inflammatory Bowel Diseases (IBD) and the Microbiome-Searching the Crime Scene for Clues. *Gastroenterology* **160**, 524–537 (2021).

46. Philpott, D. J., Sorbara, M. T., Robertson, S. J., Croitoru, K. & Girardin, S. E. NOD proteins: regulators of inflammation in health and disease. *Nature Reviews Immunology 2013 14:1* **14**, 9–23 (2013).

47.   Kufer, T. A., Nigro, G. & Sansonetti, P. J. Multifaceted Functions of NOD-Like Receptor Proteins in Myeloid Cells at the Intersection of Innate and Adaptive Immunity. *Microbiol Spectr* **4**, (2016).

48.   Neuper, T. *et al.* NOD1 modulates IL-10 signalling in human dendritic cells. *Scientific Reports 2017 7:1* **7**, 1–12 (2017).

49.   Traxinger, B. R., Richert-Spuhler, L. E. & Lund, J. M. Mucosal tissue regulatory T cells are integral in balancing immunity and tolerance at portals of antigen entry. *Mucosal Immunol* **15**, 398–407 (2022).

50.   Zhou, F. *et al.* NOD-like receptors mediate homeostatic intestinal epithelial barrier function: promising therapeutic targets for inflammatory bowel disease. *Therap Adv Gastroenterol* **16**, (2023).

51.   Seregin, S. S. *et al.* NLRP6 Protects Il10-/- Mice from Colitis by Limiting Colonization of Akkermansia muciniphila. *Cell Rep* **19**, 733–745 (2017).

52.   Liu, Z. *et al.* Role of inflammasomes in host defense against Citrobacter rodentium infection. *J Biol Chem* **287**, 16955–16964 (2012).

53.   Johnston, E. L., Heras, B., Kufer, T. A. & Kaparakis-Liaskos, M. Detection of Bacterial Membrane Vesicles by NOD-Like Receptors. *International Journal of Molecular Sciences 2021, Vol. 22, Page 1005* **22**, 1005 (2021).

54.   Shao, M. *et al.* Artemisinin analog SM934 alleviates epithelial barrier dysfunction via inhibiting apoptosis and caspase-1-mediated pyroptosis in experimental colitis. *Front Pharmacol* **13**, 849014 (2022).

55.   Biswas, A. & Kobayashi, K. S. Regulation of intestinal microbiota by the NLR protein family. *Int Immunol* **25**, 207–214 (2013).

56.   Chen, G. Y. Role of Nlrp6 and Nlrp12 in the maintenance of intestinal homeostasis. *Eur J Immunol* **44**, 321–327 (2014).

57.   Geijtenbeek, T. B. H. & Gringhuis, S. I. Signalling through C-type lectin receptors: shaping immune responses. *Nature Reviews Immunology 2009 9:7* **9**, 465–479 (2009).

58.   Li, T. H., Liu, L., Hou, Y. Y., Shen, S. N. & Wang, T. T. C-type lectin receptor-mediated immune recognition and response of the microbiota in the gut. *Gastroenterol Rep (Oxf)* **7**, 312–321 (2019).

59.   Reis e Sousa, C., Yamasaki, S. & Brown, G. D. Myeloid C-type lectin receptors in innate immune recognition. *Immunity* **57**, 700–717 (2024).

60.   Li, M., Zhang, R., Li, J. & Li, J. The Role of C-Type Lectin Receptor Signaling in the Intestinal Microbiota-Inflammation-Cancer Axis. *Front Immunol* **13**, 894445 (2022).

61.   Li, T. H., Liu, L., Hou, Y. Y., Shen, S. N. & Wang, T. T. C-type lectin receptor-mediated immune recognition and response of the microbiota in the gut. *Gastroenterol Rep (Oxf)* **7**, 312–321 (2019).

62.   Haag, L. M. & Siegmund, B. Intestinal Microbiota and the Innate Immune System - A Crosstalk in Crohn's Disease Pathogenesis. *Front Immunol* **6**, (2015).

63.   Williams, P. Role of the cell envelope in bacterial adaptation to growth in vivo in infections. *Biochimie* **70**, 987–1011 (1988).

64.   Chandhni, P. R. *et al.* Ameliorative Effect of Surface Proteins of Probiotic Lactobacilli in Colitis Mouse Models. *Front Microbiol* **12**, 679773 (2021).

65.   Le Maréchal, C. *et al.* Surface proteins of Propionibacterium freudenreichii are involved in its anti-inflammatory properties. *J Proteomics* **113**, 447–461 (2015).

66.   Nishiyama, K. *et al.* Roles of the Cell Surface Architecture of Bacteroides and Bifidobacterium in the Gut Colonization. *Front Microbiol* **12**, 754819 (2021).

67.   Liu, Q. *et al.* Surface components and metabolites of probiotics for regulation of intestinal epithelial barrier. *Microbial Cell Factories 2020 19:1* **19**, 1–11 (2020).

68.   Gonzalez-Santana, A. & Diaz Heijtz, R. Bacterial Peptidoglycans from Microbiota in Neurodevelopment and Behavior. *Trends Mol Med* **26**, 729–743 (2020).

69.   Wolf, A. J. & Underhill, D. M. Peptidoglycan recognition by the innate immune system. *Nat Rev Immunol* **18**, 243–254 (2018).

70.   Bastos, P. A. D., Wheeler, R. & Boneca, I. G. Uptake, recognition and responses to peptidoglycan in the mammalian host. *FEMS Microbiol Rev* **45**, 1–25 (2021).

71.   Travassos, L. H. *et al.* Toll-like receptor 2-dependent bacterial sensing does not occur via peptidoglycan recognition. *EMBO Rep* **5**, 1000 (2004).

72.   Wolf, A. J. Peptidoglycan-induced modulation of metabolic and inflammatory responses. *Immunometabolism (United States)* **5**, E00024 (2023).

73.   Lu, X. *et al.* Peptidoglycan recognition proteins are a new class of human bactericidal proteins. *J Biol Chem* **281**, 5895–5907 (2006).

74.   Asong, J., Wolfert, M. A., Maiti, K. K., Miller, D. & Boons, G. J. Binding and Cellular Activation Studies Reveal That Toll-like Receptor 2 Can Differentially Recognize Peptidoglycan from Gram-positive and Gram-negative Bacteria. *J Biol Chem* **284**, 8643–8653 (2009).

75.   Ren, C. *et al.* Identification of TLR2/TLR6 signalling lactic acid bacteria for supporting immune regulation. *Sci Rep* **6**, 34561 (2016).

76.   Chen, L. *et al.* Interactions between toll-like receptors signaling pathway and gut microbiota in host homeostasis. *Immun Inflamm Dis* **12**, e1356 (2024).

77.   Girardin, S. E. *et al.* Nod2 is a general sensor of peptidoglycan through muramyl dipeptide (MDP) detection. *J Biol Chem* **278**, 8869–8872 (2003).

78.   Stafford, C. A. *et al.* Phosphorylation of muramyl peptides by NAGK is required for NOD2 activation. *Nature* **609**, 590–596 (2022).

79.   Bharadwaj, R. *et al.* Methotrexate suppresses psoriatic skin inflammation by inhibiting muropeptide transporter SLC46A2 activity. *Immunity* **56**, 998-1012.e8 (2023).

80.   Trindade, B. C. & Chen, G. Y. NOD1 and NOD2 in inflammatory and infectious diseases. *Immunol Rev* **297**, 139–161 (2020).

81.   Clarke, T. B. *et al.* Recognition of peptidoglycan from the microbiota by Nod1 enhances systemic innate immunity. *Nat Med* **16**, 228–231 (2010).

82.   Garcia-Vello, P. *et al.* Peptidoglycan from Akkermansia muciniphila MucT: chemical structure and immunostimulatory properties of muropeptides. *Glycobiology* **32**, 712–719 (2022).

83.   Cañas, M. A., Fábrega, M. J., Giménez, R., Badia, J. & Baldomà, L. Outer membrane vesicles from probiotic and commensal escherichia coli activate NOD1-mediated immune responses in intestinal epithelial cells. *Front Microbiol* **9**, 341347 (2018).

84.   Toyofuku, M., Nomura, N. & Eberl, L. Types and origins of bacterial membrane vesicles. *Nature Reviews Microbiology 2018 17:1* **17**, 13–24 (2018).

85.   Martín, R. *et al.* Over-production of exopolysaccharide by Lacticaseibacillus rhamnosus CNCM I-3690 strain cutbacks its beneficial effect on the host. *Sci Rep* **13**, 6114 (2023).

86.   Salazar, N., Gueimonde, M., Hernández-Barranco, A. M., Ruas-Madiedo, P. & De Los Reyes-Gavilán, C. G. Exopolysaccharides Produced by Intestinal Bifidobacterium Strains Act as Fermentable Substrates for Human Intestinal Bacteria. *Appl Environ Microbiol* **74**, 4737 (2008).

87.   Laplanche, V. *et al.* The human gut symbiont Ruminococcus gnavus displays strain-specific exopolysaccharides modulating the host immune response. *Carbohydr Polym* **347**, 122754 (2025).

88.   Rossi, O. *et al.* Faecalibacterium prausnitzii Strain HTF-F and Its Extracellular Polymeric Matrix Attenuate Clinical Parameters in DSS-Induced Colitis. *PLoS One* **10**, e0123013 (2015).

89.   Hickey, A. *et al.* Bifidobacterium breve Exopolysaccharide Blocks Dendritic Cell Maturation and Activation of CD4+ T Cells. *Front Microbiol* **12**, 653587 (2021).

90.   Laplanche, V. *et al.* The human gut symbiont Ruminococcus gnavus displays strain-specific exopolysaccharides modulating the host immune response. *Carbohydr Polym* **347**, 122754 (2025).

91.   Sims, I. M. *et al.* Structure and functions of exopolysaccharide produced by gut commensal Lactobacillus reuteri 100-23. *The ISME Journal 2011 5:7* **5**, 1115–1124 (2011).

92.   Lee, M. G. *et al.* Potential Probiotic Properties of Exopolysaccharide-Producing Lacticaseibacillus paracasei EPS DA-BACS and Prebiotic Activity of Its Exopolysaccharide. *Microorganisms* **10**, (2022).

93.   Telesford, K. M. *et al.* A commensal symbiotic factor derived from Bacteroides fragilis promotes human CD39+Foxp3+ T cells and Treg function. *Gut Microbes* **6**, 234–242 (2015).

94.   Stephen, T. L., Groneck, L. & Kalka-Moll, W. M. The Modulation of Adaptive Immune Responses by Bacterial Zwitterionic Polysaccharides. *Int J Microbiol* **2010**, 12 (2010).

95.   Ochoa-Repáraz, J. *et al.* Central nervous system demyelinating disease protection by the human commensal Bacteroides fragilis depends on polysaccharide A expression. *J Immunol* **185**, 4101–4108 (2010).

96.   Round, J. L., Mazmanian, S. K. & Flavell, R. A. Inducible Foxp3 + regulatory T-cell development by a commensal bacterium of the intestinal microbiota. doi:10.1073/pnas.0909122107.

97.   Mazmanian, S. K., Cui, H. L., Tzianabos, A. O. & Kasper, D. L. An Immunomodulatory Molecule of Symbiotic Bacteria Directs Maturation of the Host Immune System. *Cell* **122**, 107–118 (2005).

98.   Zheng, L. *et al.* Capsular Polysaccharide From Bacteroides fragilis Protects Against Ulcerative Colitis in an Undegraded Form. *Front Pharmacol* **11**, 570476 (2020).

99.   Mazmanian, S. K., Round, J. L. & Kasper, D. L. A microbial symbiosis factor prevents intestinal inflammatory disease. *Nature 2008 453:7195* **453**, 620–625 (2008).

100.   Wang, Q. *et al.* A bacterial carbohydrate links innate and adaptive responses through Toll-like receptor 2. *J Exp Med* **203**, 2853–2863 (2006).

101.   Round, J. L. *et al.* The Toll-like receptor 2 pathway establishes colonization by a commensal of the human microbiota. *Science* **332**, 974–977 (2011).

102.   Wu, M. H. *et al.* Exopolysaccharide activities from probiotic bifidobacterium: Immunomodulatory effects (on J774A.1 macrophages) and antimicrobial properties. *Int J Food Microbiol* **144**, 104–110 (2010).

103.   Tahoun, A. *et al.* Capsular polysaccharide inhibits adhesion of Bifidobacterium longum 105-A to enterocyte-like Caco-2 cells and phagocytosis by macrophages. *Gut Pathog* **9**, (2017).

104.   Fanning, S., Hall, L. J. & van Sinderen, D. Bifidobacterium breve UCC2003 surface exopolysaccharide production is a beneficial trait mediating commensal-host interaction through immune modulation and pathogen protection. *Gut Microbes* **3**, 420–425 (2012).

105.   Fanning, S. *et al.* Bifidobacterial surface-exopolysaccharide facilitates commensal-host interaction through immune modulation and pathogen protection. *Proc Natl Acad Sci U S A* **109**, 2108–2113 (2012).

106.   Verma, R. *et al.* Cell surface polysaccharides of Bifidobacterium bifidum induce the generation of Foxp3+ regulatory T cells. *Sci Immunol* **3**, (2018).

107.   Marta Ciszek-Lenda, Magdalena Strus, Sabina Górska & Marta Targosz-Korecka. Strain specific immunostimulatory potential of lactobacilli-derived exopolysaccharides. *Central European Journal of Immunology* (2011).

108. Zhou, X. *et al.* Exopolysaccharides from Lactobacillus plantarum NCU116 Regulate Intestinal Barrier Function via STAT3 Signaling Pathway. *J Agric Food Chem* **66**, 9719–9727 (2018).

109. d'Hennezel, E., Abubucker, S., Murphy, L. O. & Cullen, T. W. Total Lipopolysaccharide from the Human Gut Microbiome Silences Toll-Like Receptor Signaling. *mSystems* **2**, (2017).

110. ANGERS, A. *et al.* The Human Gut Microbiota: Overview and analysis of the current scientific knowledge and possible impact on healthcare and well-being. *EUR 29240 EN, Publications Office of the European Union* **902**, 95–108 (2018).

111. Lin, T. L. *et al.* Like Cures Like: Pharmacological Activity of Anti-Inflammatory Lipopolysaccharides From Gut Microbiome. *Front Pharmacol* **11**, 525437 (2020).

112. Chilton, P. M., Hadelq, D. M., To, T. T., Mitchell, T. C. & Darveau, R. P. Adjuvant activity of naturally occurring monophosphoryl lipopolysaccharide preparations from mucosa-associated bacteria. *Infect Immun* **81**, 3317–3325 (2013).

113. Cullen, T. W. *et al.* Antimicrobial peptide resistance mediates resilience of prominent gut commensals during inflammation. *Science (1979)* **347**, 170–175 (2015).

114. Mancuso, G. *et al.* Bacteroides fragilis-derived lipopolysaccharide produces cell activation and lethal toxicity via toll-like receptor 4. *Infect Immun* **73**, 5620–5627 (2005).

115. Steimle, A. *et al.* Weak Agonistic LPS Restores Intestinal Immune Homeostasis. *Molecular Therapy* **27**, 1974–1991 (2019).

116. Mohr, A. E., Crawford, M., Jasbi, P., Fessler, S. & Sweazea, K. L. Lipopolysaccharide and the gut microbiota: considering structural variation. *FEBS Lett* **596**, 849–875 (2022).

117. Vatanen, T. *et al.* Variation in Microbiome LPS Immunogenicity Contributes to Autoimmunity in Humans. *Cell* **165**, 842–853 (2016).

118. Tan, H., Zhao, J., Zhang, H., Zhai, Q. & Chen, W. Novel strains of Bacteroides fragilis and Bacteroides ovatus alleviate the LPS-induced inflammation in mice. *Appl Microbiol Biotechnol* **103**, 2353–2365 (2019).

119. d'Hennezel, E., Abubucker, S., Murphy, L. O. & Cullen, T. W. Total Lipopolysaccharide from the Human Gut Microbiome Silences Toll-Like Receptor Signaling. *mSystems* **2**, e00046-17 (2017).

120. d'Hennezel, E., Abubucker, S., Murphy, L. O. & Cullen, T. W. Total Lipopolysaccharide from the Human Gut Microbiome Silences Toll-Like Receptor Signaling. *mSystems* **2**, (2017).

121. Steimle, A., Autenrieth, I. B. & Frick, J. S. Structure and function: Lipid A modifications in commensals and pathogens. *International Journal of Medical Microbiology* **306**, 290–301 (2016).

122. Rojo, Ó. P. *et al.* Serum lipopolysaccharide-binding protein in endotoxemic patients with inflammatory bowel disease. *Inflamm Bowel Dis* **13**, 269–277 (2007).

123.   Saha, S., Pupo, E., Zariri, A. & Van Der Ley, P. Lipid A heterogeneity and its role in the host interactions with pathogenic and commensal bacteria. *microLife* **3**, 1–13 (2022).

124.   Nilsen, N. J. *et al.* Cellular trafficking of lipoteichoic acid and Toll-like receptor 2 in relation to signaling: role of CD14 and CD36. *J Leukoc Biol* **84**, 280–291 (2008).

125.   Wang, Z., MacLeod, D. T. & Di Nardo, A. Commensal bacteria lipoteichoic acid increases skin mast cell antimicrobial activity against vaccinia viruses. *J Immunol* **189**, 1551–1558 (2012).

126.   Melmed, G. *et al.* Human intestinal epithelial cells are broadly unresponsive to Toll-like receptor 2-dependent bacterial ligands: implications for host-microbial interactions in the gut. *J Immunol* **170**, 1406–1415 (2003).

127.   Underhill, D. M. *et al.* The Toll-like receptor 2 is recruited to macrophage phagosomes and discriminates between pathogens. *Nature* **401**, 811–815 (1999).

128.   Claes, I. J. J. *et al.* Impact of lipoteichoic acid modification on the performance of the probiotic Lactobacillus rhamnosus GG in experimental colitis. *Clin Exp Immunol* **162**, 306–314 (2010).

129.   Friedrich, A. D., Leoni, J., Paz, M. L. & González Maglio, D. H. Lipoteichoic Acid from Lacticaseibacillus rhamnosus GG Modulates Dendritic Cells and T Cells in the Gut. *Nutrients* **14**, (2022).

130.   Ahn, Y. S., Park, M. Y., Shin, J. H., Kim, J. Y. & Kwon, O. Lysate of Probiotic Lactobacillus plantarum K8 Modulate the Mucosal Inflammatory System in Dextran Sulfate Sodium-induced Colitic Rats. *Korean J Food Sci Anim Resour* **34**, 829–835 (2014).

131.   Grangette, C. *et al.* Enhanced antiinflammatory capacity of a Lactobacillus plantarum mutant synthesizing modified teichoic acids. (2005).

132.   Wang, S. *et al.* Lipoteichoic acid from the cell wall of a heat killed Lactobacillus paracasei D3-5 ameliorates aging-related leaky gut, inflammation and improves physical and cognitive functions: from C. elegans to mice. *Geroscience* **42**, 333–352 (2020).

133.   Chaudhry, R. & Varacallo, M. Biochemistry, Glycolysis. *StatPearls* (2023).

134.   Zhang, Y. *et al.* A moonlighting role for enzymes of glycolysis in the co-localization of mitochondria and chloroplasts. *Nature Communications 2020 11:1* **11**, 1–15 (2020).

135.   Kim, J. W. & Dang, C. V. Multifaceted roles of glycolytic enzymes. *Trends Biochem Sci* **30**, 142–150 (2005).

136.   Jeffery, C. J. Moonlighting proteins. *Trends Biochem Sci* **24**, 8–11 (1999).

137.   Jeffery, C. J. Protein moonlighting: what is it, and why is it important? *Philosophical Transactions of the Royal Society B: Biological Sciences* **373**, (2018).

138.   Henderson, B. & Martin, A. Bacterial moonlighting proteins and bacterial virulence. *Curr Top Microbiol Immunol* **358**, 155–213 (2013).

139. Candela, M. *et al.* Bifidobacterial enolase, a cell surface receptor for human plasminogen involved in the interaction with the host. *Microbiology (N Y)* **155**, 3294–3303 (2009).

140. Candela, M. *et al.* Binding of Human Plasminogen to Bifidobacterium. *J Bacteriol* **189**, 5929 (2007).

141. Salzillo, M. *et al.* Identification and characterization of enolase as a collagen-binding protein in Lactobacillus plantarum. *J Basic Microbiol* **55**, 890–897 (2015).

142. Kinoshita, H. *et al.* Cell surface Lactobacillus plantarum LA 318 glyceraldehyde-3-phosphate dehydrogenase (GAPDH) adheres to human colonic mucin. *J Appl Microbiol* **104**, 1667–1674 (2008).

143. Lyu, M., Bai, Y., Orihara, K., Miyanaga, K. & Yamamoto, N. GAPDH Released from Lactobacillus johnsonii MG Enhances Barrier Function by Upregulating Genes Associated with Tight Junctions. *Microorganisms* **11**, 1393 (2023).

144. Granato, D. *et al.* Cell surface-associated elongation factor Tu mediates the attachment of Lactobacillus johnsonii NCC533 (La1) to human intestinal cells and mucins. *Infect Immun* **72**, 2160–2169 (2004).

145. Bergonzelli, G. E. *et al.* GroEL of Lactobacillus johnsonii La1 (NCC 533) is cell surface associated: Potential role in interactions with the host and the gastric pathogen Helicobacter pylori. *Infect Immun* **74**, 425–434 (2006).

146. Hurmalainen, V. *et al.* Extracellular proteins of Lactobacillus crispatus enhance activation of human plasminogen. *Microbiology (Reading)* **153**, 1112–1122 (2007).

147. Tytgat, H. L. P. *et al.* Probiotic Gut Microbiota Isolate Interacts with Dendritic Cells via Glycosylated Heterotrimeric Pili. *PLoS One* **11**, e0151824 (2016).

148. Lebeer, S. *et al.* Functional Analysis of Lactobacillus rhamnosus GG Pili in Relation to Adhesion and Immunomodulatory Interactions with Intestinal Epithelial Cells. *Appl Environ Microbiol* **78**, 185 (2012).

149. Segers, M. E. & Lebeer, S. Towards a better understanding of Lactobacillus rhamnosus GG - host interactions. *Microb Cell Fact* **13**, 1–16 (2014).

150. Tripathi, P. *et al.* Adhesion and nanomechanics of pili from the probiotic lactobacillus rhamnosus GG. *ACS Nano* **7**, 3685–3697 (2013).

151. Ganguli, K. *et al.* Lactobacillus rhamnosus GG and its SpaC pilus adhesin modulate inflammatory responsiveness and TLR-related gene expression in the fetal human gut. *Pediatric Research 2015 77:4* **77**, 528–535 (2015).

152. O'connell Motherway, M. *et al.* Functional genome analysis of Bifidobacterium breve UCC2003 reveals type IVb tight adherence (Tad) pili as an essential and conserved host-colonization factor. doi:10.1073/pnas.1105380108.

153. O'Connell Motherway, M. *et al.* A Bifidobacterial pilus-associated protein promotes colonic epithelial proliferation. *Mol Microbiol* **111**, 287–301 (2019).

154. Turroni, F. *et al.* Role of sortase-dependent pili of Bifidobacterium bifidum PRL2010 in modulating bacterium-host interactions. *Proc Natl Acad Sci U S A* **110**, 11151–11156 (2013).

155. Ottman, N. *et al.* Pili-like proteins of Akkermansia muciniphila modulate host immune responses and gut barrier function. *PLoS One* **12**, e0173004 (2017).

156. Elzinga, J. *et al.* Binding of Akkermansia muciniphila to mucin is O-glycan specific. *Nature Communications 2024 15:1* **15**, 1–10 (2024).

157. Lasaro, M. A. *et al.* F1C Fimbriae Play an Important Role in Biofilm Formation and Intestinal Colonization by the Escherichia coli Commensal Strain Nissle 1917. *Appl Environ Microbiol* **75**, 246 (2009).

158. Fischer, H., Yamamoto, M., Akira, S., Beutler, B. & Svanborg, C. Mechanism of pathogen-specific TLR4 activation in the mucosa: fimbriae, recognition receptors and adaptor protein selection. *Eur J Immunol* **36**, 267–277 (2006).

159. Yadav, A. K. *et al.* Role of surface layer collagen binding protein from indigenous Lactobacillus plantarum 91 in adhesion and its anti-adhesion potential against gut pathogen. *Microbiol Res* **168**, 639–645 (2013).

160. Vaca, D. J. *et al.* Interaction with the host: the role of fibronectin and extracellular matrix proteins in the adhesion of Gram-negative bacteria. *Med Microbiol Immunol* **209**, 277 (2020).

161. Assandri, M. H., Malamud, M., Trejo, F. M. & Serradell, M. de los A. S-layer proteins as immune players: Tales from pathogenic and non-pathogenic bacteria. *Curr Res Microb Sci* **4**, 100187 (2023).

162. MATSUO, Y., MIYOSHI, Y., OKADA, S. & SATOH, E. Receptor-like Molecules on Human Intestinal Epithelial Cells Interact with an Adhesion Factor from Lactobacillus reuteri. *Biosci Microbiota Food Health* **31**, 93–102 (2012).

163. Konstantinov, S. R. *et al.* S layer protein A of Lactobacillus acidophilus NCFM regulates immature dendritic cell and T cell functions. *Proc Natl Acad Sci U S A* **105**, 19474–19479 (2008).

164. Lightfoot, Y. L. *et al.* SIGNR3-dependent immune regulation by Lactobacillus acidophilus surface layer protein A in colitis. *EMBO J* **34**, 881–895 (2015).

165. Wang, H. *et al.* Surface-Layer Protein from Lactobacillus acidophilus NCFM Inhibits Lipopolysaccharide-Induced Inflammation through MAPK and NF-κB Signaling Pathways in RAW264.7 Cells. *J Agric Food Chem* **66**, 7655–7662 (2018).

166. Cai, Z. *et al.* S-layer protein modulates the stimulatory effects of Lactobacillus acidophilus CICC 6074 by triggering PKC signaling cascade in RAW 264.7 cells. *J Funct Foods* **67**, 103841 (2020).

167. Prado Acosta, M. *et al.* S-Layer From Lactobacillus brevis Modulates Antigen-Presenting Cell Functions via the Mincle-Syk-Card9 Axis. *Front Immunol* **12**, 602067 (2021).

168. Wang, H., Zhang, Q., Niu, Y., Zhang, X. & Lu, R. Surface-layer protein from Lactobacillus acidophilus NCFM attenuates tumor necrosis factor-α-induced intestinal barrier dysfunction and inflammation. *Int J Biol Macromol* **136**, 27–34 (2019).

169. Liu, Z., Shen, T., Zhang, P., Ma, Y. & Qin, H. Lactobacillus plantarum surface layer adhesive protein protects intestinal epithelial cells against tight junction injury induced by enteropathogenic Escherichia coli. *Mol Biol Rep* **38**, 3471–3480 (2011).

170. Mukai, T., Toba, T. & Ohori, H. Collagen binding of Bifidobacterium adolescentis. *Curr Microbiol* **34**, 326–331 (1997).

171. Li, P., Yu, Q., Ye, X., Wang, Z. & Yang, Q. Lactobacillus S-layer protein inhibition of Salmonella-induced reorganization of the cytoskeleton and activation of MAPK signalling pathways in Caco-2 cells. *Microbiology (Reading)* **157**, 2639–2646 (2011).

172. Colliou, N. *et al.* Commensal Propionibacterium strain UF1 mitigates intestinal inflammation via Th17 cell regulation. *J Clin Invest* **127**, 3970 (2017).

173. Foligné, B. *et al.* Promising immunomodulatory effects of selected strains of dairy propionibacteria as evidenced in vitro and in vivo. *Appl Environ Microbiol* **76**, 8259–8264 (2010).

174. Deutsch, S. M. *et al.* Identification of proteins involved in the anti-inflammatory properties of Propionibacterium freudenreichii by means of a multi-strain study. *Sci Rep* **7**, (2017).

175. Do Carmo, F. L. R. *et al.* Probiotic Propionibacterium freudenreichii requires SlpB protein to mitigate mucositis induced by chemotherapy. *Oncotarget* **10**, 7198 (2019).

176. Sicard, J. F., Bihan, G. Le, Vogeleer, P., Jacques, M. & Harel, J. Interactions of Intestinal Bacteria with Components of the Intestinal Mucus. *Front Cell Infect Microbiol* **7**, 387 (2017).

177. van Tassell, M. L. & Miller, M. J. Lactobacillus Adhesion to Mucus. *Nutrients* **3**, 613 (2011).

178. MacKenzie, D. A., Tailford, L. E., Hemmings, A. M. & Juge, N. Crystal Structure of a Mucus-binding Protein Repeat Reveals an Unexpected Functional Immunoglobulin Binding Activity. *Journal of Biological Chemistry* **284**, 32444–32453 (2009).

179. Buck, B. L., Altermann, E., Svingerud, T. & Klaenhammer, T. R. Functional analysis of putative adhesion factors in Lactobacillus acidophilus NCFM. *Appl Environ Microbiol* **71**, 8344–8351 (2005).

180. Lagier, J. C. *et al.* Culturing the human microbiota and culturomics. *Nat Rev Microbiol* **16**, 540–550 (2018).

181. Park, H., Yeo, S., Ryu, C. B. & Huh, C. S. A streamlined culturomics case study for the human gut microbiota research. *Scientific Reports 2024 14:1* **14**, 1–11 (2024).

182.   González-Rodríguez, I. *et al.* Role of Extracellular Transaldolase from Bifidobacterium bifidum in Mucin Adhesion and Aggregation. *Appl Environ Microbiol* **78**, 3992 (2012).

183.   Elzinga, J. *et al.* Binding of Akkermansia muciniphila to mucin is O-glycan specific. *Nature Communications 2024 15:1* **15**, 1–10 (2024).

CHAPTER I

4. CHAPTER I: MAM IS A KEY PROTEIN PROCESSED AND EXPORTED TO THE *Faecalibacterium duncaniae* ENVELOPE, WHICH IS ITS MAIN PROTEIN TO ORGANIZE ITS UNIQUE STRUCTURE

MAM is a protein that plays a pivotal role in the anti-inflammatory properties of *F. duncaniae*, a prominent member of the human gut microbiota. Despite its recognized significance in gut homeostasis, our understanding of MAM's molecular organization and cellular function remains incomplete. To assess this question, this chapter aims to elucidate MAM's localization, structural organization, and potential physiological roles within *F. duncaniae*.

Using a multidisciplinary approach that integrates mass spectrometry, bioinformatics, and advanced microscopy techniques, this chapter provides novel insights into MAM's enrichment in the bacterial envelope, its unique hexameric organization, and its hypothesized contributions to cell structure and dynamic interactions. These findings represent the first comprehensive characterization of MAM and reveal new evidence regarding the unique biology of *F. duncaniae*, highlighting MAM as a central proteinaceous component of its cell envelope.

The chapter contains a manuscript detailing the experimental characterization of MAM, submitted to the journal Gut Microbes under the manuscript ID: 255133749, and additional results expanding our understanding of *F. duncaniae's* envelope organization in relation to MAM.

1   **The Microbial anti-inflammatory Molecule (MAM) is a key protein processed and**
2   **exported to *Faecalibacterium duncaniae* envelope**

3   Thaís VILELA RODRIGUES[1,2]; Sylvain MARTHEY[3]; Sandrine AUGER[1]; Luis Lima
4   DE JESUS[1,2]; Céline HENRY[1]; Christine PECHOUX[4], Ana ARTENI[5]; Véronique
5   MARTIN[3], Philippe LANGELLA[1]; Siomar de Castro SOARES[6]; Gwenaëlle ANDRE[3;]
6   Vasco Ariston de Carvalho AZEVEDO[2]; Jean-Marc CHATEL[1].

7   [1]Université Paris Saclay, INRAE, AgroParisTech, MICALIS, Jouy-enJosas, France
8   [2]Federal University of Minas Gerais, Instituto de Ciências Biológicas, Belo Horizonte,
9   Minas Gerais, Brazil
10 [3]Université Paris Saclay, INRAE, MAIAGE, Jouy-en-Josas, France
11 [4]Université Paris Saclay, INRAE, GABI, Jouy-en-Josas, France
12 [5]Université Paris-Saclay, CEA, CNRS, Institute for Integrative Biology of the Cell, Gif-
13 sur-Yvette, France
14 [6]Federal University of Triângulo Mineiro, Instituto de Ciências Biológicas e Naturais,
15 Uberaba, Brazil

16 **Corresponding Author:** Jean-Marc Chatel - jean-marc.chatel@inrae.fr

17 **ABSTRACT**

18 MAM (Microbial-Anti-Inflammatory Molecule) is key effector protein with anti-
19 inflammatory properties in *Faecalibacterium duncaniae*, a critical human gut microbiota
20 species. Despite its importance, MAM function and molecular features remain poorly
21 understood. This study elucidates MAM's physiological importance by examining its
22 cellular localization, secretion dynamics, and structural organization. Mass spectrometry
23 and immunogold labeling confirmed MAM as the most abundant protein in the cell
24 envelope and the second most abundant in the overall proteome, localizing it to the
25 bacterial surface. Bioinformatic and *in silico* analyses suggest that MAM contains an N-
26 terminal leader peptide with motifs recognized by a Peptidase-domain-Containing ABC
27 Transporter (PCAT), enabling cargo transport to the cell envelope. After N-terminal
28 excision, the cargo protein could be transported to the cell envelope via this PCAT, where
29 it could assemble into a hexameric structure, as revealed by docking and AlphaFold3
30 modeling. Such results were supported by electron microscopy showing a lattice-like
31 organization on the bacterial surface. This work introduces a novel discussion about the
32 singular organization of the *F. duncaniae* cell envelope, having MAM as a key component
33 for the bacteria, supporting the understanding of the unique biology of *F. duncaniae* and
34 its potential as a next-generation probiotic or live biotherapeutics.

35 **KEYWORDS:** Cell envelope, Proteomics, ABC transporter, leader and cargo peptides,
36 *Faecalibacterium*, microbiota, inflammation

37

38 **INTRODUCTION**

39 *Faecalibacterium duncaniae*, formerly known as *Faecalibacterium prausnitzii*, is an
40 extremely oxygen-sensitive (EOS), non-motile, and non-spore-forming bacteria that
41 belongs to the *Clostridium* cluster IV within the *Bacillota* (*Firmicutes*) phylum. As a
42 commensal organism, *F. duncaniae* is a major component of the healthy human gut, able
43 to represent up to 5% of the total bacterial microbiota.[1] The species has garnered attention
44 as a next-generation probiotic or live biotherapeutics, due to its pivotal role in maintaining

45 gut health and modulating inflammation, in colitis murine model, mimicking symptoms
46 of Inflammatory Bowel Diseases (IBDs) such as Crohn's disease (CD) and Ulcerative
47 Colitis (UC).[2] Additionally, a lower abundance of *F. duncaniae* has been positively
48 associated with various conditions, such as obesity, diabetes, Parkinson's disease and
49 more recently, COVID-19 and influenza virus infections.[3–7]

50 Different beneficial mechanisms related to *F. duncaniae* towards the host health have
51 been described. The bacterium is a substantial producer of butyrate,[1,8] a key short-chain
52 fatty acid (SCFA) that serves as the main energy source for colonocytes, also it protects
53 the intestinal mucosa by enhancing mucin production and plays an anti-inflammatory role
54 by inhibiting the NF-kB pathway.[9,10] Another crucial factor is the production of bioactive
55 peptides attributed to MAM (Microbial Anti-Inflammatory Molecule). MAM is a 14.5
56 kDa protein produced exclusively by *Faecalibacterium* species. MAM has demonstrated
57 significant anti-inflammatory properties, particularly through inhibition of the NF-κB
58 pathway.[11,12] However, detailed insights into its physiological role within bacteria,
59 including its structure, function, possibly processing, and cognate protein-protein
60 partnering mode, remain to be deciphered.

61 MAM was primarily identified by its peptides in the *F. duncaniae* supernatant.[12] Early *in*
62 *silico* predictions revealed that MAM structure consists primarily of hydrophobic
63 residues, with a tertiary structure indicating a globular conformation, having a β-sheet
64 central core flanked with α-helices.[12,13] Although the physiological role of MAM in the
65 species remains unknown, the encoding gene for MAM was observed to be highly
66 expressed during both exponential and stationary growth phases, even in a poor
67 nutritional environment.[14] This suggests that MAM likely plays an important role in the
68 physiology of the bacteria. The genomic region of the MAM coding sequence includes
69 genes associated with various functions. In most *Faecalibacterium* species, the gene
70 encoding a Peptidase domain-containing ABC Transporter (PCAT) is located adjacent to
71 the MAM gene.[11] PCATs are key players in a specific transport system where a core ABC
72 exporter is covalently linked to a C39 peptidase and an ATP interaction chain (nucleotide-
73 binding domains - NBD). The C39 domain acts as cysteine protease, which recognizes
74 and cleaves a leader peptide, specifically after a double G motif, to facilitate the cargo
75 protein transport[15] Although a potential interaction between MAM and PCAT has been
76 suggested, and a cargo peptide identified at the N-terminal end of MAM,[11] this
77 relationship remains unclarified.

78 MAM exhibits significant diversity among the different species of *Faecalibacterium*.
79 Phylogenetic and comparative analyses of MAM demonstrated the existence of 10
80 different clusters of MAM sequences within the genus. This diversity is observed in the
81 molecular composition and in the anti-inflammatory activity of MAM, for which different
82 inhibition levels of the NF-kB pathway were observed among *Faecalibacterium*
83 species.[11]

84 In previous studies, MAM peptides demonstrated significant anti-inflammatory
85 properties in various colitis murine models and in *in vitro* assays.[11,16,17] The activity of
86 MAM was primarily tested by plasmid transfection encoding the entire protein in
87 epithelial cell lines.[12] These studies revealed MAM's capacity to inhibit the NF-κB
88 pathway in a dose-dependent manner. This influence on the NF-κB pathway was also
89 demonstrated *in vivo* through oral administration of *Lactococcus lactis*, carrying a
90 plasmid containing the cDNA of MAM. Under the control of an eukaryotic promoter, it
91 enables the production of MAM directly by the host12. Additionally, a luciferase reporter
92 assay targeting the NF-κB pathway was also performed, demonstrating MAM anti-

93 inflammatory activity in DNBS (Dinitrobenzene sulfonic acid) and DSS (Dextran Sodium
94 Sulfate)-induced colitis models.[11,16]

95 MAM has also been correlated with the maintenance of the gut barrier integrity. Studies,
96 using the gut microbiota of a diabetes mellitus mouse model and intestinal cell lines,
97 showed a positive correlation between barrier stability and permeability through the
98 interaction of recombinant MAM with tight junction proteins, demonstrating MAM's
99 multifaceted role in maintaining intestinal integrity.[18]

100 While MAM's biotherapeutic potential in gut health is evident, its functional contribution
101 to *F. duncaniae* physiology remains unexplored. To address this issue, we have
102 employed, in this work, various biochemical and molecular cell biology approaches to
103 investigate MAM's functional and structural aspects. We have performed cell
104 fractionation, proteomic analysis, and immunogold labeling with polyclonal antibodies to
105 evaluate the localization and abundance of MAM within the cell. We have also led
106 structural bioinformatics studies to explore MAM possibility to be recognized and
107 exported outside the cytoplasm by PCAT, and we have investigated MAM's capacity to
108 fold and eventually self-assemble into a supramolecular organization. We revealed
109 intriguing aspects of the envelope of *F. duncaniae* that do not follow the classical bacterial
110 cell envelope organization. Besides, the main proteinaceous component of the cell surface
111 is MAM, which forms an ordered lattice on the surface of *F. duncaniae*, suggesting a
112 possible role in maintaining envelope integrity. Thus, this study highlights the need for
113 further investigation into the architecture of the *F. duncaniae* cell envelope, opening new
114 discussions about this unique bacterium.

115

116 **METHODS**

117 **Bacterial growth and culturing conditions**

118 *F. duncaniae* A2-165 (DSM #17677) were cultivated on a BHIS agar plate enriched with
119 (Brain Heart Infusion broth 37 g/L, Difco) supplemented with yeast extract (5 g/L, Difco)
120 and 3% GAC (Glucose 6,6%, Acetate 5,5% and cysteine 1,66%). Anaerobic chamber was
121 set with N_2(nitrogen) = 90%, CO_2 = 5%, and H2 = 5%.[19] Single colonies were inoculated
122 in a liquid medium (BHIS-GAC) at 37°C degrees. Overnight pre-cultures were used to
123 prepare 10% cultures with an initial 600 nm O.D. of approximately 0.1. The experiments
124 were conducted with four replicates.

125 **Supernatant sample collection and preparation for mass spectrometry analysis**

126 For each of the four replicates, 10 ml of culture were collected. At the exponential phase
127 (EX), samples were collected at 6 and 9 hours after inoculation, and at the stationary
128 phase, the collection was made at 18 (Early Stationary – ES) and 25 hours (Late
129 Stationary – LS). Cultures were harvested for 15 minutes at 5,000g at 4°C, and the
130 supernatant was collected. The Oasis Cartridge Prime HLB column was previously
131 wetted with acetonitrile (ACN) and then equilibrated with 2% ACN and 0.1% formic
132 acid. 450 µL of supernatant was loaded and eluted with 200 µl of 40% ACN, followed by
133 80% ACN. Eluted samples were submitted to a 10 kDa Millipore cut-off centrifugation
134 at 12,000 rpm x 40 min at 4°C to remove any remaining protein. The samples were dried
135 using a speed-vac, followed by the addition of 200 µL of loading buffer (2% acetonitrile
136 and 0.08% trifluoroacetic acid). The solution was then diluted 20-fold, and 4 µL were
137 injected into the liquid chromatography-tandem mass spectrometry (LC-MS/MS) system,
138 using an Orbitrap Fusion Lumos Tribrid mass spectrometer (Thermo Fisher Scientific)
139 coupled to liquid chromatography.

140 Supernatant peptides were identified using an Orbitrap Fusion Lumos Tribrid mass
141 spectrometer (ThermoFisher Scientific, San Jose, CA) coupled to an UltiMate3000
142 RSLCnano ultraHPLC system (Dionex, Sunnyvale, CA). Each 4 µL sample was injected
143 for online desalting onto a PepMap C-18 reverse-phase (RP) nanotrap column (3 µm,
144 75 µm × 20 mm, Dionex) with nanoViper fittings (flow rate: 20 µL min^{-1}), separated on
145 a PepMap C-18 reverse-phase nano column (3 µm, 75 µm × 50 cm), and eluted with a 50
146 min gradient of 5%–35% acetonitrile in 0.1% formic acid at 250 nL min^{-1}, a 5-min ramp
147 to 40% acetonitrile/0.1% formic acid, a 3-min ramp to 98% acetonitrile/0.1% formic acid,
148 and a 5-min hold at 98% acetonitrile/0.1% formic acid. The mass spectrometer was
149 operated in positive ion mode, with the nanospray voltage set to 1.6 kV and the source
150 temperature set to 270 °C. The instrument was operated in data-dependent acquisition
151 mode and high-energy collisional dissociation fragmentation mode (collision energy:
152 30%). In all experiments, full MS scans were acquired over the 400–2000 *m/z* mass range,
153 with detection in the Orbitrap mass analyzer at a resolution of 120,000, an automatic gain
154 control set to $1 \times 10^{5,}$ and an intensity threshold of 20,000. Each precursor ion scan was
155 followed by a 2.5-s "top speed" data-dependent Orbitrap MS/MS run, with a 1.6 *m/z*
156 window for the quadrupole isolation of precursor peptides with multiply charged ions
157 from 1 to 3. Fragment ion spectra were acquired in the Orbitrap mass analyzer at a
158 resolution setting of 30,000, an automatic gain control set to 5×10^4, and a dynamic
159 maximum injection time. Polysilaxolane ions m/z 445.12002, 519.13882, and 593.15761
160 were used for internal calibration.

161 The data were converted into mzXML format using MS Convert (ProteoWizard, version
162 3.0.8934). Proteins were identified using X!Tandem v.2017.2.1.4[20] by matching peptides
163 against the MAM database. Proteins were filtered and grouped using open-source
164 X!TandemPipeline software (version 0.4.62,
165 http://pappso.inrae.fr/bioinfo/xtandempipeline/).[21] The data were compared with a
166 contaminant database to eliminate spectra due to contaminants.

167 The peptide identification process was run with a precursor mass tolerance of 10 ppm and
168 a fragment mass tolerance of 10 ppm. No digestion rule was applied. The fix modification
169 was set to cysteine carbamidomethylation, and methionine oxidation was considered a
170 potential modification. In a second pass, N-terminal acetylation was added as another
171 potential modification, whereas all the other above-mentioned settings remained
172 unchanged. Identified proteins were filtered as follows: (i) peptide E-value <0.01 and a
173 minimum of two peptides per protein, and (ii) a protein E-value of 10^{-4}.

174 **Envelope and cytoplasmic protein extraction and preparation for mass**
175 **spectrometry analysis**

176 Here, the same culture procedures were conducted as previously described. After the
177 harvesting of 30ml of culture at the early stationary phase (18 hours of growth), the cell
178 pellet was washed twice with phosphate-buffered saline (PBS) and then resuspended in
179 lysis buffer (Tris-HCl 50 mM pH 8.0; 50 µl/ml Protease Inhibitor Cocktail). To break the
180 cells, three cycles of 10 seconds of sonication were performed at a frequency of 20 kHz.
181 The supernatant containing cytoplasmic proteins was recovered by centrifugation at
182 20,000g for 15 minutes. Pellets containing the envelope fraction were washed twice with
183 PBS and then resuspended in PBS. Quantification was performed in triplicate using UV
184 absorbance at 280 nm. After quantification, 10ug of protein was submitted to a short
185 migration electrophoresis using a 1D gel (NuPAGE® 4-12% Bis-Tris Gel, novex), with
186 Coomassie G-250 (SimplyBlueTM SafeStain, Invitrogen) used as a dye. The gel was then
187 cut into small pieces and destained with Solvent A (10% v/v acetic acid, 40% v/v ethanol)
188 and Solvent B (50% v/v 50 mM ammonium bicarbonate, 50% v/v acetonitrile). Next, 10

189 mM dithiothreitol and 55 mM iodoacetamide (Sigma) were used for reduction and
190 alkylation, followed by overnight digestion with 100 ng trypsin (Promega). Peptides were
191 extracted with 0.5% v/v trifluoroacetic acid and 50% v/v acetonitrile. The samples were
192 dried using a dry-vacuum system (SavantTM SPD121D, Thermo Fisher Scientific), and
193 peptides were resuspended in 50ul of loading buffer (0.08% v/v trifluoroacetic acid, 2%
194 v/v acetonitrile) for LC-MS/MS injection. Protein identification followed the process
195 described in the previous section.

In-silico analysis of MAM motifs and modeling as monomeric and oligomeric structures

198 3D modeling of MAM was performed with AlphaFold 3 (AF3). The fasta sequence of
199 MAM from *F. duncaniae* was retrieved from Uniprot under the ID C7H4X2, and
200 submitted to the AF3 online server (https://alphafoldserver.com/) [23] to be modeled, first
201 as a monomer with the complete sequence (1-135 aa) then as homopolymers composed
202 of 2 to 8 MAM sequences (22-135 aa). For the predictions of these complexes, the MAM
203 sequence was trimmed off the first 21 amino acids corresponding to the putative signal
204 peptide. Similarly, the transporter PCAT (ID: C7H4X1) was retrieved from UniProt[22] and
205 the modeling of the PCAT dimer bound to the MAM monomer was subjected to the AF3
206 server.[23] For each prediction, five structures were computed and ranked for each
207 model, according to the global complex ranking metric with chiral mismatch and steric
208 clash penalties generated by AF3. The best model ranked by AF3 was retained for
209 subsequent analyses. Visual analyses were performed using PyMOL25. Structural
210 homologs that could have been deposited on the protein data bank were searched for using
211 the Foldseek server (https://search.foldseek.com/).[25] To evaluate the predicted oligomeric
212 structures, PDBePISA (Proteins, Interfaces, Structures and Assemblies) was used to
213 assess the interactions between the complexes' units.[26] ProtParam was utilized to compute
214 theoretical pI and the number of charged residues.[27]

Interaction of MAM leader peptide with the PCAT

216 Initially, MAM sequence was screened for signature motifs associated with the leader
217 peptide ([MMMPANx(8,11)VxGG]) and PCAT ([GIE[T/L][V/I]K]) using the Fuzzpro
218 tool.[28] For the docking, the best predicted model of MAM bound to the PCAT transporter
219 was superimposed onto the cryo-EM structure of its structural homolog PCAT1, bound
220 to CtA peptide substrate in *Clostridium thermocellum*.[29] This was performed using
221 the PyMOL align command. Next, the MAM signal peptide of 21 residue-long was cut
222 and kept to measure and characterize its molecular interaction with PCAT. To study it at
223 the excision site, the peptide encompasses on-purpose the extra Ala22, located right after
224 the cleavage site at the double G20G21. The binding energy between the MAM peptide
225 and PCAT was evaluated using Autogrid4 with the largest cubic grid, centered on the
226 middle of the peptide considered rigid, and Autodock4 with the function epdb.[30] To get a
227 positive control, the same protocol was used to measure the interaction between PCAT1
228 (chain C) and CtA (chain D between Asn8 and Thr26) of the experimental complex (PDB
229 ID: 6v9z). Last, the cryo-EM and AF3 complexes were visually inspected using PyMOL.

Lithium Chloride (LiCl) extraction and protein identification

231 This chaotropic agent LiCl was chosen to investigate the envelope of *F. duncaniae* more
232 deeply. Overnight cultures of *F. duncaniae* at stationary phase (500 mL) were harvested
233 by centrifugation at 5000 × g for 15 minutes (4°C). The supernatant was discarded,
234 and two wash cycles with 50 mL of PBS at pH 7.4 were conducted. The remaining pellet
235 was resuspended on 5 M LiCl and agitated for 15 minutes at 4°C. To obtain the enriched
236 envelope extraction, the supernatant was collected after harvesting at 9000g for 15 min

237 (4°C). Supernatants were ultracentrifuged at 49,000 × g for 3 hours to concentrate the
238 envelope proteins. The resulting pellet was resuspended in PBS, and protein
239 concentration was determined by measuring absorbance at 280 nm using a NanoDrop
240 spectrophotometer (Thermo Fisher Scientific, Waltham, MA, USA). For SDS-PAGE
241 analysis, 10µg of protein was loaded onto a pre-cast 4-15% Mini-PROTEAN® TGX™
242 gel (Bio-Rad, Hercules, CA, USA). Electrophoresis was carried out at a constant voltage
243 of 200 V until the dye front reached the bottom of the gel. In-gel digestion and protein
244 identification were conducted using LC-MS/MS, as detailed in the mass spectrometry
245 methodology described earlier.

Negative staining microscopy of LiCl extracts

247 Liquid cultures of *F. duncaniae* at stationary phase and LiCl extracts were analyzed using
248 the negative staining method. Three microliters of the nano-object suspension were
249 deposited on an air glow-discharged carbon-coated grid for 1 min. The excess liquid was
250 blotted, and the grid was rinsed with 2 % w/v aqueous uranyl acetate. The grids were
251 visualized at 120 kV with a Tecnai 12 Spirit transmission electron microscope (Thermo
252 Fisher, New York, NY, USA) equipped with a K2 Base 4 k×4 k camera (Gatan,
253 Pleasanton, CA, USA). Magnification was at 4400, 6500, or 15,000 X, corresponding to
254 a pixel size at the specimen level of 0.83, 0.55, and 0.25 nm, respectively. Image analysis
255 and dimensions calculations were obtained with ImageJ.[31]

Recombinant MAM purification and antibody production

257 The plasmid pSTABY:*mam,* conferring ampicillin resistance, was introduced into *E. coli*
258 BL21 (DE3) by transformation. The bacteria were grown in Luria-Bertani medium at
259 37°C, and the expression of the recombinant MAM (R-MAM) protein was induced using
260 1 mM isopropyl-β-D-thiogalactopyranoside (IPTG, Sigma) when the optical density
261 (OD$_{600nm}$) of the *E. coli* culture reached 0.6–0.8. Purification of R-MAM was conducted
262 under denaturing conditions (8 M urea, with 50 mM imidazole, 100 mM sodium
263 phosphate, and 10 mM Tris) utilizing Ni-NTA resin (Invitrogen) across a pH gradient
264 ranging from 8.0 to 4.15. The eluate was subsequently collected and dialyzed against a
265 Dialysis buffer containing Urea gradient (6 M, 4M, 2M, 1M, 0M) plus 50 mM TRIS, 1%
266 glycerol, and 200 mM NaCl (pH 7.4) using a SpectraPor Dialysis Membrane (10,000
267 MWCO, SpectrumLabs). This initial dialysis was performed for 5 hours, and the urea was
268 changed every 1 hour. The dialysis process continued for an additional 24 hours. Final
269 dialysis was performed in 200 mL PBS 0.1M plus glycerol 1%. The dialyzed MAM
270 protein (15 µL) was analyzed via one-dimensional SDS-PAGE (12%), quantified using
271 the BCA Protein Assay Reagent (Thermo Fisher Scientific) and subsequently sent to the
272 GeneCust company for the polyclonal antibody production in rabbits. Anti-MAM
273 antibody (1:1000) from *F. duncaniae* A2-165 was evaluated by Western Blot.

Cryo-preparation and sectioning of bacterial Cells

275 For ultrathin cryo-sectioning and immunogold labeling, bacterial cells were initially fixed
276 with 4% paraformaldehyde (PFA) in culture media under oxygen-free conditions for 1
277 hour. The cells were then transferred to an oxygen-containing environment, and the first
278 fixative was removed. Next, another fixation step was conducted using a mixture of 4%
279 PFA and 0.25% glutaraldehyde in 0.1 M phosphate buffer (pH 7.2) for 1 hour, followed
280 by another fixation step with 4% PFA for an additional hour. The cells were embedded
281 in 2.8M sucrose for cryoprotection and frozen rapidly in liquid nitrogen. Ultrathin
282 cryosections were prepared according to the Tokuyasu method,[32] optimized for
283 preserving protein localization.

284 **Immunoelectron microscopy on bacteria cryosection**

285 The grids were washed on 2% gelatine at 37°C to remove the embedding gelatin and
286 remnants of the methylcellulose; then, they were quenched with glycine 50mM in PBS,
287 blocked with a buffer containing 1% BSA. Serum anti-MAM was incubated for 1h in
288 PBS/1%BSA/0.1% saponin; the grids were washed four times, then goat anti-rabbit IgG
289 coupled to 10 nm colloidal gold particles (Aurion – Biovalley- France) and used at a 1/20
290 dilution in the presence of 0.1% saponin, for 30 min. The grids were again washed and
291 post-fixed with 1% glutaraldehyde, and cryosections were embedded with 2%
292 methylcellulose containing 4% uranyl acetate (4/1). Grids were examined with a Hitachi
293 HT7700 electron microscope operated at 80kV (Milexia – France), and images were
294 acquired with a charge-coupled device camera (AMT).

295

296 **RESULTS**

297 **MAM peptides in the supernatant are diverse and increase during bacterial growth**

298 MAM was initially identified by detecting seven specific peptides in the supernatant of
299 *F. duncaniae.*[12] To investigate this behavior more deeply, the dynamics of the production
300 of MAM peptides during bacterial growth were evaluated by collecting supernatants at
301 different stages of growth, from the early exponential to the late stationary phase. MAM
302 peptides were recovered through solid phase extraction, followed by a 10kDa filtration to
303 avoid full-length proteins. LC-MS/MS analysis followed by MAM peptides identification
304 revealed a notable increase in peptide abundance over time.

305 Our results demonstrated a great diversity of the detected MAM peptides. If we assemble
306 all the peptides across the growth stages, is it possible to cover 84.4% of MAM's total
307 length. The identified peptides spanned from the 22nd amino acid on the N-terminus to
308 the C-terminus, covering almost the entire protein. Notably, the first 21 amino acids, from
309 the initial methionine to the double glycine, were completely absent from our peptidomic
310 analysis. We detected 88 peptide variants for the 135 amino acids-long MAM protein,
311 varying in sequence, length, and abundance, with many differing by a single amino acid.

312 No indication of cleavage site by specific peptidases was observed, except for the putative
313 signal peptide (Figure 1, Supplementary table 1).

314 The identified peptides showed variable lengths, ranging from 5 to 29 amino acids long,
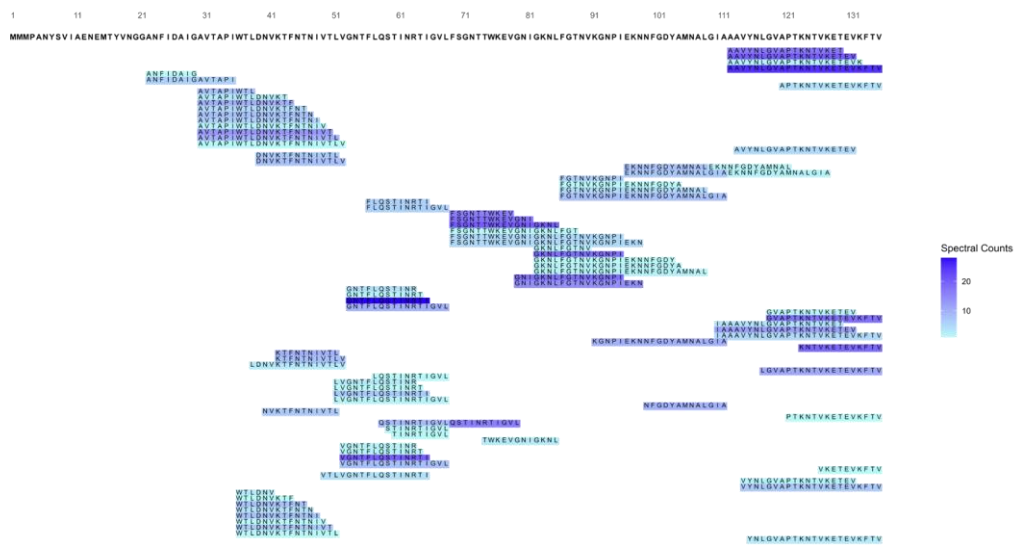
Figure 1. Peptide alignment map of MAM-identified peptides by LC-MS/MS peptidomic analysis.
The figure shows the 86 unique MAM peptides identified by LC-MS/MS analysis. Each peptide is
represented by a rectangle, with the peptide sequence within it overlapping with MAM's amino
acid sequence on the top. The rectangle's color intensity indicates the peptide's relative abundance,
as measured by the number of spectral counts.

315 with corresponding spectra counts that reflected their abundance. The most common
316 peptide lengths were 12 and 13 amino acid residues. Notably, some peptides exhibited
317 particularly high spectra counts, such as G_{53}NTFLQSTINRTI$_{65}$ (28 spectra) and
318 V_{52}GNTFLQSTINRTI$_{65}$ (20 spectra), indicating their higher relative abundance. In
319 between, a 23-amino-acid-residues-long peptide
320 (A_{112}AVYNLGVAPTKNTVKETEVKFTV$_{135}$) that covers the C-terminus of MAM was
321 also identified with an important abundance of 25 spectra (Supplementary data 1). The
322 wide range in peptide sizes and dynamics in their relative abundance suggest a non-
323 specific cleavage process, likely due to degradation mechanisms rather than active
324 secretion.

325 During the exponential phase (6 and 9 hours of growth), an average of 1.25 ± 0.96 and
326 2.75 ± 0.50 MAM peptides were detected, respectively. This number significantly
327 increased to 41.25 ± 3.50 peptides in the early stationary phase (18 hours) and reached an
328 average of 66.5 ± 2.38 peptides in the late stationary phase (25 hours) (Figure 2).
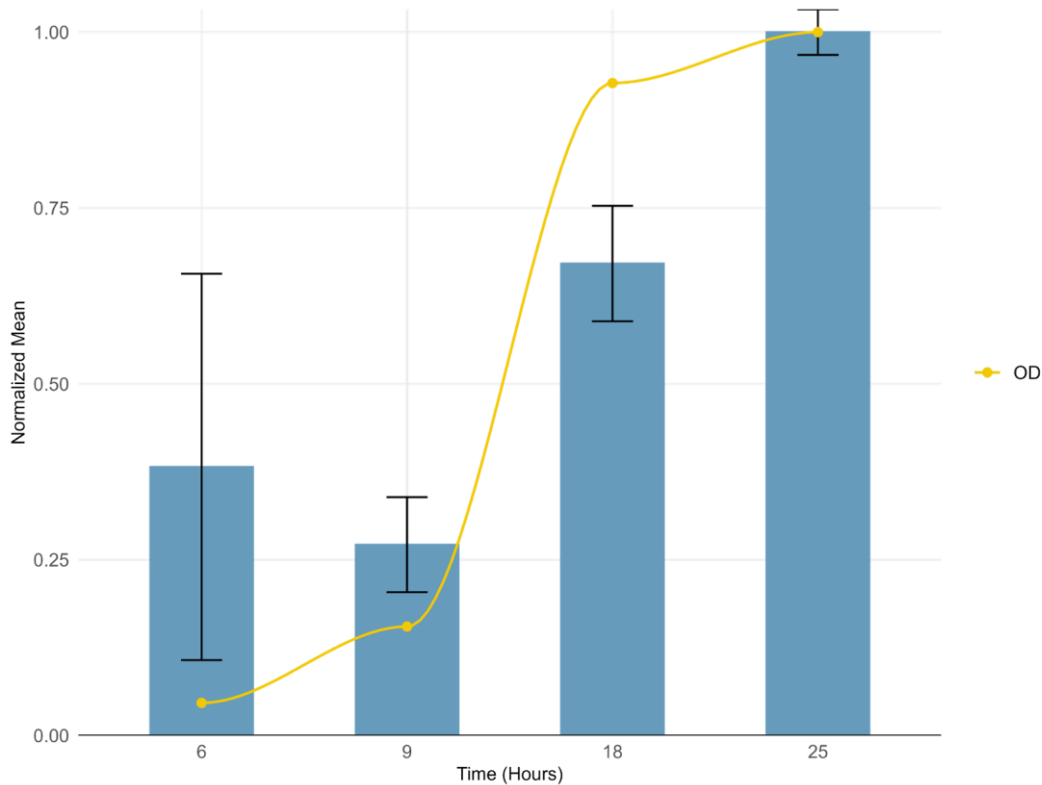
Figure 2. Dynamics of MAM peptides across different growth phases of F. duncaniae. Normalized mean number of MAM peptides identified at different growth phases: 6 hours, 9 hours (exponential phase), 18 hours (early stationary phase), and 25 hours (late stationary phase). Bars represent mean values normalized by optical density (OD), with error bars indicating standard deviation. The yellow solid line represents OD over time. Statistical significance was determined using one-way ANOVA, with significant differences indicated by asterisks (*$p < 0.05$, ****$p < 0.0001$).

MAM is the most abundant envelope protein in the proteome of *F. duncaniae*

While our results regarding MAM peptides in the supernatant suggested degradation processes, we aimed to investigate MAM's presence in other subcellular localizations. *F. duncaniae* cultures were grown to the early stationary phase (18 hours, OD ~1.6) and fractionated into cytoplasmic and envelope samples through cell lysis and centrifugation. Then, the samples were subjected to in-gel digestion and protein identification via LC-MS/MS. PCA analysis demonstrated a clear separation between cytoplasmic and envelope samples (Figure 3A, Supplementary Figure 1). The plot indicates that the first two principal components (Axis1 and Axis2) account for 43.2% and 15.6% of the variance, respectively. The separation of the cytoplasmic samples (A2-165-ENV) and envelope samples (A2-165-CYT) is evident along these axes, thus confirming the robustness of our fractionation process.
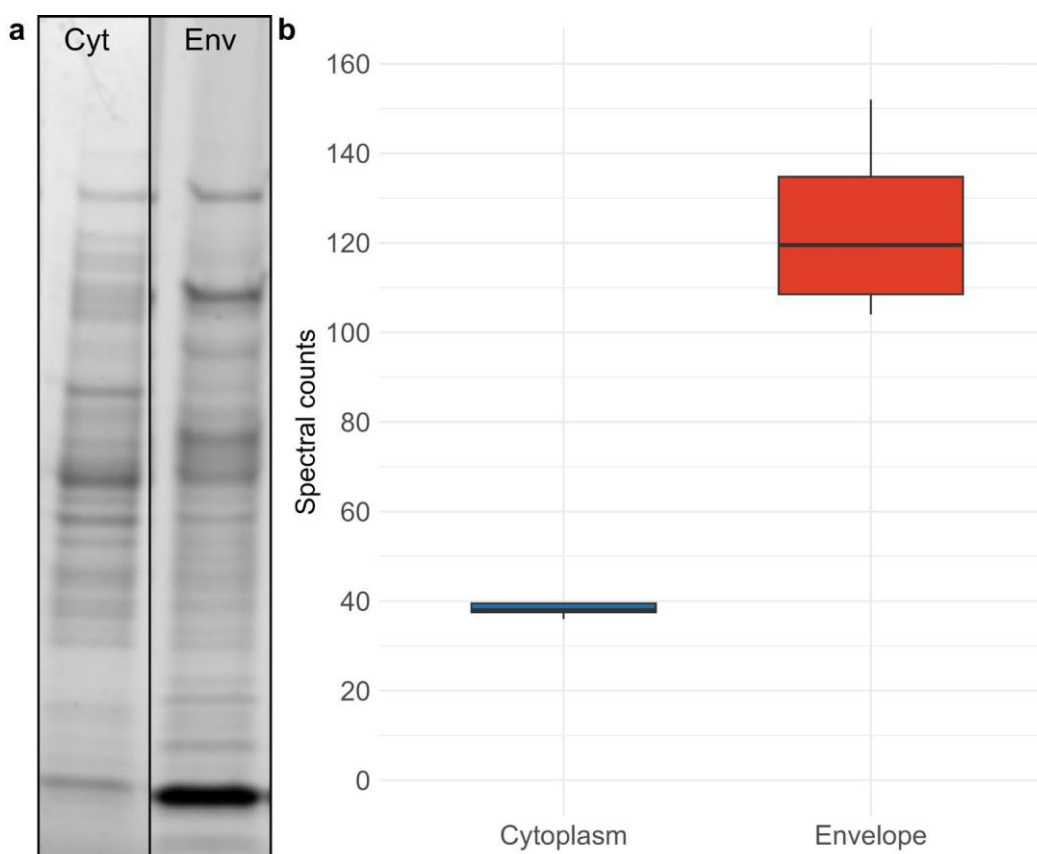
Figure 3. Abundance and localization of MAM in cytoplasmic and envelope fractions of *F. duncaniae* A) SDS-PAGE gel showing protein bands of cytoplasmic (Cyt) and envelope (Env) fractions. (B) Box plot of spectral counts representing MAM abundance in cytoplasmic (blue) and envelope (red) fractions. The box plot shows the median, interquartile range, and distribution.

MAM represents 1.15% of the envelope proteome of *F. duncaniae,* making it the most abundant protein in this fraction, as indicated by the NSAF (Normalized Spectral Abundance Factor). When combining cytoplasmic and envelope fractions, MAM is the second most abundant protein in *F. duncaniae*, comprising approximately 0.76% of the total proteome. It is surpassed only by 3-hydroxyacyl-CoA dehydrogenase, NAD binding domain protein (HADH-NBD), the most abundant cytoplasmic protein. The average NSAF score for MAM in the envelope was 0.01146, compared to 0.0037 in the cytoplasm, indicating significant enrichment of MAM at the cell envelope ($p < 0.05$) (Supplementary data 2). The SDS-PAGE gel also corroborates these results, showing that the protein band at the level of 10-15 kDa (most probably MAM) is not only the most prominent one but also the more significantly abundant one in the envelope fraction, as compared to the cytoplasm (Figure 3B). Interestingly, for the first time, with LC-MS/MS, we were able to identify the signal peptide contained in one of the four replicates of the insoluble extraction. The identified peptide is 42 amino-acid residues long (**M$_1$MMPANYSVIAENEMTYVNGG**ANFIDAIGAVTAPIWTLDNVK$_{42}$). It evidences a double glycine stretch at positions 20-21 and correlates to one spectrum count with 4,5E-09 E-value (Supplementary data 2). These results suggest that MAM plays a role in the envelope architecture of *F. duncaniae*.

AlphaFold predictions reveal the structural features of MAM and its leader peptide

The functional activity of proteins in their full-length (FL) or processed forms relies on their 3D structure, including when they harbor disordered segments. To get insight into MAM's function, we sought to model its 3D structure, considering its two putative sizes,

375   MAM full length (MAM-FL) and MAM excised of its leader peptide (MAM-ΔLP).
376   AlphaFold 3 (AF3) was employed to predict both 3D structures. Appropriately, the
377   complete and truncated sequences of MAM were submitted online to the server
378   (https://alphafoldserver.com/). Overall, the models show a pTM (predicted template
379   modeling) score of 0,63 for MAM-FL and 0,6 for MAM-ΔLP, with 82% and 72% ranking
380   scores for the best models, respectively, indicating that the folding predictions are
381   reliable. The 3D shape of MAM-FL displays a central helical core composed of two
382   orthogonal helices, from which N- and C- terminal ends both extend out (Figure 4A). The
383   N-terminal extension displays an L-shape with a helical double turn between residues 12
384   and 17, and the C-terminal end is unfolded. MAM-ΔLP, deprived of its N-terminal
385   segment, does not evidence any significant change. Markedly, the Foldseek server
386   evidences that this fold is unique and absent from the protein data bank.[25] The lowest
387   confidence in the structure is observed at the N-terminal segment, between amino acid
388   positions 1 and 35. The predicted local distance difference test (pLDDT) also shows that
389   this segment could not be highly structured (Figure 4B). In addition, the "PAE" (Predicted
390   aligned error) associated with the prediction allows us to identify three distinct structure
391   blocks 1-22, 22-35, and 36-135, whose predicted relative positions to each other are
392   uncertain, which would suggest a certain flexibility of these domains in relation to each
393   other (Figure 4C). This trait, associated with an L-shape, supports its function as a leader
394   peptide.[29]

395   From position 22 to its C-terminus, MAM presents a central core composed of three
396   helices, which are located between residues 37-70, 74-86, and 100-119, respectively. The
397   leader peptide was formerly assessed to contain a pattern [MMMPANx8/11VxGG][11]
398   where the double glycine stretch (GG) is typical of a cleavage site recognized by a
399   cysteine peptidase transporter (Figure 4D).

400   To investigate the co-occurrence of MAM and PCAT, we screened the entire non-
401   redundant FASTA database of 780 billion sequences. Using Fuzzpro, we identified
402   sequences containing either MMMPANx(8,11)VxGG or GIE[T/L][V/I]K as signature
403   motifs for MAM and PCAT, respectively. This analysis retrieved 257 MAM-like
404   proteins, all displaying the leader peptide motif at their N-terminal end. These proteins
405   were distributed across 50 genomes (Supplemental Table 2). Strikingly, MAM motifs
406   associated with *Faecalibacterium* genomes accounted for 95.33% of the identified
407   sequences, strongly supporting the hypothesis that PCAT is consistently associated with
408   MAM proteins, being involved in extremely specific interaction mechanism of
409   *Faecalibacterium*. This feature prompted us to investigate the capacity of MAM 1) to
410   have its signal peptide recognized and excised by its cognate PCAT; 2) to be contained
411   in the inner cavity of PCAT dimer; and 3) to self-assemble and oligomerize after the
412   transfer (Figure 4D).
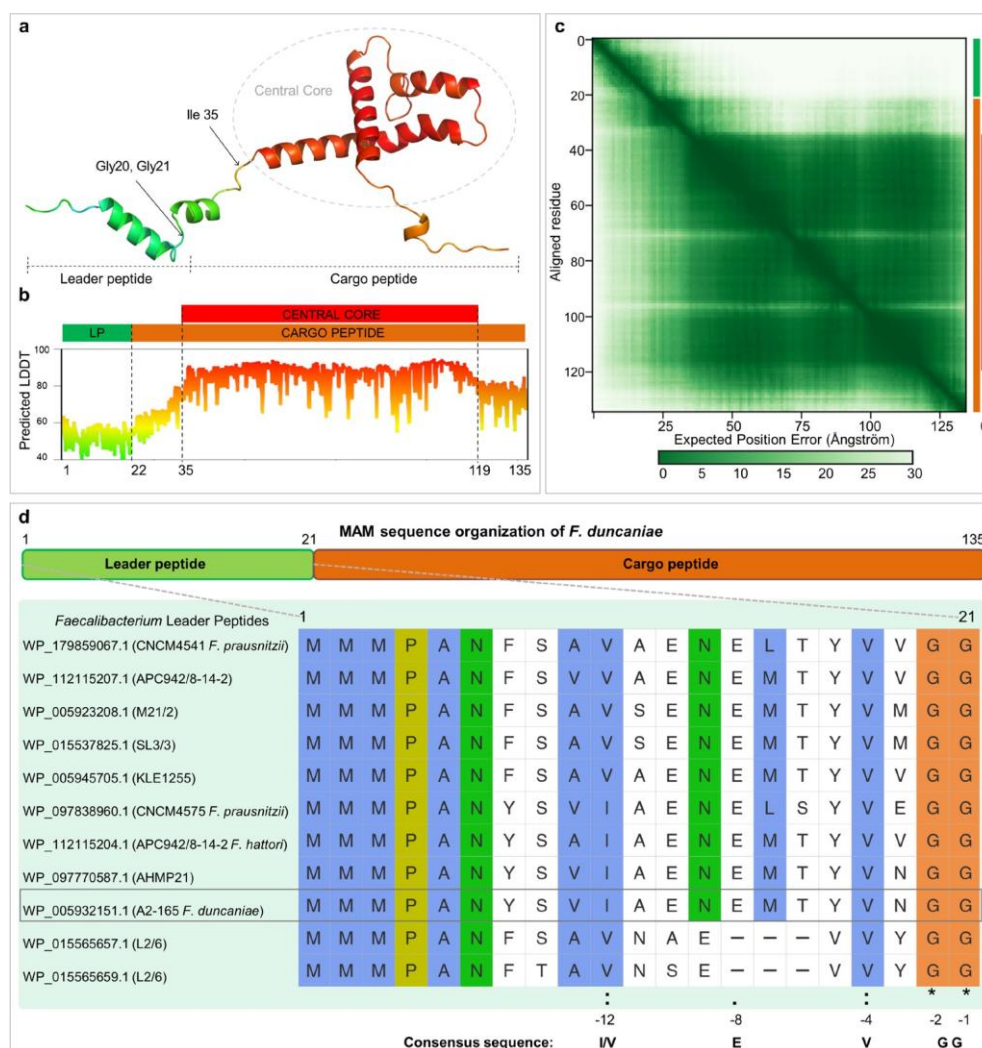
Figure 4. Schematic representation of MAM sequence and structure. A) Predicted structure of the full-length MAM protein colored by pLDDT confidence scores. The N-terminus (LP, positions 1–35) has low confidence, while the central core (positions 37–70, 74–86, 100–119) shows higher confidence (red regions). (B) Schematic of MAM structure showing the leader peptide (LP, green), cargo peptide region (orange), and central core (red). The pLDDT graph aligns with the structural elements, indicating varying confidence levels. (C) PAE plot indicating structural blocks (1–22, 22–35, 36–135), with low intrablock and high interblock PAE. (D) Sequence schematic with leader peptide (green) and cargo peptide (orange). Below, sequence alignment of leader peptides from *Faecalibacterium* strains highlights conservation and consensus sequence.

MAM is likely processed and transported by the PCAT to the cell envelope

Although displaying some substitution in amino-acid composition within the genus, the MAM's N-terminal end is highly conserved among all the *Faecalibacterium* species registered to date (Figure 4D).[11] Also, the strictly observed genetic co-occurrence of a PCAT transporter with MAM leads us to investigate the direct interaction between PCAT and MAM. Actually, the N-terminus segment describes a pattern of residues and positions with Ile/Val at position -12, Glu-Met at -8,-7, Val at -4, and Gly-Gly at -2,-1. This pattern has been previously shown to be the signature of a leader peptide and markedly the hallmark of all Gram-positive PCAT substrates, with the cleavage site nomenclature being -1 and +1 after the double Glycine stretch that pins it with Gly-2Gly-1 (Supplementary Figure 3A). Thus, it is very likely that the N-terminal segment of MAM is a leader peptide, and MAM is a substrate of PCAT.[33]

435 To further investigate this hypothesis, the molecular complex of MAM bound to the
436 PCAT was modeled with AF3 and evaluated by Autodock. It revealed a high confidence
437 zone in the position of MAM's N-terminal segment when complexed to the C39 peptidase
438 domain. The molecular docking evaluated an interaction energy of -17.3 kcal.mol^{-1},
439 evidencing a strong interaction between PCAT and MAM peptide. Also, the MAM
440 peptide displays an L-shape conformation with the double GG at 4 Å and 6 Å from the
441 catalytic residues Cys14 and His92, respectively. These features are expected to enable
442 the PCAT substrate to accommodate the narrow groove of the peptidase domain. A close
443 view of the binding shows that PCAT is also prime for MAM proteolysis. Cys14 is
444 positioned as the nucleophile, with His92 oriented to polarize the attacking cysteine.
445 Asp136 is placed to maintain His in an electronegativity and catalytically favorable
446 position, while Gln8 is able to form an oxyanion hole that should stabilize the tetrahedral
447 intermediate (Figure 5). Of note, those residues are homologous to Cys21, His99,
448 Asp115, and Gln15 in PCAT1 of *Clostridium thermocellum*, respectively (Supplementary
449 Figure 3A). Finally, our model of PCAT in complex with MAM peptide was
450 superimposed onto experimental PCAT1 bound to CtA substrate in *C. thermocellum*, with
451 the superimposition restricted to PCAT αC (alpha-carbon) traces.[29,34] Notably, MAM's
452 leader peptide was also superimposed on the crystal peptide at the peptidase site, with an
453 RMSD (Root Mean Square Deviation) of 0.590 Å (Supplementary Figure 3B). Similarly,
454 the binding energy between the 23 residue CtA peptide and its PCAT1 in the cryo-EM
455 solved structure was evaluated and showed a comparable affinity with 16.7 kcal.mol-1.
456 This strongly suggests that the N-terminal segment could be a precursor peptide that leads
457 MAM to be recognized and exported outside the cytoplasm, across the *F. duncaniae*
458 envelope, by the PCAT, co-present in the genome, and thus highly susceptible to be the
459 cognate transporter. Adequately, the mature form of MAM could be qualified as a cargo
460 peptide, starting at Alanine 23 and ending at Valine 135, according to *F. duncaniae*
461 sequence numbering.

462
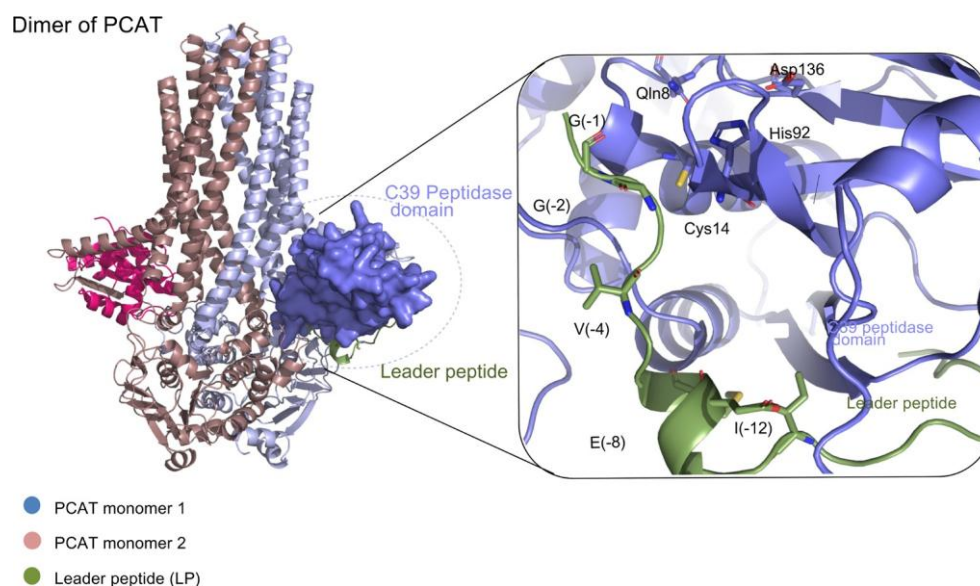
Figure 5. Interaction MAM leader peptide and the peptidase-containing ATP-binding cassette (PCAT) transporter. Predicted interaction of the MAM leader peptide (green) with the C39 peptidase domain (purple) of the PCAT transporter. The PCAT transporter consists of two monomers: monomer 1 (purple) and monomer 2 (pink). Key catalytic residues in the peptidase domain are highlighted (Asp136, His92, and Cys14), along with stabilizing residues of the leader peptide: G(-1), G(-2), V(-4), E(-8), and I(-12). The transporter domain comprises transmembrane helices, with the inset zooming into the peptidase domain.

Putative hexameric organization of MAM revealed by structural modeling after leader peptide removal

463
464

465 Proteins often become functional when assembled into supramolecular organizations
466 rather than as isolated molecules.[35] To investigate the physiological role of MAM, we
467 examined its ability to self-organize into macromolecular structures and assessed the
468 influence of its signal peptide on this arrangement. This was achieved by increasing the
469 copy numbers of MAM and using AF3 to model MAM-FL and MAM-ΔLP complexes,
470 ranging from dimers (two units) to octamers (eight units). These structures and their
471 associated metrics were thoroughly analyzed. This particular complex's organization and
472 its component units' interactions were studied visually with pymol and measured with
473 Pisa (Figure 6 and Supplementary figure 4).

474 The hexameric models of either MAM-FL or MAM-ΔLP both reveal pore-forming
475 structures with a comparable inner cavity of the buoy of 20 Å (Figure 6A). Overall, the
476 organization is the same, except for the external face of the buoy, where the N-terminal
477 end is located. Nevertheless, both predicted complexes exhibited the same regular
478 assembly concerning the position of each monomer. Despite this similarity in overall
479 structure, MAM-FL exhibits external dimensions of the wider side of 100 Å, decreasing
480 to 80 Å in MAM-ΔLP due to the lack of the first 20aa. Considering the opposite surface,
481 the diameter is about 60 Å for both structures. MAM-ΔLP has a sensibly higher ranking
482 score (0.94) than MAM-FL (0.74), suggesting a better accuracy. This is likely due to the
483 truncation of the N-terminal signal peptide in MAM-ΔLP, which exhibits lower pLDDT
484 and higher PAE values. Indeed, the disordered level was around 10% lower in MAM-
485 ΔLP compared to MAM-FL. The interface-predictable Template Modeling (ipTM) score,
486 calculated by AF3, was higher on the MAM-ΔLP (79%) in comparison to the complete
487 structure MAM-FL (54%). MAM-FL has a molecular weight of 86.9 kDa and is

488 composed of 810 amino acids, whereas MAM-ΔLP has a molecular weight of 73 kDa and
489 consists of 684 amino acids. The theoretical pI of MAM-FL is 6.59, compared to a higher
490 pI of 9.35 for MAM-ΔLP. The number of negatively charged residues (Asp + Glu) is
491 reduced from 54 in MAM-FL to 42 in MAM-ΔLP, while the number of positively charged
492 residues (Arg + Lys) remains constant at 54 for both hexamers. Fractional disorder is
493 higher in MAM-FL (0.39) compared to MAM-ΔLP (0.32) (Figure 6B, supplementary
494 figure 4). Altogether, these features emphasize that MAM-ΔLP is more stable as a
495 supramolecular assembly than MAM-FL.

496 The characteristics of the interface, measured by PISA, revealed that the contact area
497 between the six chains for MAM-FL has an average of 1744 Å², with a Gibbs free energy
498 (ΔG) associated evaluated at -27 kcal.mol-1. In MAM-ΔLP, the contact area is 1695 Å²
499 with a Gibbs free energy unchanged at -26 ΔG kcal.mol-1, one more time evidencing that
500 the N-terminal segment does not add much to the stability of the hexamer. Moreover,
501 PISA results highlighted a broad and intricate interconnectivity between all the subunits
502 of the complex. Notably, the interface is higher in the hexameric conformation, compared
503 to all the modeled complexes (Figure 6, Supplementary figure 4B). Within the hexamers,
504 the surface area is slightly larger in MAM-FL (5010Å²) as compared to MAM-ΔLP (4440
505 Å²). The analysis reveals that hydrogen bonds (H-bonds) and salt bridges strongly
506 mediate residue's connectivity and structural arrangement. Next, we augmented the
507 number of copies and found that the circular arrangement is maintained in heptamers and
508 octamers, with ranking scores of 0.94 and 0.89, respectively. This suggests comparable,
509 if not better, stability for the hexamer form. Overall, these findings indicate a particularly
510 stable and favorable edifice for MAM-ΔLP in its hexameric conformation.

511 Calculations of electrostatic potential were performed on MAM-ΔLP and MAM-FL
512 hexamers, using the PyMOL APBS plugin, to investigate the distribution and contribution
513 of charged residues. This analysis revealed distinct electrostatic profiles between the inner
514 and outer protein surfaces. The wider surface, which corresponds to the central region of
515 the amino-acid sequence, exhibits a predominance of positive charges spread across the
516 surface, with interspersed negative charges. On this side, the central pore has a dominant
517 negative potential, which might facilitate interactions or passages of positively charged
518 ions or molecules. On the opposite side, which comprises the N-terminus residues (closer
519 to the outer edge), the surface displayed more neutral charges. White regions dominate
520 this surface side, indicating charge neutrality, particularly around the C-terminus, which
521 forms the central pore. This observation is consistent with the role of envelope proteins,
522 where different surfaces may interact with the bacterial membrane on one side while
523 interacting with other extracellular or cytoplasmic components on the other. Such
524 observations are fittable for both MAM-ΔLP and MAM-FL. (Supplementary Figure 5).
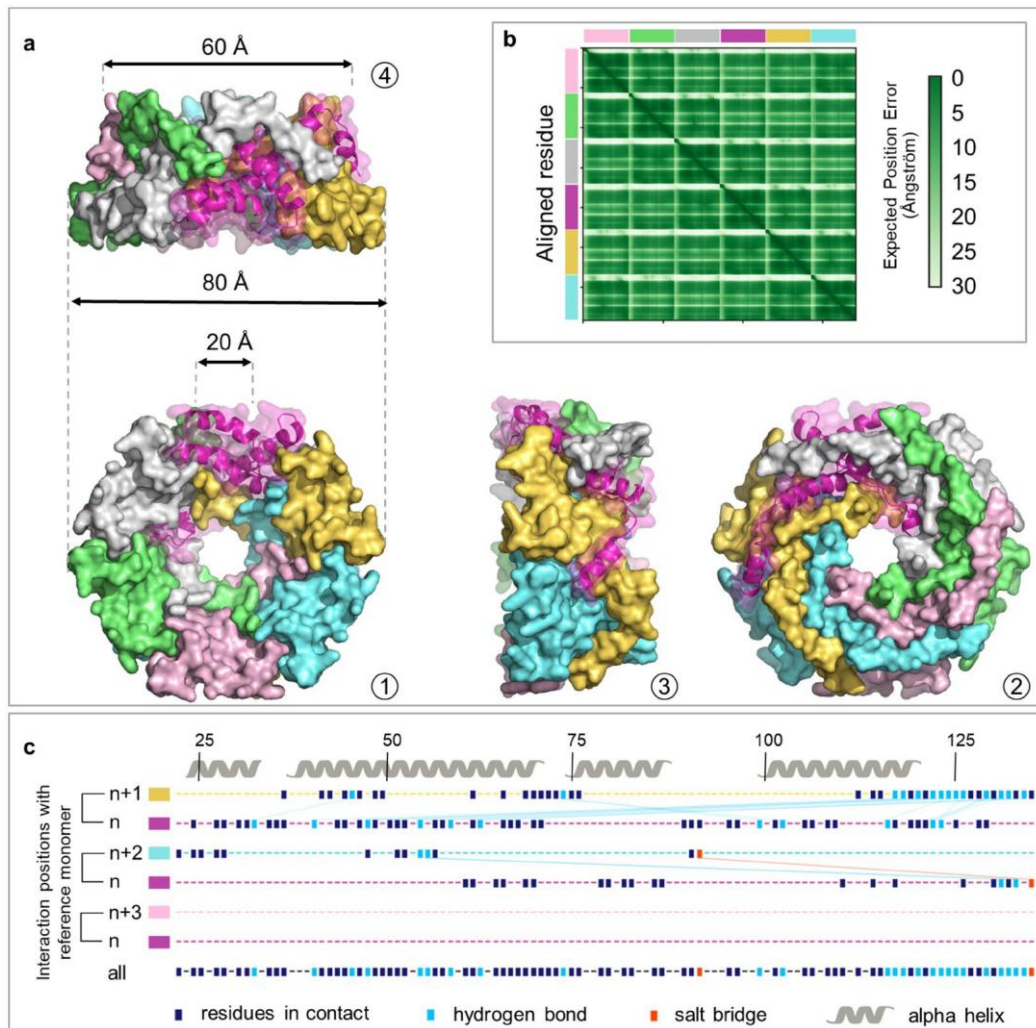
525
526 Figure 6. Predicted hexameric structure of MAM-ΔLP A) Alphafold3-predicted hexameric structure of
527 MAM-ΔLP visualized in PyMOL, with subunits colored differently. Panels A-1 and A-2 show opposite
528 faces of the hexamer, while A-3 and A-4 present the structural profile. The hexamer measures 80 Å in
529 diameter on its widest face and 60 Å on the other face. The central hole is 20 Å in diameter. (B) PAE plot
530 highlighting lower error at subunit interfaces (green blocks) and less confidence for peripheral regions. C)
531 Schematic representation of amino acid interactions involved in the stability of the predicted MAM-ΔLP
532 hexamer structure, obtained with PISA. The upper part of the figure shows the amino acid numbers and the
533 respective positions of the modeled α-helices. Bellow, each line corresponds to a subunit of the MAM-ΔLP
534 hexamer. Dark blue squares represent amino acid interaction points, light blue indicates hydrogen bonds,
535 and orange indicates salt bridges. The first two lines display level 1 interactions (n, n+1), showing contacts
536 between adjacent units. The next two lines correspond to level 2 interactions (n, n+2), indicating interactions
537 between the second-adjacent subunit. The empty third line evidences the lack of level 3 interactions (n,
538 n+3) corresponding to subunits on opposite sides. The last line represents all positions in interaction for one
539 subunit.

540 **LiCl extracts highlight MAM predominance and organized structural patterns**

541 LiCl is often used to extract surface-associated proteins and cell envelope proteinases.[36]
542 To further investigate the association of MAM with the bacterial cell surface, the LiCl-
543 extracted fraction from *F. duncaniae* was analyzed by SDS-PAGE electrophoresis
544 (Figure 7A). Overall, fewer bands were observed at this extraction than at the previous
545 cell envelope analysis. Notably, the band between 10-15 kDa was the most intense in the
546 lane, likely corresponding to MAM, as its size aligns with MAM after processing the
547 leader peptide (12,1kDa). The complete protein pool was submitted for proteomic
548 identification. This analysis revealed MAM as the most abundant protein based on the

549 NSAF score (0,0188) (Supplementary Figure 6 and Supplementary Data 3). In-depth
550 proteomic analysis of the extract resulted in MAM identification with log(E-value) of -
551 474.10, identifying peptides covering 85.19% of the full-length protein, with only the first
552 21 amino acids missing. The analysis identified 203 spectra, all of which were specific,
553 covering 49 sequences and 90 unique peptide modifications. These comprehensive results
554 strongly indicate the predominance of MAM on the envelope of *F. duncaniae*.

555 In addition to identifying MAM as the predominant protein in the LiCl extracts, we sought
556 to investigate the structural organization of these extracts using negative staining
557 microscopy. Extracted fragments appeared as larger circular structures composed of
558 smaller aggregates with similar organized patterns, exhibiting dark points and circular
559 borders. The diameters of the circular fragments were diverse, ranging from 29 nm to 220
560 nm. These observations are consistent with the predicted pore-like organization of
561 hexameric assemblies but require further confirmation to establish a direct relationship
562 (Figure 7B). Together, these findings suggest that MAM may contribute to the organized
563 structural motifs observed microscopically, consistent with its predicted hexameric
564 assembly.

565
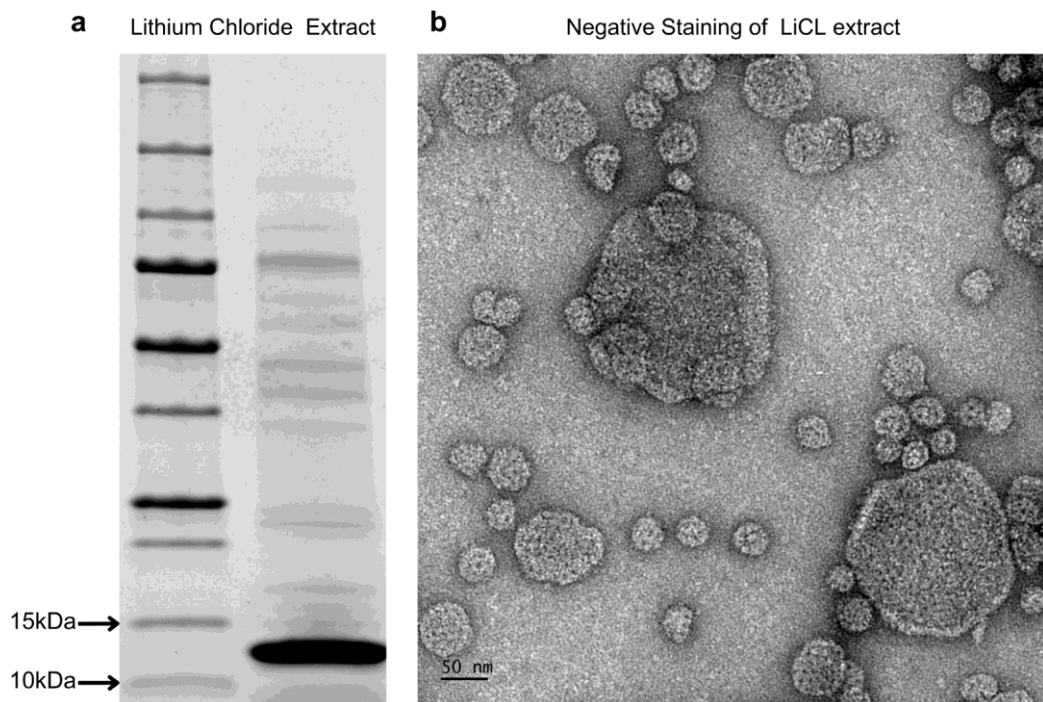
Figure 7. Proteomic Analysis of LiCl-extracted Fraction. A) SDS-PAGE electrophoresis of the LiCl-extracted fraction. The first lane contains the protein ladder, and the second lane contains the S-layer extract. (B) The negative staining microscopy of LiCl extracts reveals a complex landscape of circular fragments with varying diameters.

566 **Hexameric lattice observed in surface structures of *F. duncaniae* by *In Situ***
567 **Microscopy**

568 Electron-microscopy imaging proves to be extremely helpful in order to obtain structural
569 and functional information about cells and proteins.[37] Here, *in situ*, negative stain electron
570 microscopy of *F. duncaniae* cells revealed the bacilli expected shape of *F. duncaniae*.
571 The internal cell content is surrounded by a thick, dark layer, likely representing the cell
572 envelope. Some images showed regular cell shapes, while others showed its internal
573 content shrinking or lost, likely due to cell lysis from oxygen exposure. This led to the

appearance of a remaining shield similar to bacterial ghosts, highlighting a structured layer with a regular pattern. This ordered lattice is visible at the outermost level. Circular structures with clear surroundings and dark centers indicate depressions suggesting porosity (Figure 8 A-D).

To further evaluate this structure, Single Particle Analysis (SPA) of the bacterial lattice revealed a highly ordered hexameric structure. This periodic arrangement indicates the strong symmetry and regularity inherent in the protein assembly. The SPA images provided a detailed view of this hexameric pattern, consistently showing each central hexamer surrounded by six adjacent units, forming a macrostructure with six-fold symmetry. These units exhibited well-defined boundaries and central depressions, likely representing a porous layer. Quantitative measurements of these pores indicated an internal diameter with a mean of 14.7 nm (147 Å), varying from 12,5 to 17,4 nm in diameter. Moreover, the lattice organization suggests flexible properties, which are observed as curvatures (Figure 8 E-F). This flexibility may significantly affect the protein complexes' biological functionality and mechanical stability in the 3D bacterial conformational dynamics. These hexameric assemblies observed in the bacterial lattice are consistent with the predicted hexameric organization of MAM, as described Previously.
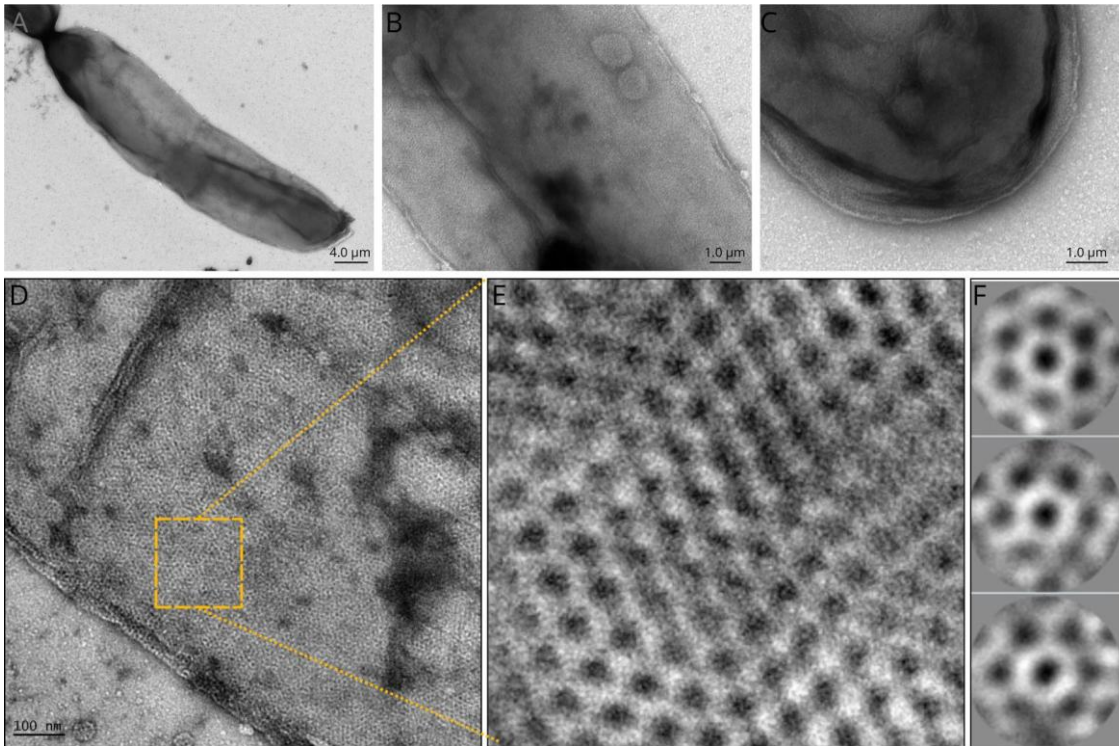
Figure 8. Electron microscopy of F. duncaniae cells. A) Full cell of F. duncaniae with signs of internal degradation. (B) Section of the cell envelope showing an organized, layered structure. (C) Close-up of the cell end, highlighting a thick cell envelope and organized coat structure. (D) Structure resembling a bacterial ghost with an intact coat but absent internal contents. (E) High-resolution microscopy of (D), showing hexameric patterns. (F) SPA transform images demonstrate the hexameric arrangement, confirming six-fold symmetry.

Immunogold labeling confirms MAM localization at the cell envelope poles

Immunoelectron microscopy of ultrathin cryosections of *F. duncaniae* cells revealed precise localization of MAM within the bacterial envelope. Bacterial cells were sectioned and labeled with polyclonal anti-MAM antibodies, followed by secondary antibodies conjugated to 10 nm colloidal gold particles for visualization. Gold particles were predominantly observed at the cell periphery, indicating a strong association of MAM

604 with the envelope layer. This peripheral distribution of MAM was consistent across
605 multiple sections and different fields of view, confirming that MAM is localized mainly,
606 more than 50%, at the outermost layer of the bacterial cell (Figure 9 A-E). In contrast,
607 minimal, less than 20%, gold labeling was detected in the cytoplasmic region, reinforcing
608 the hypothesis that MAM is rather surface-associated. The electron-dense gold particles
609 were distributed in a pattern that suggests MAM may form organized structures,
610 potentially contributing to the integrity and functionality of the cell envelope.

611
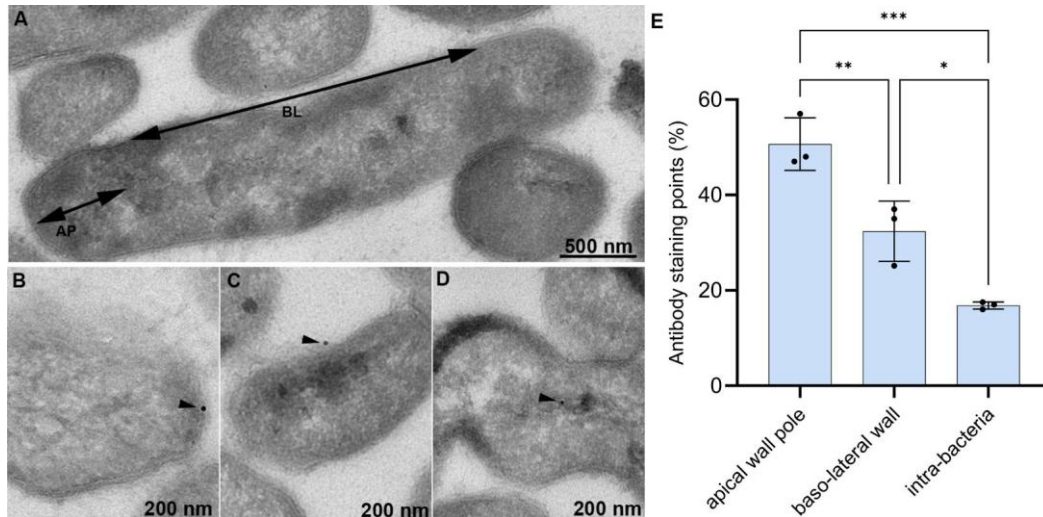
612 Figure 9. Immunolabeling of MAM in F. duncaniae Cell. A-D)Transmission electron microscopy (TEM)
613 images of ultrathin sections of F. duncaniae cells showing the localization of MAM through immunogold
614 labeling. Black dots represent the gold particles indicating the presence of MAM. A) TEM image of *F.*
615 *duncaniae* illustrating the basolateral (BL) and apical (AP) regions of the bacteria; B) Immunogold labeling
616 localized at the apical pole; C) basolateral side; and D) intra-bacteria. E) Percentage of labeling dots in each
617 cell region, highlighting the higher significant labeling signal in the apical wall pole.

619

DISCUSSION

621 *F. duncaniae* is a dominant species in the gut microbiota of healthy adults, known for its
622 unique capacity to produce MAM, a protein with significant anti-inflammatory
623 properties.[11] However, the molecular characteristics and physiological role of MAM have
624 not been well-documented until now. Here, we reported in vitro, that MAM is the first
625 protein, ranked by abundance, and primarily localized in the envelope fraction of *F.*
626 *duncaniae*. We also demonstrated, in silico, compelling evidence that MAM could be
627 the substrate of the adjacent Peptidase-Containing-ABC-Transporter (PCAT), which is
628 also remarkably expressed,[11]. We maje here that PCAT translocate MAM out, to the cell
629 envelope. MAM could be recognized with its N-terminal leader peptide to be excised by
630 the adjacent, and possibly cognate, PCAT. Moreover, MAM evidences in silico intrinsic
631 ability to self-arrange into a hexameric complex, hence creating a pore-like
632 supramolecular structure, secured by an intensive network of hydrogen bonds and salt
633 bridges. In line with that, we reported in vitro, using microscopy techniques the detection
634 of a hexameric edifice with physical characteristics compatible with our in silico
635 predictions and immunogold labelling of MAM especially localized at the envelope of
636 cell poles. These novel conclusions emphasize that MAM could shape the cell envelope
637 and bolster *F. duncaniae*'s cell integrity while mediating interactions between the
638 bacterial internal cell, the environment, and the host.

MAM's known anti-inflammatory properties and beneficial effects observed in colitis mice models have diverted investigations on MAM's physiological and functional significance within the bacterium. MAM was primarily identified as peptides in the supernatant of *F. duncaniae*.[11] Early structural predictions determined that MAM has more than 50% hydrophobic residues disseminated onto a putative globular organization. Low sequence complexity and intrinsic disorder were not predicted, and no transmembrane domain was correlated with MAM. Those earliest models were obtained by homology modeling, with the amino acid sequence indicating MAM having multiple β-sheet forming a core region flanked by α-helices.[12] Ji-Hee Shin and collaborators also hypothesized on MAM tertiary structure, sharing features with the previously mentioned model.[13] In addition, Auger et al. investigated the diversity of MAM based on genetic features and phylogenetic assays, highlighting MAM's great phenotypic heterogeneity reflected in its anti-inflammatory potential.[11] Hence, we aimed to investigate MAM's physiological, structural, and functional features in *F. duncaniae*. Appropriately, we explore MAM traits using numerous methodological strategies to describe this protein extensively and assess its physiological role in the cell.

The first experimental identification of MAM was performed on the bacterial supernatant, which contains several fractions of MAM peptides, suggesting that MAM was a secreted protein.[12] To confirm such behavior and the secretion dynamics of MAM peptides during the *F. duncaniae*'s growth, liquid culture supernatant was collected at different time steps, covering the bacterium growth from 6 to 25 hours. This broad analysis revealed that MAM peptides are rarely detected in the early stages of growth, contrasting with a higher abundance at the stationary phase. Also, the peptides did not follow a specific pattern of secretion, neither in size nor in amino acid composition; many differed by just one amino acid from others. Such randomness is also observed on the first identified peptides. The four different peptides detected in the early stages of *F. duncaniae* growth (between 6 and 9 hours) do not belong to a specific region but instead cover the middle-end of the protein (amino acid positions 52-65 and 112-135) (Figures 1 and 2). Markedly, none of them detects any N-terminal-containing peptides.

When comparing our results with those of the previous MAM identification performed by Quévrain et al[12], a significant discrepancy in the number of identified MAM peptides is evident. While the earlier research identified only seven peptides using MALDI-TOF (Matrix-Assisted Laser Desorption/Ionization Time-of-Flight) and FT-ICR (Fourier Transform Ion Cyclotron Resonance) mass spectrometry, our approach identified 86 MAM peptides. Several factors could explain this difference. Firstly, the sensitivity and the resolution of the Orbitrap Fusion Lumos Tribrid mass spectrometer employed in our study are superior, enabling largely comprehensive peptide detection and identification.[38,39] Additionally, our methodological approach involved a more extensive fractionation process, with samples collected at various growth phases (6, 9, 18, and 25 hours) and from four replicates, increasing the likelihood of detecting a broader range of peptides. Furthermore, using the X! Tandem software for data processing may have contributed to more robust peptide identification compared to the methodologies used in the previous study.[21,38] This significant increase in the number of identified peptides underscores the effectiveness of our methodological enhancements and, importantly, highlights the complexity of MAM peptide and the abundance of MAM production in *F. duncaniae*. Consequently, we hypothesize that MAM is not a secreted protein per se but is likely present in the supernatant due to a non-specific degradation process, possibly cell death, lacking distinct cleavage sites. This is fully consistent with the capacity of MAM leader peptide to be recognized and cleaved off by PCAT, which strictly co-occurs

688 and is located in the vicinity of MAM. This explains why the leader peptide/N-terminus
689 is not detectable in our proteomic and peptidomics analysis. Notably, MAM is able to be
690 embodied within the inner groove formed by the PCAT dimer.

691 The evidence that MAM is not actively secreted raises the question of its subcellular
692 localization. Several cell fractionation procedures have been established, each adapted to
693 specific bacterial envelope compositions.[36] However, the cell envelope characteristics of
694 *F. duncaniae* remain undescribed. Therefore, we employed a preliminary method to
695 separate the envelope from cytoplasmic fractions and investigate MAM localization. Cell
696 pellets were subjected to chemical and physical lysis, followed by high-speed
697 centrifugation to separate the internal soluble (cytoplasmic fraction) from the envelope
698 (insoluble fraction) content.[40,41] Samples were then submitted to LC-MS/MS for protein
699 identification and i2MassChroq[42] was used for spectral counting quantification.

700 Our results assessed that MAM is one of the most abundant proteins in *F. duncaniae*'s
701 proteome and the most abundant protein in the envelope fraction (Figure 3). Principal
702 Component Analysis (PCA) demonstrates that our separation approach effectively
703 differentiated cytoplasm from envelope proteins. Notably, the NSAF score, which
704 normalizes spectral counts by protein length to account for differences in protein size,
705 identified MAM as the most abundant protein in the envelope fraction. This normalization
706 is particularly relevant for accurately comparing the relative abundance of proteins within
707 complex mixtures.[43] In addition, our findings suggest that the conventional cell
708 fractionation method, which typically treats the envelope fraction as cellular debris, may
709 not be optimal for *F. duncaniae*.[44] This approach could hide critical insights into MAM's
710 subcellular localization and abundance. Moreover, *F. duncaniae* is a fragile bacterium
711 that is difficult to cultivate due to its extreme oxygen sensitivity, presenting significant
712 challenges during cell manipulation. While refined fractionation techniques exist, our
713 approach provided sufficient resolution under experimental conditions, highlighting
714 MAM as a key envelope component. However, these results also underscore the necessity
715 of future investigations into *F. duncaniae*'s cell organization, with further optimization
716 of cell fractionation methods specific to this bacterium.

717 MAM's amino acid composition, genetic organization, structural conformation, and
718 supramolecular assembling capacity were also investigated. MAM is exclusively
719 produced by the genus Faecalibacterium. Other studies from the group have recently
720 highlighted this singularity.[11] Having such a distinctive sequence, no relevant homology
721 with other proteins is observed, and no known domains were identified. The MAM
722 sequence of *F. duncaniae* differs from the MAM of other Faecalibacterium species by up
723 to 40%. The genomic region of MAM's coding sequence harbors several proteins,
724 including the Peptidase-Containing ABC Transporters (PCATs).[11]

725 ATP-binding cassette (ABC) transporters integrate a large group of integral membrane
726 proteins present in a vast number of living organisms. They are composed of two
727 Nucleotide-Binding Domains (NBD) responsible for the processing of ATP and two
728 Transmembrane Domains (TMDs), which form the core of the active export of diverse
729 substrates, including proteins, ions, lipids, and peptides.[45] PCATs are unique members of
730 the ABC transporter group. They are formed by two peptidases capable of transporting
731 peptides and proteins across membranes and acting on the maturation process through
732 their proteolytic activity. They act, for example, on the secretion of quorum-sensing and
733 antimicrobial peptides.[15,46] PCATs in Gram-positive bacteria are known to recognize and
734 cleave off leader peptides that specifically display an L-shaped N-terminal segment with
735 a double glycine stretch (GG) while being able to embody the cargo protein to be exported
736 in a disordered shape. This step is next followed by transferring the remaining cargo

protein outside the cytosol. In Gram-negative bacteria, PCATs are involved in a complex formation of membrane proteins in a secretion system Type I (T1SS). They compose a transport core between the inner and outer membranes; in this case, the proteolytic process is absent, resulting in the maintenance of the leader peptide.[29,33]

In this study, Alphafold3 was used to model the MAM structure as a monomer, followed by docking the MAM leader peptide in a complex with the ABC transporter, considered as a functional dimer. AlphaFold is considered the most accurate tool for structural predictions, with the added capability of predicting complex interactions.[23]Although the sequence of MAM can be variable among different species of Faecalibacterium, three motifs recapitulate all MAM sequences. The predicted monomeric structure of MAM revealed a core region consisting of three alpha-helices connected by flexible coil regions with a potentially unfolded C-terminus (Figure 4A). Remarkably, the N-terminus is strictly conserved if we consider the [MMMPANx8/11VxGG] motif, and it has been shown that it is necessary and sufficient to retrieve MAM-like protein in a dataset of hundreds of millions of sequences.

Indeed, the structure prediction of MAM and docking of its 22-residue-long extended leader peptide into the PCAT active site highlight a strong interaction at the cysteine peptidase domain of the PCAT. The N-terminal segment of MAM evidences an L-shape feature, which is required to accommodate into the PCAT conserved active site and to prime the GG stretch for proteolysis. The process leads to the excision of the leader peptide, in which a consensus sequence has been previously identified in other organisms, also located at the N-terminus and formed by Ile/Leu/Val(-12)-(X)3-Glu(-8)-Leu(-7)-Val(-4)-Gly(-2)Gly(-1).[33,46] Markedly, this pattern sticks to the MAM's consensus sequence described above Leu(−12)-(X)3-Glu(−8)-Leu(−7)-Gly(-2)Gly(-1) (Figure 4D and Supplementary figure 3A). This observation strengthens the indication of PCATs as the cognate transporter of MAM.

These in silico interactions strongly correlate with those observed in the recently solved cryo-EM structure of the PCAT1 transporter bound to a 21-residue CtA substrate in Clostridium thermocellum.[47] The conserved amino acid residues at the active site, the shared pattern of substrate binding, and similar interaction energies suggest that PCAT recognizes and cleaves the MAM leader peptide, acting as its cognate transporter. Supporting this hypothesis, the MAM leader peptide has been detected by LC-MS/MS only once, with one related spectra count. In contrast, the MAM cargo peptide has been consistently identified as a cell envelope component. This evidence indicates that MAM is likely a physiological substrate of PCAT, which processes and exports it to participate into the assembly of the *F. duncaniae* cell envelope (Figure 5).

The subcellular localization of MAM at the cell envelope, the absence of a strong secretion pattern, the high abundance and the putative transportation through PCAT led us to use AlphaFold again to investigate the capability of a structural super-organization of MAM. Starting from dimers and extending to octamers, our modeling indicated that MAM is likely arranged in a pore-organized structure, with the highest confidence attributed to the hexameric assembly of MAM cargo peptide. Moreover, the electrostatic potential map of the hexameric model indicates its charge distribution is suitable for interaction with the bilipid membrane (Supplementary figure 4-5).[48] The presence of negative and positive charges across the protein's surface suggests that MAM may interact with polar heads and hydrophobic tails of the lipid bilayer. This feature can act to facilitate protein anchoring and interactions and maintain the proper orientation of MAM within the membrane. These findings suggest that once exported to the cell

785 envelope, after N-terminal cleavage by the PCAT, MAM would predominantly organize
786 in a stable oligomeric complex, forming a pore with a central hole.

787 Recent microscopy techniques were applied to visualize and analyze *F. duncaniae* cells
788 accurately. Our findings revealed significant insights into the cell envelope's architecture
789 and functionality. The in situ negative stain electron microscopy confirmed the bacilli
790 shape of *F. duncaniae* and highlighted a porous bacterial coat. The observed shrinkage
791 and cell lysis from oxygen exposure resulted in cells with the appearance of bacterial
792 ghosts, which persisted possibly after cell lysis[49](Figure 8A-D). Fast Fourier Transform
793 and Single Particle Analysis revealed a crystalline pattern with six-fold symmetry by
794 exhibiting a regular, hexameric lattice structure. The flexibility observed in the lattice's
795 curvature may contribute to its biological function and mechanical stability (Figure 8 E-
796 F).

797 Among the different pore-organized proteins, MAM's subcellular localization, the
798 absence of structural homologs, it's high abundance and putative hexameric organization
799 indicate a fittable role as an S-layer protein. For example, Haloferax volcanii is an
800 archaeon that has a protein with self-arrangement properties organized into hexameric or
801 pentameric structures, forming the S-layer coat on the cell surface and the surface of
802 exomes.[50] S-layer proteins from the bacteria *Deinococcus radiodurans* and the archaea
     Sulfolobus acidocaldarius also have the capacity to create hexamers, with the central pore
     structure.
803 The assembly of several hexamers forms an ordered lattice, which provides structural
804 integrity and protection to the organism.[51,52] In beneficial bacterial species like *L.*
805 *acidophilus,*[53] *L. brevis,*[54] *L. crispatus,*[55,56] *L. helveticus,*[57,58] and *P. freudenreichii,*[59] S-
806 layers were identified. However, such structures are poorly described between human gut
807 commensals.

808 After using LiCl, a common surface proteins extraction agent,[60,61] through proteomic
809 analysis, we obtained an enriched envelope sample in which MAM was identified as the
810 most abundant protein. Negative staining microscopy of the LiCl extract supported the
811 visualization of an ordered porous lattice, this time in circular fragments but with the same
812 pattern as the surrounding *F. duncaniae* cells. The hexameric structure of MAM modeled
813 by AlphaFold matched the organization observed in these networks regarding dimension
814 and hexametrical arrangement (Figure 6-7). These findings support the possibility that
815 MAM could function as an S-layer protein. However, further research is necessary to
816 confirm this, particularly to determine whether there is a complete proteinaceous bacterial
817 coat or if MAM is a membrane-associated protein.

818 Immunogold labeling of *F. duncaniae* cells obtained with polyclonal antibodies raised
819 against recombinant purified MAM revealed black dots on the peripheral bacterial
820 surface, confirming the presence of MAM in the cell envelope (Figure 9).

821 Interestingly, MAM detection in *F. duncaniae* cells was more pronounced at the bacterial
822 poles than in the mid-cell region (Figure 9). Polar proteins are known to play roles in
823 genome segregation, cell division, septum formation, signal transduction, and dynamic
824 regulation, all of which are crucial for determining protein functionality.[62,63] These
825 findings strengthen the hypothesis that MAM is essential for maintaining cell envelope
826 integrity and facilitating interactions with the host and environment. Additionally, they
827 open new avenues for exploring MAM's potential role in the cell cycle. This highlights
828 the need for further investigation to precisely determine the positioning and organization
829 of MAM within cell envelope layers, as well as its temporal and spatial dynamics.

831

ACKNOWLEDGMENTS

DISCLOSURE STATEMENT

All authors declare no competing financial or non-financial interests.

FUNDING

DATA AVAILABILITY

The mass spectrometry proteomics data reported in this work have been deposited in the ProteomeXchange Consortium database (http://proteomecentral.proteomexchange.org) via the PRIDE partner repository, with the dataset identifier PXD057939.

CORRESPONDING AUTHORS

Correspondence to Jean-Marc Chatel: jean-marc.chatel@inrae.fr

AUTHORS CONTRIBUTIONS

T.V.R. participated in all stages of the study, including bacterial culture, extraction, sample preparation for peptidomics and proteomics, bioinformatic analysis, microscopy, writing the main manuscript and prepared the figures. C.H. conducted the complete peptidomics and proteomics workflow, including sample preparation, data acquisition and processing. V.M. performed database searches to identify homologs of the MAM leader peptide across various organisms. G.A. led the bioinformatic analysis, focusing on the detailed investigation of the interaction between PCAT and the leader peptide, and contributed to the manuscript writing. S.M. carried out the structural predictions of MAM and performed comprehensive analyses of its structural properties. C.P. was responsible for electron microscopy and immunogold labeling of bacterial cells and LiCl extracts. A.A. conducted electron microscopy and single-particle analysis of bacterial cells and LiCl extracts. L.L.J. handled the production and purification of recombinant MAM. V.A.C.A. and J.M.C. supervised the research as primary advisors. P.L. and S.C.S. contributed to the manuscript revision. All authors read and approved the final manuscript.

REFERENCES

1. Miquel, S. *et al.* Faecalibacterium prausnitzii and human intestinal health. *Curr Opin Microbiol* **16**, 255–261 (2013).

2. Sokol, H. *et al.* Faecalibacterium prausnitzii is an anti-inflammatory commensal bacterium identified by gut microbiota analysis of Crohn disease patients. *Proc Natl Acad Sci U S A* **105**, 16731–16736 (2008).

3. Maioli, T. U. *et al.* Possible Benefits of Faecalibacterium prausnitzii for Obesity-Associated Gut Disorders. *Front Pharmacol* **12**, 740636 (2021).

4. Martín, R. *et al.* Faecalibacterium: a bacterial genus with promising human health applications. *FEMS Microbiol Rev* **47**, (2023).

875   5.   Nishiwaki, H. *et al.* Meta-Analysis of Gut Dysbiosis in Parkinson's Disease. *Movement*
876   *Disorders* **35**, 1626–1635 (2020).

877   6.   Liu, Y. *et al.* Roles of the gut microbiota in severe SARS-CoV-2 infection. *Cytokine*
878   *Growth Factor Rev* **63**, 98–107 (2022).

879   7.   Chollet, L. *et al.* Faecalibacterium duncaniae as a novel next generation probiotic against
880   influenza. *Front Immunol* **15**, 1347676 (2024).

881   8.   Duncan, S. H., Hold, G. L., Harmsen, H. J. M., Stewart, C. S. & Flint, H. J. Growth
882   requirements and fermentation products of Fusobacterium prausnitzii, and a proposal to
883   reclassify it as Faecalibacterium prausnitzii gen. nov., comb. nov. *Int J Syst Evol Microbiol*
884   **52**, 2141–2146 (2002).

885   9.   Schwab, M. *et al.* Involvement of different nuclear hormone receptors in butyrate-
886   mediated inhibition of inducible NFκB signalling. *Mol Immunol* **44**, 3625–3632 (2007).

887   10.   Fusco, W. *et al.* Short-Chain Fatty-Acid-Producing Bacteria: Key Components of the
888   Human Gut Microbiota. *Nutrients* **15**, (2023).

889   11.   Auger, S. *et al.* Intraspecific Diversity of Microbial Anti-Inflammatory Molecule (MAM)
890   from Faecalibacterium prausnitzii. *Int J Mol Sci* **23**, (2022).

891   12.   Quévrain, E. *et al.* Identification of an anti-inflammatory protein from Faecalibacterium
892   prausnitzii, a commensal bacterium deficient in Crohn's disease. *Gut* **65**, 415 (2016).

893   13.   Shin, J. H. *et al.* Faecalibacterium prausnitzii prevents hepatic damage in a mouse model
894   of NASH induced by a high-fructose high-fat diet. *Front Microbiol* **14**, 1123547 (2023).

895   14.   Verstraeten, S. *et al.* Faecalibacterium duncaniae A2-165 regulates the expression of
896   butyrate synthesis, ferrous iron uptake, and stress-response genes based on acetate
897   consumption. *Scientific Reports 2024 14:1* **14**, 1–12 (2024).

898   15.   Rahman, S. & McHaourab, H. S. ATP-dependent interactions of a cargo protein with the
899   transmembrane domain of a polypeptide processing and secretion ABC transporter.
900   *Journal of Biological Chemistry* **295**, 14678–14685 (2020).

901   16.   Breyner, N. M. *et al.* Microbial Anti-Inflammatory Molecule (MAM) from
902   Faecalibacterium prausnitzii Shows a Protective Effect on DNBS and DSS-Induced
903   Colitis Model in Mice through Inhibition of NF-κB Pathway. *Front Microbiol* **8**, (2017).

904   17.   Seo, B. *et al.* Strain-Specific Anti-Inflammatory Effects of Faecalibacterium prausnitzii
905   Strain KBL1027 in Koreans. *Probiotics Antimicrob Proteins* (2024) doi:10.1007/S12602-
906   024-10213-7.

907   18.   Xu, J. *et al.* Faecalibacterium prausnitzii-derived microbial anti-inflammatory molecule
908   regulates intestinal integrity in diabetes mellitus mice via modulating tight junction protein
909   expression普拉梭菌活性产物-微生物抗炎分子通过调控细胞紧密连接蛋白表达修复
910   糖尿病小鼠肠道屏障. *J Diabetes* **12**, 224–236 (2020).

911   19.   Martín, R. *et al.* The commensal bacterium Faecalibacterium prausnitzii is protective in
912   DNBS-induced chronic moderate and severe colitis models. *Inflamm Bowel Dis* **20**, 417–
913   430 (2014).

914   20.   Craig, R. & Beavis, R. C. TANDEM: matching proteins with tandem mass spectra.
915   *Bioinformatics* **20**, 1466–1467 (2004).

21. Langella, O. *et al.* X!TandemPipeline: A Tool to Manage Sequence Redundancy for Protein Inference and Phosphosite Identification. *J Proteome Res* **16**, 494–503 (2017).

22. Bateman, A. *et al.* UniProt: the Universal Protein Knowledgebase in 2023. *Nucleic Acids Res* **51**, D523–D531 (2023).

23. Abramson, J. *et al.* Accurate structure prediction of biomolecular interactions with AlphaFold 3. *Nature 2024 630:8016* **630**, 493–500 (2024).

24. Schrödinger L & Warren DeLano. PyMOL. Preprint at http://www.pymol.org/pymol (2020).

25. van Kempen, M. *et al.* Fast and accurate protein structure search with Foldseek. *Nature Biotechnology 2023 42:2* **42**, 243–246 (2023).

26. Krissinel, E. & Henrick, K. Inference of macromolecular assemblies from crystalline state. *J Mol Biol* **372**, 774–797 (2007).

27. Gasteiger, E. *et al.* Protein Identification and Analysis Tools on the ExPASy Server. in *The Proteomics Protocols Handbook* 571–607 (Humana Press, Totowa, NJ, 2005). doi:10.1385/1-59259-890-0:571.

28. Rice, P., Longden, L. & Bleasby, A. EMBOSS: The European Molecular Biology Open Software Suite. *Trends in Genetics* **16**, 276–277 (2000).

29. Kieuvongngam, V. *et al.* Structural basis of substrate recognition by a polypeptide processing and secretion transporter. *Elife* **9**, (2020).

30. Morris, G. M. *et al.* AutoDock4 and AutoDockTools4: Automated docking with selective receptor flexibility. *J Comput Chem* **30**, 2785–2791 (2009).

31. Schneider, C. A., Rasband, W. S. & Eliceiri, K. W. NIH Image to ImageJ: 25 years of image analysis. *Nature Methods 2012 9:7* **9**, 671–675 (2012).

32. Tokuyasu, K. T. A technique for ultracryotomy of cell suspensions and tissues. *J Cell Biol* **57**, 551–565 (1973).

33. Bobeica, S. C. *et al.* Insights into AMS/PCAT transporters from biochemical and structural characterization of a double Glycine motif protease. *Elife* **8**, (2019).

34. Kieuvongngam, V. & Chen, J. Structures of the peptidase-containing ABC transporter PCAT1 under equilibrium and nonequilibrium conditions. *Proc Natl Acad Sci U S A* **119**, (2022).

35. Bludau, I. *et al.* Rapid Profiling of Protein Complex Reorganization in Perturbed Systems. *J Proteome Res* **22**, 1520–1536 (2023).

36. Ji, D., Ma, J., Xu, M. & Agyei, D. Cell-envelope proteinases from lactic acid bacteria: Biochemical features and biotechnological applications. *Compr Rev Food Sci Food Saf* **20**, 369–400 (2021).

37. Franken, L. E. *et al.* A Technical Introduction to Transmission Electron Microscopy for Soft-Matter: Imaging, Possibilities, Choices, and Technical Developments. *Small* **16**, 1906198 (2020).

38. Zhao, Y. *et al.* Evolution of Mass Spectrometry Instruments and Techniques for Blood Proteomics. *J Proteome Res* **22**, 1009–1023 (2023).

956   39.   Luo, Y., Li, T., Yu, F., Kramer, T. & Cristea, I. M. Resolving the Composition of Protein
957   Complexes Using a MALDI LTQ Orbitrap. *J Am Soc Mass Spectrom* **21**, 34–46 (2010).

958   40.   Solis, N. & Cordwell, S. J. Current methodologies for proteomics of bacterial surface-
959   exposed and cell envelope proteins. *Proteomics* **11**, 3169–3189 (2011).

960   41.   Henry, C. *et al.* Identification of Hanks-type kinase PknB-specific targets in the
961   Streptococcus thermophilus phosphoproteome. *Front Microbiol* **10**, 452274 (2019).

962   42.   Valot, B., Langella, O., Nano, E. & Zivy, M. MassChroQ: A versatile tool for mass
963   spectrometry quantification. *Proteomics* **11**, 3572–3577 (2011).

964   43.   Millán-Oropeza, A., Blein-Nicolas, M., Monnet, V., Zivy, M. & Henry, C. Comparison of
965   Different Label-Free Techniques for the Semi-Absolute Quantification of Protein
966   Abundance. *Proteomes* **10**, (2022).

967   44.   Santos, T. & Hébraud, M. Extraction and Preparation of Listeria monocytogenes
968   Subproteomes for Mass Spectrometry Analysis. *Methods Mol Biol* **2220**, 137–153 (2021).

969   45.   Wilkens, S. Structure and mechanism of ABC transporters. *F1000Prime Rep* **7**, (2015).

970   46.   Yu, L. *et al.* Structural basis of peptide secretion for Quorum sensing by ComA. *Nature
971   Communications 2023 14:1* **14**, 1–17 (2023).

972   47.   Bhattacharya, S. & Palillo, A. Structural and dynamic studies of the peptidase domain
973   from Clostridium thermocellum PCAT1. *Protein Sci* **31**, 498 (2022).

974   48.   Samanta, R. & Gray, J. J. Implicit model to capture electrostatic features of membrane
975   environment. *PLoS Comput Biol* **20**, e1011296 (2024).

976   49.   Lanzoni-Mangutchi, P. *et al.* Structure and assembly of the S-layer in C. difficile. *Nat
977   Commun* **13**, (2022).

978   50.   von Kügelgen, A., Alva, V. & Bharat, T. A. M. Complete atomic structure of a native
979   archaeal cell surface. *Cell Rep* **37**, 110052 (2021).

980   51.   Gambelli, L. *et al.* Structure of the two-component S-layer of the archaeon Sulfolobus
981   acidocaldarius. *Elife* **13**, (2024).

982   52.   Farci, D. *et al.* ll Structural analysis of the architecture and in situ localization of the main
983   S-layer complex in Deinococcus radiodurans. *Structure* **29**, (2021).

984   53.   Grosu-Tudor, S. S. *et al.* S-layer production by Lactobacillus acidophilus IBB 801 under
985   environmental stress conditions. *Appl Microbiol Biotechnol* **100**, 4573–4583 (2016).

986   54.   De Leeuw, E., Li, X. & Lu, W. Binding characteristics of the Lactobacillus brevis ATCC
987   8287 surface layer to extracellular matrix proteins. *FEMS Microbiol Lett* **260**, 210–215
988   (2006).

989   55.   Horie, M. *et al.* Inhibition of the adherence of Escherichia coli strains to basement
990   membrane by Lactobacillus crispatus expressing an S-layer. *J Appl Microbiol* **92**, 396–
991   403 (2002).

992   56.   Chen, X. *et al.* The S-layer proteins of Lactobacillus crispatus strain ZJ001 is responsible
993   for competitive exclusion against Escherichia coli O157:H7 and Salmonella typhimurium.
994   *Int J Food Microbiol* **115**, 307–312 (2007).

995 57. Beganović, J. *et al.* Functionality of the S-layer protein from the probiotic strain
996   Lactobacillus helveticus M92. *Antonie van Leeuwenhoek, International Journal of*
997   *General and Molecular Microbiology* **100**, 43–53 (2011).

998 58. Johnson-henry, K. C., Hagen, K. E., Gordonpour, M., Tompkins, T. A. & Sherman, P. M.
999   Surface-layer protein extracts from Lactobacillus helveticus inhibit enterohaemorrhagic
1000   Escherichia coli O157:H7 adhesion to epithelial cells. *Cell Microbiol* **9**, 356–367 (2007).

1001 59. do Carmo, F. L. R. *et al.* Extractable bacterial surface proteins in probiotic-host
1002   interaction. *Front Microbiol* **9**, 341730 (2018).

1003 60. Angelescu, I. R., Zamfir, M., Ionetic, E. C. & Grosu-Tudor, S. S. The Biological Role of
1004   the S-Layer Produced by Lactobacillus helveticus 34.9 in Cell Protection and Its Probiotic
1005   Properties. *Fermentation 2024, Vol. 10, Page 150* **10**, 150 (2024).

1006 61. Rojas, M., Ascencio, F. & Conway, P. L. Purification and characterization of a surface
1007   protein from Lactobacillus fermentum 104R that binds to porcine small intestinal mucus
1008   and gastric mucin. *Appl Environ Microbiol* **68**, 2330–2336 (2002).

1009 62. Treuner-Lange, A. & Søgaard-Andersen, L. Regulation of cell polarity in bacteria. *J Cell*
1010   *Biol* **206**, 7 (2014).

1011 63. Chaudhary, R., Mishra, S., Kota, S. & Misra, H. Molecular interactions and their
1012   predictive roles in cell pole determination in bacteria. *Crit Rev Microbiol* **47**, 141–161
1013   (2021).

1014

4.1.   Additional Results

To investigate the cellular organization of *F. duncaniae* and the localization of MAM as close as possible to its native conformation, Cryo-electron microscopy (Cryo-EM) was used. This technology enables the visualization of biological complexes with high fidelity, preserving their near-native structural integrity.

4.1.1. Methodology

Cryo-EM of F. duncaniae cells and LiCl extracts

Cryo-electron microscopy was performed with liquid cultures of *F.duncaniae* at the exponential phase. Samples were submitted to rapid freezing in liquid ethane in order to visualize intact cells. The cryo-EM grids were prepared using a Vitrobot Mark IV (ThermoFisher) at 20 C and 100% humidity. 3 uL of sample were applied onto freshly glow-discharged Quantifoil grids (R2/2), 200 mesh grids. The grids were blotted for 4.5 s with blot force 2, then plunge-frozen in liquid-nitrogen-cooled ethane. Cryo-EM images were observed in a Tecnai Spirit electron microscope (Thermo Fischer) operating at 120 kV and equipped with a DDC K2 Base direct-detection camera (Gatan Inc.). Images were recorded at 15,000 magnification, with a pixel size of 2.5 Å at the specimen level and 20 e/Å2. This methodological process is referent the Figure 6 obtained from CEA, CNRS, Institute for Integrative Biology of the Cell. The other figures (7-9) were obtained from were obtained from the MRC Laboratory of Molecular Biology from Structural Studies Division (Tanmay Bharat's lab) – Cambridge, UK.

LiCl extracts were obtained following the protocol described in the manuscript included in this chapter (page 93), and submitted to cryo-EM.

Envelope proteome of F. duncaniae screening

Protein BLAST (https://blast.ncbi.nlm.nih.gov/Blast.cgi) was used to screen the proteins related to the envelope of *F. duncaniae* proteome, focusing on homologs of proteins typically associated with the outer membrane (OM) in Gram-negative bacteria. In Gram-negative bacteria, the OM is organized with various proteins that serve as key structural and functional markers. Proteins such as OmpA, OmpC, OmpF, and LamB are integral OM components, each contributing to the membrane's integrity and selective permeability. The β-barrel assembly machinery (Bam) complex, comprising essential proteins like BamA and BamD, along with accessory proteins BamB, BamC, and BamE, orchestrates the proper folding

and insertion of these outer membrane proteins (OMPs) into the OM. Additionally, the Tol-Pal system, including proteins like TolA and TolB, plays a crucial role in maintaining OM stability and facilitating its invagination during cell division[306,307]. Moreover, MlaF is an ATP-binding component of the MlaFEDB complex, an inner membrane (IM) ABC transporter in *E. coli* involved in maintaining OM lipid asymmetry by facilitating the retrograde transport of phospholipids from the OM to the inner membrane[308]. LptA is a periplasmic protein that binds lipopolysaccharide (LPS) and is essential for transporting LPS from the IM to the OM, playing a crucial role in outer membrane biogenesis[309]. Collectively, these proteins and systems are crucial for the structural integrity, functionality, and biogenesis of the Gram-negative bacterial outer membrane. Their sequence was obtained in the Uniprot database and checked for homology with the 1469 identified proteins in the proteome of *F. duncaniae*.

4.1.2. Results

Cryo-EM of F. duncaniae cells reveal a double-layered cell envelope

To investigate the organization of the *F. duncaniae* cell envelope and its relation to MAM, Cryo-EM micrographs of *F. duncaniae* cells were obtained. The images reveal a potentially dermic organization, with a well-defined and intact IM (Figure 16). Since the composition of the external layer remains unknown, we refer to it as the outer layer (OL) rather than the outer membrane (OM).
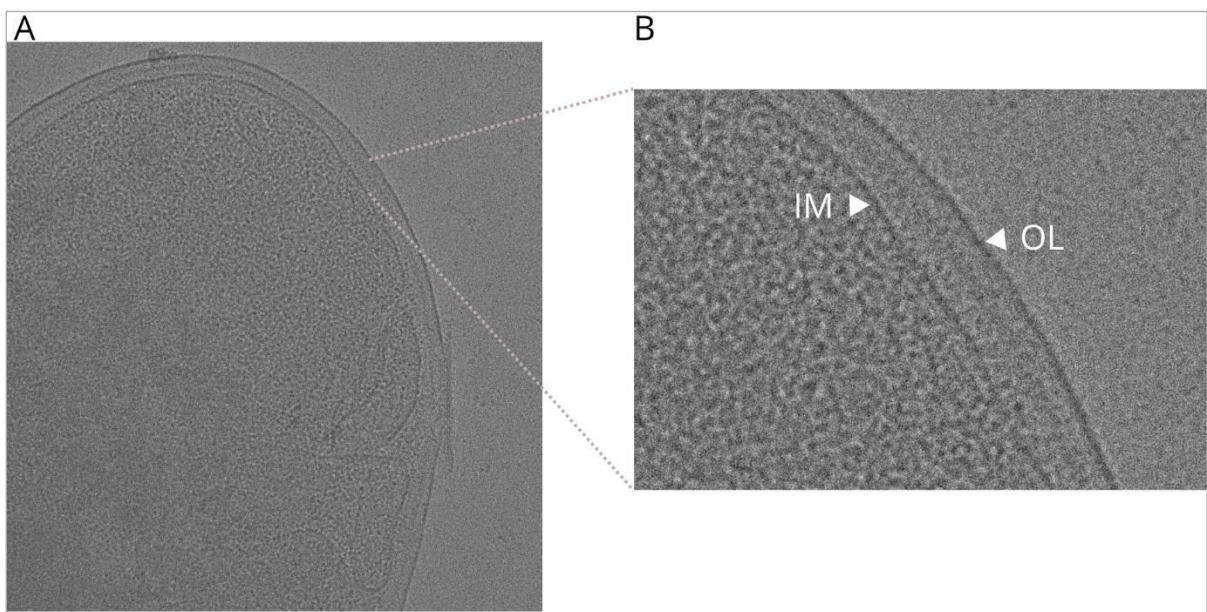
Figure 16. Cryo-EM of *F. duncaniae* cell. The image reveals the cell's surface with a clear view of its double membranes. In a close-up of the cell's membrane, the outer layer (OL) and the inner membrane (IM) are labeled, highlighting the separation between these two layers. Source: Images obtained at ImagerieGif.

In some images, the OL appears discontinuous in some regions, displaying structural disruptions and possible outward-extending invaginations. Figures 17 and 18 present Cryo-EM images of *F. duncaniae* cells in the exponential and stationary phases, respectively, showing minor structural differences among them. However, in the magnified view (Figure 18B), an interesting distinction between the IM and the OL can be observed. The OL appears darker in contrast to the IM, suggesting a difference in composition or density. Additionally, a row of dot-like structures is visible along specific regions of the external layer, a feature not observed in the IM.
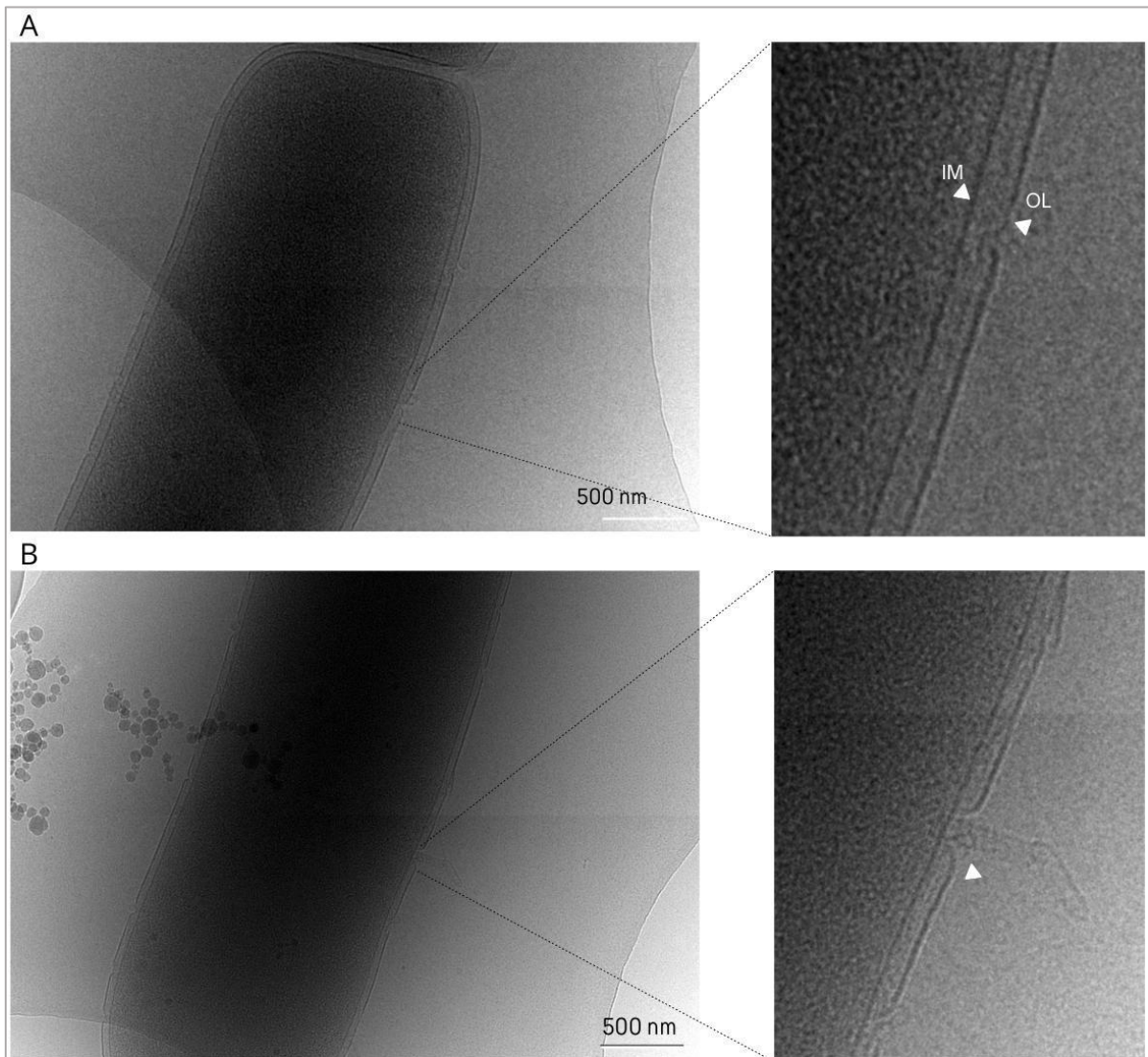
Figure 17. *F. duncaniae* cells at exponential phase. The figures (A and B) show the double-layered cell envelope surrounding the cell. A magnification of the cell envelope is on the right, indicating the continuous IM and the OL having disruptions with protrusions (arrows) to the extracellular environment. Source: Images obtained at Tanmay Bharat's lab.
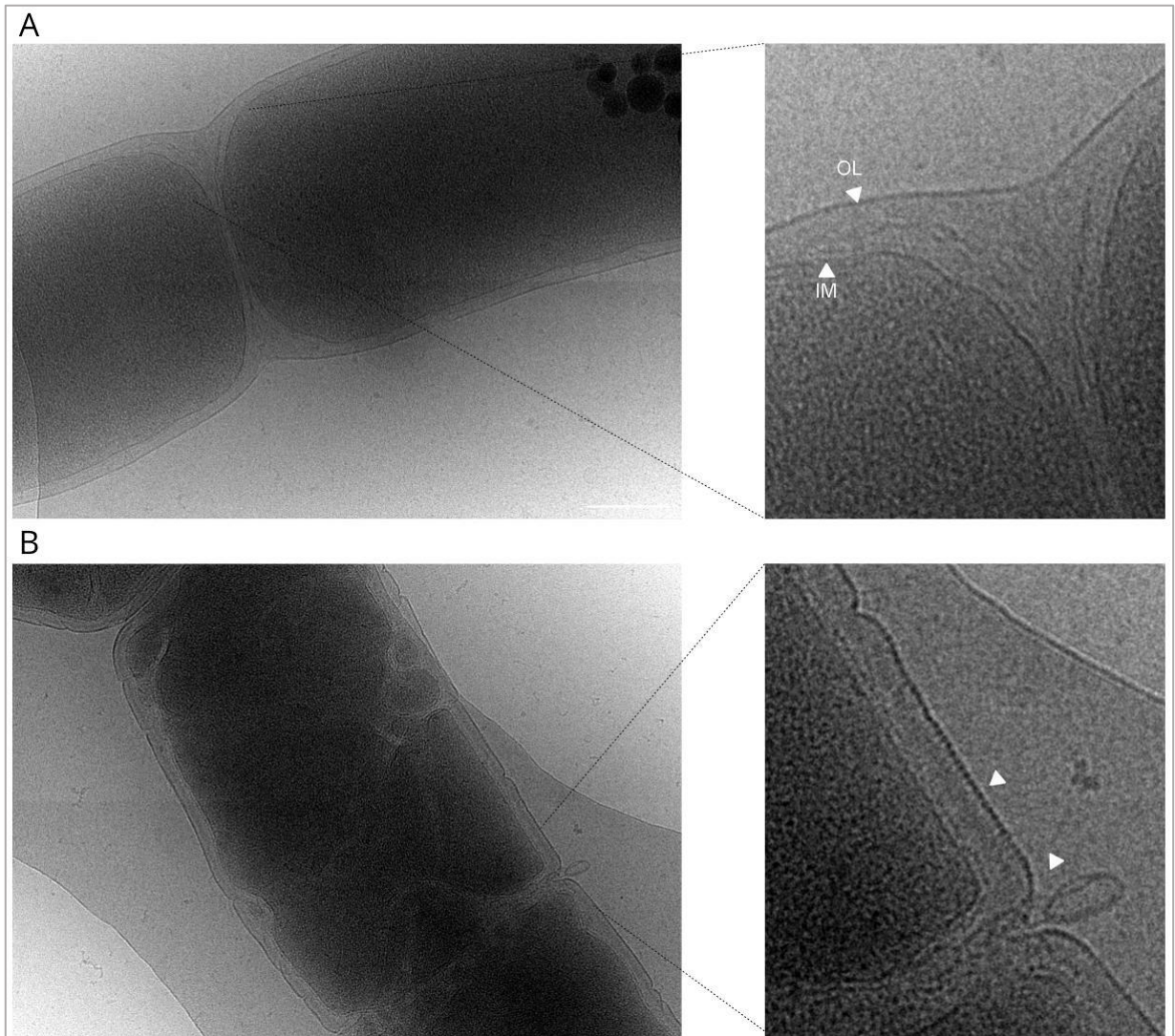
Figure 18. Cryo-EM of *F. duncaniae* at stationary phase. A) Image showing a smooth envelope organization at the poles of the bacilli, where adjacent cells are closely positioned. Arrows indicate IM and OL. B) Another *F. duncaniae* cell, with a magnified view highlighting extracellular protrusions, as well as the irregular OL structure and its distinct organization compared to the IM. Arrows indicate the OL and a protrusion.

Cryo-EM of LiCl (Lithium chloride) extracts from F. duncaniae cells

Lastly, the figure presents Cryo-EM images of LiCl extracts, revealing a regular lattice with pore-like structures (Figure 19) similar to the patterns observed in previous EM analyses (Figure 7 (page 105) in the included manuscript in Chapter I). Notably, the most abundant protein identified within this lattice was MAM, suggesting its structural role in the observed organization.
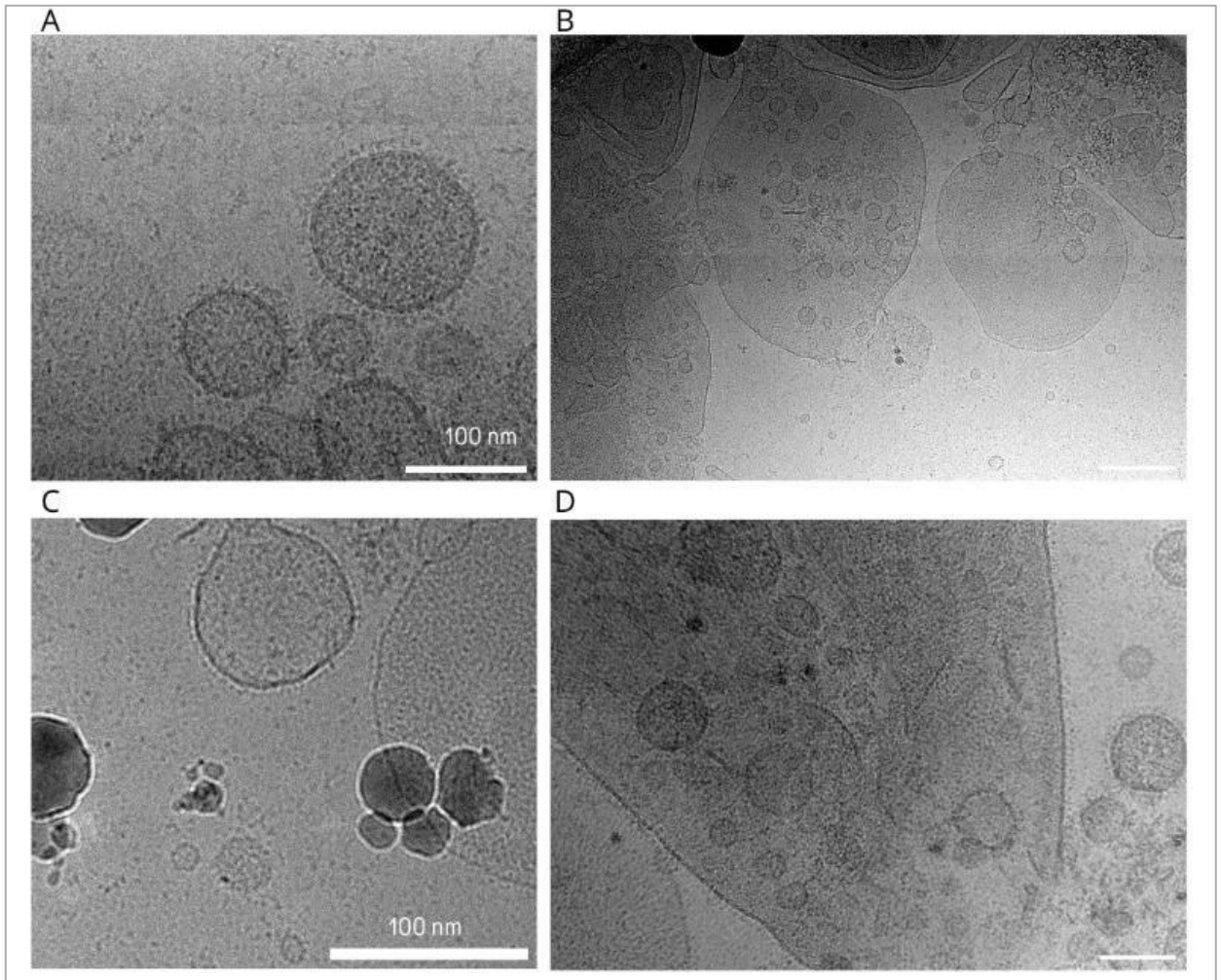
Figure 19. Cryo-EM of LiCl extractions of *F. duncaniae* cells. Figures A, C) Circular fragments of LiCl extractions having different sizes and pattern organisation filled with dark points are observed. B,D) Display a similar structural arrangement, though with larger fragments overlapping the circular ones. Source: Images obtained at Tanmay Bharat's lab.

Proteomic screening of F. duncaniae

Building on the intriguing images of *F. duncaniae* cells suggesting a double-layered cell envelope, we further investigated its envelope proteome to identify potential OM markers. While Maier and collaborators previously searched for OM-associated markers in the *F. duncaniae* genome, specifically heat shock proteins Hsp60 and Hsp70, we extended our analysis to explore additional proteins typically associated with the outer membrane[247].

Our BLAST analysis of *F. duncaniae*'s proteome against known OM proteins from Gram-negative bacteria revealed limited homology. The lipopolysaccharide export system protein LptA exhibited 41.1% identity, and the intermembrane phospholipid transport system ATP-binding protein MlaF showed 37.8%, both matching with proteins annotated as ABC transporters in *F. duncaniae's* proteome. Thus, the observed sequence identity may result from

conserved ATPase or transporter-related domains, as both MlaF and Lpt systems involve transport mechanisms, with MlaF being part of an ABC transporter system and LptA associated with an LPS transport pathway. Thus, the observed identity might be explained by conserved domains related to transporters in general. In contrast, other OM-associated proteins, including BamA, BamE, TolB, TolR, and OmpA, displayed no significant similarity with our database.

4.1.3. Discussion and conclusion

In addition to the findings presented in the submitted paper, this chapter highlights important observations derived from additional Cryo-EM analyses that provide significant knowledge regarding *F. duncaniae*'s envelope organization. The Cryo-EM imaging revealed a putative didermic architecture, distinguishing *F. duncaniae* from classical Gram-positive but also Gram-negative bacteria. Notably, the OL lacks proteins commonly associated with classical outer membranes, such as LPS-related markers. This suggests a novel organization of the outer layer, which differs structurally and functionally from the inner membrane, as indicated by our images. Those results, together with the confirmation of MAM at the envelope by immunogold labeling (Figure 9 (page 107) in the included manuscript in Chapter I), highlight the unique envelope characteristics of *F. duncaniae* having MAM as one of the main structural components. These findings are further supported by LiCl extractions, where Cryo-EM revealed a lattice-like organization, consistent with the patterns observed in negative staining EM indicated in the submitted manuscript (Figure 7 (page 105) in the included manuscript in Chapter I), reinforcing the hypothesis of MAM's role in forming an atypical structural layer.

Collectively, these findings expand our understanding of *F. duncaniae*'s envelope biology, emphasizing MAM as a central component in its structural organization and function. Nevertheless, further efforts are needed to fully characterize the composition of the outer layer of *F. duncaniae* and how MAM is organized within this structure.

CHAPTER II

5. CHAPTER II – IMMUNOMODULATORY CHARACTERIZATION OF MAM FROM *F. DUNCANIAE*

Understanding the intricate interactions between the gut microbiota and the host immune system is fundamental to elucidating the mechanisms related to intestinal homeostasis and inflammation. In this context, the *Faecalibacterium* genus has demonstrated to be a key player due to its recognized immunomodulatory properties, with *F. duncaniae* A2-165 being one of its most studied representatives. MAM has gained particular attention among its effector molecules due to its potential therapeutic activity in IBD. However, despite previous efforts in MAM's biological activity, those studies have predominantly relied on bacterial supernatants, synthetic peptides, or plasmid-based expression systems, limiting a direct evaluation of the purified protein in inflammation models.

To address this gap, this chapter presents the first direct assessment of recombinant MAM (R-MAM) in the intestinal DNBS-induced colitis murine model. The study also explores its immunomodulatory potential by evaluating its effects on human intestinal epithelial cells and peripheral blood mononuclear cells (PBMCs). The findings demonstrate that R-MAM significantly reduces inflammation by preventing weight loss, decreasing macroscopic disease scores, and promoting an anti-inflammatory cytokine profile.

Apart from its therapeutic relevance, the study also highlights technical challenges, particularly regarding purified R-MAM's solubility and conformational stability. Thus, future efforts should focus on optimizing protein stability and delivery mechanisms to maximize its therapeutic efficacy. Moreover, a comprehensive evaluation of the modulation of key cytokine networks in colonic tissues and its effects at the tissue level, including histological analyses of inflammatory infiltrates and epithelial integrity, will be crucial to determine MAM's precise role in immune homeostasis.

Integrating those key experimental approaches may advance our understanding of MAM's function and biotechnological potential, explaining the molecular and immunological basis of *F. duncaniae*'s health-promoting properties.

Article

Recombinant MAM from *Faecalibacterium duncaniae* exhibits protective effect in DNBS-induced colitis

Thaís Vilela Rodrigues [1,2]**, Luís Lima de Jesus** [1,2]**, Monique Ferrary Américo** [1,2]**, Florian Chain** [2]**, Laura Creusot** [3,4] **Nathalie Rolhion** [3,4]**, Anne Aucouturier** [2]**, Luis Bermudez-humaran** [2]**, Philippe Langella**[2]**, Vasco Ariston de Carvalho Azevedo** [1]**, Jean-Marc Chatel**[*]

[1] Federal University of Minas Gerais, Instituto de Ciências Biológicas, Belo Horizonte, Minas Gerais
[2] Université Paris Saclay, INRAE, AgroParisTech, MICALIS, Jouy-en-Josas, France
[3] Sorbonne Université, Inserm, Centre de Recherche Saint-Antoine, CRSA, F-75012 Paris, France
[4] Gut, Liver & Microbiome Research FHU, Paris, France
[*] Correspondence: jean-marc.chatel@inrae.

Abstract: Microbial Anti-Inflammatory Molecule (MAM) is a key effector of the next-generation probiotic *Faecalibacterium duncaniae* A2-165, a species whose depletion in the gut microbiota is strongly linked to inflammatory bowel disease (IBD) and other conditions. Despite its importance, the direct anti-inflammatory effects of purified MAM have never been evaluated *in vitro* or in intestinal inflammation models. Prior studies have relied on bacterial supernatants, synthetic peptides, or DNA delivery systems, each with inherent limitations. Here, we produced and purified recombinant MAM (R-MAM) under denaturing conditions and, for the first time, demonstrated its direct anti-inflammatory activity *in vitro* and protective effects in a colitis murine model. Despite numerous attempts, we were not able to obtain a non-aggregated R-MAM. Therefore, we can assume that the R-MAM used here is partly or totally denatured. Nevertheless, *in vitro* assays with human intestinal epithelial cells (HT-29) and peripheral blood mononuclear cells (PBMCs) confirmed the ability of MAM to induce an anti-inflammatory cytokine profile. In addition, in a DNBS-induced colitis model, oral administration of R-MAM significantly prevented weight loss and reduced colon weight and thickness, key macroscopic indicators of inflammation. Additionally. These findings provide a critical validation step for the therapeutic potential of MAM in intestinal inflammation, despite its purification under denaturing conditions. Future studies should focus on optimizing protein stability and conformational integrity to increase its therapeutic potential as a biotherapeutic agent.

Keywords: Inflammatory Bowel Disease; Next-generation Probiotic, Peptide, Effector Molecule, Purification

01. Introduction

Inflammatory bowel diseases are chronic disorders of the gastrointestinal tract that result from a complex interplay between genetic, immune, microbial, and environmental factors[1–3]. This condition includes Crohn's disease (CD) and ulcerative colitis (UC). A central aspect of IBD pathogenesis is the imbalance in cytokine signaling, where excessive pro-inflammatory mediators, such as TNFα, IL6, and IL1β, drive chronic inflammation and tissue damage. This process is further exacerbated by gut dysbiosis. While targeted biologic therapies such as anti-TNF, anti-IL12/23, and integrin inhibitors have improved disease management, the therapeutic

response remains highly variable, emphasizing the need for precision medicine approaches based on molecular and microbiota-based profiling[4,5].

A key marker of IBD patients is the significant depletion of the *F. duncaniae* (previously named *F. prausnitzii*) strain A2-165 within the gut microbiome[6–9]. *F. duncaniae* is an extremely oxygen-sensitive Bacillus belonging to the Bacillota phylum (formerly Firmicutes) that constitutes a substantial proportion of the gut microbiota. This genus represents rates ranging from 5--15% of the bacterial community composition[8,10]. This abundance is associated with a healthy gut environment, whereas reduced levels of *F. duncaniae* have been correlated with IBD and various disorders, including colorectal cancer, diabetes and obesity[11–16].

Several beneficial properties are attributed to *F. duncaniae*, such as anti-inflammatory properties, reinforcement of the intestinal barrier, and maintenance of gut homeostasis[17–19]. This activity is attributed mainly to its remarkable capacity for butyrate production and its exclusive ability to synthesize MAM[18,19]. MAM is a 15 kDa protein with potent anti-inflammatory properties that was first identified in the supernatant of *F. duncaniae*[20,21]. Using cDNA delivery systems, MAM has been shown to modulate the NF-κB signaling pathway and reduce pro-inflammatory cytokine secretion *in vitro* and *in vivo*, particularly in colitis models[19,22,23]. However, these approaches, while demonstrating the biological activity, rely on indirect expression systems that introduce variability in protein availability and function.

Despite its promising anti-inflammatory effects, the therapeutic potential of purified recombinant MAM (R-MAM) remains largely unexplored. To date, only one study has evaluated purified R-MAM, which showed benefits in a diabetes mellitus (DM) model, particularly in enhancing intestinal barrier integrity[24]. However, its direct effects *in vivo* in intestinal inflammation models have not yet been assessed. This study aims to address this gap by investigating the impact of purified R-MAM in both *in vitro* models (HT-29 cells and PBMCs) and in a DNBS-induced colitis mouse model. Despite the fact that R-MAM is probably denatured, by using purified R-MAM, we reduce the bias associated with cDNA-based expression systems and enable a more controlled and direct assessment of its therapeutic potential, providing new insights into R-MAM activity in intestinal inflammation.

2. Materials and methods

2.1 Recombinant expression and purification of MAM under denaturing conditions

2.1.1 Protein expression induction

The coding sequence of the MAM from *F. duncaniae* A2-165 (WP_005932151) was inserted into the pStaby vector with restriction enzymes (Xhol and Nhel). The resulting recombinant plasmid was transformed into chemically competent *Escherichia coli* T7 Express (BL21) for protein expression. A single colony was inoculated into 10 mL of Luria–Bertani (LB) medium supplemented with 100 μg/mL ampicillin and incubated overnight at 37°C with shaking (180 rpm). Subsequently, 5 mL of the overnight culture was transferred into 500 mL of LB medium containing 100 μg/mL ampicillin. When the culture reached an optical density at 600 nm (OD600) of 0.6--0.8, the expression of recombinant MAM (R-MAM) was induced by adding 1 mM isopropyl β-D-thiogalactoside (IPTG), followed by incubation at 37°C for 19 hours with shaking (180 rpm). The cells were then harvested via centrifugation (2,500 ×g for 10 minutes at 4°C), washed twice with ice-cold 0.1 M phosphate-buffered saline (PBS; pH 7.0), and centrifuged again under the same conditions. The resulting bacterial pellets were stored at -20°C for a maximum period of 24 hours until protein extraction.

2.1.2 Protein Extraction and Purification

A maximum of four bacterial pellets, each obtained from 125 mL of culture, were utilized for protein extraction and purification. The frozen pellets were thawed and subsequently

resuspended in Buffer B (8 M urea, 100 mM NaH2PO4, 10 mM Tris, and 50 mM imidazole; pH 8.0) at a ratio of 15 mL of buffer per pellet. The suspensions were incubated at room temperature for 1 hour, with intermittent homogenization every 20 minutes. Following incubation, the samples were sonicated on ice for 4 cycles of 20 s each. The homogenate was then centrifuged at 10,000 ×g for 25 minutes at 21°C to remove insoluble debris. The resulting supernatant was carefully collected and loaded onto a Ni-NTA resin column (1.5 mL) (Invitrogen) preequilibrated with Buffer B.

The column was sequentially washed twice with 5 mL of Buffer C (8 M urea, 100 mM NaH2PO4, 10 mM Tris, 50 mM imidazole, and 500 mM NaCl; pH 6.3), once with Buffer D1 (8 M urea, 100 mM NaH2PO4, 10 mM Tris, 50 mM imidazole, and 200 mM NaCl; pH 5.9), and finally once with Buffer D2 (8 M urea, 100 mM NaH2PO4, 10 mM Tris, 50 mM imidazole, and 300 mM NaCl; pH 5.3). Following the washing steps, the purified MAM was eluted in 500 µL fractions via Buffer E (8 M urea, 100 mM NaH2PO4, and 10 mM Tris; pH 4.2). To optimize purity, this step was performed at pH 4.2 instead of the recommended pH of 4.5, as a lower pH improved the specificity of MAM recovery by reducing the coelution of contaminant proteins. Aliquots (20 µl) of the eluted fractions were visualized via SDS–PAGE.

The purification procedures were adapted from the Expression and Purification of Proteins via the 6x Histidine-Tag Manual (https://www.iba-lifesciences.com/media/a8/ee/aa/1631860506/Manual-6xHistidine-tag.pdf), with modifications to optimize protein yield and purity.

2.1.3 R-MAM protein Dialysis

Dialysis of the purified R-MAM protein was conducted via a stepwise protocol to gradually reduce the urea concentration. Approximately 5 mL of purified protein (~2.5 mg/mL) was loaded into a 10 kDa molecular weight cutoff dialysis cassette (Spectra/Por® 7 Dialysis Membrane). The cassette was sequentially dialyzed against 200 mL of buffers with decreasing urea concentrations as follows: Buffer 1 (6 M urea, 50 mM Tris, 1% glycerol, and 200 mM NaCl; pH 7.4) for 1 hour, followed by Buffer 2 (4 M urea, 50 mM Tris, 1% glycerol, and 200 mM NaCl; pH 7.4); Buffer 3 (2 M urea, 50 mM Tris, 1% glycerol, and 200 mM NaCl; pH 7.4); Buffer 4 (1 M urea, 50 mM Tris, 1% glycerol, and 200 mM NaCl; pH 7.4); and Buffer 5 (0.1 M PBS containing 1% glycerol; pH 7.4). After 1 h of dialysis in Buffer 5, the buffer was replaced twice, and the dialysis process was continued for an additional 24 hours. The dialyzed protein mixture was then collected directly from the cassette (Supplementary Figure 1), analyzed via SDS–PAGE, quantified via bicinchoninic acid (BCA) assay (Thermo Fisher), and stored at -80°C for subsequent *in vitro* and *in vivo* assays.

2.2 *F. duncaniae culture and dose preparation*

The strain *Faecalibacterium duncaniae* A2-165 (DSM #17677) was cultivated in BHIS liquid medium (Brain Heart Infusion broth, 37 g/L, Difco) supplemented with yeast extract (5 g/L, Difco) and 3% GAC (glucose, acetate, cysteine), a mixture composed of 6.6% glucose, 5.5% acetate, and 1.66% cysteine. GAC supplementation was used to support bacterial growth, where acetate serves as the main energy source, cysteine protects against oxygen, and glucose provides additional metabolic support. The cultures were incubated at 37°C in an anaerobic chamber under an atmosphere consisting of 90% nitrogen (N_2), 5% carbon dioxide (CO_2), and 5% hydrogen (H_2). Bacterial growth was monitored until the cultures reached the stationary phase, as indicated by an optical density at 600 nm (OD_{600}) of approximately 1.6–1.7. The samples were collected at this point and stored at -80°C with 20% glycerol for future use.

2.3 *In vitro anti-inflammatory assays*

2.3.1 HT-29 culture

Human colon carcinoma cells (HT-29 ATCC HTB-38) were grown in Dulbecco's modified Eagle's minimal essential medium (DMEM) with 4.5 g/L glucose (Sigma–Aldrich) supplemented with 10% (v/v) heat-inactivated fetal bovine serum (FCS; Eurobio, France) and 0.1% penicillin/streptomycin (P/S). The cultures were maintained at 37°C in a 10% (v/v) CO_2 atmosphere until 100% confluence, and the medium was replaced every two days.

2.3.2 HT-29 *in vitro* anti-inflammatory assay

For an anti-inflammatory assay with the HT-29 cell line, 1×10^5 cells were seeded in 24-well plates and cultivated in DMEM supplemented with 10% FBS and 0.1% P/S. On the 6th day after seeding, the medium was changed to DMEM supplemented with 5% FBS and 0.1% P/S. Co-incubation started on the same day, with the cells at the confluence. The cells were stimulated for 24 h at 37°C in 10% CO_2 with recombinant TNFα (5 ng/mL; PeproTech, NJ, USA) to induce a pro-inflammatory state and simultaneously coincubated with simultaneously coincubated with 50 µL of either recombinant MAM (R-MAM) at final concentrations of 0.05 mg/mL or 0.1 mg/mL, or 50 µL of PBS as the vehicle control. The experiments were conducted in triplicate following standardized conditions in the protocols established by our facility[25–27]. The supernatants were collected and used for IL8 concentration measurement via ELISA (BioLegend, San Diego, CA). The procedures were performed according to the manufacturer's instructions.

2.3.3 PBMC *in vitro* anti-inflammatory assay

Fresh peripheral blood mononuclear cells (PBMCs) were obtained from four healthy donors. Approval for blood collection was obtained from the local ethics committee (Comité de Protection de Personnes Ile de France IV, IRB 00003835 Suivitheque study). Sepmate tubes (STEMCELL Technologies, 85450) were used for cell isolation via density gradient centrifugation, following the manufacturer's instructions. PBMCs were resuspended in RPMI-1640 Glutamax (Gibco, 61870-010) supplemented with 10% FBS (Sigma #F7524), 1% P/S (Gibco, #15140-122), 1% pyruvate (Gibco, #11360-039), and 1% nonessential amino acids (Gibco, #11140-035), and $1x10^6$ PBMCs per well were seeded. The cells were subsequently stimulated for 16 hours with doses of MAM ranging from 0.5 mg/ml to 0.001 mg/ml final concentration, and 1 µg/mL *E. coli* K12 lipopolysaccharide (LPS, InvivoGen, tlrl-eklps) was used as a positive control.

To account for the potential effects of cell viability on cytokine measurements, cytokine levels (IL10 (Invitrogen, #88-7106-88) and TNFα (Invitrogen, #88-7346-88)) were normalized to lactate dehydrogenase (LDH) activity in the culture supernatant. LDH release, measured via a cytotoxicity detection kit (Roche, 04744934001), served as an indicator of cell lysis. Cytokine concentrations are expressed relative to LDH levels in the corresponding wells to adjust for variations in cell integrity. The experiments were conducted in duplicate.

2.4 *In vivo* colitis mouse model

The experiment was conducted according to ethics committee guidelines. Six-week-old male C57BL/6JRj mice (Janvier, France) (n = 8 mice per group) were maintained in the animal facilities of the French National Institute of Agricultural Research (IERP; INRA Jouy-en-Josas, France) under specific pathogen-free (SPF) conditions. Animals were kept in plastic cages with 4 mice per cage under the temperature of 21°C, with unrestricted access to food and water. A 12-hour light/dark cycle was provided. To ensure acclimatization, the animals were maintained under these conditions for one week prior to the start of the experiments. Intragastric gavage was initiated on day 1 with 200 µl of *F. duncaniae* at a concentration of 1×10^9 CFU/ml, recombinant MAM (R-MAM) at concentrations of 1.0 mg/ml, 0.1 mg/ml, or 0.01 mg/ml, or PBS containing 16% glycerol, used as vehicle control for both R-MAM and *F. duncaniae* cell resuspension. Doses of R-MAM were chosen on the basis of previous studies investigating similar bioactive proteins in murine models [20–22]. Treatments were administered daily for

the duration of the assay. On the 8th day, the mice were anesthetized and subjected to intrarectal injections of DNBS (100 mg/kg of body weight) diluted in 30% ethanol to induce colitis. The body weights of the mice were monitored daily throughout the experiment, and the animals were euthanized 4 days after the induction of DNBS-induced colitis (Figure 4A). Mice that exhibited weight loss of 20% due to disease severity were euthanized according to established criteria.

Macroscopic scores were calculated for each mouse on the basis of ulcerations (scored 0–5), adhesions (presence/absence: 0/1), hyperemia (presence/absence: 0/1), altered transit, such as diarrhea or constipation (presence/absence: 0/1), and increased colon wall thickness (presence/absence: 0/1), which was measured via an electronic caliper (Control Company, WVR, United States)[28]. The total macroscopic score was determined by summing the individual scores for each animal.

2.5 Statistical analysis

Prism version 8 (GraphPad Software, San Diego, USA) was used to plot the results. Data are presented as the mean ± standard deviation (SD). Normality was assessed using the Shapiro-Wilk test. Depending on the results of the normality test, data were analyzed using Dunn's test, Dunnett's multiple comparisons test, the Kruskal-Wallis test, or analysis of variance (ANOVA). The specific statistical tests and post-tests analyses used are indicated in the figure legends. Significance levels are represented as follows *: $p < 0.05$, **: $p < 0.01$, ***: $p < 0.001$, ****: $p < 0.0001$.

3. Results

3.1 Recombinant MAM displays anti-inflammatory activity in vitro in HT-29 cells

After dialysis, the protein was obtained as aggregates indicating probably a non-native folding. We used this insoluble form for our *in vitro* and *in vivo* assays (Figure 1A and Supplementary Figure 1).

The intestinal cell line HT-29 secreting IL8 in response to TNFα stimulation, was used to assess the immunomodulatory effects of R-MAM. Compared with TNFα, R-MAM significantly reduced IL8 levels at the highest concentration tested (0.1 mg/mL) (p = 0.0012), resulting in a 56.32% reduction in IL8 secretion relative to that of the TNFα-treated control (Figure 1B). Interestingly, no significant difference was observed between the R-MAM 0.1 mg/mL group and the untreated control group (p = 0.3993), suggesting that this concentration tends to restore IL8 levels to basal levels. In contrast, a lower dose of R-MAM (0.05 mg/mL) tended to reduce IL8 levels (114,957 pg/mL vs 151,423 pg/mL for TNFα), although this reduction was not statistically significant (p = 0.1684). The greater reduction observed at 0.1 mg/mL supports a dose-dependent effect, with higher concentrations of R-MAM more effectively suppressing IL8 secretion. PBS, used as the vehicle for MAM, was also tested under TNFα stimulation, and no significant difference in IL8 levels was observed compared with the TNFα-stimulated control.
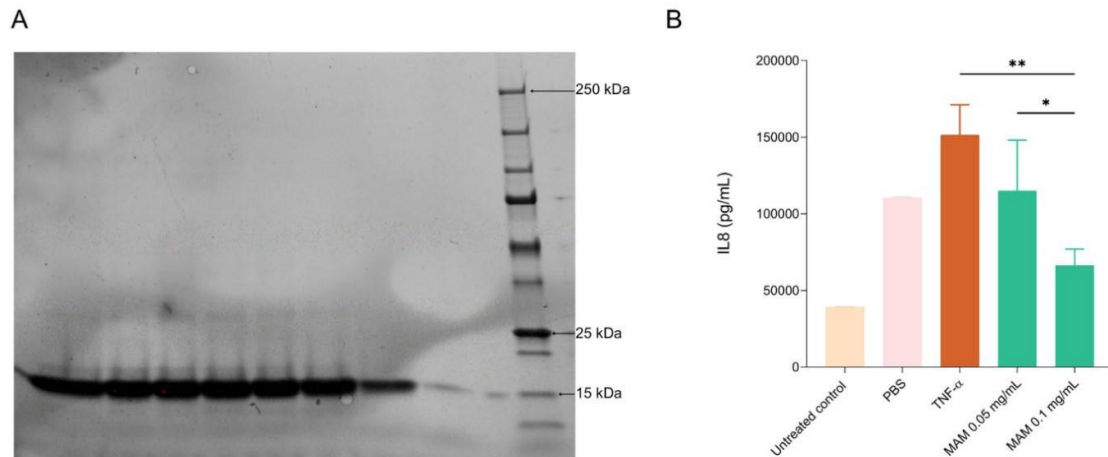
Figure 1. (**a**) SDS–PAGE gel of purified MAM highlighting an intense band of MAM (expected size ~15 kDa) in all wells. (**b**) IL8 secretion by HT-29 cells subjected to inflammatory conditions by TNFα. The treatment groups included TNFα alone, TNFα with PBS, and TNFα with recombinant MAM (R-MAM) at concentrations of 0.05 mg/mL and 0.1 mg/mL. The beige and light pink bars represent the growth media for the HT-29 cells and the PBS controls, respectively. Statistical analysis was performed via ANOVA followed by Tukey's multiple comparisons post test. Significant comparisons are indicated: $p < 0.01$ (**) and $p < 0.05$ (*).

3.2 Recombinant MAM induces IL10 and TNFα production by PBMCs in a dose-dependent manner

To evaluate the anti-inflammatory properties of MAM, PBMCs isolated from four healthy donors were stimulated with R-MAM at five different concentrations ranging from 0.5 mg/ml to 0.0001 mg/ml. LPS (100 ng/ml) was used as a positive control, and PBS was used as a negative control. After 16 h of stimulation, R-MAM significantly induced IL10 secretion in a dose-dependent manner. Higher concentrations of R-MAM (0.5 mg/mL and 0.1 mg/mL) induced significantly greater IL10 than did PBS ($p < 0.0001$), although the difference was not significant
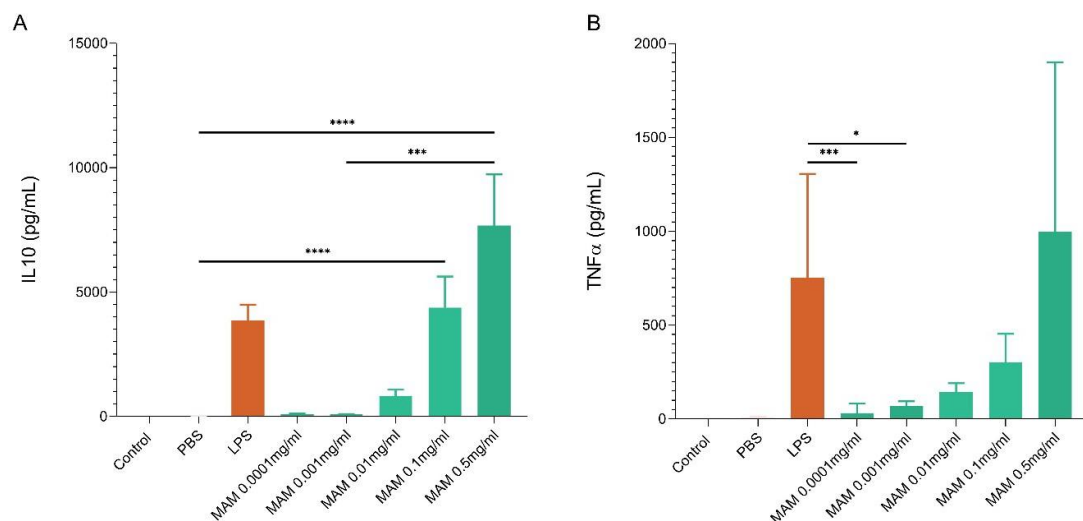
compared with that of LPS ($p > 0.9999$) (Figure 2A). Compared with LPS, lower concentrations of R-MAM (0.001 mg/mL and 0.0001 mg/mL) resulted in significantly lower TNFα levels, whereas higher doses, such as 0.1 mg/mL R-MAM, did not significantly differ from those of LPS ($p > 0.05$), resulting in higher TNFα levels (Figure 2B).

Figure 2. (**a**) Quantification of IL10 and (**b**) TNFα production by PBMCs stimulated with R-MAM via ELISA. The beige and light pink bars, which represent the growth media for the PBMCs and PBS controls, respectively, are not visually discernible due to their minimal values. The orange bars represent the LPS-stimulated control, whereas the green bars indicate the responses to different doses of R-MAM. Statistical analysis was performed via the Kruskal–Wallis test followed by Dunn's multiple comparisons post test. Significant comparisons are indicated: $p < 0.0001$ (****), $p < 0.001$ (***), and $p < 0.05$ (*).

To better evaluate the anti-inflammatory properties of R-MAM, we expressed the previous results as the IL10/TNFα ratio, which indicates the balance between anti-inflammatory (IL10) and pro-inflammatory (TNFα) responses. Notably, R-MAM at a concentration of 0.1 mg/ml had a significantly greater ratio than did LPS ($p < 0.05$), supporting its anti-inflammatory profile. The effect diminished with lower concentrations of R-MAM, which induced ratios similar to those of the PBS or LPS controls (Figure 3A). Interestingly, the individual responses among donors varied, as shown in the donor-specific graphs (Figure 3B).
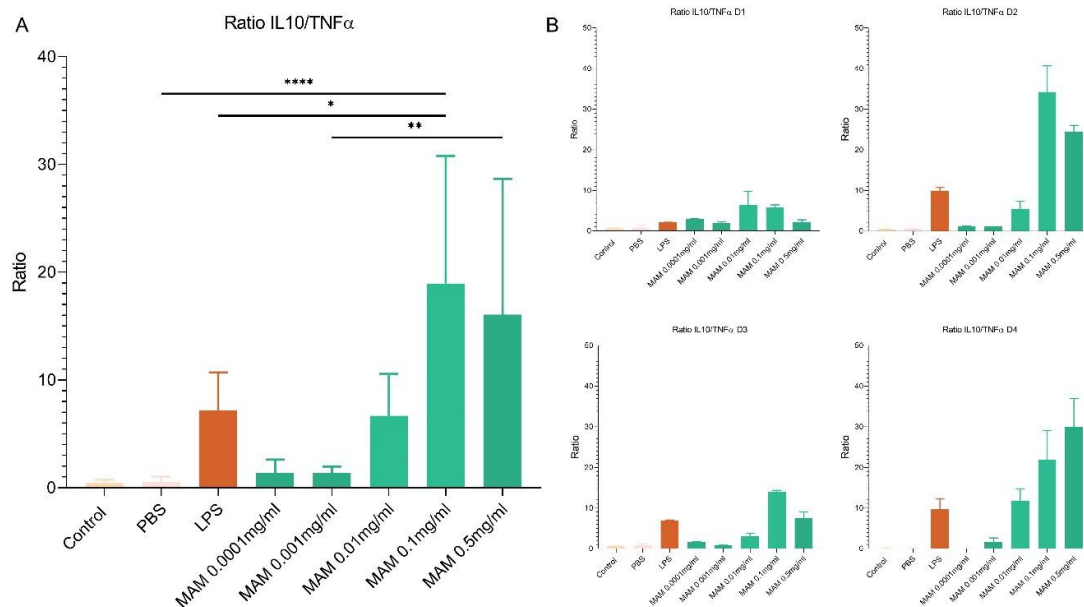
Figure 3. (**a**) The global panel shows the mean IL10/TNFα ratio across all donors, whereas the donor-specific panels (**b**) illustrate individual responses to R-MAM stimulation at concentrations ranging from 0.5 to 0.0001 mg/mL (green bars). LPS was used as an inflammatory control. Ratios were calculated on the basis of cytokine levels quantified via ELISA. Statistical analysis was performed via ANOVA followed by Tukey's multiple comparisons post test. Significant comparisons are indicated: $p < 0.0001$ (****), $p < 0.01$ (**) and $p < 0.05$ (*).

3.3 3. R-MAM alleviates DNBS-induced colitis in mice

After the *in vitro* studies, the effect of R-MAM was evaluated *in vivo*. The mice (n=8 per group) were orally administered 1.0 mg/mL, 0.1 mg/mL, or 0.01 mg/mL R-MAM for 8 days as a pretreatment and 4 days following the intrarectal injection of DNBS to induce colitis (Figure 4A). The higher doses (1.0 mg/mL and 0.1 mg/mL) did not significantly affect any of the analyzed parameters, including weight loss, macroscopic scores, or bowel measurements, compared with those of the sick control group (data not shown). These findings suggest that higher concentrations may not confer additional benefits, in contrast with the therapeutic effects observed at lower doses. On the basis on these findings and previous *in vitro* analyses, we focused our investigation on the group that received the lower dose of R-MAM (0.01 mg/mL).

The weights of the mice were monitored during the 12 days of the experiment, and the mice were euthanized on day 12. Overall, R-MAM treatment (0.01 mg/mL) resulted in significant anti-inflammatory activity *in vivo*. R-MAM significantly protected mice from weight loss during DNBS-induced colitis compared with the sick control group (p = 0.0046) (Figure 4B). While no significant differences were observed in the macroscopic disease scores, the scores were lower in the groups administered R-MAM. Furthermore, colon weight was significantly lower in the group treated with R-MAM than in the DNBS group, reaching levels similar to those of the healthy control group (p = 0.0301). A similar pattern was observed in the measurement of bowel thickness, where the thickness was significantly reduced in the R-MAM group (p = 0.0455), reinforcing the anti-inflammatory potential of R-MAM. No significant differences in colon length were detected between the treatment and control groups (Figure 4C–F).
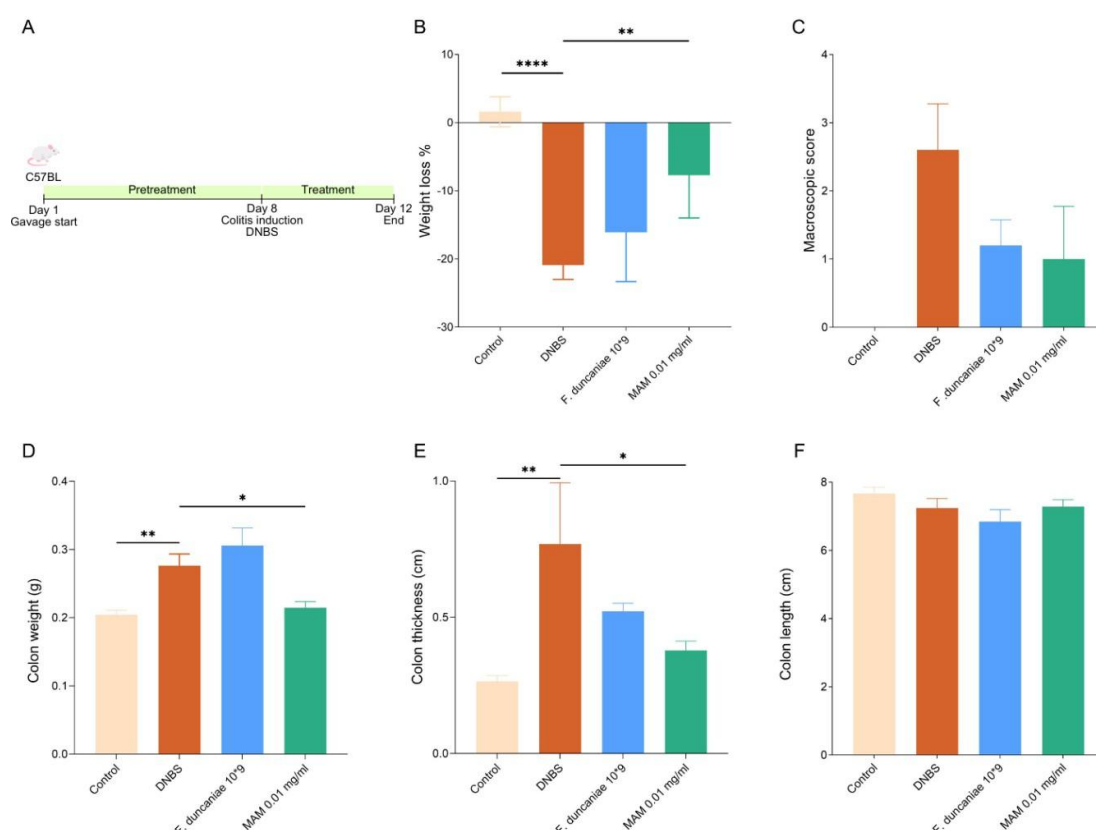
Figure 4. (**a**) Experimental design: Mice received oral R-MAM during the 12 days of the experiment. Colitis was induced by the intrarectal administration of DNBS on the 8th day. (**b**) Percentage of weight loss 96 hours after DNBS administration. (**c**) Macroscopic score (n=5–8 mice/group). (**d**) Colon weight (n=5–8 mice/group). (**e**) Colon thickness (n=5–8 mice/group). (**f**) Colon length (n=5–8 mice/group). The orange bars represent the sick control, the blue bars represent the group treated with *F. duncaniae*, and the green bars represent the group that received R-MAM. Statistical analysis was performed via Dunnett's test for weight loss, colon weight, and colon thickness. Dunn's test was used for macroscopic scores. Significant comparisons are indicated: $p < 0.0001$ (****), $p < 0.01$ (**) and $p < 0.05$ (*).

4. Discussion

F. duncaniae is one of the most abundant species in the gut microbiota, with the protein MAM identified as a key effector molecule mediating its beneficial effects, particularly in IBD [8,17,22,29]. While earlier studies assessed MAM activity through cDNA delivery or eukaryotic expression systems [14,17,18], this study evaluated the direct effects of purified recombinant

MAM *in vitro* using blood mononuclear cells and HT-29 cells, and on an intestinal colitis mouse model.

The direct exposure of TNFα-stimulated HT-29 intestinal cells to R-MAM significantly reduced the secretion of the pro-inflammatory cytokine IL8. R-MAM at 0.05 and 0.1 mg/mL effectively decreased the IL8 level, with the 0.1 mg/mL concentration resulting in a statistically significant reduction compared with that in TNFα-stimulated cells without R-MAM. Thus, these findings suggest that R-MAM can modulate immune signaling pathways in human intestinal cells associated with TNFα-induced IL8 production and that a minimum effective dose of R-MAM is required to achieve anti-inflammatory effects.

Human mononuclear blood cells were also evaluated for their responsiveness to different doses of R-MAM without prior induction of inflammation, using LPS as a pro-inflammatory agent control. IL10 plays an important role in the intestinal anti-inflammatory pathway regulation by inducing Th17 responses and regulating macrophages that support intestinal barrier integrity[30–32]. Here, R-MAM triggered a dose-dependent increase in the secretion of the anti-inflammatory cytokine IL10. This finding aligns with previous reports highlighting the role of R-MAM in modulating immune responses via IL10 induction[22,23].

TNFα is a major driver of inflammation in IBD, but it also plays regulatory roles in immune priming and tissue repair[33,34]. TNFα is elevated in patients with intestinal inflammation, particularly in IBD, where maintaining a balanced TNFα level is crucial for preserving gut homeostasis and preventing excessive inflammation[35,36]. In this context, our results demonstrated that R-MAM also induces TNFα production in a dose-dependent manner, with higher concentrations leading to higher TNFα levels.

The IL10/TNFα ratio was subsequently evaluated as an indicator of immune homeostasis, where a higher ratio suggests a shift toward an anti-inflammatory response, which is crucial for preventing excessive immune activation and tissue damage in the context of gut inflammation[37,38]. R-MAM at a concentration of 0.1 mg/mL elicited a strong anti-inflammatory profile response, with IL10 levels approximately 14 times higher than those of TNFα (p < 0.0001), suggesting that this concentration provides the most favorable anti-inflammatory profile.

In contrast, we also observed a concurrent increase in TNFα at higher concentrations, particularly at 0.5 mg/mL. This raises questions about whether the observed TNFα induction represents an exacerbated pro-inflammatory response or transient activation involved in immune priming and tissue repair. Given the dual role of TNFα in inflammation and regulation, future studies should investigate the kinetics of cytokine production and assess whether prolonged exposure to high doses of R-MAM shifts the immune response toward a pathological inflammatory state or regulatory adaptation, raising questions about the balance between its pro- and anti-inflammatory effects[39].

With respect to the donor variations (healthy males and females aged 28–40), cytokine production among the four PBMC donors followed similar trends, although some donors presented higher cytokine levels. Except for donor 4, 0.1 mg/mL R-MAM consistently induced the highest IL10/TNFα ratio, reinforcing its potential immunomodulatory role.

Since higher doses of purified R-MAM had no beneficial effects *in vitro*, we similarly observed that, among the three doses tested *in vivo* (0.5 mg/mL, 0.1 mg/mL, and 0.01 mg/mL), only the lowest dose (0.01 mg/mL) exhibited significant protective activity. This outcome may be attributed to immune overactivation, where excessive stimulation triggers exacerbated inflammatory responses instead of mitigating inflammation[40,41]. Therefore, we focused on this dose to evaluate its anti-inflammatory potential in colitis.

Previous studies have evaluated MAM activity in intestinal models via eukaryotic expression systems or supernatants containing MAM peptides[21,22]. While mRNA quantification confirmed MAM production in the gut, these indirect methods present challenges, such as the

inability to control protein concentration precisely or assess its availability in the intestinal environment. In contrast, our study utilized purified R-MAM to directly evaluate its immunomodulatory activity, minimizing potential biases associated with delivery precision and accurate dose control, thereby addressing reproducibility concerns.

The administration of purified denatured R-MAM to DNBS-induced colitis model mice significantly ameliorated weight loss, colon weight, and colon thickness, which are well-established macroscopic markers of disease severity and inflammation in murine models[42]. Although the reduction in macroscopic disease scores was not statistically significant, the observed trend suggests a partial mitigation of inflammation and ulceration in R-MAM-treated mice. Similarly, no significant differences in colon length were detected between the groups, possibly reflecting the role of the early stage of colitis or R-MAM in preventing tissue remodeling.

To date, the only study using purified recombinant MAM *in vivo* was conducted by Xu *et al*. in a type 2 diabetes mellitus (DM) model. They employed intragastric gavage, similar to our approach, but at a substantially higher daily dose of 200 µg of protein over four weeks[24]. In contrast, our highest tested dose (100 µg/day) had no protective effects, suggesting that the therapeutic window of MAM may vary depending on the disease model. Chronic metabolic inflammation in DM may require higher MAM concentrations to elicit beneficial effects, whereas acute inflammatory models such as DNBS-induced colitis may be more sensitive to immune modulation. These findings highlight the complexity of anti-inflammatory therapeutics and the importance of disease-specific responses.

Although the precise mechanisms underlying the effects of MAM remain unclear, its known properties suggest two potential modes of action: the modulation of anti-inflammatory responses and the restoration of mucosal barrier integrity. MAM's ability to mitigate colitis symptoms by reducing the levels of pro-inflammatory cytokines, particularly TNFα, was demonstrated here through *in vitro* studies and in the literature[21–23]. Additionally, MAMs were associated with the regulation of tight junction proteins, which are critical for maintaining epithelial integrity[24]. Such assays align with our observations of reduced weight loss and colon thickness in R-MAM-treated mice, suggesting that MAM supports gut barrier function and intestinal homeostasis.

Despite these important achievements, further analyses, including cytokine quantification, immune cell profiling, and histological evaluation, would provide deeper insights into the MAM's mechanisms of action in intestinal inflammation[43]. Additional efforts with larger sample sizes and extended observation periods are also essential to validate and refine these findings, guiding preclinical trials in human models[44].

The purification of recombinant MAM was previously described by Xu *et al*. Similarly to our protocol, they used an *E. coli* expression vector to synthesize the protein, followed by purification through His-tag affinity chromatography.[24] Although these properties are beneficial, the authors did not provide further details regarding the stability of the purified protein. In the present study, R-MAM probably was not in its native conformation. This conclusion is supported by the presence of visible precipitates in the purified solution, indicating protein aggregation and potential misfolding under the applied purification conditions. This outcome was anticipated because of the hydrophobic nature of MAMs, which introduces challenges during purification, resulting in aggregation and potential misfolding[45]. Thus, the stability of purified R-MAM in the gastrointestinal tract remains a critical consideration of this work, as proteolytic degradation may limit its availability and activity in the intestinal environment. These structural alterations could partially impair its biological function by masking critical epitopes necessary for immune recognition and interactions with host molecules.[46]

Despite this limitation, we proceeded with the experiments and observed significant anti-inflammatory activity, indicating the robustness of the effects of MAM, even under potentially suboptimal conditions. A possible explanation is that since R-MAM is likely processed in peptides via immune cells[47], its peptides retain anti-inflammatory activity. This hypothesis is supported by studies in which *F. duncaniae* supernatants containing MAM peptides were proven to be effective[19,48]. Nevertheless, to increase the conformational stability of purified R-MAM and fully explore its therapeutic potential, future studies should consider optimizing purification methods. Strategies such as testing alternative expression systems, employing solubility enhancers, or coexpressing molecular chaperones during purification could be beneficial[49,50].

Understanding these aspects is essential to elucidate the role and activity of MAMs in the host and unravel their full therapeutic potential. Thus, R-MAM holds potential as an adjuvant therapy alongside established IBD treatments, such as anti-TNF agents or immunosuppressants, potentially enhancing their efficacy while mitigating adverse effects. Additionally, its ability to modulate cytokine balance and support gut barrier integrity suggests that R-MAM could be developed as a postbiotic formulation, offering a safer and more stable alternative to live probiotics. Future studies should focus on optimizing its delivery, stability, and synergistic effects with existing therapies to explore and maximize its potential therapeutic applications in intestinal inflammatory diseases[51].

5. Conclusions

Our study identified purified R-MAM as a novel effector molecule capable of stimulating anti-inflammatory responses in a dose-dependent manner, besides its protective effects observed *in vivo* intestinal colitis model. These results provide new opportunities for the use of R-MAM in the treatment of IBD and associated inflammatory diseases, although more research is needed to improve its formulation and investigate its mechanism of action and clinical uses.

Abbreviations

The following abbreviations are used in this manuscript:

MAM	Microbial Anti-inflammatory Molecule
DNBS	Di-nitrobenzene sulfate
DSS	Dextran sulfate sodium
IBD	Inflammatory Bowel Diseases
R-MAM	Recombinant MAM
IL10	Interleukin-10
NF-κB	Nuclear factor kappa B
IFNγ	Interferon-gamma
cDNA	Complementary DNA
MLN	Mesenteric Lymph nodes
LB	Luria–Bertani
IPTG	Isopropyl β-D-thiogalactoside
OD	Optical Density
PBS	Phosphate-buffered saline
BCA	Bicinchoninic acid
DMEM	Dulbecco's Modified Eagle Medium
PBMC	Peripheral Blood Mononuclear Cells
ELISA	Enzyme Linked Immunosorbent Assay
ZO-1	Zona Occludens-1
LPS	Lipopolysaccharides
DM	Diabetes Mellitus

References

1.   Liu, J., Di, B. & Xu, L. li. Recent advances in the treatment of IBD: Targets, mechanisms and related therapies. *Cytokine Growth Factor Rev* **71–72**, 1–12 (2023).

2.   McDowell, C., Farooq, U. & Haseeb, M. Inflammatory Bowel Disease. *StatPearls* (2023).

3.   Sairenji, T., Collins, K. L. & Evans, D. V. An Update on Inflammatory Bowel Disease. *Prim Care* **44**, 673–692 (2017).

4.   Saez, A., Herrero-Fernandez, B., Gomez-Bris, R., Sánchez-Martinez, H. & Gonzalez-Granado, J. M. Pathophysiology of Inflammatory Bowel Disease: Innate Immune System. *Int J Mol Sci* **24**, 1526 (2023).

5.   Chang, J. T. Pathophysiology of Inflammatory Bowel Diseases. *New England Journal of Medicine* **383**, 2652–2664 (2020).

6.   Lopez-Siles, M. *et al.* Alterations in the Abundance and Co-occurrence of Akkermansia muciniphila and Faecalibacterium prausnitzii in the Colonic Mucosa of Inflammatory Bowel Disease Subjects. *Front Cell Infect Microbiol* **8**, 334070 (2018).

7.   Lopez-Siles, M. *et al.* Mucosa-associated Faecalibacterium prausnitzii phylotype richness is reduced in patients with inflammatory bowel disease. *Appl Environ Microbiol* **81**, 7582–7592 (2015).

8.   Miquel, S. *et al.* Faecalibacterium prausnitzii and human intestinal health. *Curr Opin Microbiol* **16**, 255–261 (2013).

9.   Sokol, H. *et al.* Faecalibacterium prausnitzii is an anti-inflammatory commensal bacterium identified by gut microbiota analysis of Crohn disease patients. *Proc Natl Acad Sci U S A* **105**, 16731–16736 (2008).

10.   Fitzgerald, C. B. *et al.* Comparative analysis of Faecalibacterium prausnitzii genomes shows a high level of genome plasticity and warrants separation into new species-level taxa. *BMC Genomics* **19**, 931 (2018).

11.   Vallianou, N. G. *et al.* The Role of Next-Generation Probiotics in Obesity and Obesity-Associated Disorders: Current Knowledge and Future Perspectives. *International Journal of Molecular Sciences 2023, Vol. 24, Page 6755* **24**, 6755 (2023).

12.   Kaźmierczak-Siedlecka, K. *et al.* Next-generation probiotics - do they open new therapeutic strategies for cancer patients? *Gut Microbes* **14**, (2022).

13.   Lopez-Siles, M. *et al.* Changes in the Abundance of Faecalibacterium prausnitzii Phylogroups I and II in the Intestinal Mucosa of Inflammatory Bowel Disease and Patients with Colorectal Cancer. *Inflamm Bowel Dis* **22**, 28–41 (2016).

14.   Wang, J. *et al.* A metagenome-wide association study of gut microbiota in type 2 diabetes. *Nature 2012 490:7418* **490**, 55–60 (2012).

15.   Ullah, H. *et al.* The gut microbiota-brain axis in neurological disorder. *Front Neurosci* **17**, (2023).

16.   Chollet, L. *et al.* Faecalibacterium duncaniae as a novel next generation probiotic against influenza. *Front Immunol* **15**, 1347676 (2024).

17.   Martín, R. *et al.* Faecalibacterium: a bacterial genus with promising human health applications. *FEMS Microbiol Rev* **47**, (2023).

18.   Verstraeten, S. *et al.* Faecalibacterium duncaniae A2-165 regulates the expression of butyrate synthesis, ferrous iron uptake, and stress-response genes based on acetate consumption. *Scientific Reports 2024 14:1* **14**, 1–12 (2024).

19.   Quévrain, E., Maubert, M. A., Sokol, H., Devreese, B. & Seksik, P. The presence of the anti-inflammatory protein MAM, from Faecalibacterium prausnitzii, in the intestinal ecosystem. *Gut* **65**, 882–882 (2016).

20.   Zhang, M. *et al.* Faecalibacterium prausnitzii Inhibits Interleukin-17 to Ameliorate Colorectal Colitis in Rats. *PLoS One* **9**, e109146 (2014).

21.   Quévrain, E. *et al.* Identification of an anti-inflammatory protein from Faecalibacterium prausnitzii, a commensal bacterium deficient in Crohn's disease. *Gut* **65**, 415 (2016).

22.   Auger, S. *et al.* Intraspecific Diversity of Microbial Anti-Inflammatory Molecule (MAM) from Faecalibacterium prausnitzii. *Int J Mol Sci* **23**, (2022).

23.   Breyner, N. M. *et al.* Microbial Anti-Inflammatory Molecule (MAM) from Faecalibacterium prausnitzii Shows a Protective Effect on DNBS and DSS-Induced Colitis Model in Mice through Inhibition of NF-κB Pathway. *Front Microbiol* **8**, (2017).

24.   Xu, J. *et al.* Faecalibacterium prausnitzii-derived microbial anti-inflammatory molecule regulates intestinal integrity in diabetes mellitus mice via modulating tight junction protein expression普拉梭菌活性产物-微生物抗炎分子通过调控细胞紧密连接蛋白表达修复糖尿病小鼠肠道屏障. *J Diabetes* **12**, 224–236 (2020).

25.   Pápai, G. *et al.* The Administration Matrix Modifies the Beneficial Properties of a Probiotic Mix of Bifidobacterium animalis subsp. lactis BB-12 and Lactobacillus acidophilus LA-5. *Probiotics Antimicrob Proteins* **13**, 484–494 (2021).

26.   Carbonne, C. *et al.* Ligilactobacillus salivarius CNCM I-4866, a potential probiotic candidate, shows anti-inflammatory properties in vitro and in vivo. *Front Microbiol* **14**, 1270974 (2023).

27.   Martín, R., Martín, C., Escobedo, S., Suárez, J. E. & Quirós, L. M. Surface glycosaminoglycans mediate adherence between HeLa cells and Lactobacillus salivarius Lv72. *BMC Microbiol* **13**, 1–11 (2013).

28.   Barone, M. *et al.* A versatile new model of chemically induced chronic colitis using an outbred murine strain. *Front Microbiol* **9**, 326524 (2018).

29.   Sokol, H. *et al.* Low counts of Faecalibacterium prausnitzii in colitis microbiota. *Inflamm Bowel Dis* **15**, 1183–1189 (2009).

30.   Morhardt, T. L. *et al.* IL-10 produced by macrophages regulates epithelial integrity in the small intestine. *Scientific Reports 2019 9:1* **9**, 1–10 (2019).

31.   Brockmann, L. *et al.* Intestinal microbiota-specific Th17 cells possess regulatory properties and suppress effector T cells via c-MAF and IL-10. *Immunity* **56**, 2719-2735.e7 (2023).

32.   Koelink, P. J. *et al.* Anti-TNF therapy in IBD exerts its therapeutic effect through macrophage IL-10 signalling. *Gut* **69**, 1053 (2019).

33.   Leppkes, M., Roulis, M., Neurath, M. F., Kollias, G. & Becker, C. Pleiotropic functions of TNFα in the regulation of the intestinal epithelial response to inflammation. *Int Immunol* **26**, 509–515 (2014).

34.   Bradford, E. M. *et al.* Epithelial TNF Receptor Signaling Promotes Mucosal Repair in Inflammatory Bowel Disease. *J Immunol* **199**, 1886–1897 (2017).

35.   Xiao, P. *et al.* Mannose metabolism normalizes gut homeostasis by blocking the TNFα-mediated pro-inflammatory circuit. *Cell Mol Immunol* **20**, 119 (2022).

36.   Ruder, B., Atreya, R. & Becker, C. Tumour Necrosis Factor Alpha in Intestinal Homeostasis and Gut Related Diseases. *Int J Mol Sci* **20**, (2019).

37.   Bashashati, M. *et al.* Cytokine imbalance in irritable bowel syndrome: a systematic review and meta-analysis. *Neurogastroenterology & Motility* **26**, 1036–1048 (2014).

38.   Cherukuri, A. *et al.* Immunologic human renal allograft injury associates with an altered IL-10/TNFα expression ratio in regulatory B cells. *J Am Soc Nephrol* **25**, 1575–1585 (2014).

39.   Li, W., Liu, Q., Shi, J., Xu, X. & Xu, J. The role of TNFα in the fate regulation and functional reprogramming of mesenchymal stem cells in an inflammatory microenvironment. *Front Immunol* **14**, 1074863 (2023).

40.   Dutcher, J. P. *et al.* High dose interleukin-2 (Aldesleukin) - expert consensus on best management practices-2014. *J Immunother Cancer* **2**, 26 (2014).

41.   Schreiber, S. *et al.* Safety and efficacy of recombinant human interleukin 10 in chronic active Crohn's disease. *Gastroenterology* **119**, 1461–1472 (2000).

42.   Morampudi, V. *et al.* DNBS/TNBS Colitis Models: Providing Insights Into Inflammatory Bowel Disease and Effects of Dietary Fat. *J Vis Exp* 51297 (2014) doi:10.3791/51297.

43.   Alex, P. *et al.* Distinct Cytokine Patterns Identified from Multiplex Profiles of Murine DSS and TNBS-Induced Colitis. *Inflamm Bowel Dis* **15**, 341–352 (2009).

44.   Yan, Y. *et al.* Temporal and Spatial Analysis of Clinical and Molecular Parameters in Dextran Sodium Sulfate Induced Colitis. *PLoS One* **4**, e6073 (2009).

45.   Bai, Y. *et al.* Advanced Techniques for Detecting Protein Misfolding and Aggregation in Cellular Environments. *Chem Rev* **123**, 12254–12311 (2023).

46.   Pirkalkhoran, S. *et al.* Bioengineering of Antibody Fragments: Challenges and Opportunities. *Bioengineering 2023, Vol. 10, Page 122* **10**, 122 (2023).

47.   Pishesha, N., Harmand, T. J. & Ploegh, H. L. A guide to antigen processing and presentation. *Nature Reviews Immunology 2022 22:12* **22**, 751–764 (2022).

48.   Carlsson, A. H. *et al.* Faecalibacterium prausnitzii supernatant improves intestinal barrier function in mice DSS colitis. *Scand J Gastroenterol* **48**, 1136–1144 (2013).

49.   De Marco, A. Protocol for preparing proteins with improved solubility by co-expressing with molecular chaperones in Escherichia coli. *Nature Protocols 2007 2:10* **2**, 2632–2639 (2007).

50.   Remans, K. *et al.* Protein purification strategies must consider downstream applications and individual biological characteristics. *Microb Cell Fact* **21**, 1–16 (2022).

51.   Klojdová, I., Milota, T., Smetanová, J. & Stathopoulos, C. Encapsulation: A Strategy to Deliver Therapeutics and Bioactive Compounds? *Pharmaceuticals* **16**, 362 (2023).

CHAPTER III

6. CHATER III – MAM: MOLECULAR DIVERSITY WITHIN THE GENUS *FAECALIBACTERIUM*

One of the important characteristics of MAM is its great diversity within the genus *Faecalibacterium*, which may impact the function and relation with the host[303]. Here, we aim to explore this diversity regarding its structure predictions between species, as well as MAM's localization, and interactions with the ABC transporter.

To further elucidate the structural and functional diversity of MAM, this study focuses on three variants of *Faecalibacterium* with distinct anti-inflammatory profiles: *F. duncaniae* A2-165, *F. prausnitzii* M21/2, and *F. prausnitzii* CNCM4541. The MAM of A2-165 strain has been widely used as a reference in *Faecalibacterium* research. The MAM of M21/2 strain has shown the highest anti-inflammatory activity, achieving 96% inhibition of NF-κB *in vitro* and demonstrating protective effects in murine models of colitis. In contrast, the MAM of CNCM4541 exhibited no detectable suppression of NF-κB, making it a crucial negative control to investigate molecular determinants associated with MAM function[303].

Briefly, our findings demonstrated that all selected MAMs from 3 different species/strains are able to organize in a hexameric complex, as well as forming the same ordered lattice visible through EM. MAM is among the top 10 most abundant proteins in the *Faecalibacterium* proteome across all evaluated species. Although having strong structural diversity, similarities between the species were observed in the predicted pore-like organization, abundance, cell envelope localization, and the ability to arrange in an ordered lattice. However, no correlation was found between MAM and its differential anti-inflammatory activity within the genus. This indicates that further studies are needed to clarify what other MAM from *Faecalibacterium* features determine its species-specific anti-inflammatory properties.

6.1.   Methodology

MAM structural predictions

The amino acid sequences of MAM proteins were obtained from Auger et al., 2022. Structural predictions of the A2-165, M21/2, and CNCM4541 MAM monomeric forms were performed using AlphaFold3[310,311]. The selected proteins and their corresponding strains are as follows: WP_005923208.1 (M21/2), WP_005932151.1 (A2-165). The interactions between the three main selected variants were evaluated with PISA interface toll[312], and structures were analyzed with Pymol[313].

For docking with the PCAT ABC transporter, the protein sequence of each respective variant was selected (Protein IDs: A2165: WP_005932148, M21/2: WP_005926821, CNCM4541: WP_097801715). Both MAM and the PCAT ABC transporter sequences were submitted to AlphaFold3 for complex modeling.

MAM in the cell envelope of Faecalibacterium

To validate whether the subcellular localization of MAM in *Faecalibacterium* species follows the pattern previously observed in *F. duncaniae* A2-165, cytoplasm, and envelope protein fractions were isolated from cultures of *F. prausnitzii* M21/2 and *Faecalibacterium* CNCM4541. The methodology was conducted as described in Chapter I. Spectral counting, and NSAF (Normalized Spectral Abundance Factor) were used to compare and quantify MAM abundance in each fraction. Statistical significance was assessed using a one-way ANOVA, followed by Tukey's multiple comparisons test.

Envelope-associated protein extraction, identification, and visualization

Two extraction approaches were employed to isolate envelope-associated fractions enriched with MAM: RIPA buffer and LiCl. These methods are commonly used to isolate S-layer-like proteins, though MAM is not classified as an S-layer component[314–316]. For all extractions, *Faecalibacterium* cultures from the three selected variants were grown to stationary phase (~18hrs of growth) and harvested by centrifugation at $5000 \times g$ for 15 minutes. To isolate the envelope-associated fraction of *Faecalibacterium* with RIPA buffer, cell pellets were surface-washed with cold PBS (pH 7.4) before resuspension in 60 mL of cold 0.1 M Tris–HCl buffer (pH 7.2). To disrupt the cells and release envelope-associated components, six cycles of sonication (10 seconds each) were performed. Differential centrifugation was used to isolate the envelope fraction, first pelleting whole bacterial cells at $6,000 \times g$ for 10 minutes at 4°C,

then collecting the supernatant. The fraction was further concentrated by ultracentrifugation at 49,000 × g for 3 hours at 4°C. The resulting pellet was resuspended in 50 µL of cold 0.1 M Tris–HCl buffer and incubated for 48 hours at 4°C to stabilize the extracted envelope-associated proteins.

RIPA buffer (1% v/v final concentration) was added to solubilize MAM from the envelope fraction, and the suspension was gently mixed on ice for 30 minutes to disrupt non-covalent interactions between MAM and the bacterial cell wall. The reaction was quenched by adding cold 0.1 M Tris–HCl buffer (pH 7.2) at a 3:1 ratio, followed by centrifugation at 13,000 × g for 30 minutes at room temperature to pellet the MAM-enriched envelope fraction. To further purify the sample, the pellet was washed twice with PBS using a 50 kDa centrifugal filter, centrifuged at 13,000 × g for 5 minutes at 4°C, and stored at −80°C. The RIPA buffer used in this protocol consisted of NaCl (0.88 g), EDTA (0.15 g), NP-40 (1 mL, 100%), sodium deoxycholate (1 g), SDS (0.10 g), and Tris–HCl (1 M, 2.5 mL, pH 7.6) per 100 mL solution. Extraction with LiCl was performed as described in Chapter I.

For RIPA buffer extraction, four intense gel bands visible in the SDS-page gel were excised to identify the respective protein content separately. In parallel, LiCl-extracted fractions from *F. duncaniae* A2-165, *F. prausnitzii* M21/2, and *Faecalibacterium* CNCM4541 were completely subjected to protein identification to assess the presence and composition of envelope-associated proteins across strains. Electronic Microscopy of RIPA buffer extracts was performed with the three selected *Faecalibacterium* species, following the procedures in the methods section of Chapter 1.

6.2. Results

MAM monomer structure diversity

The predicted structures of the MAM proteins from the three selected *Faecalibacterium* species reveal a conserved core helix-rich region interconnected by disordered segments and a prominently unfolded N-terminal region across all three variants. The three structures demonstrated high divergence from each other, especially regarding the positioning of the helices. (Figure 20).
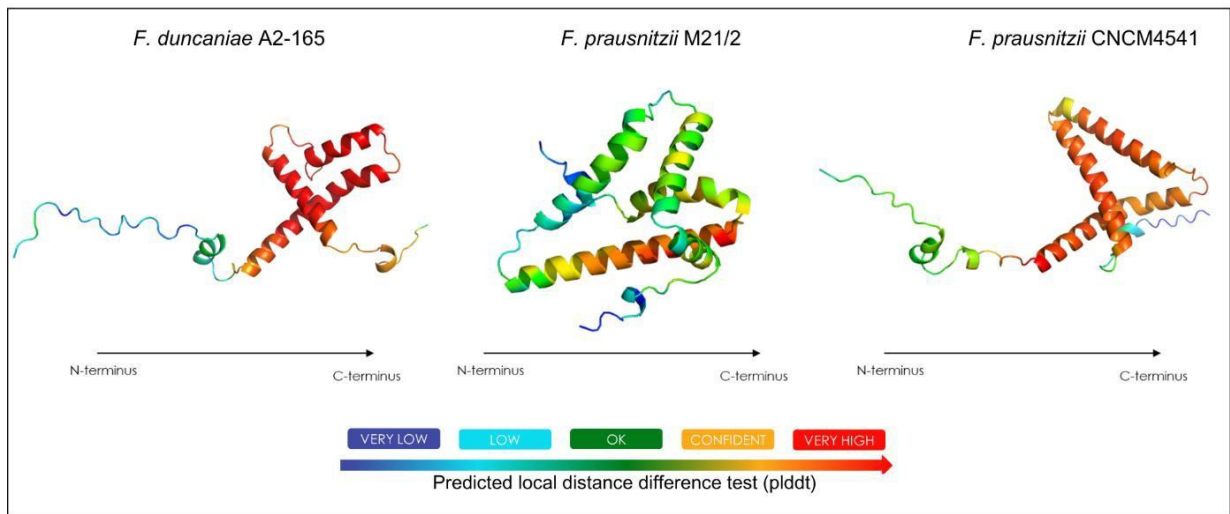
Figure 20. Structural Comparison of monomeric MAM proteins from *Faecalibacterium* strains. Predicted AlphaFold 3D models of MAM proteins from *F. duncaniae* A2-165, *F. prausnitzii* M21/2, and *F. prausnitzii* CNCM4541, with color-coded pLDDT scores indicating confidence levels range in structural prediction (blue – low confidence to red indicating high confidence. Arrows indicate the position of N-terminus and C-terminus.

MAM interaction with the ABC transporter

The structural modeling of MAM proteins in complex with the ABC transporter revealed conserved features across the three *Faecalibacterium* variants, particularly in the orientation of the N-terminal leader peptide (LP), which interacts with the peptidase domain (PCAT), as described in Chapter I. The LP region consistently displayed the highest structural confidence, indicated by PLDDT scores in yellow-red (Figure 20), although, for *F. prausnitzii* M21/2, this confidence was lower. On the other hand, the central and C-terminal regions exhibited significantly lower structural quality (PLDDT scores in blue-green) for the three variants, indicating potential flexibility or disorder in these areas (Figure 21).
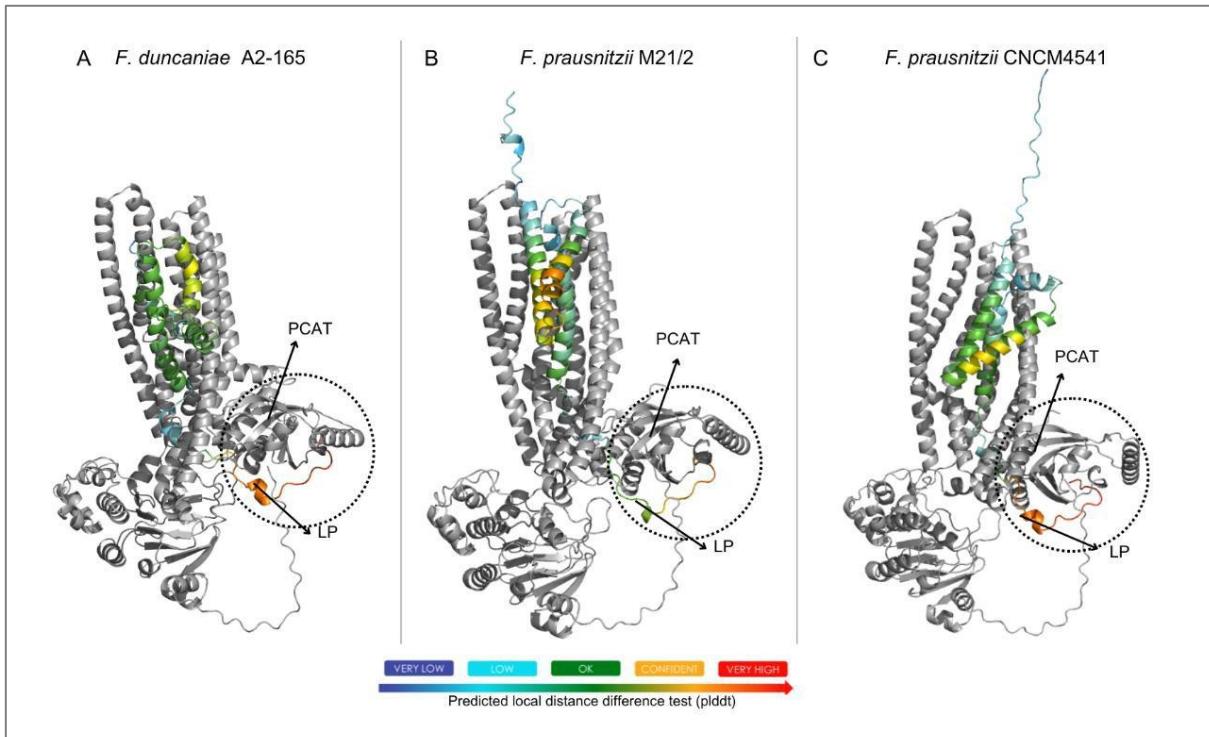
Figure 21. Interaction between MAM and PCAT ABC transporter in *Faecalibacterium* strains. Predicted structural models of MAM-ABC transporter complexes for A*)* *F. duncaniae* A2-165, B) *F. prausnitzii* M21/2, and C) *F. prausnitzii* CNCM4541. MAM proteins are colored according to PLDDT scores (color-coded bar below), and the ABC transporter domains are in gray. The PCAT peptidase is highlighted with a dashed circle. MAM's N-terminal LP shows expected positioning within the PCAT across all strains. High-confidence regions visualized in yellow/red indicate high structural confidence and low-confidence regions are observed in shades of blue.

Conserved hexameric organization in MAM-ΔLP predictions

The structural modeling of MAM-ΔLP hexamers from *F. duncaniae* A2-165, *F. prausnitzii* M21/2, and CNCM4541 revealed conserved pore-like hexameric arrangements, characterized by interlaced subunits forming ring-like complexes with central pores of varying diameters (Figure 22). *F. duncaniae* A2-165 displayed a compact structure with an 80 Angstroms (Å) outer diameter and a 20 Å central pore, while *F. prausnitzii* M21/2 exhibited the largest hexameric assembly, with 110 Å of diameter and a 22 Å pore. Conversely, CNCM4541 presented a more condensed configuration with an 87 Å outer diameter and the smallest pore at 17 Å. The hexameric model selected for A2-165 was predicted with AlphaFold 3, while for M21/2 and CNCM4541, predictions with AlhaFold 2 had higher confidence scores, thus selected to be shown in this manuscript.
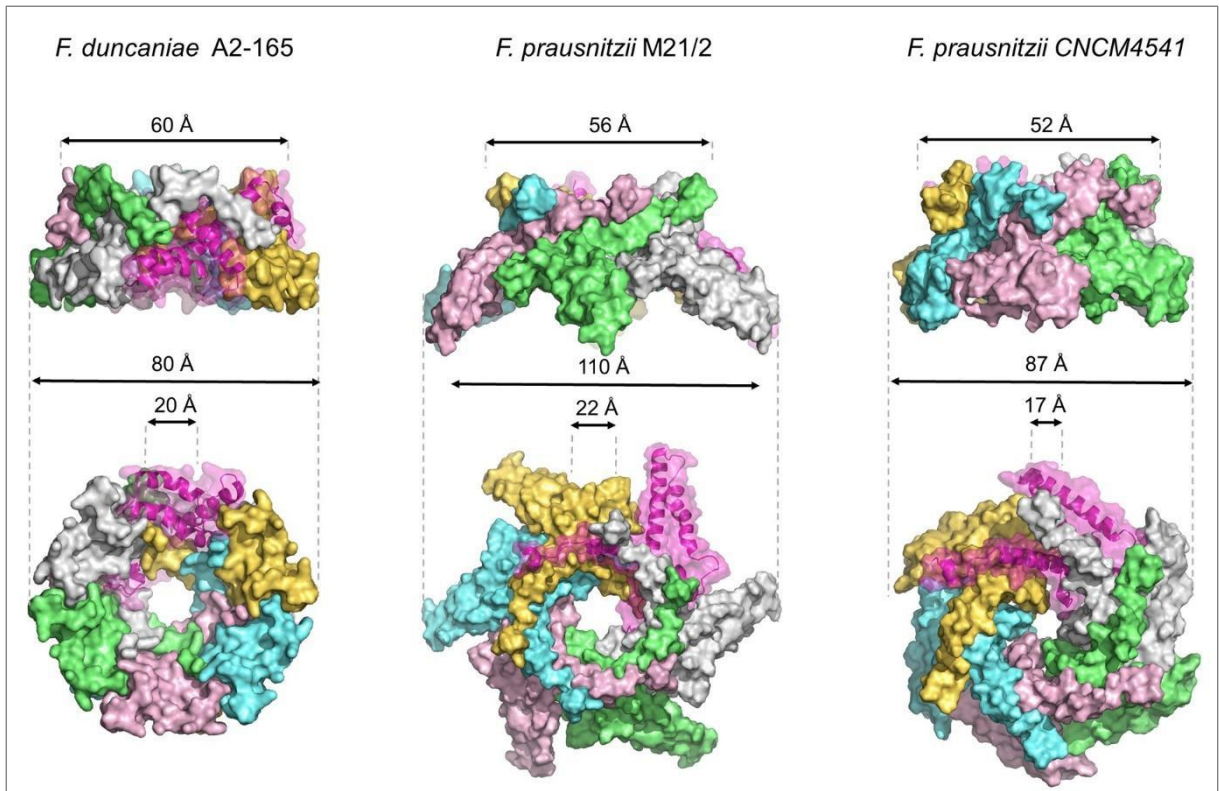
Figure 22. Hexameric complexes of *Faecalibacterium* species. A) *F. duncaniae* A2-165, B) *F. prausnitzii* M21/2, and C) *F. prausnitzii* CNCM4541, hexamers colored by subunit. One face and lateral structural profiles are observed. Arrows and dashed lines indicate the structural dimension in Angstroms (Å).

Interaction interfaces

Proteins that form oligomeric structures rely on multiple levels of interactions to maintain their stability and function[317]. In MAM hexameric assembly, each monomer interacts with its immediate neighbor (Level 1, n, n+1) and, in some cases (A2-165 and M21/2), with a second-adjacent monomer (Level 2, n, n+2). Level 1 interactions provide direct monomer-to-monomer binding, contributing to the overall stability of the hexamer, while Level 2 interactions reflect broader interconnectivity between non-adjacent monomers. The absence of Level 3 interactions (n, n+3) across all strains suggests that the hexameric organization remains consistent without requiring additional long-range contacts (Figure 23).

Nevertheless, the predicted MAM hexameric structures exhibited notable differences in both stability and interconnectivity across the three strains. *F. duncaniae* A2-165 displayed the highest stability and interconnectivity, with the largest interface area (1695.5 Å², Level 1), a dense hydrogen bond network, and additional salt bridges stabilizing Level 2 interactions. *F. prausnitzii* M21/2 exhibited moderate stability and interconnectivity, characterized by a more compact interface (1483.2 Å², Level 1), fewer hydrogen bonds in Level 1, and an average of two salt bridges per interaction level. CNCM4541 had the weakest interconnectivity, with the

smallest interface area (1210.9 Å², Level 1) and 11 hydrogen bonds. Despite showing 5 salt bridges, it lacked Level 2 interactions entirely.
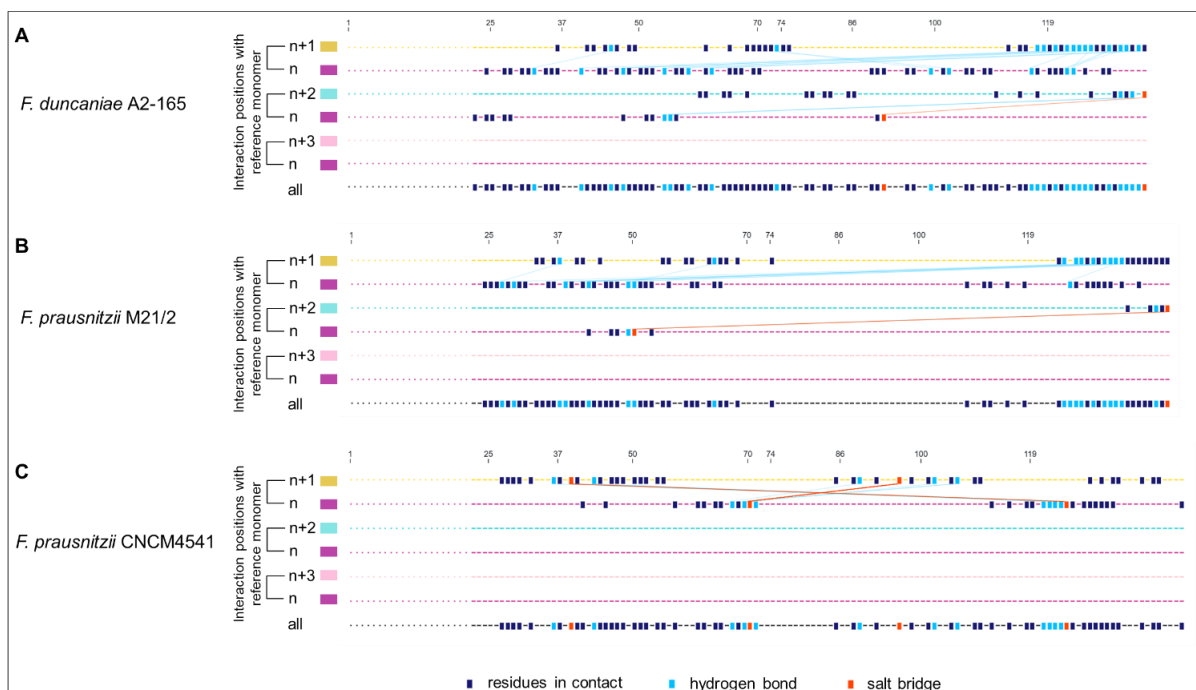
Figure 23. Representation of the interconnectivity of monomers in the hexameric complex. Schematic representation of amino acid interactions involved in the stability of the predicted MAM-ΔLP hexamer structure from A) A2-165, B) M21/2, C) CNCM4541. The upper part of each panel (A-C) shows the amino acid numbers and the respective positions of the modeled α-helices. Below, each line corresponds to a subunit of the MAM-ΔLP hexamer. Dark blue squares represent amino acid interaction points, light blue indicates hydrogen bonds, and orange indicates salt bridges. The first two lines display level 1 interactions (n, n+1), showing contacts between adjacent units. The next two lines correspond to level 2 interactions (n, n+2), indicating interactions between the second-adjacent subunit. The empty third line evidences the lack of level 3 interactions (n, n+3) corresponding to subunits on opposite sides. The last line represents all positions in interaction for one subunit. The colored boxes and lines (yellow, dark pink, light pink, and blue) follow the colors of the monomers indicated in the hexameric assembly (Figure 22).

Binding free energy (ΔiG) was used to quantify interaction interactions strength. *F. duncaniae* A2-165 exhibited the most negative ΔiG (-26.2 kcal/mol, Level 1), indicating strong monomer binding. *F. prausnitzii* M21/2 had a slightly higher ΔiG (-25.9 kcal/mol, Level 1), suggesting similar but weaker monomer interactions. *F. prausnitzii* CNCM4541 had the least negative ΔiG (-15.3 kcal/mol, Level 1), indicating weaker monomeric interactions within the studied hexamers (Figure 23, Table 1).

Table 1. Comparison of interface interactions across MAM variants.

	Species	Interaction Level	Structure 1	Surface Å² 1	Structure 2	Surface Å² 2	Interface Area (Å²)	ΔiG (kcal/mol)	Hydrogen Bonds	Salt Bridges
1	A2-165	Level 1	A	9773	F	9773	1701.4	-26.3	17	0
2	A2-165	Level 1	D	9776	E	9767	1697.9	-26.3	17	0
3	A2-165	Level 1	C	9782	D	9776	1695.0	-26.1	17	0
4	A2-165	Level 1	B	9770	C	9782	1694.1	-26.1	17	0
5	A2-165	Level 1	E	9767	F	9773	1693.2	-26.0	17	0
6	A2-165	Level 1	A	9773	B	9770	1691.3	-26.1	16	0
	A2-165	**Mean (Level 1)**	-	**9773.5**	-	**9773.5**	**1695.5**	**-26.2**	**17**	**0**
7	A2-165	Level 2	A	9773	C	9782	530.5	-12.3	3	1
8	A2-165	Level 2	C	9782	E	9767	529.9	-12.3	3	1
9	A2-165	Level 2	B	9770	F	9773	528.4	-12.2	3	1
10	A2-165	Level 2	B	9770	D	9776	528.3	-12.2	3	1
11	A2-165	Level 2	A	9773	E	9767	525.7	-12.2	3	1
12	A2-165	Level 2	D	9776	F	9773	523.6	-12.2	3	1
	A2-165	**Mean (Level 2)**	-	**9773.5**	-	**9773.5**	**527.7**	**-12.2**	**3**	**1**
1	M21/2	Level 1	E	9766	F	9782	1489.6	-26.1	11	2
2	M21/2	Level 1	D	9758	E	9766	1484.1	-26.1	11	2
3	M21/2	Level 1	A	9768	B	9746	1483.8	-25.9	11	2
4	M21/2	Level 1	B	9746	C	9767	1481.6	-25.9	11	2
5	M21/2	Level 1	A	9768	F	9782	1480.7	-25.9	11	2
6	M21/2	Level 1	C	9767	D	9758	1479.3	-25.8	11	2
	M21/2	**Mean (Level 1)**	-	**9762.2**	-	**9766.8**	**1483.2**	**-25.9**	**11**	**2**
7	M21/2	Level 2	A	9768	E	9766	214.3	-2.7	1	2
8	M21/2	Level 2	C	9767	E	9766	214.0	-2.8	1	2
9	M21/2	Level 2	A	9768	C	9767	213.9	-2.7	1	2
10	M21/2	Level 2	D	9758	F	9782	213.6	-2.7	1	2
11	M21/2	Level 2	B	9746	F	9782	212.6	-2.7	1	2
12	M21/2	Level 2	B	9746	D	9758	212.4	-2.7	1	2
	M21/2	**Mean (Level 2)**	-	**9762.2**	-	**9766.8**	**213.5**	**-2.7**	**1**	**2**
1	CNCM4541	Level 1	C	9786	D	9740	1224.8	-15.3	11	5
2	CNCM4541	Level 1	D	9740	E	9743	1221.6	-15.1	11	5
3	CNCM4541	Level 1	A	9668	E	9743	1215.7	-15.1	10	5
4	CNCM4541	Level 1	A	9668	F	9744	1207.8	-15.6	11	6
5	CNCM4541	Level 1	B	9741	F	9744	1202.3	-14.7	11	5
6	CNCM4541	Level 1	B	9741	C	9786	1193.1	-15.9	11	5

CNCM4541	**Mean (Level 1)**	-	**9724**	-	**9750**	**1210.9**	**-15.9**	**10,83333**	**5,166667**

The table presents the interaction parameters of MAM hexamers from *F. duncaniae* A2-165*, F. prausnitzii* M21/2, and *F. prausnitzii* CNCM4541. The interacting monomers are identified in the columns Structure 1 and Structure 2, with letters from A to F to indicate each of the 6 monomers. Interface area (Å²), binding free energy (ΔiG, kcal/mol), number of hydrogen bonds, and salt bridges were compared across Level 1 (n, n+1) and Level 2 (n, n+2) interactions.

MAM abundance in the envelope is characteristic of the targeted Faecalibacterium variants

Here, we demonstrated that a substantial abundance of MAM in the envelope fraction in relation to the cytoplasm is characteristic of the three tested species of *Faecalibacterium* (Figures 24 and 25). Moreover, proteomic analysis confirmed that MAM is predominantly localized in the envelope fraction across all analyzed *Faecalibacterium* strains, consistent with previous observations in *F. duncaniae* A2-165. The highest spectral counts in the envelope fraction were detected in *F. duncaniae* A2-165 and CNCM4541 ($p < 0.0001$), while *F. prausnitzii* M21/2 exhibited a more balanced distribution between envelope and cytoplasm, but still with significant enrichment in the envelope ($p < 0.05$) (Figure 24).
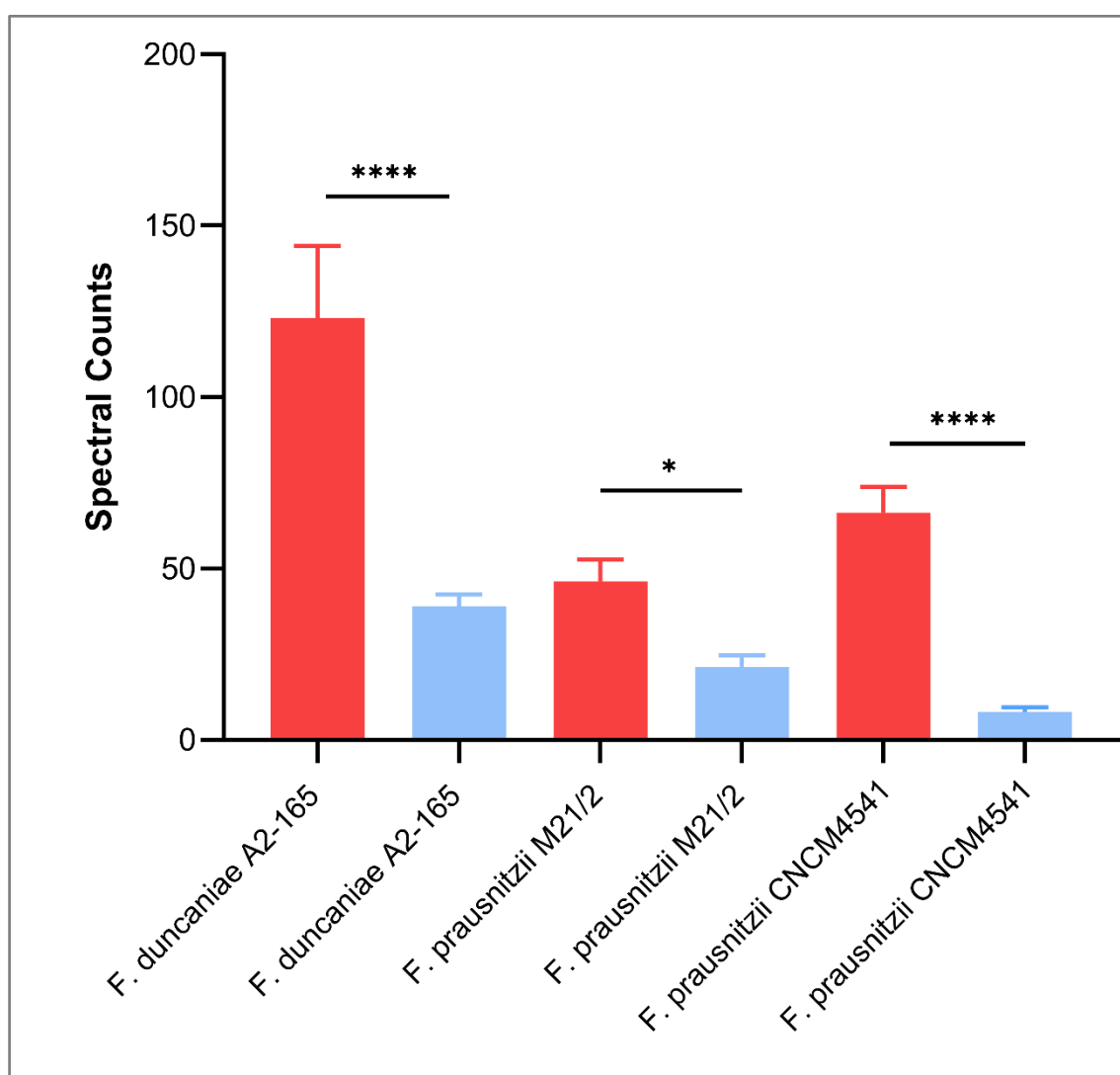
Figure 24. Subcellular localization of MAM in *Faecalibacterium* strains based on proteomic analysis. The Y axis indicates spectral counts of MAM in the envelope (red) and cytoplasm (blue) fractions of *F. duncaniae* A2-165, *F. prausnitzii* M21/2, and *F. prausnitzii* CNCM4541. Significant comparisons are indicated: $p < 0.0001$(****), $p < 0.05$(***). Data normality was assessed using the Shapiro-Wilk test, and statistical significance was determined by Tukey's multiple comparisons test.
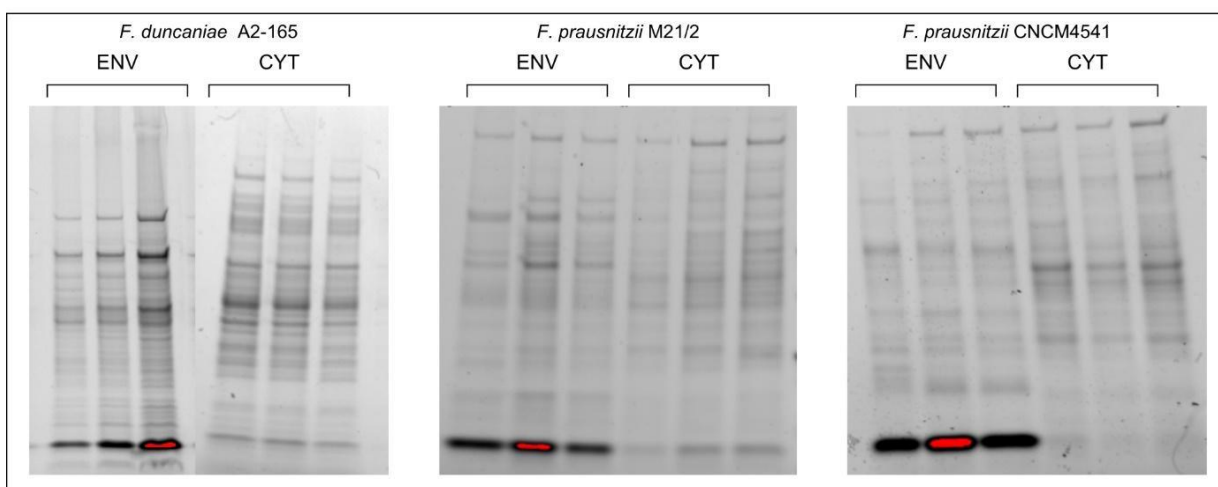
Figure 25. Cell envelope and cytoplasm protein profiles between *Faecalibacterium* variants. The figure shows the contrasting pattern of bands in SDS-page gell between cytoplasm (CYT) and envelope (ENV) proteins in addition to the differences between the three representatives of the genus. Triplicates are shown and 10ug of protein was loaded in each well, indicating the massive abundance of ~15kDa protein in the envelope fraction for all variants.

MAM remains largely abundant in targeted envelope extraction among variants

Given the observed enrichment of MAM in envelope fractions, we sought to further evaluate the biochemical nature of this localization using targeted extraction protocols. To assess MAM enrichment, total protein extracts and membrane-associated fractions obtained via LiCl and RIPA buffer extractions were analyzed by SDS-PAGE. As expected, in total extracts, a dominant band at ~15 kDa was observed in all strains, corresponding to the predicted molecular weight of MAM. This band remained the most intense in total protein samples, suggesting a high relative abundance of MAM among extracted proteins (Figure 26).

LiCl extraction showed a cleaner protein profile compared to total extracts and RIPA extractions, suggesting less cytoplasmic contamination. The 15 kDa band was present in all three strains, indicating that this method effectively supported the obtaining of envelope-associated MAM. Despite *F. prausnitzii* CNCM4541 RIPA extractions showing that the band corresponding to MAM was less evident when compared to LiCl extraction, this result was not consistently reproducible and should be considered with caution (Figure 26).
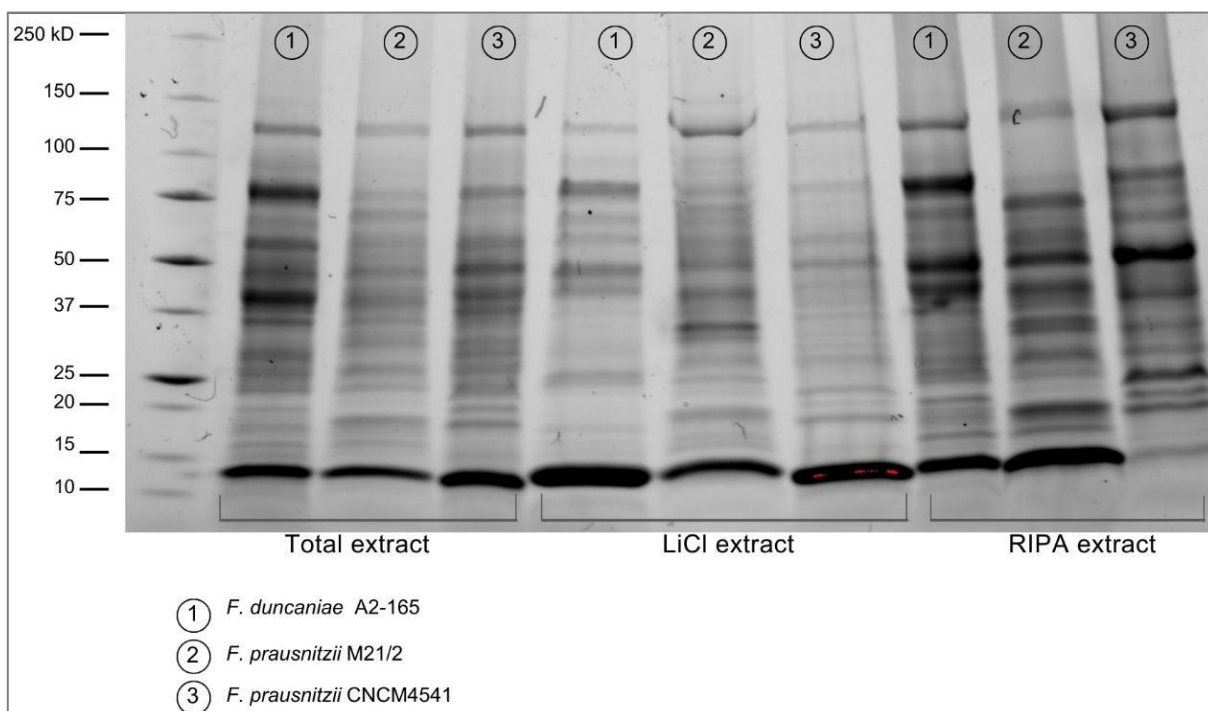
Figure 26. SDS-PAGE protein profiles of bacterial total extract and envelope extractions using LiCl and RIPA buffer for the 3 selected strains. Protein extracts from *F. duncaniae* A2-165 (1), *F. prausnitzii* M21/2 (2), and *F. prausnitzii CNCM4541* (3) analyzed by SDS-PAGE. Total extracts, LiCl extracts, and RIPA extracts are shown from the right to the left.

Proteomic analysis of excised SDS-PAGE bands from RIPA buffer extracts of *F. duncaniae* A2-165 confirmed the dominance of MAM corresponding to the ~15 kDa band. Specific spectra and and emPAI (Exponentially Modified Protein Abundance Index) were used to assess the abundance of proteins in each extracted band. The emPAI is a label-free quantitative method that estimates protein abundance based on the number of observed peptides relative to theoretically detectable peptides. The most abundant protein indicated by both specific spectra and emPAI is the 3-hydroxy acyl-CoA dehydrogenase, suggesting important contamination of RIPA extracts with cytoplasmic proteins. MAM exhibited the second-highest specific spectra count (81) and emPAI value (4.6×10^9), indicating its significant enrichment compared to other proteins identified in the gel. MAM's protein coverage of 70.37% indicates the lack of the LP, which was not identified between MAM peptides. Those parameters and the low log(E-value) further validate MAM's identity as the most envelope-related abundant protein in this fraction (Figure 27).

Sample	Uniprot ID	Description	log(E-value)	coverage	MW	size	Specific spectra	emPAI
1	C7H507	Tat pathway signal sequence domain protein	-135,1052312	34,32%	75214,1063	676	76	$5,523 \times 10^7$
2	C7H5K9	3-hydroxyacyl-CoA dehydrogenase, NAD binding domain protein	-651,780897	86,21%	31089,07145	290	449	$1,64 \times 10^{10}$
3	C7H933	30S ribosomal protein S5	-67,2870375	53,61%	16999,21943	166	17	$1,9207 \times 10^2$
4	C7H4X2	Microbial anti-inflammatory molecule	-149,4513482	70,37%	14491,3565	135	81	$4,64 \times 10^9$

Figure 27. Identification and quantification of proteins in SDS-PAGE-excised bands of RIPA extract via proteomics analysis of the species *F. duncaniae* A2-165. A) The table presents the most abundant protein identified in each excised SDS-PAGE band, listing Uniprot ID, description, log(E-value), coverage, molecular weight (MW), size (amino acids), specific spectra, and emPAI values. The order of the table follows the order of bands indicated in panel B. B) SDS-PAGE gel with excised bands (1–4) for proteomic analysis. The molecular weight ladder (kDa) is on the left.

Proteomic analysis was then conducted with LiCl-extracted fractions with the three target variants. The results revealed distinct patterns of protein enrichment across the three *Faecalibacterium* strains, with variability in MAM abundance and evidence of cytoplasmic protein presence. In *F. duncaniae* A2-165, MAM was the most abundant protein based on the NSAF (Normalized Spectral Abundance Factor) score (NSAF = 0.0188). NSAF is a metric that normalizes spectral counts by protein length, allowing for a better comparison of protein abundances than emPAI. This significantly exceeds the levels of other abundant identified proteins, such as the TAT signal peptide and 50S ribosomal protein. Conversely, in *F. prausnitzii* M21/2, cytoplasmic contamination was strongly evident, as indicated by the prominence of small ribosomal subunit proteins (e.g., uS8, NSAF = 0.0112) and other ribosomal and metabolic proteins. At the same time, MAM exhibited a lower NSAF (0.0041), although visibly, the most intense band remains the one matching MAM's size. In CNCM4541, MAM stayed among the most abundant proteins (NSAF = 0.0071), though glyceraldehyde-3-phosphate dehydrogenase (NSAF = 0.0080) dominated, further suggesting cytoplasmic contamination in this sample (Figure 28).
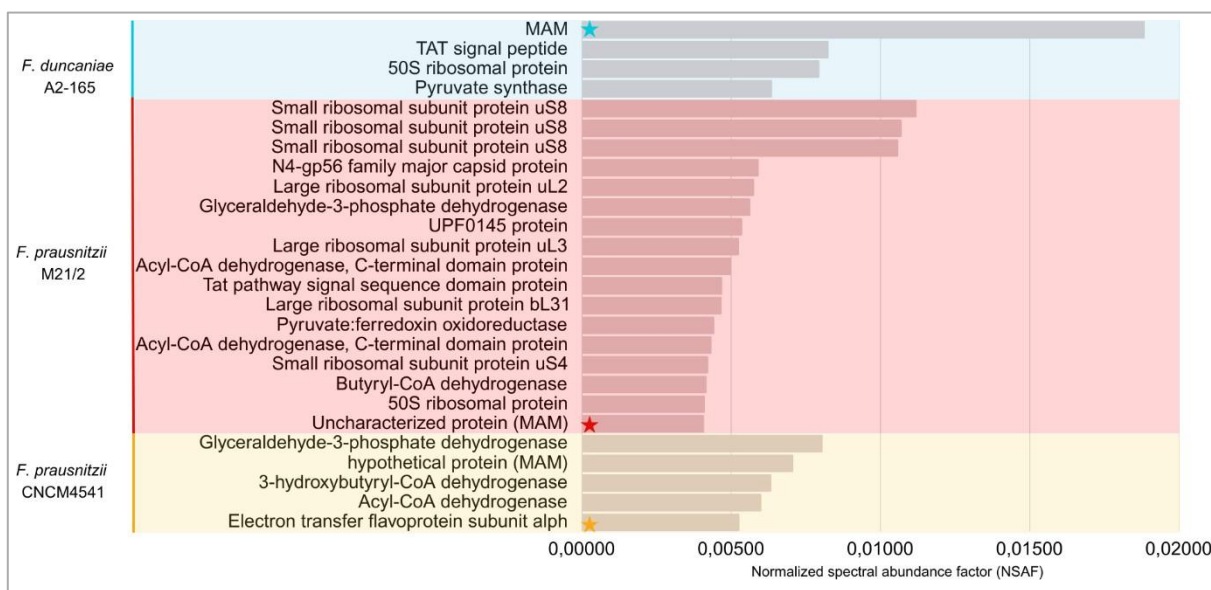
Figure 28. Normalized Spectral Abundance Factor (NSAF) ranking of LiCl-extracted proteins across *Faecalibacterium* strains. Relative protein abundance based on NSAF scores reveals variability in MAM in LiCl extracts from *F. duncaniae* A2-165 (blue panel), *F. prausnitzii* M21/2 (red channel), and *F. prausnitzii* CNCM4541 (yellow panel). Stars indicate the MAM position in the ranking for each strain.

Microscopy analysis showed a similar organized pore-like pattern in RIPA buffer extracts

Electron microscopy (EM) analysis of RIPA-extracted fractions revealed structural patterns across the three *Faecalibacterium* species. In *F. duncaniae* A2-165 and *F. prausnitzii* M21/2 (Figure 29, A, and B), a network of pore-like arrangements was consistently observed, highlighting a recurring putative hexameric organization. These structures were characterized by regular spacing and a lattice-like organization, suggesting preserved oligomeric assemblies of MAM after the extraction. Additionally, irregularly shaped fragments, potentially corresponding to disrupted envelope components, were also present. In contrast, CNCM4541 (Figure 29 C) exhibited fewer identifiable fragments, with the characteristic pore-like networks being less evident.
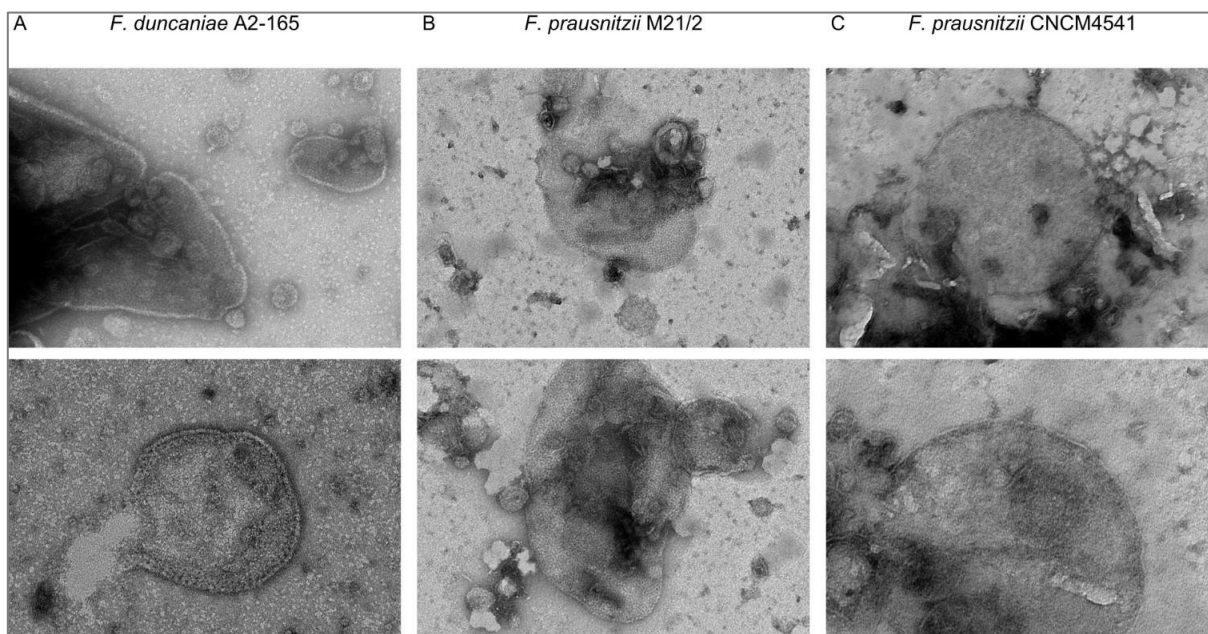
Figure 29. Electron Microscopy analysis of RIPA-extracted fractions from *Faecalibacterium* strains. The figure shows irregular fragments with variable sizes in all variants. Pore-like network structures are visible in extracts from A) *F. duncaniae* A2-165 and B) *F. prausnitzii* M21/2, while such arrangements are less evident in C) *F. prausnitzii* CNCM4541.

These findings collectively highlight the conserved structural and functional features of MAM across *Faecalibacterium* strains, emphasizing its role as a key envelope-associated protein with a putative pore-like organization. Moreover, important strain-specific differences were observed in structural stability, abundance, and extractability, which may have implications for its biological functions and interactions.

6.3 Discussion

Our results indicated that despite the high variability among MAM protein sequences, many features are conserved among *Faecalibacterium* variants, especially regarding MAM's abundance in the envelope and the putative oligomeric organization.

Despite the conserved predicted arrangement in hexamers of MAM from different strains, the structural analysis revealed notable differences in interface area, binding strength (ΔiG), and secondary interactions, highlighting strain-specific structural adaptations.

The PISA interface data indicates that *F. duncaniae* A2-165, with the largest buried surface area and extensive hydrogen bonding, exhibits a balanced stabilization mechanism, combining hydrophobic interactions (interface residues) with electrostatic forces (salt bridges and hydrogen bonds). In contrast, CNCM4541 relies heavily on salt bridges for stabilization but exhibits fewer hydrophobic interactions due to its smaller interface area[318,319].

Intriguingly, despite the hexameric predictions indicating CNCM4541 harboring the least stable structure, the bare absence of the MAM-related band in CNCM4541 RIPA extract, contrasting with its clear presence in both total extracts and LiCl extractions suggests structural and connecting differences in MAM from CNCM4541 that prevent solubilization by RIPA buffer. Unlike LiCl, which primarily disrupts ionic interactions, RIPA buffer is a detergent-based lysis solution that disrupts lipid-protein and non-covalent protein-protein interactions, including hydrophobic interactions[320–322].

The pores observed in the hexameric predictions ranged from 17 to 22 Å of diameters across the three used *Faecalibacterium* strains. This suggests that MAM likely maintains a conserved hexameric arrangement with a putative role in the envelope permeability. Larger pores could facilitate molecular passage, promoting solute exchange and external interactions, whereas smaller pores might result in a more rigid, tightly packed hexamer, enhancing stability but restricting molecular diffusion[323,324]. Such observations are an important step to be considered in the future as this suggested porosity may profoundly affect the biological function of *Faecalibacterium* cells. The recurrence of similar features indicates a conserved biological role, but structural and physicochemical differences may indicate variable selectivity.

It's important to remember that the accuracy of AlphaFold's predictions is influenced by the presence of homologous sequences in its training datasets, as the algorithm relies heavily on evolutionary information from Multiple Sequence alignments (MSAs) to infer structural architecture[325]. Despite the significant confidence in MAM hexameric predictions, the lack of homologs in existing protein databases may have reduced the prediction reliability, particularly in regions with low sequence conservation or flexibility, as indicated by the lower pLDDT scores, thus indicating the absolute need for experimental validation.

Nevertheless, the ranking of the MAM abundance in the envelope based on specific spectra count and NSAF revealed differences in its relative abundance across the three strains. In *F. duncaniae* A2-165, MAM ranked as the second most abundant protein, indicating its prominent presence in this strain. For *F. prausnitzii* M21/2, MAM was less abundant, ranking 9th, after the important presence of cytoplasmic-related proteins. In contrast, for CNCM4541, MAM ranked 7th, reflecting a moderate abundance. These findings highlight variability in MAM enrichment among the strains but, most importantly, reveal a massive presence of cytoplasmic proteins. This aspect might hinder the real abundance of envelope proteins, further indicating the development of new protocols for more properly extracting envelope-associated proteins.

Regarding the demonstrated microscopy of RIPA extracts, visual simmilatity in a porous-like network was evident between A2-165 and M21/2 variants. Despite the important decreased intensity of the band related to MAM in the observed SDS-PAGE gel of CNCM4541, some fragments were still found. However, those fragments were less abundant and not identified at the same detail level as the other variants.

The findings presented in this chapter, despite some differences, consistently suggest that MAM may play an important role in the structure and function of the cell envelope. This implies that MAM could be crucial for maintaining cell integrity and permeability across various species and strains. Sequent steps involving cryo-electron microscopy (cryo-EM) and antibody labeling will be essential for determining whether the bi-layered cell envelope is a characteristic shared by the *Faecalibacterium* genus representatives. Additionally, structural validation may help confirm the oligomerization state of MAM in the specific variants studied.

6.4 Conclusion

These structural insights into MAM oligomerization and subcellular localization across *Faecalibacterium* strains provided in this chapter are evidence of the suggested conserved structural and functional characteristics of MAM in the *Faecalibacterium* genus. The observed enrichment of MAM in the envelope fractions and its predicted hexameric organization in a network suggests a critical role in maintaining cell integrity and permeability, with notable variability across strains across the genus that must be investigated in the future.

7. GENERAL DISCUSSION

The human gut microbiota, an intricate ecosystem of diverse microbial species, having indispensable role in maintaining host homeostasis by contributing to nutrient metabolism, immune modulation, and barrier integrity. Within this complex ecosystem, the genus *Faecalibacterium* has been described as an essential microorganism for gut health. *Faecalibacterium* accounts for up to 15% of gut microbial populations and has been linked to protective effects against IBD, colorectal cancer, and metabolic disorders. Its importance is associated particularly with its production of beneficial metabolites like butyrate and bioactive peptides such as those derived from MAM.

MAM is an exclusive protein produced by the *Faecalibacterium* genus and has demonstrated anti-inflammatory effects, supporting its potential as a biotherapeutic through *in vitro* and *in vivo* models. Those studies about MAM have primarily focused on its presence in bacterial supernatants or its synthetic peptide derivatives, leaving critical gaps in our understanding of its structural organization, biochemical properties, and physiological roles. To date, one study evaluated the purified protein in a diabetes model, providing valuable insights into its role in intestinal barrier protection. Still, no research has yet investigated the effects of purified MAM in gut inflammation models such as colitis. Furthermore, the remarkable diversity of MAM within the *Faecalibacterium* genus, both in molecular and functional properties, remains largely unexplored. Thus, this thesis aims to answer what are the aspects of MAM that embrace its physiological role regarding *Faecalibacterium* and its relation with the host.

This work evaluated molecular aspects of MAM, such as its structure, localization, and interactions, providing insights into the potential functional roles of this protein and regarding the cell biology of *Faecalibacterium*. Moreover, by integrating molecular biology and biochemistry, purified recombinant MAM was obtained and its anti-inflammatory properties were evaluated *in vitro* and in murine model. Lastly, important findings regarding MAM presence and diversity within the genus *Faecalibacterium* were also assessed. Thus, this research not only addresses key gaps in our understanding of *Faecalibacteirum* physiology but also reinforces the potential of microbiota-derived molecules such as MAM in clinical applications, particularly in inflammatory diseases.

The key findings of this thesis

Our *in silico* modeling characterization suggested that MAM is likely organized as a hexamer, and together with proteomic analysis, its massive abundance in the envelope indicates

its potential role as a structural component of the cell architecture of *F. duncaniae*. A putative mechanism for MAM secretion via a PCAT ABC transporter system was also observed, highlighting its likely pathway of translocation from the intracellular compartments to the outer layer. Furthermore, our analysis provided critical insights into the organization of the cell envelope in *F. duncaniae*, revealing features of an outer layer that challenge the traditional classification of *Faecalibacterium* in Gram-positive or Gram-negative bacteria.

Our diversity investigations highlighted that MAM from species such as *F. prausnitzii* M21/2 and CNCM4541 also occupies a prominent position in the envelope fraction, having hexameric arrangement as a consistent feature among *Faecalibacterium* species, suggesting a conserved cell envelope architecture within the genus. Lastly, purified recombinant MAM demonstrated its protective effects in colitis models, with anti-inflammatory properties demonstrated *in vitro*, reinforcing its potential as a therapeutic target.

MAM is the most abundant envelope protein of F. duncaniae

Through peptidomics LC-MS/MS, we demonstrate that the probable reason for the identification of MAM peptides in the supernatant is due to degradative processes. Thus, to evaluate the subcellular localization of MAM, a simple fractionation process was employed to separate *F. duncaniae* cells into cytoplasmic and envelope-enriched fractions. Although MAM was detected in the cytoplasmic fraction, it was predominantly localized in the envelope, where it emerged as the most abundant protein in this fraction.

The uniqueness of MAM's sequence presents a significant challenge for its characterization, as no motifs or domains, apart from its signal peptide, are identifiable in existing databases. Advances in protein structural modeling by AlphaFold enabled the prediction of MAM's organization as both a monomer and a complex. The monomeric structure revealed a lack of evident stability, characterized by helices connected by disordered regions and an unfolded N-terminus. However, important ideas about its potential properties and associated functions began to emerge through the subcellular localization and the modeling of MAM complexes. From dimers to octamers, the putative suprastructure of MAM highlights a pore-like organization in which the hexameric complex has the highest prediction score.

F. duncaniae likely has an ordered envelope layer composed of oligomeric MAM

With the notable progress of imaging at high resolutions emerging, microscopy was the next reasonable step to take in order to investigate the association of MAM with the envelope of *F. duncaniae*. Thus, electron microscopy and single particle analyses of *F. duncaniae* cells

revealed a surface network filled with dark spots surrounded by hexameric borders, precisely organized in a regular patterned layer. Those observations actively align with the predicted modeling of MAM as a hexamer, although the precise nature and function of those "pores" remained uncertain. Those findings conducted the hypothesis that MAM organizes as hexamers, contributing to the formation of a lattice-like structure, with a six-fold symmetry defining its organization.

In prokaryotes, pore-organized structures are present in different cell layers and are essential for various cellular processes. The Mechanosensitive Ion Channel (MscL) of *Escherichia coli* is a well-characterized pentameric protein that protects cells from osmotic stress. With a molecular weight of 15 kDa, similar to MAM's weight, this protein is embedded in the lipidic cytoplasmic membrane[326–328]. Pore-forming Proteins (PFPs) are a heterogeneous group capable of creating membrane pores, crucial for processes like apoptosis[329]. Present in a broad range of organisms, PFPs are also structurally diverse, many related to toxicity and defense mechanisms[330]. In addition, surface layer proteins or S-layer proteins (SLPs) build the outermost coat of prokaryotic cells, forming crystalline and porous sheaths composed of repetitive units of a single protein, which often represents the most numerous proteins of the organism[321,331].

Among the different pore-organized proteins, MAM's subcellular localization and abundance, together with its lack of homology and putative hexameric organization, strongly match with descriptions of S-layer proteins[332]. Hexameric protein organizations are found in different organisms with S-layers. For example, *Haloferax volcanii* is an archaeon that has a protein with self-arrangement properties to organize into hexameric or pentameric structures, forming the S-layer coat on the cell surface and on the surface of exomes[333]. Structurally similar to the MAM's putative organization proposed here, S-layer proteins from the bacteria *Deinococcus radiodurans* and the archaea *Sulfolobus acidocaldarius* also have the capacity to self-arrange in a hexameric structure with a central pore. The assembly of several hexamers forms an ordered lattice, which provides structural integrity and protection to the organism[334,335]. In Gram- positive commensal species like *L. acidophilus*[336], and *Propionibacterium freudenreichii*[337], their S-layer can be visualized as an additional surface coat after the cell membrane and the peptidoglycan wall. Although these organisms are phylogenetically distinct from *F. duncaniae*, and despite the absence of S-layer homology (SLH) domains, their structural characteristics lead to further investigation into the possibility of MAM being an S-layer protein.

Morphological differences are common among S-layers, leading to difficulties in their characterization and isolation. The biochemical extraction of S-layers consists of removing the

cytoplasmic cell components after cell disruption, followed by dissociating hydrogen bonds to remove the cellular membrane. Solutions capable of breaking hydrogen bonds include Guanidine hydrochloride (GuHCL), LiCl, urea, trichloroacetic acid, ethylene diamine tetra acetic acid (EDTA), or Sodium Dodecyl Sulfate (SDS)[338,339]. Interestingly, some S-layer proteins, after being detached from the bacterial cell envelope, were observed to be able to self-assemble into regular lattice structures *in vitro* under specific conditions. The addition of divalent cations such as Ca2+ and Mg2+ can enhance this reassembly process, promoting the formation of a stable and uniform lattice[340]. EM-related techniques are the primary choices for S-layer identification and SLP structure characterization on the bacterial or archaeal cell envelope. Cryo-EM is the most advanced method containing broad modalities for high-resolution visualization of biological structures at the molecular level in their native state[341,342]. 3D X-ray crystallography, together with cryo-EM, was used to solve both the structure and assembly of SLPs from *Clostridioides difficile* S-layer[343]. Small angle X-ray scattering nanometer scale (SAXS), single-molecular force spectroscopy (SMFS), and atomic force microscopy (AFM) can be also helpful in depicting the topography and symmetry features of the S-layer mesh at the nanometer scale[344]. Further, even though sequence homology modeling (SHM) systems had a huge improvement in the structural predictions with artificial intelligence algorithms, as is the case with AlphaFold, the reduced homology between SLPs is a significant obstacle to structural delineation. Moreover, there isn't a unique standard methodology for S-layer characterization. Thus, a combination of the existing methodologies, aligned with detailed specifications based on the organism type, needs to be considered[342].

In our analysis, LiCl and RIPA buffer were employed to attempt the enrichment of a putative S-layer fraction. However, RIPA buffer extracts exhibited significant cytoplasmic contamination, whereas LiCl extractions resulted in fewer such issues. On SDS-PAGE gels, a prominent band corresponding to a molecular size of approximately 12–15 kDa was observed, and subsequent LC-MS/MS analysis identified MAM as the most abundant protein in these extracts. LiCl extracts were subjected to negative staining microscopy and Cryo-EM to further characterize this enriched fraction. Both techniques revealed circular cell envelope fragments of variable sizes, with internal regions displaying an organized pattern reminiscent of the lattice structures previously observed in *situ* electron microscopy of *F. duncaniae* cells. Despite these observations and the physicochemical characteristics shared with known SLP assemblies[345], it remains challenging to definitively classify MAM as an SLP, especially as it does not contain an SLH motif. Indeed, not all known S-layers have the SLH motif; thus, alternatively, MAM may constitute an atypical S-layer[346,347].

The unique envelope organization of Faecalibacterium and its relation with MAM

One of the most important results of this work was the pioneering findings regarding the non-classical organization of *F. duncaniae* cell envelopes. In the literature, *F. duncaniae* has been variably characterized as Gram-negative or Gram-positive, reflecting a lack of consensus regarding its cell envelope structure. Phylogeny studies indicate *F. duncaniae* as Gram-negative, while other studies refer to having a cell envelope similar to Gram-positive[348]. Furthermore, *F. duncaniae* lacks genes responsible for the synthesis of LPS and other membrane protein markers, as demonstrated by Maier et collaborators, 2017 and further analyzed in Chapter I of this work[247]. This highlights the existence of organisms with more diverse cell envelopes than are traditionally described and the fact that *F. duncaniae* may have cell envelope organization that remains unexplored.

Recent advances in phylogenomics have significantly reshaped our understanding of bacterial cell envelope evolution, challenging the classical dichotomy of monoderms and diderms. These studies indicate that a subgroup of diderm bacteria within the Terrabacteria lineage, which includes Bacillota, has likely lost the outer membrane independently on multiple occasions, giving rise to monoderm species. In contrast, this group is evolutionarily distinct from the Gracilicutes branch, encompassing well-characterized diderm bacteria such as *Escherichia coli* and lacking monoderm representatives. The term "neoderm" has been proposed to describe bacteria that possess an outer layer whose composition and origin differ from the classical outer membranes of diderm bacteria. However, the exact nature of this outer layer in neoderms remains a subject of ongoing research[349,350]. In the case of *F. duncaniae*, it is still to be determined whether its outer layer comprises lipids, a structured lattice formed by MAM, or a combination of both. Further biochemical and structural analyses are essential to elucidate the composition and organization of this outer layer, specifically the precise location of MAM within those layers. Therefore, understanding the biological architecture of the *F. duncaniae* envelope, involving the localization and organization of MAM can provide critical insights regarding its unique architecture, evolutionary origins, and functional adaptations.

MAM's strong association with the cell envelope of *F. duncaniae*, as evidenced by a mesh-like layer observed in EM and proteomic studies, highlights the importance of cryo-EM for further investigation into this cellular architecture. Our cryo-EM analysis revealed a distinct double-layer envelope surrounding the bacterial surface, with a thin, likely PG layer in between.

Interestingly, while the IM appears to enclose the cell completely, the outer layer shows disruptions with protuberances, suggesting structural differences from the IM. This observation

points to an atypical OL with an unknown composition. Despite not identifying transmembrane domains (TMDs) in the MAM sequence that could tether the outer membrane to the cell or motifs for peptidoglycan attachment, such as SLH domains, the electrostatic potential of MAM hexameric complex's two faces reveals charge patterns compatible with membrane interactions (Supplementary data available in Annex 1). However, several critical questions remain unanswered: i) Is the outer layer surrounding the cell composed of MAM?

ii)   Is   this   layer   composed   of   lipids   associated   with   MAM?

iii)   Is   this   coat   located   externally   to   the   PG   layer?

iv) Or is MAM positioned between the PG layer and the cellular membrane?

Addressing these questions will be essential to fully understand the role and organization of MAM within the cell envelope.

The ABC transporter in relation to MAM and F. duncaniae envelope

In an attempt to identify the possible nature of *F. duncaniae*'s outer layer, we search protein markers of OM to screen the proteome of *F. duncaniae*. Our analysis revealed a low-identity match with two related proteins, MlaF, which acts in the lipid asymmetry, and the lipopolysaccharide export system protein LptA, which assembles a complex structure spanning the cytoplasm to the outer membrane[351,352]. However, these matching proteins had very low identity with *F. duncaniae* proteome, and the hits were annotated as ABC transporters, including the PCAT ABC transporter, which is likely responsible for MAM translocation, as indicated in this study.

Recent analyses of the transition from diderm to monoderm bacteria have highlighted the existence of previously unknown mechanisms for lipid trafficking and tethering of the OM to the cell wall[353,354]. The limited sequence similarity between *F. duncaniae* proteins and known OM-associated proteins suggests the possible existence of novel mechanisms in its OL organization and assembly. In this context, the evidence presented here strongly suggests that the PCAT transporter mediates the translocation of MAM from the cytoplasm to the cell envelope in *F. duncaniae*. PCAT is very abundant among the Bacillota. They are known for participating in both proteolysis and export of proteins, such as bacteriocins, and in bacterial communication through signaling peptides and quorum sensing[355]. Therefore, our work indicates that a possible new role of PCATs in transporting outer-layer proteins should be evaluated.

Antibodies labeling indicates MAM's increased presence at the cell poles

Specific antibodies generated in rabbits against recombinant R-MAM were produced to define the subcellular cell localization of MAM accurately (Figure 9 (page 107) in the manuscript included in Chapter I). Initially, we attempted to induce antibodies using LiCl extracts; however, despite achieving strong enrichment of MAM, the resulting antibodies primarily targeted contaminants rather than MAM. This observation raises intriguing questions about the immunological response towards MAM, as microbiota-derived components constantly interact with the immune system without inducing inflammation[356]. Later, purified recombinant MAM successfully induced specific antibodies, and immunogold labeling was applied to determine MAM's localization.

Based on the abundance of MAM observed through proteomic assays, we expected to observe more immunogold labeling dots. Several factors may explain this discrepancy. First, we were unable to properly refold R-MAM, which resulted in precipitated aggregates. Also, if we consider the presence of lipids in the OM, its important to point that membrane proteins are notoriously difficult to solubilize in non-native environments due to their hydrophobic nature and the loss of lipid support[357]. Nonetheless, the preparation successfully induced specific antibodies, as shown by the absence of cross-reactivity with MAM from other *Faecalibacterium* species. While we confirmed the specificity of the antibodies, the misfolding of R-MAM may have altered the exposure of specific epitopes. This could lead to either the exposure of usually hidden epitopes or the masking of epitopes exposed in the native form[358,359]. Additionally, membrane-associated components such as lipids can conceal epitopes from antibodies, while transmembrane proteins and mucin domains are also known to mask epitopes by steric hindrance[360–362].

Interestingly, MAM detection in *F. duncaniae* cells was more pronounced at the bacterial poles than in the mid-cell region. Polar proteins are known to play roles in genome segregation, cell division, septum formation, signal transduction, and dynamic regulation, all of which are crucial for determining protein functionality[363]. For example, the DivIVA protein in *B. subtilis* localizes to the poles and septa, playing a key role in morphogenesis and cell division.[363] Similarly, *Caulobacter crescentus* exhibits polar proteins such as TipN, essential for cell polarity and proper organization of cell proteins and organelles,[364] and PopZ, which anchors chromosomes and facilitates segregation[365]. These findings strengthen the hypothesis that MAM is essential for maintaining cell envelope integrity and may have other roles in the cell cycle. Additionally, SLP, which typically form continuous surface layers, can exhibit specific localization patterns, as observed in *Ca. Viridilinea mediisalina*. In this organism, the S-layer forms exclusively at the apices, suggesting a specialized function at the terminal ends of the cell[366]. These findings strengthen the hypothesis that MAM is essential for maintaining cell

envelope integrity and facilitating interactions with the host and environment. Additionally, they are opening new discussions to explore MAM's potential role in the cell cycle. Thus, improving purification and folding protocols, besides the combination of cryo-EM and immunogold labeling, are further steps to conduct and precisely determine MAM's localization within the cell envelope to evaluate whether the outer layer of *F. duncaniae* cell envelope is composed of MAM.

MAM is a beneficial effector molecule derived from Faecalibacterium

One of the key attributes of MAM is its potent anti-inflammatory activity. In this study, we were the first to demonstrate the direct effects of purified recombinant MAM in a murine model of colitis. Administration of R-MAM improves disease-related observations, as evidenced by reduced weight loss, decreased bowel weight, and diminished bowel thickness in DNBS-induced colitis mice. Additionally, *in vitro* assays revealed that R-MAM modulates immune signaling pathways, notably reducing TNF-α and IL8 production in PBMC and in human intestinal epithelial cells, respectively, supporting its anti-inflammatory properties. Despite the limitations of our study (Manuscript included in Chapter 2), our work strengthens the potential bioterapheutical activity of MAM.

The activity of MAM with respect to intestinal inflammation leads to the investigation of other cell envelope molecules from gut commensals that have beneficial effects on the host. Particularly cell envelope effector molecules from the gut microbiota are closely related to host-microbe interactions, contributing to gut homeostasis and immune modulation. These molecules, which include SLP, mucus and collagen binding proteins, and polysaccharides, among others, mediate key functions such as adhesion to the intestinal epithelium, immune system modulation, and maintenance of barrier integrity, as described in the review manuscript included in this thesis[367,368]. Thus, MAM's molecular characterization as an envelope protein described by this work, suggests that its benefits towards the host may be driven not only by its peptides in the supernatant but also by its abundant presence in the bacterial surface, facilitating *Faecalibacterium*-host and environmental interactions. This evidence paves the way for evaluating not only MAM but also other uncharacterized effector molecules that may possess similar beneficial properties and hold biotechnological potential.

MAM diversity across the Faecalibacterium genus

The diversity of MAM proteins across *Faecalibacterium* strains, reflected in their sequence variability, highlights the complexity of this unique bacterial effector. Interestingly,

our findings consistently demonstrate conserved structural features, including a hexameric, pore-like organization predicted through modeling and supported by electron microscopy observations. This conservation across strains highlights MAM's likely fundamental role in cell envelope architecture and integrity. The revealed results regarding structural variations, such as differences in hexameric stability, pore sizes, and envelope abundance, do not currently provide evidence to link structural diversity with MAM's differential anti-inflammatory activity. Further studies should explore whether this structural conservation correlates with functional consistency and immunomodulatory properties or whether MAM's sequence variability enables strain-specific adaptations to distinct environmental or host niches.

A significant barrier to understanding the role of MAM in *Faecalibacterium* cell biology is the current lack of genetic engineering protocols adapted for this genus. Most available protocols are optimized for diderm model organisms, such as *Escherichia coli* and *Bacillus subtilis*. Given that the envelope of *F. duncaniae* likely includes a porous layer composed of MAM, this structure may impede DNA uptake during genetic manipulation procedures. Although this hypothesis requires experimental validation, future approaches could explore using LiCl to remove the outer layer, as demonstrated in protocols for S-layer removal. LiCl has been shown to extract SLP in some bacterial species without compromising the integrity of the underlying cell wall structure[369]. Applying this method could clarify whether the MAM-based envelope hinders transformation and inform the development of optimized genetic engineering protocols. Such improvements could enable the generation of MAM or ABC transporter knockouts, further elucidating their roles in cell envelope architecture and integrity, in addition to a broad understanding of the role of MAM in *Faecalibacterium's* beneficial properties to the host.

8. CONCLUSION

This work presents the first comprehensive characterization of MAM, a key effector molecule derived from the next-generation probiotic *Faecalibacterium duncaniae*. Here, we demonstrate that MAM is a structurally conserved yet molecularly diverse cell envelope protein within *Faecalibacterium*, highlighting its essential role in both bacterial organization and host interactions. This study establishes MAM as a fundamental component of *F. duncaniae*'s envelope architecture and, for the first time, provides direct evidence of its anti-inflammatory and protective effects *in vitro* and in a colitis model.

These findings not only expand our understanding of *Faecalibacterium*'s physiology and unique cell envelope organization but also highlight MAM's potential as a therapeutic target for inflammatory diseases. By assessing its structural and functional properties, this research paves the way for future studies aimed at elucidating MAM's precise molecular mechanisms and its broader implications for gut health.

9. PERSPECTIVES

Future efforts should prioritize the comprehensive characterization of the *Faecalibacterium* cell envelope through a combination of structural validations, proteomics, and imaging techniques. Approaches targeting MAM are essential to understand its distribution within the envelope layers and to determine whether it forms oligomeric structures. Such efforts are crucial for refining genetic engineering protocols focused on *Faecalibacterium* cell biology. This research will not only enable a deeper understanding of MAM's physiological role in the bacterium but also facilitate a clearer identification of its contribution to the beneficial effects of *Faecalibacterium*, and the corresponding mechanisms involved in host interactions.

10.   REFERENCES

1. Gest, H. The discovery of microorganisms by Robert Hooke and Antoni Van Leeuwenhoek, fellows of the Royal Society. *Notes Rec R Soc Lond* **58**, 187–201 (2004).

2. Dethlefsen, L., McFall-Ngai, M. & Relman, D. A. An ecological and evolutionary perspective on human–microbe mutualism and disease. *Nature 2007 449:7164* **449**, 811–818 (2007).

3. Round, J. L. & Mazmanian, S. K. The gut microbiota shapes intestinal immune responses during health and disease. *Nature Reviews Immunology 2009 9:5* **9**, 313–323 (2009).

4. Ursell, L. K., Metcalf, J. L., Parfrey, L. W. & Knight, R. Defining the Human Microbiome. *Nutr Rev* **70**, S38 (2012).

5. Hou, K. *et al.* Microbiota in health and diseases. *Signal Transduction and Targeted Therapy 2022 7:1* **7**, 1–28 (2022).

6. Berg, G. *et al.* Microbiome definition re-visited: old concepts and new challenges. *Microbiome* **8**, 1–22 (2020).

7. Turnbaugh, P. J. *et al.* The human microbiome project: exploring the microbial part of ourselves in a changing world. *Nature* **449**, 804 (2007).

8. Thursby, E. & Juge, N. Introduction to the human gut microbiota. *Biochemical Journal* **474**, 1823 (2017).

9. Neish, A. S. Microbes in Gastrointestinal Health and Disease. *Gastroenterology* **136**, 65 (2009).

10. Hildebrand, F. *et al.* Dispersal strategies shape persistence and evolution of human gut bacteria. *Cell Host Microbe* **29**, 1167-1176.e9 (2021).

11. Bengmark, S. Ecological control of the gastrointestinal tract. The role of probiotic flora. *Gut* **42**, 2–7 (1998).

12. Lozupone, C. A., Stombaugh, J. I., Gordon, J. I., Jansson, J. K. & Knight, R. Diversity, stability and resilience of the human gut microbiota. *Nature* **489**, 220 (2012).

13. Daliri, E. B. M., Ofosu, F. K., Xiuqin, C., Chelliah, R. & Oh, D. H. Probiotic Effector Compounds: Current Knowledge and Future Perspectives. *Front Microbiol* **12**, 655705 (2021).

14. Cryan, J. F. *et al.* The microbiota-gut-brain axis. *Physiol Rev* **99**, 1877–2013 (2019).

15. Orozco-Mosqueda, M. del C., Rocha-Granados, M. del C., Glick, B. R. & Santoyo, G. Microbiome engineering to improve biocontrol and plant growth-promoting mechanisms. *Microbiol Res* **208**, 25–31 (2018).

16. Lagier, J. C. *et al.* Culturing the human microbiota and culturomics. *Nat Rev Microbiol* **16**, 540–550 (2018).

17. Kim, C. Y., Ma, J. & Lee, I. HiFi metagenomic sequencing enables assembly of accurate and complete genomes from human gut microbiota. *Nature Communications 2022 13:1* **13**, 1–11 (2022).

18. Hitch, T. C. A. *et al.* Microbiome-based interventions to modulate gut ecology and the immune system. *Mucosal Immunol* **15**, 1095 (2022).

19. Ma, Z., Zuo, T., Frey, N. & Rangrez, A. Y. A systematic framework for understanding the microbiome in human health and disease: from basic principles to clinical translation. *Signal Transduction and Targeted Therapy 2024 9:1* **9**, 1–36 (2024).

20. Valdes, A. M., Walter, J., Segal, E. & Spector, T. D. Role of the gut microbiota in nutrition and health. *BMJ* **361**, 36–44 (2018).

21. Martinez-Guryn, K., Leone, V. & Chang, E. B. Regional Diversity of the Gastrointestinal Microbiome. *Cell Host Microbe* **26**, 314–324 (2019).

22. Olsson, L. M. *et al.* Dynamics of the normal gut microbiota: A longitudinal one-year population study in Sweden. *Cell Host Microbe* **30**, 726-739.e3 (2022).

23. Benson, A. K. *et al.* Individuality in gut microbiota composition is a complex polygenic trait shaped by multiple environmental and host genetic factors. *Proc Natl Acad Sci U S A* **107**, 18933–18938 (2010).

24. Tian, L. *et al.* Deciphering functional redundancy in the human microbiome. *Nature Communications 2020 11:1* **11**, 1–11 (2020).

25. Visconti, A. *et al.* Interplay between the human gut microbiome and host metabolism. *Nature Communications 2019 10:1* **10**, 1–10 (2019).

26. Van Hul, M. *et al.* What defines a healthy gut microbiome? *Gut* **73**, 1893–1908 (2024).

27. Tanca, A. *et al.* Metaproteomic portrait of the healthy human gut microbiota. *npj Biofilms and Microbiomes 2024 10:1* **10**, 1–12 (2024).

28. Qin, J. *et al.* A human gut microbial gene catalogue established by metagenomic sequencing. *Nature* **464**, 59–65 (2010).

29. Rinninella, E. *et al.* What is the Healthy Gut Microbiota Composition? A Changing Ecosystem across Age, Environment, Diet, and Diseases. *Microorganisms* **7**, 14 (2019).

30. Miquel, S. *et al.* Faecalibacterium prausnitzii and human intestinal health. *Curr Opin Microbiol* **16**, 255–261 (2013).

31. Hold, G. L., Schwiertz, A., Aminov, R. I., Blaut, M. & Flint, H. J. Oligonucleotide probes that detect quantitatively significant groups of butyrate-producing bacteria in human feces. *Appl Environ Microbiol* **69**, 4320–4324 (2003).

32. Fitzgerald, C. B. *et al.* Comparative analysis of Faecalibacterium prausnitzii genomes shows a high level of genome plasticity and warrants separation into new species-level taxa. *BMC Genomics* **19**, 931 (2018).

33. Piquer-Esteban, S., Ruiz-Ruiz, S., Arnau, V., Diaz, W. & Moya, A. Exploring the universal healthy human gut microbiota around the World. *Comput Struct Biotechnol J* **20**, 421 (2022).

34. Kennedy, K. M. *et al.* Questioning the fetal microbiome illustrates pitfalls of low-biomass microbial studies. *Nature 2023 613:7945* **613**, 639–649 (2023).

35. Suárez-Martínez, C., Santaella-Pascual, M., Yagüe-Guirao, G. & Martínez-Graciá, C. Infant gut microbiota colonization: influence of prenatal and postnatal factors, focusing on diet. *Front Microbiol* **14**, 1236254 (2023).

36. Joos, R. *et al.* Examining the healthy human microbiome concept. *Nature Reviews Microbiology 2024 23:3* **23**, 192–205 (2024).

37. Wang, J., Zhu, N., Su, X., Gao, Y. & Yang, R. Gut-Microbiota-Derived Metabolites Maintain Gut and Systemic Immune Homeostasis. *Cells* **12**, (2023).

38. Liu, X. F. *et al.* Regulation of short-chain fatty acids in the immune system. *Front Immunol* **14**, 1186892 (2023).

39. Den Besten, G. *et al.* The role of short-chain fatty acids in the interplay between diet, gut microbiota, and host energy metabolism. *J Lipid Res* **54**, 2325 (2013).

40. Tang, W. H. W., Kitai, T. & Hazen, S. L. Gut microbiota in cardiovascular health and disease. *Circ Res* **120**, 1183–1196 (2017).

41. Mutuyemungu, E., Singh, M., Liu, S. & Rose, D. J. Intestinal gas production by the gut microbiota: A review. *J Funct Foods* **100**, 105367 (2023).

42. Van Hul, M. *et al.* Role of the intestinal microbiota in contributing to weight disorders and associated comorbidities. *Clin Microbiol Rev* **37**, (2024).

43. Jandhyala, S. M. *et al.* Role of the normal gut microbiota. *World J Gastroenterol* **21**, 8836–8847 (2015).

44. LeBlanc, J. G. *et al.* Bacteria as vitamin suppliers to their host: a gut microbiota perspective. *Curr Opin Biotechnol* **24**, 160–168 (2013).

45. Robinson, K., Deng, Z., Hou, Y. & Zhang, G. Regulation of the intestinal barrier function by host defense peptides. *Front Vet Sci* **2**, 166366 (2015).

46. Ghosh, S., Whitley, C. S., Haribabu, B. & Jala, V. R. Regulation of Intestinal Barrier Function by Microbial Metabolites. *Cell Mol Gastroenterol Hepatol* **11**, 1463–1482 (2021).

47. Yang, S. & Yu, M. Role of goblet cells in intestinal barrier and mucosal immunity. *J Inflamm Res* **14**, 3171–3183 (2021).

48. Barreto e Barreto, L., Rattes, I. C., da Costa, A. V. & Gama, P. Paneth cells and their multiple functions. *Cell Biol Int* **46**, 701–710 (2022).

49. Gieryńska, M., Szulc-Dąbrowska, L., Struzik, J., Mielcarska, M. B. & Gregorczyk-Zboroch, K. P. Integrity of the Intestinal Barrier: The Involvement of Epithelial Cells and Microbiota—A Mutual Relationship. *Animals 2022, Vol. 12, Page 145* **12**, 145 (2022).

50. Loh, J. S. *et al.* Microbiota–gut–brain axis and its therapeutic applications in neurodegenerative diseases. *Signal Transduction and Targeted Therapy 2024 9:1* **9**, 1–53 (2024).

51. Olivares-Villagómez, D. & Van Kaer, L. Intestinal Intraepithelial Lymphocytes: Sentinels of the Mucosal Barrier. *Trends Immunol* **39**, 264 (2017).

52. Nguyen, H. D., Aljamaei, H. M. & Stadnyk, A. W. The Production and Function of Endogenous Interleukin-10 in Intestinal Epithelial Cells and Gut Homeostasis. *Cell Mol Gastroenterol Hepatol* **12**, 1343–1352 (2021).

53. Belkaid, Y. & Hand, T. W. Role of the Microbiota in Immunity and inflammation. *Cell* **157**, 121 (2014).

54. Zheng, D., Liwinski, T. & Elinav, E. Interaction between microbiota and immunity in health and disease. *Cell Research 2020 30:6* **30**, 492–506 (2020).

55. Magalhães, M. I. *et al.* The link between obesity and the gut microbiota and immune system in early-life. *Crit Rev Microbiol* (2024) doi:10.1080/1040841X.2024.2342427.

56. Morais, L. H., Schreiber, H. L. & Mazmanian, S. K. The gut microbiota–brain axis in behaviour and brain disorders. *Nature Reviews Microbiology 2020 19:4* **19**, 241–255 (2020).

57. Morton, J. T. *et al.* Multi-level analysis of the gut-brain axis shows autism spectrum disorder-associated molecular and microbial profiles. *Nat Neurosci* **26**, 1208–1217 (2023).

58. Sharon, G. *et al.* Human Gut Microbiota from Autism Spectrum Disorder Promote Behavioral Symptoms in Mice. *Cell* **177**, 1600-1618.e17 (2019).

59. Wilson, D. M. *et al.* Hallmarks of neurodegenerative diseases. *Cell* **186**, 693–714 (2023).

60. Valles-Colomer, M. *et al.* The neuroactive potential of the human gut microbiota in quality of life and depression. *Nature Microbiology 2019 4:4* **4**, 623–632 (2019).

61. Needham, B. D. *et al.* A gut-derived metabolite alters brain activity and anxiety behaviour in mice. *Nature 2022 602:7898* **602**, 647–653 (2022).

62. Buffington, S. A. *et al.* Dissecting the contribution of host genetics and the microbiome in complex behaviors. *Cell* **184**, 1740-1756.e16 (2021).

63. Cook, J. & Prinz, M. Regulation of microglial physiology by the microbiota. *Gut Microbes* **14**, (2022).

64. Dohnalová, L. *et al.* A microbiome-dependent gut–brain pathway regulates motivation for exercise. *Nature 2022 612:7941* **612**, 739–747 (2022).

65. Wang, H. X. & Wang, Y. P. Gut microbiota-brain axis. *Chin Med J (Engl)* **129**, 2373–2380 (2016).

66. Thomas, C. M. *et al.* Histamine derived from probiotic Lactobacillus reuteri suppresses TNF via modulation of PKA and ERK signaling. *PLoS One* **7**, (2012).

67. De Biase, D. & Pennacchietti, E. Glutamate decarboxylase-dependent acid resistance in orally acquired bacteria: function, distribution and biomedical implications of the gadBC operon. *Mol Microbiol* **86**, 770–786 (2012).

68. Lombardi, C. & Dicks, L. M. T. Gut Bacteria and Neurotransmitters. *Microorganisms* **10**, 1838 (2022).

69. Ullah, H. *et al.* The gut microbiota-brain axis in neurological disorder. *Front Neurosci* **17**, (2023).

70. Campbell, C. *et al.* Crosstalk between Gut Microbiota and Host Immunity: Impact on Inflammation and Immunotherapy. *Biomedicines 2023, Vol. 11, Page 294* **11**, 294 (2023).

71. Karlsson, F. H. *et al.* Symptomatic atherosclerosis is associated with an altered gut metagenome. *Nature Communications 2012 3:1* **3**, 1–8 (2012).

72. Wang, J. *et al.* A metagenome-wide association study of gut microbiota in type 2 diabetes. *Nature 2012 490:7418* **490**, 55–60 (2012).

73. Shahgoli, V. K. *et al.* Inflammatory bowel disease, colitis, and cancer: unmasking the chronic inflammation link. *Int J Colorectal Dis* **39**, 173 (2024).

74. Lopez-Siles, M. *et al.* Changes in the Abundance of Faecalibacterium prausnitzii Phylogroups I and II in the Intestinal Mucosa of Inflammatory Bowel Disease and Patients with Colorectal Cancer. *Inflamm Bowel Dis* **22**, 28–41 (2016).

75. Krukowski, H. *et al.* Gut microbiome studies in CKD: opportunities, pitfalls and therapeutic potential. *Nature Reviews Nephrology 2022 19:2* **19**, 87–101 (2022).

76. Amini Khiabani, S., Asgharzadeh, M. & Samadi Kafil, H. Chronic kidney disease and gut microbiota. *Heliyon* **9**, e18991 (2023).

77. Petersen, C. & Round, J. L. Defining dysbiosis and its influence on host immunity and disease. *Cell Microbiol* **16**, 1024 (2014).

78. Winter, S. E. & Bäumler, A. J. Gut dysbiosis: Ecological causes and causative effects on human disease. *Proc Natl Acad Sci U S A* **120**, e2316579120 (2023).

79. Degruttola, A. K., Low, D., Mizoguchi, A. & Mizoguchi, E. Current understanding of dysbiosis in disease in human and animal models. *Inflamm Bowel Dis* **22**, 1137 (2016).

80. Scott, K. P., Jean-Michel, A., Midtvedt, T., Van Hemert, S. & Antoine, J.-M. Manipulating the gut microbiota to maintain health and treat disease. *Microb Ecol Health Dis* **26**, (2015).

81. Shin, N. R., Whon, T. W. & Bae, J. W. Proteobacteria: microbial signature of dysbiosis in gut microbiota. *Trends Biotechnol* **33**, 496–503 (2015).

82. DAS, B. & Nair, G. B. Homeostasis and dysbiosis of the gut microbiome in health and disease. *J Biosci* **44**, 1–8 (2019).

83. Sekirov, I. & Finlay, B. B. The role of the intestinal microbiota in enteric infection. *J Physiol* **587**, 4159 (2009).

84. Chassaing, B. *et al.* Randomized Controlled-Feeding Study of Dietary Emulsifier Carboxymethylcellulose Reveals Detrimental Impacts on the Gut Microbiota and Metabolome. *Gastroenterology* **162**, 743–756 (2022).

85. Martinez, J. E. *et al.* Unhealthy Lifestyle and Gut Dysbiosis: A Better Understanding of the Effects of Poor Diet and Nicotine on the Intestinal Microbiome. *Front Endocrinol (Lausanne)* **12**, 667066 (2021).

86. Wang, B. *et al.* A High-Fat Diet Increases Gut Microbiota Biodiversity and Energy Expenditure Due to Nutrient Difference. *Nutrients* **12**, 3197 (2020).

87. Levy, M., Kolodziejczyk, A. A., Thaiss, C. A. & Elinav, E. Dysbiosis and the immune system. *Nature Reviews Immunology 2017 17:4* **17**, 219–232 (2017).

88. Gasaly, N. *et al.* Impact of Bacterial Metabolites on Gut Barrier Function and Host Immunity: A Focus on Bacterial Metabolism and Its Relevance for Intestinal Inflammation. *Front Immunol* **12**, 658354 (2021).

89. Bosi, A., Banfi, D., Bistoletti, M., Giaroni, C. & Baj, A. Tryptophan Metabolites Along the Microbiota-Gut-Brain Axis: An Interkingdom Communication System Influencing the Gut in Health and Disease. *Int J Tryptophan Res* **13**, 1178646920928984 (2020).

90. Dmytriv, T. R., Storey, K. B. & Lushchak, V. I. Intestinal barrier permeability: the influence of gut microbiota, nutrition, and exercise. *Front Physiol* **15**, 1380713 (2024).

91. Burgueño, J. F. & Abreu, M. T. Epithelial Toll-like receptors and their role in gut homeostasis and disease. doi:10.1038/s41575-019-0261-4.

92. Weaver, C. T., Elson, C. O., Fouser, L. A. & Kolls, J. K. The Th17 Pathway and Inflammatory Diseases of the Intestines, Lungs and Skin. *Annu Rev Pathol* **8**, 477 (2012).

93. Li, C.-J., Wang, Y.-K., Zhang, S.-M., Ren, M.-D. & He, S.-X. Global burden of inflammatory bowel disease 1990-2019: A systematic examination of the disease burden and twenty-year forecast. *World J Gastroenterol* **29**, 5751 (2023).

94. Wang, R., Li, Z., Liu, S. & Zhang, D. Global, regional and national burden of inflammatory bowel disease in 204 countries and territories from 1990 to 2019: a systematic analysis based on the Global Burden of Disease Study 2019. *BMJ Open* **13**, e065186 (2023).

95. Kamp, K., Dudley-Brown, S., Heitkemper, M., Wyatt, G. & Given, B. Symptoms Among Emerging Adults With Inflammatory Bowel Disease: A Descriptive Study. *Res Nurs Health* **43**, 48 (2019).

96. Bhayani, P., Natarajan, K. & Coelho-Prabhu, N. Rising Incidence of Inflammatory Bowel Disease in the Asian Subcontinent—An Exploration of Causative Factors. *Gastrointestinal Disorders 2024, Vol. 6, Pages 549-556* **6**, 549–556 (2024).

97. Hendrickson, B. A., Gokhale, R. & Cho, J. H. Clinical Aspects and Pathophysiology of Inflammatory Bowel Disease. *Clin Microbiol Rev* **15**, 79 (2002).

98. Friedrich, M., Pohin, M. & Powrie, F. Cytokine Networks in the Pathophysiology of Inflammatory Bowel Disease. *Immunity* **50**, 992–1006 (2019).

99. Santana, P. T., Rosas, S. L. B., Ribeiro, B. E., Marinho, Y. & de Souza, H. S. P. Dysbiosis in Inflammatory Bowel Disease: Pathogenic Role and Potential Therapeutic Targets. *International Journal of Molecular Sciences 2022, Vol. 23, Page 3464* **23**, 3464 (2022).

100. Cheng, L., Qi, C., Zhuang, H., Fu, T. & Zhang, X. gutMDisorder: a comprehensive database for dysbiosis of the gut microbiota in disorders and interventions. *Nucleic Acids Res* **48**, D554–D560 (2020).

101. Saez, A., Herrero-Fernandez, B., Gomez-Bris, R., Sánchez-Martinez, H. & Gonzalez-Granado, J. M. Pathophysiology of Inflammatory Bowel Disease: Innate Immune System. *International Journal of Molecular Sciences 2023, Vol. 24, Page 1526* **24**, 1526 (2023).

102. Lechuga, S., Braga-Neto, M. B., Naydenov, N. G., Rieder, F. & Ivanov, A. I. Understanding disruption of the gut barrier during inflammation: Should we abandon traditional epithelial cell lines and switch to intestinal organoids? *Front Immunol* **14**, 1108289 (2023).

103. Saez, A., Herrero-Fernandez, B., Gomez-Bris, R., Sánchez-Martinez, H. & Gonzalez-Granado, J. M. Pathophysiology of Inflammatory Bowel Disease: Innate Immune System. *Int J Mol Sci* **24**, 1526 (2023).

104. Xin, S. *et al.* Inflammation accelerating intestinal fibrosis: from mechanism to clinic. *Eur J Med Res* **29**, 335 (2024).

105. Cao, H. *et al.* The Pathogenicity and Synergistic Action of Th1 and Th17 Cells in Inflammatory Bowel Diseases. *Inflamm Bowel Dis* **29**, 818–829 (2023).

106. Muro, P. *et al.* The emerging role of oxidative stress in inflammatory bowel disease. *Front Endocrinol (Lausanne)* **15**, 1390351 (2024).

107. Chang, J. T. Pathophysiology of Inflammatory Bowel Diseases. *New England Journal of Medicine* **383**, 2652–2664 (2020).

108. Saez, A., Herrero-Fernandez, B., Gomez-Bris, R., Sánchez-Martinez, H. & Gonzalez-Granado, J. M. Pathophysiology of Inflammatory Bowel Disease: Innate Immune System. *Int J Mol Sci* **24**, 1526 (2023).

109. Wang, H., Foong, J. P. P., Harris, N. L. & Bornstein, J. C. Enteric neuroimmune interactions coordinate intestinal responses in health and disease. *Mucosal Immunology 2021 15:1* **15**, 27–39 (2021).

110. Günther, C., Rothhammer, V., Karow, M., Neurath, M. & Winner, B. The Gut-Brain Axis in Inflammatory Bowel Disease—Current and Future Perspectives. *Int J Mol Sci* **22**, 8870 (2021).

111. Huang, H. *et al.* Fine-mapping inflammatory bowel disease loci to single-variant resolution. *Nature* **547**, 173–178 (2017).

112. Guan, Q. A Comprehensive Review and Update on the Pathogenesis of Inflammatory Bowel Disease. *J Immunol Res* **2019**, 7247238 (2019).

113. Ashton, J. J., Seaby, E. G., Beattie, R. M. & Ennis, S. NOD2 in Crohn's Disease—Unfinished Business. *J Crohns Colitis* **17**, 450 (2022).

114. Annese, V. Genetics and epigenetics of IBD. *Pharmacol Res* **159**, 104892 (2020).

115. Foerster, E. G. *et al.* How autophagy controls the intestinal epithelial barrier. *Autophagy* **18**, 86 (2021).

116. Pigneur, B. *et al.* Phenotypic characterization of very early-onset IBD due to mutations in the IL10, IL10 receptor alpha or beta gene: a survey of the Genius Working Group. *Inflamm Bowel Dis* **19**, 2820–2828 (2013).

117. Khakoo, N. S. *et al.* Early Life and Childhood Environmental Exposures, More Than Genetic Predisposition, Influence Age of Diagnosis in a Diverse Cohort of 2952 Patients With IBD. *Clinical Gastroenterology and Hepatology* **22**, 1462-1474.e5 (2024).

118. Ananthakrishnan, A. N. Epidemiology and risk factors for IBD. *Nature Reviews Gastroenterology & Hepatology 2015 12:4* **12**, 205–217 (2015).

119. Lo Sasso, G. *et al.* Inflammatory Bowel Disease–Associated Changes in the Gut: Focus on Kazan Patients. *Inflamm Bowel Dis* **27**, 418 (2020).

120. Alam, M. T. *et al.* Microbial imbalance in inflammatory bowel disease patients at different taxonomic levels. *Gut Pathog* **12**, 1–8 (2020).

121. Santana, P. T., Rosas, S. L. B., Ribeiro, B. E., Marinho, Y. & de Souza, H. S. P. Dysbiosis in Inflammatory Bowel Disease: Pathogenic Role and Potential Therapeutic Targets. *Int J Mol Sci* **23**, 3464 (2022).

122. Lin, Z., Luo, W., Zhang, K. & Dai, S. Environmental and Microbial Factors in Inflammatory Bowel Disease Model Establishment: A Review Partly through Mendelian Randomization. *Gut Liver* **18**, 370–390 (2024).

123. Chen, B. C., Weng, M. T., Chang, C. H., Huang, L. Y. & Wei, S. C. Effect of smoking on the development and outcomes of inflammatory bowel disease in Taiwan: a hospital-based cohort study. *Scientific Reports 2022 12:1* **12**, 1–9 (2022).

124. De Castro, M. M. *et al.* Role of diet and nutrition in inflammatory bowel disease. *World J Exp Med* **11**, 1 (2021).

125. Venegas, D. P. *et al.* Short Chain Fatty Acids (SCFAs)-Mediated Gut Epithelial and Immune Regulation and Its Relevance for Inflammatory Bowel Diseases. *Front Immunol* **10**, 277 (2019).

126. Rohr, M. W., Narasimhulu, C. A., Rudeski-Rohr, T. A. & Parthasarathy, S. Negative Effects of a High-Fat Diet on Intestinal Permeability: A Review. *Advances in Nutrition* **11**, 77 (2019).

127. Bancil, A. S. *et al.* Food Additive Emulsifiers and Their Impact on Gut Microbiome, Permeability, and Inflammation: Mechanistic Insights in Inflammatory Bowel Disease. *J Crohns Colitis* **15**, 1068–1079 (2021).

128. Narula, N. *et al.* Associations of Antibiotics, Hormonal Therapies, Oral Contraceptives, and Long-Term NSAIDS With Inflammatory Bowel Disease: Results From the Prospective Urban Rural Epidemiology (PURE) Study. *Clinical Gastroenterology and Hepatology* **21**, 2649-2659.e16 (2023).

129. Chen, X. *et al.* Adverse health effects of emerging contaminants on inflammatory bowel disease. *Front Public Health* **11**, 1140786 (2023).

130. Belei, O. *et al.* The Interaction between Stress and Inflammatory Bowel Disease in Pediatric and Adult Patients. *J Clin Med* **13**, 1361 (2024).

131. Stengel, A. *et al.* Depression and Anxiety Disorders in Patients With Inflammatory Bowel Disease. *Front Psychiatry* **12**, 714057 (2021).

132. Ordille, A. J. & Phadtare, S. Intensity-specific considerations for exercise for patients with inflammatory bowel disease. *Gastroenterol Rep (Oxf)* **11**, goad004 (2023).

133. Hendrickson, B. A., Gokhale, R. & Cho, J. H. Clinical Aspects and Pathophysiology of Inflammatory Bowel Disease. *Clin Microbiol Rev* **15**, 79 (2002).

134. Rogler, G., Singh, A., Kavanaugh, A. & Rubin, D. T. Extraintestinal Manifestations of Inflammatory Bowel Disease: Current Concepts, Treatment, and Implications for Disease Management. *Gastroenterology* **161**, 1118–1132 (2021).

135. Magro, F. *et al.* European consensus on the histopathology of inflammatory bowel disease. *J Crohns Colitis* **7**, 827–851 (2013).

136. Fakhoury, M., Negrulj, R., Mooranian, A. & Al-Salami, H. Inflammatory bowel disease: Clinical aspects and treatments. *J Inflamm Res* **7**, 113–120 (2014).

137. Hong, S. M. & Baek, D. H. Diagnostic Procedures for Inflammatory Bowel Disease: Laboratory, Endoscopy, Pathology, Imaging, and Beyond. *Diagnostics (Basel)* **14**, (2024).

138. Vitello, A. *et al.* Current Approaches for Monitoring of Patients with Inflammatory Bowel Diseases: A Narrative Review. *Journal of Clinical Medicine 2024, Vol. 13, Page 1008* **13**, 1008 (2024).

139. Vernuccio, F. *et al.* The Role of Magnetic Resonance Enterography in Crohn's Disease: A Review of Recent Literature. (2022) doi:10.3390/diagnostics12051236.

140. Hong, S. M. & Baek, D. H. Diagnostic Procedures for Inflammatory Bowel Disease: Laboratory, Endoscopy, Pathology, Imaging, and Beyond. *Diagnostics* **14**, 1384 (2024).

141. Cappello, M. & Morreale, G. C. The Role of Laboratory Tests in Crohn's Disease. *Clin Med Insights Gastroenterol* **9**, 51 (2016).

142. Hanauer, S. B. & Leighton, J. A. Capsule Endoscopy in the Evaluation of Small-Bowel Inflammation. *Gastroenterol Hepatol (N Y)* **4**, 771 (2008).

143. Kaplan, G. G. & Windsor, J. W. The four epidemiological stages in the global evolution of inflammatory bowel disease. *Nature Reviews Gastroenterology & Hepatology 2020 18:1* **18**, 56–66 (2020).

144. McDowell, C., Farooq, U. & Haseeb, M. Inflammatory Bowel Disease. *StatPearls* (2023).

145. Solitano, V. *et al.* Advanced Combination Treatment With Biologic Agents and Novel Small Molecule Drugs for Inflammatory Bowel Disease. *Gastroenterol Hepatol (N Y)* **19**, 251 (2023).

146. GREENFIELD, S. M., PUNCHARD, N. A., TEARE, J. P. & THOMPSON, R. P. H. Review article: the mode of action of the aminosalicylates in inflammatory bowel disease. *Aliment Pharmacol Ther* **7**, 369–383 (1993).

147. Barrett, K., Saxena, S. & Pollok, R. Using corticosteroids appropriately in inflammatory bowel disease: a guide for primary care. *The British Journal of General Practice* **68**, 497 (2018).

148. Dubois-Camacho, K. *et al.* Glucocorticosteroid therapy in inflammatory bowel diseases: From clinical practice to molecular biology. *World J Gastroenterol* **23**, 6628 (2017).

149. Liu, J., Di, B. & Xu, L. li. Recent advances in the treatment of IBD: Targets, mechanisms and related therapies. *Cytokine Growth Factor Rev* **71–72**, 1–12 (2023).

150. Cai, Z., Wang, S. & Li, J. Treatment of Inflammatory Bowel Disease: A Comprehensive Review. *Front Med (Lausanne)* **8**, 765474 (2021).

151. Al Radi, Z. M. A. *et al.* Exploring the Predictive Value of Gut Microbiome Signatures for Therapy Intensification in Patients With Inflammatory Bowel Disease: A 10-Year Follow-up Study. *Inflamm Bowel Dis* **30**, 1642–1653 (2024).

152. Sica, G. S. & Biancone, L. Surgery for inflammatory bowel disease in the era of laparoscopy. *World J Gastroenterol* **19**, 2445–2448 (2013).

153. Seifarth, C., Kreis, M. E. & Gröne, J. Indications and Specific Surgical Techniques in Crohn's Disease. *Viszeralmedizin* **31**, 273 (2015).

154. Ferreira, S. da C. *et al.* Factors associated with surgical resection in patients with Crohn's disease: long-term evaluation. *Acta Cir Bras* **39**, e391924 (2024).

155. Reddy, K. *et al.* Advancements in Robotic Surgery: A Comprehensive Overview of Current Utilizations and Upcoming Frontiers. *Cureus* **15**, e50415 (2023).

156. Karimi, M. *et al.* Safety and efficacy of fecal microbiota transplantation (FMT) as a modern adjuvant therapy in various diseases and disorders: a comprehensive literature review. *Front Immunol* **15**, 1439176 (2024).

157. Cheng, Y. W. & Fischer, M. Fecal Microbiota Transplantation. *Clin Colon Rectal Surg* **36**, 151 (2023).

158. Li, Q. *et al.* Fecal Microbiota Transplantation for Ulcerative Colitis: The Optimum Timing and Gut Microbiota as Predictors for Long-Term Clinical Outcomes. *Clin Transl Gastroenterol* **11**, e00224 (2020).

159. Xiang, L. *et al.* Efficacy of faecal microbiota transplantation in Crohn's disease: a new target treatment? *Microb Biotechnol* **13**, 760 (2020).

160. Larsen, O. F. A. & Brummer, R. J. M. Perspective: on the future of fecal microbiota transplantation. *Front Microbiol* **15**, 1449133 (2024).

161. Akutko, K. & Stawarski, A. Probiotics, Prebiotics and Synbiotics in Inflammatory Bowel Diseases. *J Clin Med* **10**, 2466 (2021).

162. Oka, A. & Sartor, R. B. Microbial-Based and Microbial-Targeted Therapies for Inflammatory Bowel Diseases. *Dig Dis Sci* **65**, 757 (2020).

163. Hill, C. *et al.* Expert consensus document. The International Scientific Association for Probiotics and Prebiotics consensus statement on the scope and appropriate use of the term probiotic. *Nat Rev Gastroenterol Hepatol* **11**, 506–514 (2014).

164. Hill, C. *et al.* The International Scientific Association for Probiotics and Prebiotics consensus statement on the scope and appropriate use of the term probiotic. *Nature Reviews Gastroenterology & Hepatology 2014 11:8* **11**, 506–514 (2014).

165. Andreoletti, O. *et al.* Statement on the update of the list of QPS-recommended biological agents intentionally added to food or feed as notified to EFSA. 2: Suitability of taxonomic units notified to EFSA until March 2015. *EFSA Journal* **13**, 4138 (2015).

166. Ma, T. *et al.* Targeting gut microbiota and metabolism as the major probiotic mechanism - An evidence-based review. *Trends Food Sci Technol* **138**, 178–198 (2023).

167. Al-Fakhrany, O. M. & Elekhnawy, E. Next-generation probiotics: the upcoming biotherapeutics. *Mol Biol Rep* **51**, 1–14 (2024).

168. Azad, M. A. K., Sarker, M., Li, T. & Yin, J. Probiotic Species in the Modulation of Gut Microbiota: An Overview. *Biomed Res Int* **2018**, 9478630 (2018).

169. Huang, S. *et al.* Propionic fermentation by the probiotic Propionibacterium freudenreichii to functionalize whey. *J Funct Foods* **52**, 620–628 (2019).

170. Ansari, F. *et al.* Health-promoting properties of Saccharomyces cerevisiae var. boulardii as a probiotic; characteristics, isolation, and applications in dairy products. *Crit Rev Food Sci Nutr* **63**, 457–485 (2023).

171. Zhou, P., Chen, C., Patil, S. & Dong, S. Unveiling the therapeutic symphony of probiotics, prebiotics, and postbiotics in gut-immune harmony. *Front Nutr* **11**, 1355542 (2024).

172. Zhou, J. *et al.* Programmable probiotics modulate inflammation and gut microbiota for inflammatory bowel disease treatment after effective oral delivery. *Nature Communications 2022 13:1* **13**, 1–14 (2022).

173. Tamaki, H. *et al.* Efficacy of probiotic treatment with Bifidobacterium longum 536 for induction of remission in active ulcerative colitis: A randomized, double-blinded, placebo-controlled multicenter trial. *Dig Endosc* **28**, 67–74 (2016).

174. Abdulqadir, R., Engers, J. & Al-Sadi, R. Role of Bifidobacterium in Modulating the Intestinal Epithelial Tight Junction Barrier: Current Knowledge and Perspectives. *Curr Dev Nutr* **7**, 102026 (2023).

175. Pagnini, C. *et al.* Safety and Potential Role of Lactobacillus rhamnosus GG Administration as Monotherapy in Ulcerative Colitis Patients with Mild–Moderate Clinical Activity. *Microorganisms* **11**, 1381 (2023).

176. Martín, R. *et al.* Effects in the use of a genetically engineered strain of Lactococcus lactis delivering in situ IL-10 as a therapy to treat low-grade colon inflammation. *Hum Vaccin Immunother* **10**, 1611–1621 (2014).

177. Gibson, G. R. *et al.* Expert consensus document: The International Scientific Association for Probiotics and Prebiotics (ISAPP) consensus statement on the definition and scope of prebiotics. *Nature Reviews Gastroenterology & Hepatology 2017 14:8* **14**, 491–502 (2017).

178. Slavin, J. Fiber and Prebiotics: Mechanisms and Health Benefits. *Nutrients 2013, Vol. 5, Pages 1417-1435* **5**, 1417–1435 (2013).

179. Davani-Davari, D. *et al.* Prebiotics: Definition, Types, Sources, Mechanisms, and Clinical Applications. *Foods* **8**, 92 (2019).

180. Peluso, I., Romanelli, L. & Palmery, M. Interactions between prebiotics, probiotics, polyunsaturated fatty acids and polyphenols: diet or supplementation for metabolic syndrome prevention? *Int J Food Sci Nutr* **65**, 259–267 (2014).

181. Markowiak, P. & Ślizewska, K. Effects of Probiotics, Prebiotics, and Synbiotics on Human Health. *Nutrients* **9**, (2017).

182. Roy, S. & Dhaneshwar, S. Role of prebiotics, probiotics, and synbiotics in management of inflammatory bowel disease: Current perspectives. *World J Gastroenterol* **29**, 2078 (2023).

183. Casellas, F. *et al.* Oral oligofructose-enriched inulin supplementation in acute ulcerative colitis is well tolerated and associated with lowered faecal calprotectin. *Aliment Pharmacol Ther* **25**, 1061–1067 (2007).

184. Akutko, K. & Stawarski, A. Probiotics, Prebiotics and Synbiotics in Inflammatory Bowel Diseases. *Journal of Clinical Medicine 2021, Vol. 10, Page 2466* **10**, 2466 (2021).

185. Hughes, R. L., Alvarado, D. A., Swanson, K. S. & Holscher, H. D. The Prebiotic Potential of Inulin-Type Fructans: A Systematic Review. *Advances in Nutrition* **13**, 492–529 (2022).

186. Aguilar-Toalá, J. E. *et al.* Postbiotics — when simplification fails to clarify. *Nature Reviews Gastroenterology & Hepatology 2021 18:11* **18**, 825–826 (2021).

187. Żółkiewicz, J., Marzec, A., Ruszczyński, M. & Feleszko, W. Postbiotics-A Step Beyond Pre- and Probiotics. *Nutrients* **12**, 1–17 (2020).

188. Rafique, N. *et al.* Promising bioactivities of postbiotics: A comprehensive review. *J Agric Food Res* **14**, 100708 (2023).

189. Nataraj, B. H., Ali, S. A., Behare, P. V. & Yadav, H. Postbiotics-parabiotics: The new horizons in microbial biotherapy and functional foods. *Microb Cell Fact* **19**, 1–22 (2020).

190. Kango, N. & Nath, S. Prebiotics, Probiotics and Postbiotics: The Changing Paradigm of Functional Foods. *J Diet Suppl* **21**, 709–735 (2024).

191. Salminen, S. *et al.* The International Scientific Association of Probiotics and Prebiotics (ISAPP) consensus statement on the definition and scope of postbiotics. *Nature Reviews Gastroenterology & Hepatology 2021 18:9* **18**, 649–667 (2021).

192. Zagato, E. *et al.* Lactobacillus paracasei CBA L74 metabolic products and fermented milk for infant formula have anti-inflammatory activity on dendritic cells in vitro and protective effects against colitis and an enteric pathogen in vivo. *PLoS One* **9**, (2014).

193. Gonzalez-Santana, A. & Diaz Heijtz, R. Bacterial Peptidoglycans from Microbiota in Neurodevelopment and Behavior. *Trends Mol Med* **26**, 729–743 (2020).

194. Clarke, T. B. *et al.* Recognition of peptidoglycan from the microbiota by Nod1 enhances systemic innate immunity. *Nat Med* **16**, 228–231 (2010).

195. Garcia-Vello, P. *et al.* Peptidoglycan from Akkermansia muciniphila MucT: chemical structure and immunostimulatory properties of muropeptides. *Glycobiology* **32**, 712–719 (2022).

196. Xu, H., Bian, X., Wang, H., Huang, L. & Chen, X. Akkermansia muciniphila postbiotic administration mitigates choline-induced plasma Trimethylamine-N-Oxide production in mice. *Appl Biol Chem* **67**, 1–12 (2024).

197. Buckley, M., Lacey, S., Doolan, A., Goodbody, E. & Seamans, K. The effect of Lactobacillus reuteri supplementation in Helicobacter pylori infection: A placebo-controlled, single-blind study. *BMC Nutr* **4**, 1–8 (2018).

198. Barros, C. P. *et al.* Ohmic heating as a method of obtaining paraprobiotics: Impacts on cell structure and viability by flow cytometry. *Food Res Int* **140**, (2021).

199. Gibson, G. R. & Roberfroid, M. B. Dietary modulation of the human colonic microbiota: introducing the concept of prebiotics. *J Nutr* **125**, 1401–1412 (1995).

200. Markowiak, P. & Ślizewska, K. Effects of Probiotics, Prebiotics, and Synbiotics on Human Health. *Nutrients 2017, Vol. 9, Page 1021* **9**, 1021 (2017).

201. Sharma, A. N., Chaudhary, P., Kumar, S., Grover, C. R. & Mondal, G. Effect of synbiotics on growth performance, gut health, and immunity status in pre-ruminant buffalo calves. *Scientific Reports 2023 13:1* **13**, 1–12 (2023).

202. van Zanten, G. C. *et al.* The effect of selected synbiotics on microbial composition and short-chain fatty acid production in a model system of the human colon. *PLoS One* **7**, (2012).

203. Panigrahi, P. *et al.* A randomized synbiotic trial to prevent sepsis among infants in rural India. *Nature 2017 548:7668* **548**, 407–412 (2017).

204. Phavichitr, N. *et al.* Impact of synbiotics on gut microbiota during early life: a randomized, double-blind study. *Scientific Reports 2021 11:1* **11**, 1–12 (2021).

205. Bijle, M. N., Neelakantan, P., Ekambaram, M., Lo, E. C. M. & Yiu, C. K. Y. Effect of a novel synbiotic on Streptococcus mutans. *Sci Rep* **10**, (2020).

206. Rufino, M. N. *et al.* Synbiotics improve clinical indicators of ulcerative colitis: systematic review with meta-analysis. *Nutr Rev* **80**, 157–164 (2022).

207. Furrie, E. *et al.* Synbiotic therapy (Bifidobacterium longum/Synergy 1) initiates resolution of inflammation in patients with active ulcerative colitis: a randomised controlled pilot trial. *Gut* **54**, 242–249 (2005).

208. Park, H., Yeo, S., Ryu, C. B. & Huh, C. S. A streamlined culturomics case study for the human gut microbiota research. *Scientific Reports 2024 14:1* **14**, 1–11 (2024).

209. O'Toole, P. W., Marchesi, J. R. & Hill, C. Next-generation probiotics: the spectrum from probiotics to live biotherapeutics. *Nature Microbiology 2017 2:5* **2**, 1–6 (2017).

210. Martín, R. & Langella, P. Emerging health concepts in the probiotics field: Streamlining the definitions. *Front Microbiol* **10**, 457799 (2019).

211. Abouelela, M. E. & Helmy, Y. A. Next-Generation Probiotics as Novel Therapeutics for Improving Human Health: Current Trends and Future Perspectives. *Microorganisms 2024, Vol. 12, Page 430* **12**, 430 (2024).

212. Kaźmierczak-Siedlecka, K. *et al.* Next-generation probiotics - do they open new therapeutic strategies for cancer patients? *Gut Microbes* **14**, (2022).

213. Zhou, K. Strategies to promote abundance of Akkermansia muciniphila, an emerging probiotics in the gut, evidence from dietary intervention studies. *J Funct Foods* **33**, 194–201 (2017).

214. Pellegrino, A., Coppola, G., Santopaolo, F., Gasbarrini, A. & Ponziani, F. R. Role of Akkermansia in Human Diseases: From Causation to Therapeutic Properties. *Nutrients 2023, Vol. 15, Page 1815* **15**, 1815 (2023).

215. Derrien, M., Belzer, C. & de Vos, W. M. Akkermansia muciniphila and its role in regulating host functions. *Microb Pathog* **106**, 171–181 (2017).

216. Al-Fakhrany, O. M. & Elekhnawy, E. Next-generation probiotics: the upcoming biotherapeutics. *Mol Biol Rep* **51**, 1–14 (2024).

217. Al-Fakhrany, O. M. & Elekhnawy, E. Next-generation probiotics: the upcoming biotherapeutics. *Mol Biol Rep* **51**, 505 (2024).

218. Gubernatorova, E. O. *et al.* Akkermansia muciniphila - friend or foe in colorectal cancer? *Front Immunol* **14**, (2023).

219. Wang, F. *et al.* Akkermansia muciniphila administration exacerbated the development of colitis-associated colorectal cancer in mice. *J Cancer* **13**, 124–133 (2022).

220. Zhang, C. *et al.* Assessment of the safety and probiotic properties of Roseburia intestinalis: A potential 'Next Generation Probiotic'. *Front Microbiol* **13**, (2022).

221. Kang, X. *et al.* Roseburia intestinalis generated butyrate boosts anti-PD-1 efficacy in colorectal cancer by activating cytotoxic CD8+ T cells. *Gut* **72**, 2112–2122 (2023).

222. Song, W. S. *et al.* Multiomics analysis reveals the biological effects of live Roseburia intestinalis as a high-butyrate-producing bacterium in human intestinal epithelial cells. *Biotechnol J* **18**, (2023).

223. Udayappan, S. *et al.* Oral treatment with Eubacterium hallii improves insulin sensitivity in db/db mice. *npj Biofilms and Microbiomes 2016 2:1* **2**, 1–10 (2016).

224. Engels, C., Ruscheweyh, H. J., Beerenwinkel, N., Lacroix, C. & Schwab, C. The Common Gut Microbe Eubacterium hallii also Contributes to Intestinal Propionate Formation. *Front Microbiol* **7**, (2016).

225. Morotomi, M., Nagai, F. & Watanabe, Y. Description of Christensenella minuta gen. nov., sp. nov., isolated from human faeces, which forms a distinct branch in the order Clostridiales, and proposal of Christensenellaceae fam. nov. *Int J Syst Evol Microbiol* **62**, 144–149 (2011).

226. Kropp, C. *et al.* The Keystone commensal bacterium Christensenella minuta DSM 22607 displays anti-inflammatory properties both in vitro and in vivo. *Scientific Reports 2021 11:1* **11**, 1–12 (2021).

227. Mazier, W. *et al.* A new strain of christensenella minuta as a potential biotherapy for obesity and associated metabolic diseases. *Cells* **10**, 823 (2021).

228. Hayashi, H., Shibata, K., Sakamoto, M., Tomita, S. & Benno, Y. Prevotella copri sp. nov. and Prevotella stercorea sp. nov., isolated from human faeces. *Int J Syst Evol Microbiol* **57**, 941–946 (2007).

229. Zang, X. *et al.* Prevotella copri—a potential next-generation probiotic. *Food Front* **5**, 1391–1409 (2024).

230. Gong, J. *et al.* Effects of Prevotella copri on insulin, gut microbiota and bile acids. *Gut Microbes* **16**, (2024).

231. Yang, C. *et al.* Prevotella copri alleviates hyperglycemia and regulates gut microbiota and metabolic profiles in mice . *mSystems* (2024) doi:10.1128/MSYSTEMS.00532-24/SUPPL_FILE/REVIEWER-COMMENTS.PDF.

232. Alpizar-Rodriguez, D. *et al.* Prevotella copri in individuals at risk for rheumatoid arthritis. *Ann Rheum Dis* **78**, 590–593 (2019).

233. Scher, J. U. *et al.* Expansion of intestinal Prevotella copri correlates with enhanced susceptibility to arthritis. *Elife* **2013**, (2013).

234. Sedighi, M. *et al.* Comparison of gut microbiota in adult patients with type 2 diabetes and healthy individuals. *Microb Pathog* **111**, 362–369 (2017).

235. Liu, J. *et al.* Association Between Intestinal Prevotella copri Abundance and Glycemic Fluctuation in Patients with Brittle Diabetes. *Diabetes, Metabolic Syndrome and Obesity* **16**, 1613–1621 (2023).

236. Tan, H., Zhai, Q. & Chen, W. Investigations of Bacteroides spp. towards next-generation probiotics. *Food Research International* **116**, 637–644 (2019).

237. Ramakrishna, C. *et al.* Bacteroides fragilis polysaccharide A induces IL-10 secreting B and T cells that prevent viral encephalitis. *Nature Communications 2019 10:1* **10**, 1–13 (2019).

238. He, Q. *et al.* Protective effects of a new generation of probiotic Bacteroides fragilis against colitis in vivo and in vitro. *Sci Rep* **13**, (2023).

239. Martín, R. *et al.* Faecalibacterium: a bacterial genus with promising human health applications. *FEMS Microbiol Rev* **47**, (2023).

240. Sokol, H. *et al.* Faecalibacterium prausnitzii is an anti-inflammatory commensal bacterium identified by gut microbiota analysis of Crohn disease patients. *Proc Natl Acad Sci U S A* **105**, 16731–16736 (2008).

241. Chollet, L. *et al.* Faecalibacterium duncaniae as a novel next generation probiotic against influenza. *Front Immunol* **15**, 1347676 (2024).

242. Ferreira-Halder, C. V., Faria, A. V. de S. & Andrade, S. S. Action and function of Faecalibacterium prausnitzii in health and disease. *Best Pract Res Clin Gastroenterol* **31**, 643–648 (2017).

243. Dikeocha, I. J., Al-Kabsi, A. M., Chiu, H. T. & Alshawsh, M. A. Faecalibacterium prausnitzii Ameliorates Colorectal Tumorigenesis and Suppresses Proliferation of HCT116 Colorectal Cancer Cells. *Biomedicines* **10**, (2022).

244. Maioli, T. U. *et al.* Possible Benefits of Faecalibacterium prausnitzii for Obesity-Associated Gut Disorders. *Front Pharmacol* **12**, 740636 (2021).

245. Savin, K. W. *et al.* Faecalibacterium diversity in dairy cow milk. *PLoS One* **14**, e0221055 (2019).

246. Duncan, S. H., Hold, G. L., Harmsen, H. J. M., Stewart, C. S. & Flint, H. J. Growth requirements and fermentation products of Fusobacterium prausnitzii, and a proposal to reclassify it as Faecalibacterium prausnitzii gen. nov., comb. nov. *Int J Syst Evol Microbiol* **52**, 2141–2146 (2002).

247. Maier, E., Anderson, R. C., Altermann, E. & Roy, N. C. Live Faecalibacterium prausnitzii induces greater TLR2 and TLR2/6 activation than the dead bacterium in an apical anaerobic co-culture system. *Cell Microbiol* **20**, e12805 (2018).

248. Botin, T. *et al.* The Tolerance of Gut Commensal Faecalibacterium to Oxidative Stress Is Strain Dependent and Relies on Detoxifying Enzymes. *Appl Environ Microbiol* **89**, (2023).

249. Koga, Y. *et al.* Age-associated effect of kestose on Faecalibacterium prausnitzii and symptoms in the atopic dermatitis infants. *Pediatr Res* **80**, 844–851 (2016).

250. Laursen, M. F. *et al.* Faecalibacterium Gut Colonization Is Accelerated by Presence of Older Siblings. *mSphere* **2**, (2017).

251. De Filippis, F., Pasolli, E. & Ercolini, D. Newly Explored Faecalibacterium Diversity Is Connected to Age, Lifestyle, Geography, and Disease. (2020) doi:10.1016/j.cub.2020.09.063.

252. Prausnitz, C. Der Bacillus mucosus anaerobius. *Zentralbl Bakteriol Parasitenk Infektionskr Hyg Abt Orig* **89**, (1922).

253. Hauduroy P., Ehringer G., Guillot G., Urbain Ach. & Magrou J. Compte-rendu: Dictionnaire des bactéries pathogènes. *Bull Acad Vet Fr* **90**, 178–179 (1937).

254. Cato, E. P., Salmon, C. W. & Moore, W. E. C. Fusobacterium prausnitzii (Hauduroy et al.) Moore and Holdeman: emended description and designation of neotype strain. *Int J Syst Bacteriol* **24**, 225–229 (1974).

255. Lopez-Siles, M. *et al.* Cultured representatives of two major phylogroups of human colonic Faecalibacterium prausnitzii can utilize pectin, uronic acids, and host-derived substrates for growth. *Appl Environ Microbiol* **78**, 420–428 (2012).

256. Benevides, L. *et al.* New Insights into the Diversity of the Genus Faecalibacterium. *Front Microbiol* **8**, 1790 (2017).

257. Zou, Y. *et al.* Characterization and description of Faecalibacterium butyricigenerans sp. nov. and F. longum sp. nov., isolated from human faeces. *Sci Rep* **11**, (2021).

258. Sakamoto, M. *et al.* Genome-based, phenotypic and chemotaxonomic classification of Faecalibacterium strains: proposal of three novel species Faecalibacterium duncaniae sp. nov., Faecalibacterium hattorii sp. nov. and Faecalibacterium gallinarum sp. nov. *Int J Syst Evol Microbiol* **72**, 005379 (2022).

259. Liou, J. S. *et al.* Faecalibacterium taiwanense sp. nov., isolated from human faeces. *Int J Syst Evol Microbiol* **74**, (2024).

260. Plomp, N. & Harmsen, H. J. M. Description of Faecalibacterium wellingii sp. nov. and two Faecalibacterium taiwanense strains, aiding to the reclassification of Faecalibacterium species. *Anaerobe* **89**, (2024).

261. Verstraeten, S. *et al.* Faecalibacterium duncaniae A2-165 regulates the expression of butyrate synthesis, ferrous iron uptake, and stress-response genes based on acetate consumption. *Scientific Reports 2024 14:1* **14**, 1–12 (2024).

262. Miquel, S. *et al.* Identification of Metabolic Signatures Linked to Anti-Inflammatory Effects of Faecalibacterium prausnitzii. (2015) doi:10.1128/mBio.00300-15.

263. Rios-Covian, D., Gueimonde, M., Duncan, S. H., Flint, H. J. & De Los Reyes-Gavilan, C. G. Enhanced butyrate formation by cross-feeding between Faecalibacterium prausnitzii and Bifidobacterium adolescentis. *FEMS Microbiol Lett* **362**, 176 (2015).

264. Park, J. H. *et al.* An Integrative Multiomics Approach to Characterize Prebiotic Inulin Effects on Faecalibacterium prausnitzii. *Front Bioeng Biotechnol* **10**, 825399 (2022).

265. Kang, D. *et al.* Functional dissection of the phosphotransferase system provides insight into the prevalence of Faecalibacterium prausnitzii in the host intestinal environment. *Environ Microbiol* **23**, 4726–4740 (2021).

266. Lopez-Siles, M. *et al.* Cultured Representatives of Two Major Phylogroups of Human Colonic Faecalibacterium prausnitzii Can Utilize Pectin, Uronic Acids, and Host-Derived Substrates for Growth. *Appl Environ Microbiol* **78**, 420 (2012).

267. Wang, P. *et al.* Avenanthramide Metabotype from Whole-Grain Oat Intake is Influenced by Faecalibacterium prausnitzii in Healthy Adults. *J Nutr* **151**, 1426–1435 (2021).

268. Lopez-Siles, M. *et al.* Mucosa-associated Faecalibacterium prausnitzii phylotype richness is reduced in patients with inflammatory bowel disease. *Appl Environ Microbiol* **81**, 7582–7592 (2015).

269. Frank, D. N. *et al.* Molecular-phylogenetic characterization of microbial community imbalances in human inflammatory bowel diseases. *Proc Natl Acad Sci U S A* **104**, 13780 (2007).

270. Sokol, H. *et al.* Low Counts of Faecalibacterium prausnitzii in Colitis Microbiota. *Inflamm Bowel Dis* **15**, 1183–1189 (2009).

271. Varela, E. *et al.* Colonisation by Faecalibacterium prausnitzii and maintenance of clinical remission in patients with ulcerative colitis. *Aliment Pharmacol Ther* **38**, 151–161 (2013).

272. Machiels, K. *et al.* A decrease of the butyrate-producing species Roseburia hominis and Faecalibacterium prausnitzii defines dysbiosis in patients with ulcerative colitis. *Gut* **63**, 1275–1283 (2014).

273. Kallassy, J., Gagnon, E., Rosenberg, D., Silbart, L. K. & McManus, S. A. Strains of Faecalibacterium prausnitzii and its extracts reduce blood glucose levels, percent HbA1c, and improve glucose tolerance without causing hypoglycemic side effects in diabetic and prediabetic mice. *BMJ Open Diabetes Res Care* **11**, e003101 (2023).

274. Lopez-Siles, M. *et al.* Alterations in the Abundance and Co-occurrence of Akkermansia muciniphila and Faecalibacterium prausnitzii in the Colonic Mucosa of Inflammatory Bowel Disease Subjects. *Front Cell Infect Microbiol* **8**, 334070 (2018).

275. Zhao, H. *et al.* Systematic review and meta-analysis of the role of Faecalibacterium prausnitzii alteration in inflammatory bowel disease. *J Gastroenterol Hepatol* **36**, 320–328 (2021).

276. Qiu, X., Zhang, M., Yang, X., Hong, N. & Yu, C. Faecalibacterium prausnitzii upregulates regulatory T cells and anti-inflammatory cytokines in treating TNBS-induced colitis. *J Crohns Colitis* **7**, e558–e568 (2013).

277. Martín, R. *et al.* The commensal bacterium Faecalibacterium prausnitzii is protective in DNBS-induced chronic moderate and severe colitis models. *Inflamm Bowel Dis* **20**, 417–430 (2014).

278. Carlsson, A. H. *et al.* Faecalibacterium prausnitzii supernatant improves intestinal barrier function in mice DSS colitis. *Scand J Gastroenterol* **48**, 1136–1144 (2013).

279. Martín, R. *et al.* Faecalibacterium prausnitzii prevents physiological damages in a chronic low-grade inflammation murine model. *BMC Microbiol* **15**, 67 (2015).

280. Touch, S. *et al.* Human CD4+CD8α+ Tregs induced by Faecalibacterium prausnitzii protect against intestinal inflammation. *JCI Insight* **7**, e154722 (2022).

281. Sarrabayrouse, G. *et al.* CD4CD8αα Lymphocytes, A Novel Human Regulatory T Cell Subset Induced by Colonic Bacteria and Deficient in Patients with Inflammatory Bowel Disease. *PLoS Biol* **12**, e1001833 (2014).

282. Jiang, S. *et al.* A reduction in the butyrate producing species Roseburia spp. and Faecalibacterium prausnitzii is associated with chronic kidney disease progression. *Antonie van Leeuwenhoek, International Journal of General and Molecular Microbiology* **109**, 1389–1396 (2016).

283. Hu, S. *et al.* Gut Microbiota Changes in Patients with Bipolar Depression. *Advanced Science* **6**, 1900752 (2019).

284. Huang, Y. *et al.* Possible association of Firmicutes in the gut microbiota of patients with major depressive disorder. *Neuropsychiatr Dis Treat* **14**, 3329–3337 (2018).

285. Liu, R. T. *et al.* Reductions in anti-inflammatory gut bacteria are associated with depression in a sample of young adults. *Brain Behav Immun* **88**, 308–324 (2020).

286. Hao, Z., Wang, W., Guo, R. & Liu, H. Faecalibacterium prausnitzii (ATCC 27766) has preventive and therapeutic effects on chronic unpredictable mild stress-induced depression-like and anxiety-like behavior in rats. *Psychoneuroendocrinology* **104**, 132–142 (2019).

287. Li, S. *et al.* Altered gut microbiota associated with symptom severity in schizophrenia. *PeerJ* **8**, e9574 (2020).

288. Ueda, A. *et al.* Identification of Faecalibacterium prausnitzii strains for gut microbiome-based intervention in Alzheimer's-type dementia. *Cell Rep Med* **2**, 100398 (2021).

289. Hazan, S. *et al.* Lost microbes of COVID-19: Bifidobacterium, Faecalibacterium depletion and decreased microbiome diversity associated with SARS-CoV-2 infection severity. *BMJ Open Gastroenterol* **9**, e000871 (2022).

290. Ye, L. *et al.* F. prausnitzii-derived extracellular vesicles attenuate experimental colitis by regulating intestinal homeostasis in mice. *Microb Cell Fact* **22**, 1–15 (2023).

291. Quévrain, E., Maubert, M. A., Sokol, H., Devreese, B. & Seksik, P. The presence of the anti-inflammatory protein MAM, from Faecalibacterium prausnitzii, in the intestinal ecosystem. *Gut* **65**, 882–882 (2016).

292. Rossi, O. *et al.* Faecalibacterium prausnitzii Strain HTF-F and Its Extracellular Polymeric Matrix Attenuate Clinical Parameters in DSS-Induced Colitis. *PLoS One* **10**, e0123013 (2015).

293. Tremaroli, V. & Bäckhed, F. Functional interactions between the gut microbiota and host metabolism. *Nature 2012 489:7415* **489**, 242–249 (2012).

294. Liu, H. *et al.* Butyrate: A Double-Edged Sword for Health? *Advances in Nutrition* **9**, 21–29 (2018).

295. Siddiqui, M. T. & Cresci, G. A. M. The Immunomodulatory Functions of Butyrate. *J Inflamm Res* **14**, 6025 (2021).

296. Di Bella, M. A. Overview and Update on Extracellular Vesicles: Considerations on Exosomes and Their Application in Modern Medicine. *Biology (Basel)* **11**, 804 (2022).

297. Yaghoubfar, R. *et al.* Effect of Akkermansia muciniphila, Faecalibacterium prausnitzii, and Their Extracellular Vesicles on the Serotonin System in Intestinal Epithelial Cells. *Probiotics Antimicrob Proteins* **13**, 1546–1556 (2021).

298. Yabut, J. M. *et al.* Emerging Roles for Serotonin in Regulating Metabolism: New Implications for an Ancient Molecule. *Endocr Rev* **40**, 1092 (2019).

299. Margolis, K. G., Cryan, J. F. & Mayer, E. A. The Microbiota-Gut-Brain Axis: From Motility to Mood. *Gastroenterology* **160**, 1486 (2021).

300. Ghia, J. E. *et al.* Serotonin Has a Key Role in Pathogenesis of Experimental Colitis. *Gastroenterology* **137**, 1649–1660 (2009).

301. Wang, Y. *et al.* Faecalibacterium prausnitzii-derived extracellular vesicles alleviate chronic colitis-related intestinal fibrosis by macrophage metabolic reprogramming. *Pharmacol Res* **206**, 107277 (2024).

302. Huang, X. L. *et al.* Faecalibacterium prausnitzii supernatant ameliorates dextran sulfate sodium induced colitis by regulating Th17 cell differentiation. *World J Gastroenterol* **22**, 5201 (2016).

303. Auger, S. *et al.* Intraspecific Diversity of Microbial Anti-Inflammatory Molecule (MAM) from Faecalibacterium prausnitzii. *Int J Mol Sci* **23**, (2022).

304. Quévrain, E. *et al.* Identification of an anti-inflammatory protein from Faecalibacterium prausnitzii, a commensal bacterium deficient in Crohn's disease. *Gut* **65**, 415 (2016).

305. Breyner, N. M. *et al.* Microbial Anti-Inflammatory Molecule (MAM) from Faecalibacterium prausnitzii Shows a Protective Effect on DNBS and DSS-Induced Colitis Model in Mice through Inhibition of NF-κB Pathway. *Front Microbiol* **8**, (2017).

306. Thewasano, N., Germany, E. M., Maruno, Y., Nakajima, Y. & Shiota, T. Categorization of Escherichia coli outer membrane proteins by dependence on accessory proteins of the β-barrel assembly machinery complex. *J Biol Chem* **299**, 104821 (2023).

307. Fitzmaurice, D., Amador, A., Starr, T., Hocky, G. M. & Rojas, E. R. β-barrel proteins dictate the effect of core oligosaccharide composition on outer membrane mechanics. *bioRxiv* 2024.09.02.610904 (2024) doi:10.1101/2024.09.02.610904.

308. Chi, X. *et al.* Structural mechanism of phospholipids translocation by MlaFEDB complex. *Cell Research 2020 30:12* **30**, 1127–1135 (2020).

309. Tran, A. X., Trent, M. S. & Whitfield, C. The LptA Protein of Escherichia coli Is a Periplasmic Lipid A-binding Protein Involved in the Lipopolysaccharide Export Pathway. *J Biol Chem* **283**, 20342 (2008).

310. Abramson, J. *et al.* Accurate structure prediction of biomolecular interactions with AlphaFold 3. *Nature 2024 630:8016* **630**, 493–500 (2024).

311. Bertoline, L. M. F., Lima, A. N., Krieger, J. E. & Teixeira, S. K. Before and after AlphaFold2: An overview of protein structure prediction. *Frontiers in Bioinformatics* **3**, 1120370 (2023).

312. Krissinel, E. & Henrick, K. Inference of macromolecular assemblies from crystalline state. *J Mol Biol* **372**, 774–797 (2007).

313. Schrödinger L & Warren DeLano. PyMOL. Preprint at http://www.pymol.org/pymol (2020).

314. Tiong, H. K., Hartson, S. & Muriana, P. M. Comparison of five methods for direct extraction of surface proteins from Listeria monocytogenes for proteomic analysis by orbitrap mass spectrometry. *J Microbiol Methods* **110**, 54–60 (2015).

315. Olaya-Abril, A., Gómez-Gascón, L., Jiménez-Munguía, I., Obando, I. & Rodríguez-Ortega, M. J. Another turn of the screw in shaving Gram-positive bacteria: Optimization of proteomics surface protein identification in Streptococcus pneumoniae. *J Proteomics* **75**, 3733–3746 (2012).

316. Ali, S. *et al.* Slr4, a newly identified S-layer protein from marine Gammaproteobacteria, is a major biofilm matrix component. *Mol Microbiol* **114**, 979–990 (2020).

317. Hashimoto, K. & Panchenko, A. R. Mechanisms of protein oligomerization, the critical role of insertions and deletions in maintaining different oligomeric states. *Proc Natl Acad Sci U S A* **107**, 20352–20357 (2010).

318. Bosshard, H. R., Marti, D. N. & Jelesarov, I. Protein stabilization by salt bridges: concepts, experimental approaches and clarification of some misunderstandings. *J Mol Recognit* **17**, 1–16 (2004).

319. Baldwin, R. L. Energetics of protein folding. *J Mol Biol* **371**, 283–301 (2007).

320. Pum, D., Toca-Herrera, J. L. & Sleytr, U. B. S-Layer Protein Self-Assembly. *Int J Mol Sci* **14**, 2484 (2013).

321. Fagan, R. P. & Fairweather, N. F. Biogenesis and functions of bacterial S-layers. *Nat Rev Microbiol* **12**, 211–222 (2014).

322. Islam, M. S., Aryasomayajula, A. & Selvaganapathy, P. R. A Review on Macroscale and Microscale Cell Lysis Methods. *Micromachines (Basel)* **8**, 83 (2017).

323. Teilum, K., Olsen, J. G. & Kragelund, B. B. Functional aspects of protein flexibility. *Cell Mol Life Sci* **66**, 2231 (2009).

324. Adamson, L. S. R. *et al.* Pore structure controls stability and molecular flux in engineered protein cages. *Sci Adv* **8**, 7346 (2022).

325. Jumper, J. *et al.* Highly accurate protein structure prediction with AlphaFold. *Nature 2021 596:7873* **596**, 583–589 (2021).

326. Lane, B. J. & Pliotas, C. Approaches for the modulation of mechanosensitive MscL channel pores. *Front Chem* **11**, 1162412 (2023).

327. Van Den Berg, J., Galbiati, H., Rasmussen, A., Miller, S. & Poolman, B. On the mobility, membrane location and functionality of mechanosensitive channels in Escherichia coli. *Scientific Reports 2016 6:1* **6**, 1–11 (2016).

328. Cruickshank, C. C., Minchin, R. F., Le Dain, A. C. & Martinac, B. Estimation of the pore size of the large-conductance mechanosensitive ion channel of Escherichia coli. *Biophys J* **73**, 1925–1931 (1997).

329. Margheritis, E., Kappelhoff, S. & Cosentino, K. Pore-Forming Proteins: From Pore Assembly to Structure by Quantitative Single-Molecule Imaging. *Int J Mol Sci* **24**, (2023).

330. Parker, M. W. & Feil, S. C. Pore-forming protein toxins: from structure to function. *Prog Biophys Mol Biol* **88**, 91–142 (2005).

331. Assandri, M. H., Malamud, M., Trejo, F. M. & Serradell, M. de los A. S-layer proteins as immune players: Tales from pathogenic and non-pathogenic bacteria. *Curr Res Microb Sci* **4**, 100187 (2023).

332. Pum, D., Breitwieser, A. & Sleytr, U. B. Patterns in Nature—S-Layer Lattices of Bacterial and Archaeal Cells. *Crystals 2021, Vol. 11, Page 869* **11**, 869 (2021).

333. von Kügelgen, A., Alva, V. & Bharat, T. A. M. Complete atomic structure of a native archaeal cell surface. *Cell Rep* **37**, 110052 (2021).

334. Gambelli, L. *et al.* Structure of the two-component S-layer of the archaeon Sulfolobus acidocaldarius. *Elife* **13**, (2024).

335. Farci, D. *et al.* ll Structural analysis of the architecture and in situ localization of the main S-layer complex in Deinococcus radiodurans. *Structure* **29**, (2021).

336. Grosu-Tudor, S. S. *et al.* S-layer production by Lactobacillus acidophilus IBB 801 under environmental stress conditions. *Appl Microbiol Biotechnol* **100**, 4573–4583 (2016).

337. Do Carmo, F. L. R. *et al.* Propionibacterium freudenreichii surface protein SlpB is involved in adhesion to intestinal HT-29 cells. *Front Microbiol* **8**, 269595 (2017).

338. Sára, M. & Sleytr, U. B. S-Layer Proteins. *J Bacteriol* **182**, 859 (2000).

339. Sleytr, U. B., Schuster, B., Egelseer, E. M. & Pum, D. S-layers: principles and applications. *FEMS Microbiol Rev* **38**, 823–864 (2014).

340. Pavkov-Keller, T., Howorka, S. & Keller, W. The structure of bacterial S-layer proteins. *Prog Mol Biol Transl Sci* **103**, 73–130 (2011).

341. Shepherd, D. C., Dalvi, S. & Ghosal, D. From cells to atoms: Cryo-EM as an essential tool to investigate pathogen biology, host–pathogen interaction, and drug discovery. *Mol Microbiol* **117**, 610–617 (2022).

342. Turk, M. & Baumeister, W. The promise and the challenges of cryo-electron tomography. *FEBS Lett* **594**, 3243–3261 (2020).

343. Lanzoni-Mangutchi, P. *et al.* Structure and assembly of the S-layer in C. difficile. *Nat Commun* **13**, (2022).

344. Oh, Y. J. *et al.* Characterizing the S-layer structure and anti-S-layer antibody recognition on intact Tannerella forsythia cells by scanning probe microscopy and small angle X-ray scattering. *Journal of Molecular Recognition* **26**, 542–549 (2013).

345. Li, W. W. *et al.* Characterization of a Putative S-layer Protein of a Colonial Microcystis Strain. *Curr Microbiol* **75**, 173–178 (2018).

346. Blackler, R. J. *et al.* Structural basis of cell wall anchoring by SLH domains in Paenibacillus alvei. *Nat Commun* **9**, 1–11 (2018).

347. Kern, J. *et al.* Structure of Surface Layer Homology (SLH) Domains from Bacillus anthracis Surface Array Protein. *J Biol Chem* **286**, 26042 (2011).

348. Munukka, E. *et al.* Faecalibacterium prausnitzii treatment improves hepatic health and reduces adipose tissue inflammation in high-fat fed mice. *The ISME Journal 2017 11:7* **11**, 1667–1679 (2017).

349. Beaud Benyahia, B., Taib, N., Beloin, C. & Gribaldo, S. Terrabacteria: redefining bacterial envelope diversity, biogenesis and evolution. *Nat Rev Microbiol* **23**, (2025).

350. Megrian, D., Taib, N., Witwinowski, J., Beloin, C. & Gribaldo, S. One or two membranes? Diderm Firmicutes challenge the Gram-positive/Gram-negative divide. *Mol Microbiol* **113**, 659–671 (2020).

351. Sperandeo, P., Martorana, A. M. & Polissi, A. The lipopolysaccharide transport (Lpt) machinery: A nonconventional transporter for lipopolysaccharide assembly at the outer membrane of Gram-negative bacteria. *Journal of Biological Chemistry* **292**, 17981–17990 (2017).

352. Tang, X. *et al.* Structural insights into outer membrane asymmetry maintenance in Gram-negative bacteria by MlaFEDB. *Nature Structural & Molecular Biology 2020 28:1* **28**, 81–91 (2020).

353. Witwinowski, J. *et al.* An ancient divide in outer membrane tethering systems in bacteria suggests a mechanism for the diderm-to-monoderm transition. *Nat Microbiol* **7**, 411–422 (2022).

354. Grasekamp, K. P. *et al.* The Mla system of diderm Firmicute Veillonella parvula reveals an ancestral transenvelope bridge for phospholipid trafficking. *Nat Commun* **14**, (2023).

355. Beis, K. & Rebuffat, S. Multifaceted ABC transporters associated to microcin and bacteriocin export. *Res Microbiol* **170**, 399–406 (2019).

356. Ansaldo, E., Farley, T. K. & Belkaid, Y. Control of Immunity by the Microbiota. *Annu Rev Immunol* **39**, 449–479 (2021).

357. Danmaliki, G. I. & Hwang, P. M. Solution NMR spectroscopy of membrane proteins. *Biochimica et Biophysica Acta (BBA) - Biomembranes* **1862**, 183356 (2020).

358. Teif, V. B. *et al.* Linker histone epitopes are hidden by in situ higher-order chromatin structure. *Epigenetics Chromatin* **13**, 1–16 (2020).

359. Paramithiotis, E. *et al.* A prion protein epitope selective for the pathologically misfolded conformation. *Nature Medicine 2003 9:7* **9**, 893–899 (2003).

360. Sánchez-Martínez, S., Lorizate, M., Katinger, H., Kunert, R. & Nieva, J. L. Membrane Association and Epitope Recognition by HIV-1 Neutralizing Anti-gp41 2F5 and 4E10 Antibodies. *https://home.liebertpub.com/aid* **22**, 998–1006 (2006).

361. Reynard, O. *et al.* Ebolavirus Glycoprotein GP Masks both Its Own Epitopes and the Presence of Cellular Surface Proteins. *J Virol* **83**, 9596–9601 (2009).

362. Huarte, N., Lorizate, M., Kunert, R. & Nieva, J. L. Lipid modulation of membrane-bound epitope recognition and blocking by HIV-1 neutralizing antibodies. *FEBS Lett* **582**, 3798–3804 (2008).

363.   Hamoen, L. W. & Errington, J. Polar Targeting of DivIVA in Bacillus subtilis Is Not Directly Dependent on FtsZ or PBP 2B. *J Bacteriol* **185**, 693 (2003).

364.   Lam, H., Schofield, W. B. & Jacobs-Wagner, C. A Landmark Protein Essential for Establishing and Perpetuating the Polarity of a Bacterial Cell. *Cell* **124**, 1011–1023 (2006).

365.   Ptacin, J. L. *et al.* Bacterial scaffold directs pole-specific centromere segregation. *Proc Natl Acad Sci U S A* **111**, (2014).

366.   Gaisin, V. A., Kooger, R., Grouzdev, D. S., Gorlenko, V. M. & Pilhofer, M. Cryo-Electron Tomography Reveals the Complex Ultrastructural Organization of Multicellular Filamentous Chloroflexota (Chloroflexi) Bacteria. *Front Microbiol* **11**, 548235 (2020).

367.   Yin, R. *et al.* Immunogenic molecules associated with gut bacterial cell walls: chemical structures, immune-modulating functions, and mechanisms. *Protein Cell* **14**, 776–785 (2023).

368.   Lebeer, S., Vanderleyden, J. & De Keersmaecker, S. C. J. Host interactions of probiotic bacterial surface molecules: comparison with commensals and pathogens. *Nat Rev Microbiol* **8**, 171–184 (2010).

369.   Lortal, S. S. *et al.* S-layer of Lactobacillus helveticus atcc 12046: isolation, chemical characterization and re-formation after extraction with lithium chloride Slayer of Lactobacillus helveticus ATCC 12046: isolation, chemical characterization and re-formation after extraction with lithium chloride. *J Gen Microbiol* **138**, 61–62 (1992).

ANNEXES

Annex 1

CHAPTER I: MAM IS A KEY PROTEIN PROCESSED AND EXPORTED TO THE *Faecalibacterium duncaniae* **ENVELOPE, WHICH IS ITS MAIN PROTEIN TO ORGANIZE ITS UNIQUE STRUCTURE**

[ANNEX 1](#)

Annex 2

CHAPTER II – IMMUNOMODULATORY CHARACTERIZATION OF MAM FROM *F. duncaniae*

ANNEX 2